final report

Grant number 0327687

Measurement of the operating noise of offshore wind turbines to determine the noise input through the noise transfer function between the tower and the water on systems in the offshore test field

dr Hermann van Radecke and Dr. Michael Benesch[1]
Flensburg University of Applied Sciences
and CEwind
Kanzleistr. 91-93 24943 Flensburg

June 2012

[1] Since May 1, 2012: BSH, Hamburg

Gefördert durch:

aufgrund eines Beschlusses
des Deutschen Bundestages

The project on which this report is based was funded by the

Federal Ministry for the Environment, Nature Conservation and Nuclear Safety

funded under the funding code 0327687.

The responsibility for the content of this publication lies
with the authors.

This research project was named

RAVE operating noise

as part of the research initiative RAVE - Research at alpha ventus

carried out.

Contents

1. Summary As part of
the present research project, the Flensburg University of Applied Sciences examined the operating noise under water from wind turbines in the Alpha Ventus offshore wind farm in the North Sea.

The aim of the project was to measure underwater noise, to analyze the noise using various methods, to identify the noise sources and the noise paths as transfer functions into the water, and to place the noise in the context of its biological significance for marine mammals.
The alpha ventus wind farm is located in the North Sea 45 km from Borkum at a water depth of 30 m and consists of 12 turbines, 6 REpower 5M and 6 AREVA M5000, each 800 m apart. Two systems, a REpower and an AREVA system, were equipped with hydrophones, acceleration sensors under and above water to measure the vibration and measuring computers for data acquisition. The FINO1 research platform, 400 m away, was equipped with a hydrophone and a measuring computer. The noise measurements were carried out at the edge of the wind farm.
The measuring computers were synchronized with GPS signals so that cross-correlations could be carried out.
The data acquisition was high-resolution at 50 kHz for measuring the time series. Measurements were taken three times a day for a period of 300 seconds each. The measurement data was transmitted ashore via the park's internal RAVE network.

The sound could be measured with 3 hydrophones (two at one of the systems and one at FINO1) on 27 days in 2010 and on 138 days in 2011.
The sound levels could be determined. The mean value of all measurements was approx. 118 dB re 1 ÿPa as the equivalent continuous sound level Leq.
A comparative value for airborne noise is obtained by subtracting 62 dB, which would correspond to 56 dB in air.
The peak value Lpeak is the maximum level that occurs for a short time and was approx. 15 dB higher than the mean value.
The dependency of the noise level at different capacities of the wind farm and with different environmental parameters could be determined. It has been proven that overall in the wind farm it became quieter with increasing power, especially with increasing wave height. The reason is that the background noise was of the same order of magnitude as the turbine noise, the background noise decreased with increasing wind and more than compensated for the increase in turbine noise. The background noise was most likely generated by ships, some of which came from the shipping lanes 14 km away. With a lot of wind and waves, these noises were heard

Air intake dampened, so that the overall noise level decreased.
All distinctive tonal noises could be identified with accelerometers on the two plant types.

A very distinctive tonal noise with 90 Hz could be clearly assigned to a system type. This sound dominated the sound in the wind farm, especially at full load. In addition, the harmonics of the sound were detectable in the spectrum up to 1 kHz. The source strength of this type of system was determined with the tonal noise as an equivalent continuous sound level Leq at a distance of 100 m to be 129 dB re 1ÿPa re 100 m.

The noise from the second type of turbine is so weak relative to the background noise that it was almost impossible to measure it, even though the hydrophones were in front of the turbine.
Driving impacts from the construction areas for the offshore wind farms Borkum West II and BARD Offshore 1, 7 km and 50 km away respectively, were identified and removed from the operational noise measurements.
The results confirm measurements in the alpha ventus wind farm by Betke et al (2012).
It can be assumed that the wind turbines will not cause any damage to harbor porpoises and seals from noise emissions during operation. The sound levels were sometimes below the hearing threshold or very probably not harmful above the hearing threshold of the species. However, no hearing thresholds were available for the tone at 90 Hz, so that no statement could be made about the audibility for the most prominent tonal noise. Statements by marine biologists and bioacousticians and the resulting legal requirements for avoiding noise are still required, particularly because of the long-term exposure to noise from background and system noise.

2. Introduction and task With the 5th
Energy Research Program of the Federal Government, the goal of funding, research and development in the field of renewable energies is to ensure an environmentally friendly and nature-friendly expansion of wind power at sea.
The aim of this project was to investigate the environmental and natural compatibility of offshore wind turbines by measuring the sound radiation under water during the operation of wind turbines in Germany's first offshore wind farm in the North Sea. By measuring not only the sound but also the vibrations at the plants to a previously unavailable extent according to the state of research, both the pollution of the environment as an immission and the allocation to the sound sources as an emission should be possible. This goal has been achieved. With the continuation of a noise working group, in which the measurements were or will be included, the interpretation of the biologically relevant noise components and a specification of the low-noise required in the approval process according to the state of the art1 of offshore wind turbines are possible, so that the expansion of offshore wind farms (by 2030 according to the Federal Government's strategy for the use of wind energy at sea 1/2002) can be promoted in a nature-friendly manner. The specification provided by the measurement data provided here increases the state of the art and, together with the partners of the RAVE project, it was possible to provide information on particularly critical frequency intervals for avoidance. References to operational or structural measures to reduce emissions or ultimately the setting of limit values can be expanded on the basis of the data.
The scientific prospects for success of the project consisted in creating extensive sound data. After the end of the project, the analyzes of the data will be made available to the project partners in consultation with the RAVE project partners for processing under biological, physical, technically constructive and planning aspects.
To carry out the project, firstly two hydrophones were permanently installed under water at a sufficient distance on two wind turbines in the apha ventus wind farm, which were intended as research facilities in the RAVE project, secondly both wind turbines were equipped with acceleration sensors below and above water and thirdly one another hydrophone installed at the nearby research platform FINO1. With three measuring computers, the signals of the sound and the vibrations were recorded as a time series with high temporal resolution and finally stored on a computer on land.

For subsequent data evaluation, the time series could be accessed and the noise-relevant variables calculated, such as the equivalent continuous noise level Leq, peak level Lpeak, and individual event level SEL averaged over various averaging times. In the frequency domain, third-octave spectra and narrow-band spectra could be carried out both for sound and for vibration, which led to coherence and transfer functions, among other things. The comparison of the frequency analyzes made it possible to identify the sources of the sound.

[1] Abromeit C. (2007): BARD approval notice of April 11, 2007, issued by BSH, Section 4.1: The physical structures must be designed in such a way that neither during construction nor during operation according to the state of the art avoidable emissions of pollutants, noise and light into the marine environment.

3. Alpha ventus, description, location, turbine types, integration into RAVE The alpha ventus wind farm is located 45 km north of Borkum in the North Sea, see Fig. 3.1. Two traffic separation schemes pass at a distance of 14 km, one in the north and one in the south. A third shipping route, a little further away, lies to the west and connects the Traffic Separation Schemes.
There is a lot of ship traffic on the routes, which the hydrophones measure as a background.
There are 12 turbines installed in the wind farm, 6 turbines from REpower, 6 turbines from AREVA Wind GmbH.
The usual designation system is: AV for alpha ventus with system numbers AV01 to AV12.
The turbines each have a nominal output of 5 MW, are power and speed controlled by pitch control and variable speed by means of inverters (load control through blade angle speed control with electric motorized individual blade adjustment). Their properties are shown in Table 3.1. The two foundation types are four-legged jacket constructions, Annexes AV01 to AV06, and three-legged tripod construction, Annexes AV07 to AV12, see Fig.3.2, both foundations are shown to the same scale, so that the dimensions and, important here, the radiating surfaces can be seen in comparison.

Fig. 3.1: Position of the alpha ventus wind farm 45 km north of Borkum in the North Sea between two traffic separation areas, a third not shown connects the two areas to the west (image: DOTI, own supplement)

alpha ventus turbine number AV01 to AV06 turbine type		AV07 to AV12
REpower 5M nominal output 5075 kW nominal wind		AREVA M5000
approx. 13 m/s cut-in wind 3.5 to 4 m/s rotor		5000 kW
diameter 126 m		12,4 m/s
		3,5 bis 4 m/s
		116 m
Rotor speed	6.9 to 12.1 min-1 +15% 2	5.9 to 14.8 rpm +10%
Lager	main bearings	moment bearing
transmission	planetary/spur gear transmission ratio approx. 1:97	Planetary gear transmission ratio 1 : 9.92
Generator	double-sp. Asynchronous rated power 5.4MW 6 poles	Synchronous, permanent Rated power 5.26 MW Multipole
generator speed	670 to 1170 rpm +15%	(24) 45.1 to 148.5 rpm (up to 2.475 Hz)
inverter	In the exciter circle	full inverter
Foundation	Jacket	Tripod

Tab. 3.1: Turbine types and foundations (own research by Husum Wind 2010 and Betke 2012)

Fig. 3.3 shows the layout of the systems. The plants (red dots) are set up in an almost regular and almost rectangular 4 by 3 pattern. REpower's turbines are in the northern half, and AREVA's turbines are in the southern half. The systems on which measuring devices were installed are the systems AV04 and AV07, each marked with a yellow dot. Two hydrophones were installed near each facility, shown as yellow dots. To the west of the AV04 facility is the FINO1 research platform, on which a hydrophone was also installed. Three hydrophones were functional during the measurement period, two on AV04 and one on FINO1. The

Noise measurements were thus carried out at the geometric edge of the wind farm. The distances between the turbines in east-west and north-south direction are about 800 m. FINO1 is about 400 m away from AV04. The exact coordinates of the systems are shown in Tab. 6.1. Their distances result geometrically (distance = ÿ((x1-x2)²+(y1-y2)²) with sufficient accuracy.

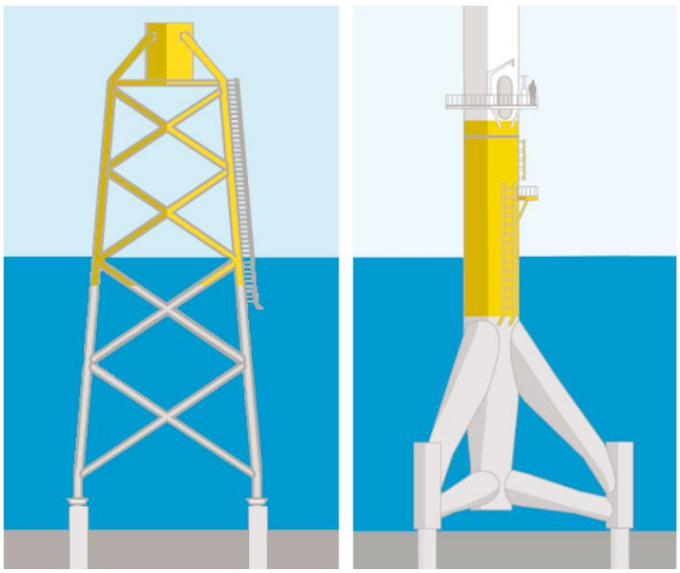

Fig. 3.2: The two foundation types, jacket constructions for plants AV01 to AV06 on the left, tripod for plants AV07 to AV12 on the right, same scale according to Betke (2012), see also RAVE (2012)

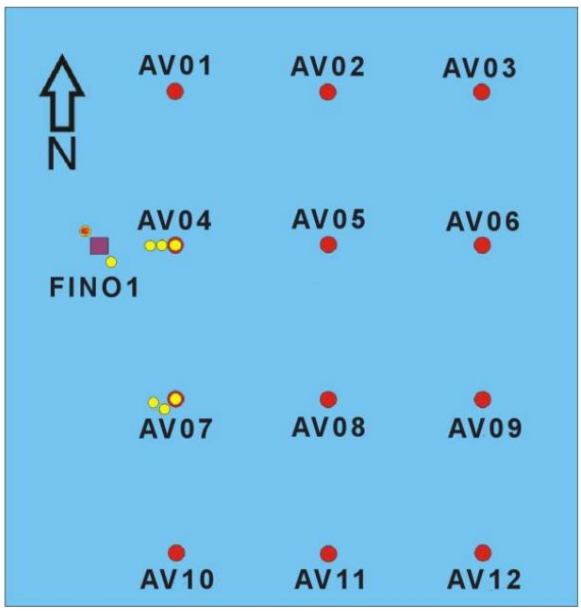

Fig.3.3: List of the 12 turbines (red dots) in the alpha ventus wind farm REpower turbines
(AV01-AV06)
AREVA plants (AV07-AV12)
2 systems with measuring devices (red-yellow dots)
Measuring station FINO1 (rectangle)
5 hydrophones (yellow dots, light red 1 substitute position) at the geometric edge of the wind farm, data that can be evaluated from 3 hydrophones (2 on AV04, 1 on FINO1)
Distances between the systems (north-south and east-west) approx. 800 m distance between FINO1 and AV04 approx. 400 m

This project was part of the overall RAVE project, an abbreviation of Research at Alpha VENtus. The project could only be carried out with integration into RAVE due to its complexity and the difficult offshore conditions. Many coordination meetings and consultations were necessary to plan and coordinate the implementation of the project. A detailed description of all projects and project partners can be found in RAVE (2012). In particular, the participation and assistance of the project partners Federal Maritime and Hydrographic Agency BSH, German Wind Energy Institute DEWI, Windtest (now: GL Garrad Hassan) and Fraunhofer Institute IWES were of exceptional importance in carrying out the project.

4. Basics of underwater noise and evaluation The basics of underwater noise and data evaluation are presented below. With regard to sound, the generation of sound, levels and propagation of sound are explained. Third-octave, narrowband, cross spectra, coherence and transfer functions are explained with regard to data evaluation.

4.1 Noise generation The generation of underwater noise during the operation of wind turbines has been described many times, see references, most recently by Betke (2012).

Airborne noise is irrelevant. The noise that can be heard on land is mainly generated by the rotor blades and transmitted through the air. However, the sound impedances Z of air and water are so different that the sound pressure according to Urban (2002) p. 86 penetrates the water during reflection, but the intensity is hardly. The characteristic impedances are given in Tab. 4.1.1 (Urban 2002 p. 83 and p. 91 supplemented with own calculations). The reflection of the intensity at an interface is given by the equation for ar according to Urban (2002) p. 79, which applies to perpendicular incidence, ar = I2/I1 = ((Z2-Z1)/(Z2+Z1))² and the data from Tab. 4.1.1 (sea water has a salt content of approx. 30 ‰).

(4.1.1)

Structure-borne noise is important. Vibrations arise in the machine and are conducted as structure-borne noise via the tower into the foundation under water and from there radiated into the water. The main source of vibrations are the gearbox, the generator, bearings and also the transformer.

In the transmission, the frequencies of the various speeds of the stages, the overrun frequencies of the various gears and the meshing frequencies are excited. The rollover frequencies of the inner and outer rings and the rolling elements are also excited in the bearings. Magnetic forces occur in the generator, so that the number of pole pairs has an influence, among other things. Magnetic forces also occur in the transformer and create vibrations. The inverters can generate vibrations. Harmonics are to be expected with all excitations. The turbines in the wind farm are speed-variable, so that the frequency of the vibrations depends on the load.

Overall, a variety of tonal noises can be expected. The main cause, however, are mechanically rotating parts, so that low frequencies below 1 kHz are to be expected (CRI, DEWI, ITAP 2007, Betke 2012).

It is to be expected that the vibrations will increase in amplitude as the load increases.
It is to be expected that the transmission of structure-borne noise depends on the construction of the tower, the connection between the tower and the foundation (transition piece) and the foundation.
It is to be expected that certain vibration modes develop well or badly.
It is to be expected that the radiation of structure-borne noise into the water depends on the shape and type of the surface of the foundation.
It is therefore difficult to derive from structural elements how the spectrum of the underwater radiation is formed.

physical quantities symbol Unit	density r [kg/m³]	Speed characteristic impedance Z0 c [m/s]	 [106.Pa/(m/s)]	at 100Hz ÿ = c/f [m]
Water 30 ‰ salidity (3% salinity)	1026	1500	1,54	15,0
Seabed Sand Silt Clay (typical)	1601	1545	2,48	15,5
Stahl	7700	5690	44,00	56,9
Air	1,2	340	0,000414	3,4

Tab. 4.1.1: Sound-relevant properties of water, seabed, steel, air (Urban 2002, own calculation)

4.2 Level variables

Sound pressure p in Pa and sound velocity v in m/s are the primary sound field variables. Both are alternating variables and can be described with p(t) and v(t) each with the mean value zero. in one

formed sound field they are in the same phase. Its quotient is the impedance introduced above in Pa/(m/s) and can be calculated as the product of density ÿ in kg/m³ times the speed of sound c in m/s. Its product p times v is the intensity in W/m². (Urban 2002, pp. 63 to 68) The decisive sound quantity, with which the sound can usually be described completely, as here, is the pressure, more precisely the alternating pressure. As pressure receivers, the hydrophones measure the sound pressure p in Pa. The sound pressure is usually not specified directly but as an equivalent continuous sound level Leq and as a peak level Lpeak, both of which are discussed. The single event level SEL is not explained in detail here. This level is used for piling noise, which is not the subject of this project. In Section 7.8.1 under Pile-driving noise that appeared as background noise, the single-event level is explained and estimated by calculation.

4.2.1 Equivalent continuous sound level Leq

The most important level variable in sound engineering is the equivalent continuous sound level, also known as the energy-equivalent level. The level is defined as the time integral over the square of the sound pressure p(t), which leads to power via the energy, normalized with a square of reference pressure p0, which is 1 ÿPa in water. In contrast, the reference pressure in air is 20 ÿPa = 2. 10-5 Pa.

It is averaged over time T and, as is usual for dB, the logarithm of 10 is given 10 times:

$$L_{eq} = 10 \log \left(\frac{1}{T} \int_0^T \frac{p(t)^2}{p_0^2} dt \right) \text{ dB} \quad . \qquad (4.2.1.1)$$

The sound level in water has the unit dB re 1 ÿPa.

The core of the equation, the integral over the square of the pressure without normalization by the reference sound pressure p0 but with normalization by the measurement time T, is identical to the variance, which is the square of the standard deviation. The variance is also called effective value peff² = p², see et al Müller (2011) p. 5.

The averaging time here is T = 300 s, which is the measurement time, and is given as Leq 300 s. This size is suitable for keeping track of the series of measurements.

On the other hand, the averaging time is T = 5 s. The measurement time is divided into 60 sections. The result is referred to as Leq 5 s. This quantity scatters more and is suitable for specifying percentiles, see below.

The signals for the Leq values (and the Lpeak values below) are essentially band filtered, removing the spurious noise below 10 Hz and above 3 kHz. Reasons for this and effects, shown as differences in Leq values, filtered and unfiltered, see below.

The Leq values are also given as third-octave spectra as a function of frequency, see below.

The airborne noise level, which is felt to be just as loud, is occasionally used as a comparison value for the underwater noise level. There is no doubt that there is a difference between airborne and waterborne noise due to the different reference values, which means 10. log((20 ÿPa / 1 ÿPa)²) = 26 dB. With the same feeling of pressure, the impedance is taken into account with 36 ÿ 35.7 = 10 . log(ZW/ZL), impedances see above, so Leq(air) = Leq(water) - 62 dB. However, this reference is controversial because while it accounts for the pressure in human hearing, which is tied to the perception of pressure, it does not consider the velocity of sound.

4.2.2 Peak level Lpeak The peak level is the maximum measured positive or negative sound pressure in the measurement period:

$$L_{peak} = 10 \log \left(\frac{|p_{peak}|^2}{p_0^2} \right) \text{ dB} \qquad (4.2.2.1)$$

It is remarkable that a single very brief peak, e.g. B. protrudes from the slow signal p with the positive height ÿp, depending on the phase position of the slow signal p can be of different heights, because ppeak = ÿp+p applies. Different phase positions of p can be determined by different Fre

frequency filtering are caused because band filters change not only the amplitude but also the phase.

4.3 Sound propagation in the North Sea The sound propagation path r in this part of the North Sea with a depth of 30 m is in a disk. However, the weakening of the intensity is not proportional to r to the power of 1, as is to be expected from the cylinder geometry, nor is it proportional to r to the power of 2, as is to be expected from the spherical geometry, but through many meetings in the committees one has settled on r to the power of 1 ,5 so that the geometric decrease in the sound level, also referred to as transmission loss TL, can be specified with

Leq in North Sea **TL = 15. log(r2/r1)** Unit dB, r1 = 1 m or r1 = 100 m. (4.3.1)

The reason is that although the water surface reflects almost completely because it represents a soft interface, the sea floor does not represent a completely hard interface.

The source level Lwa, unit dB re 1 ÿPa re 1 m, here that of a wind turbine or below that of a ship, is related to the theoretical distance 1 m, so that the sound level Leq at a distance r is Leq /(dB re 1 ÿPa) = Lwa /(dB re 1ÿPa re 1m) - 15th log(r/1m) = Lwa /(dB re 1ÿPa re 100m) – 15th log(r/100m), (4.3.2.)

where occasionally for technical reasons the source strength is related to 100 m, then the second part of Eq. 4.3.2, see also Betke (2012). The formula according to Thiele (2002) is used for the frequency-dependent calculation of the attenuation, taking into account the geometry and the frequency-dependent absorption in the water, see also CRI, DEWI, ITAP (2004). It applies

TL (16.07 0.185 FL) (log(r/km) 3) (0.174 0.046 FL 0.005 FL) r/km) with FL 10 log(f/kHz) ÿ((4.3.3)

and TL = Transmission Loss in dB
r = distance in km f =
frequency in kHz

The distance is given in km and the frequency in kHz, FL is an intermediate size.
If the spectrum is not known, the attenuation for Leq according to Eq. 4.3.2 is a good approximation for Thiele's equation. According to the two equations, at 1000 m and a frequency of 100 Hz, the attenuation (45.0 dB, 42.6 dB) differs by 2.1 dB, see Table 4.3.1.
Betke (2008) gives the adapted approximation equation for the North Sea in the alpha ventus area

TL = [10+2. log(f)+(2,5. 10-8.f+2,0. 10-5) . r]. log(r) (4.3.4)

for TL in dB with r in m and f in Hz, the results of which are similar to those of Thiele.
In the case of frequency-dependent attenuations, the equation according to Thiele Eq. 4.3.3 and in the case of broadband attenuation without taking the frequency into account Eq. 4.3.1.

Attenuation TL 15 log	r [m]	f [Hz] TL [dB] (-) 45.0	
r TL Thiele	1000	100 42.9 42.1	
(2002)	1000		
TL Betke (2008)	1000	100	

Tab. 4.3.1: Attenuation due to geometry and possible absorption according to different approaches

4.4 Third-octave

spectra The first step in frequency analysis is the third-octave spectrum. A third is 1/3 octave. The Leq values are specified in thirds, the center frequency fm is specified as the frequency. The ratio of the upper f2 to the lower cut-off frequency f1 is constant, k = f2 / f1, = spectral width of the thirds increases with the ÿ2, which causes the higher frequencies and basically contains more energy. The center frequency is the multiplicative mean **f** = **f ÿf .** According to Urban (2002) p. 35, DIN 45651 lists the third-octave filters with their center and cut-off frequencies in Table 4.4.1.

$f_m = \sqrt{f_1 f_2}$

For the present report, the third-octave spectra were calculated with the LabView subprogram "SVT Fractional-Octave Analysis" from National Instruments, which allows calculation of the third-octave levels according to IEC 1260:1995 and ANSI S1.11-2004 (2008).
A significant tonal component as a peak at 90 Hz is shown below and lies on a third-octave boundary at 89.1 Hz, so that the line appears at 100 Hz or 80 Hz depending on the spectral distribution of the signal and the specific structure of the filter. Here in LabView, the 90 Hz line is mapped to the 1/3 octave 100 Hz, see below.

No.	1	2	3	4	5	6	7	8	9	10	11	12	13	14	15	16	17	18
f1 / Hz	14,1	17,8	22,4	28,2	35,5	44,7	56,2	70,7	89,1	112	141	178	224	282	355	447	562	708
fm / Hz	**16**	**20**	**25**	**31,5**	**40**	**50**	**63**	**80**	**100**	**125**	**160**	**200**	**250**	**315**	**400**	**500**	**630**	**800**
f2 / Hz	17.8	22.4	28.2	35.5	44.7	56.2	70.7	89.1	112	141	178	224	282	355	447	562	708	891

No.	19	20	21	22	23	24	25	26	27	28	29	30	31	32
f1 / Hz	891	1122	1413	1778	2239	2818	3548	4467	5623	7079	8913	11220	14130	17780
fm / Hz	**1000**	**1250**	**1600**	**2000**	**2500**	**3150**	**4000**	**5000**	**6300**	**8000**	**10000**	**12500**	**16000**	**20000**
f2 / Hz	1122	1413	1778	2239	2818	3548	4467	5623	7079	8913	11220	14130	17780	22390

Tab. 4.4.1: Third-octave filter with center frequency fm and limit frequencies f1, f2 (Urban 2002 according to DIN 45651)

4.5 Perzentile

Percentiles are used here as statistical statements of the excess. As the lower limit, L95 specifies the value that is exceeded in its frequency of 95% of all values. L50 is the median and is exceeded by 50%, see Fig. 4.5.1. As the upper limit, L5 specifies the value that is only exceeded by 5%. For this definition, see Müller (2011) and Betke (2008). In the scale from bottom to top, the minimum and maximum are in the order Min, L95, L50, middle. Leq, L5, Max. As already stated by Betke (2012), L95 and L5 are better suited to describe the scattering of the sound measurement values, because the extreme sound events, which represent the minimum and the maximum, have little statistical relevance and with the percentiles not be shown. Percen tiles are used here when specifying the level in dB and in thirds related to the measured values in a third. The energetic mean (mean Leq) is also given here, which is always higher than the usual arithmetic mean due to the energetic averaging based on the logarithmic dB scale. For symmetrical distributions, the arithmetic mean is identical to L50. Thus, here in Fig. 4.5.1 and in the results in Section 7, the energetic mean Mean Leq is always greater than L50.

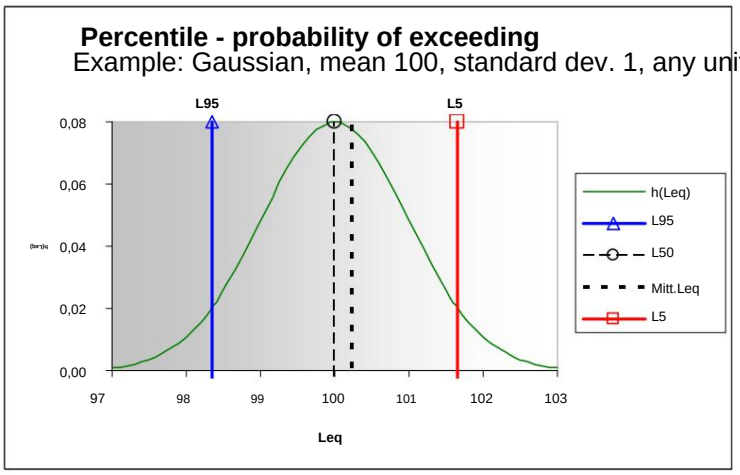

Fig.4.5.1: Percentiles as used here, example frequency h(Leq) over Leq of a Gaussian distribution, mean 100, standard deviation 1, L95 = 95% of the measured values exceed this Leq value, L5 only 5% of the values exceed this Leq value L50 = median, with symmetrical distribution identical arithmetic mean Avg.Leq = energetically mean Leq (greater than arithmetic mean due to logarithmic dB scale)

4.6 Narrow Band Spectrum

The next step in frequency analysis is narrow band analysis with the narrow band spectrum.
The bandwidth ÿf is constant, here ÿf = 1 Hz.
To form the power density spectrum Sxx(f), the time series x(t) is Fourier transformed to form the complex amplitude spectrum X(f) with the real part, which contains the cosine part, or co-spectrum for short, and with

Imaginary part that contains the sine or quadrature part, or quad spectrum for short. The complex spectrum contains magnitude and phase. Only the amount is evaluated here. The power density spectrum Sxx(f), which indicates the variances of the individual frequencies, is formed by forming the absolute value with the conjugate complex spectrum (*). Parseval's theorem applies, according to which the integral of the power density spectrum is equal to the variance of the signal in the time domain ÿ². If the variance is normalized, the spectrum is called variance-preserving. See the equations 4.6.1. For details see Bendat and Piersol (1980).

$$x(t) \quad \ddot{y} > \quad \frac{1}{2T} \int_{-T}^{+T} x(t)\, e^{-i\omega t}\, dt \quad \ddot{y}\, \ddot{y} > X(f)\, C(f) - iQ(f) \qquad \ddot{y} > \ddot{y}\, X(f)\, X^{*}(f)\, S_{xx}(f) \ddot{y} > \qquad (4.6.1, a,b)$$

$$\ddot{y}^2 \ddot{y} = \int S_{xx}(f) \ddot{y} df$$

The calculation of the power density spectra was performed with a 50,000-point DFT according to the overlap add method (Welch 1967) using a Hanning window. With a measurement time of 300 seconds per measurement, a sampling rate of 50 kHz and an overlap of 50%, each spectrum from 599 individual spectra is averaged.

However, since the time series of a measurement were divided into 10 sub-files in order to keep the size of the individual files manageable, the 9 segments that are half in the nth and half in the (n+1)th sub-file were not evaluated. Thus, the spectra were averaged from 590 individual spectra.

Using a DFT instead of an FFT has the advantage that the frequency resolution in the spectra is exactly 1.0 Hz for the selected parameters. The greater computing effort of a DFT compared to an FFT, on the other hand, hardly plays a role, since with the computing speed of today's CPUs the "bottleneck" is mainly when reading the time series from the hard disk.
A peak-true representation of the spectra is achieved by multiplying by a factor that results from the parameters of the FFT and the Hanning filter according to DIN 456681 tonality.

4.7 Cross Spectrum

For a cross spectrum Sxy(f), two time series x(t) and y(t) are sampled simultaneously, Co and Quad spectra are formed with Fourier transformations and the squared magnitudes are formed crosswise, see Equations 4.7.1. Sxz(f) is Hermitian, Lxy(f) = Lyx(f) and Qxy(f) = -Qyx(f) (Bendat, Piersold 1980).

$$x(t) \quad \ddot{y} > \quad X(f)\, C(f) - iQ(f) \qquad y(t) \quad \ddot{y} > \quad Y(f)\, C(f) - iQ(f)$$

$$L(f) = C(f)\, C(f) + Q(f)\, Q(f) \qquad Q(f) = C(f)\, Q(f) - Q(f)\, C(f)$$

$$S_{xy}(f) = X(f)\, Y^{*}(f) = L(f) + iQ(f) \qquad (4.7.1)$$

4.8 Transfer function

In electrical systems, the transfer function IH(f)I² indicates the proportion that is given from the input x via the system H to the output y. H is a frequency resolved gain factor, see Eq. 4.8.1.

$$\left|H(f)\right|^2 = \frac{S_{yy}(f)}{S_{xx}(f)} \qquad (4.8.1)$$

If the noise emissions of a facility are superimposed with the presence of background noise, sound from other sources can be found in Syy(f) and is calculated as amplification in relation to the acceleration signals Sxx(f) of the facility, which is mathematically correct, but causal is not correct. Since the background noise is very strong, the transfer function is not unambiguous and is only meaningful in connection with the consideration of the individual spectra Syy(f) and Sxx(f) from see Section 7.7 Acceleration spectra and sound sources.

4.9 Coherence function

The coherence function gxy²(f) tests the connection between two spectra in a similar way to the correlation coefficient and supplies a frequency-resolved number between 0 and 1. The coherence function is formed with the square of the absolute value of the cross spectrum and normalized with the two power density spectra, see Eq. 4.9.1. Values of 0.5 to 0.3 are actually achieved here and are rated as high because of the additional signal sources.

$$g_{xy}(f)^2 = \frac{\left|S_{xy}(f)\right|^2}{S_{xx}(f)\,S_{yy}(f)} \qquad (4.9.1)$$

4.10 Filtering It
was used to suppress low frequencies below 10 Hz, which are not acoustic vibrations but rather have their origin in currents, e.g. B. frequencies of the Strouhal number (Prandtl 2008) when flowing around the hydrophone, and to suppress the high frequencies above 3.0 kHz, which are caused by electromagnetic radiation, e.g. B. in the cables of the systems, a bandpass filter 10 Hz to 3.0 kHz of the 8th order Butterworth bandpass type is used.
The bandpass filter was used in the calculation of the Leq values and the peak values. The effect of the bandpass filter is shown in Section 7.
The bandpass filter was not used when calculating the third-octave spectra.
The bandpass filter was used when calculating the narrowband spectra. Only frequencies in the passband are shown here, so that there is no attenuation in the shown range due to the steep edge steepness.

There are exceptions to the procedure mentioned here in the evaluation, which are marked or are obvious.

4.11 Wind Classes

Three wind classes were defined to describe the load states of the wind turbines. In the lower class, the wind is below and close to the cut-in speed of 3.5 m/s to 4 m/s, see Table 3.1, the system delivers little or no power. In the upper class, the system delivers nominal power or just below, the nominal wind speed is typically 11.5 m/s to 13 m/s, see ibid.
The middle class covers the middle speeds with the partial load range. The Meteorological Institute of Denmark forms three classes: calm, 0.2 m/s to 5.0 m/s, 5.0 to 11.0 m/s, which corresponds to Beaufort 3 to 6, and over 11.0 m /s (Cappelen 1999). Due to the machine properties, there is a slight deviation from this standard here.

Wind speed and significant wave height are coupled, see next section, and wave height classes are formed accordingly. It is remarkable that the service ships in the wind farm can only operate up to a significant wave height of approx. 2 m.
Three wind classes are formed with speeds below, between and above 4 m/s and 11.5 m/s.

Three performance classes are formed with performance below, between and above 1% and 90% of the nominal output.
Two wave classes are formed with significant wave heights below and above 2.5 m.
For details on the formation of classes, see Section 7 of the evaluation.

4.12 Other parameters The
power, speed and wind speed on the nacelle were measured on the AV04 and AV07 systems. The power was measured for all systems, and the power of the wind farm was summed up. The averaging times for the power at the systems were 15 minutes.
The wind speed at a height of 100 m was evaluated on FINO1, averaging time 10 minutes.
The significant wave height hS was measured at FINO1, averaging time 30 minutes. The wave height was evaluated. The significant wave height is the mean for the third of the tallest waves

a wave collective recorded over a defined period of time (Lesny, 2008, p. 24). The wave height depends on the local wind (wind-induced), with the strike length and thus the wind direction having an influence, and on the large-scale waves (swell). According to Kyrow in Heinemann (2003), a Froude number ($1/Fr^2 = 0.16$) can be used to roughly estimate the wind-induced portion of the significant wave height without taking into account the strike length with the wind speed v as $hS = 0.16/ g . v^2$ with g typical for Froude number $g = 9.81 m/s^2$. Fig. 4.12.1 shows the significant wave height over the wind speed at a height of 100 m measured at FINO1 for June to December 2011 and the calculation according to Kyrow. The maximum values in the 2011 measurement period occurred on December 9 with vmax = 27.5 m/s and hsmax = 8.26 m.

At FINO1, the water level is measured as a level and was evaluated, whereby the water level is given as a pressure in dBar, which is equal to one meter of water column.

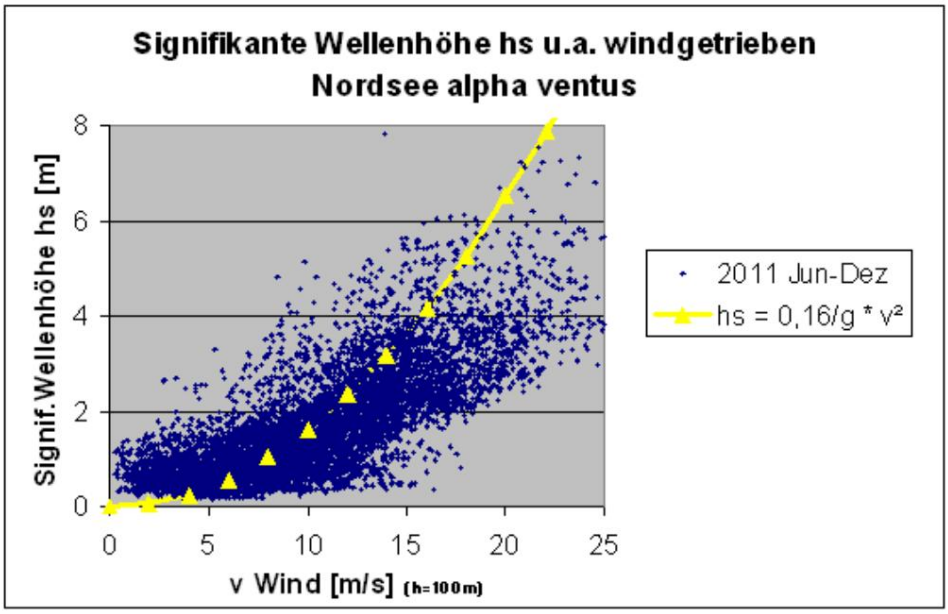

Fig. 4.12.1 Significant wave height hs over wind speed v at a height of 100 m measured at FINO1 Jun. - Dec. 2011, approx. 8200 pairs of values (blue dots) and simple equation hs = hs(v) (yellow line with triangles)

5. Measurement setup, measurement technology Section 5.1 describes the measurement setup with measurement concept and measurement points, and Section 5.2 describes the measurement technology with its measurement devices and the measurement procedure.

5.1 Measurement setup The measurement setup for the hydrophones and the accelerometers is shown below.

The core of the measurement setup are the hydrophones. Two hydrophones were set down on tripods on the seabed near the two systems AV04 and AV07 and connected to the system by a cable each. The hydrophones thus had a position of about 3 m above the sea floor. The planned distance to the plant was approx. 75 m and approx. 140 m, the actual distances are given below. Fig. 5.1.1 shows the measurement setup on the AV07 system.

The measurement setup on the AV04 system is correspondingly the same. The measurement setup on the AV04 system was functional for six months and could be evaluated. Measurements were taken with a third hydrophone at the FINO1 measuring station about 400 m away. In 2011, the hydrophone was also mounted on a tripod standing on the seabed and connected to FINO1 with a cable, see Fig. 5.1.1 in the box. According to measurements by the BSH, the actual distances of the three hydrophones to the next AV04 system were approx. 92 m, 159 m and 446 m (2011) and to the second closest system, which is the AV07 system, approx. 785 m, 791 m and 914 m (2011), see Table 6.1 for details.

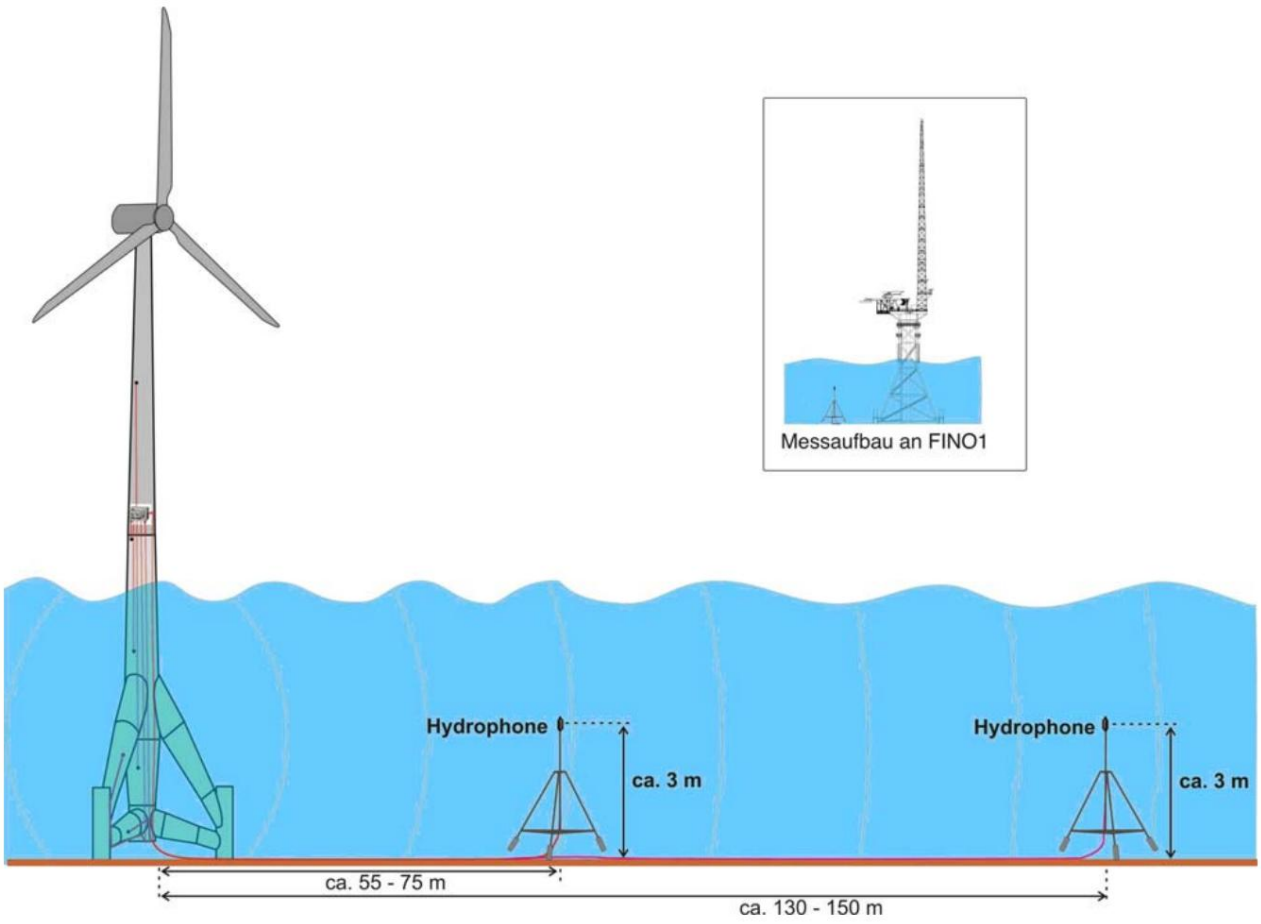

Fig. 5.1.1: Measurement setup. At the AV04 system, here the AV07 system is shown, two hydrophones on a tripod were anchored at a distance of approx. 75 m and 140 m (key figures for planning) on the seabed, 3 m above the seabed, water depth approx. 30 m In addition, acceleration sensors were installed in the foundation and tower. Box: Measurement setup on FINO1 with another hydrophone on a tripod (not to scale)

The structure of the accelerometers is shown below.
In order to record vibrations in the tower and in the foundation, acceleration sensors were installed from the inside and from the outside on the metal surfaces above and below the water on two systems.
With the method of coherent attachment, care was taken to ensure that the structure was not weakened by notch effects and that no electrical corrosion was provoked. For this purpose, among other things, metal bases were welded onto the AV07 system, to which the acceleration sensors were glued. The same applies to the fastening of the cables with regard to notch effects and corrosion. 2 sensors were installed above the water and 4 below the water on the AV04 plant, 4 above the water and 3 below the water on the AV07 plant, see Fig. 5.1.2 and Fig. 5.1.3.

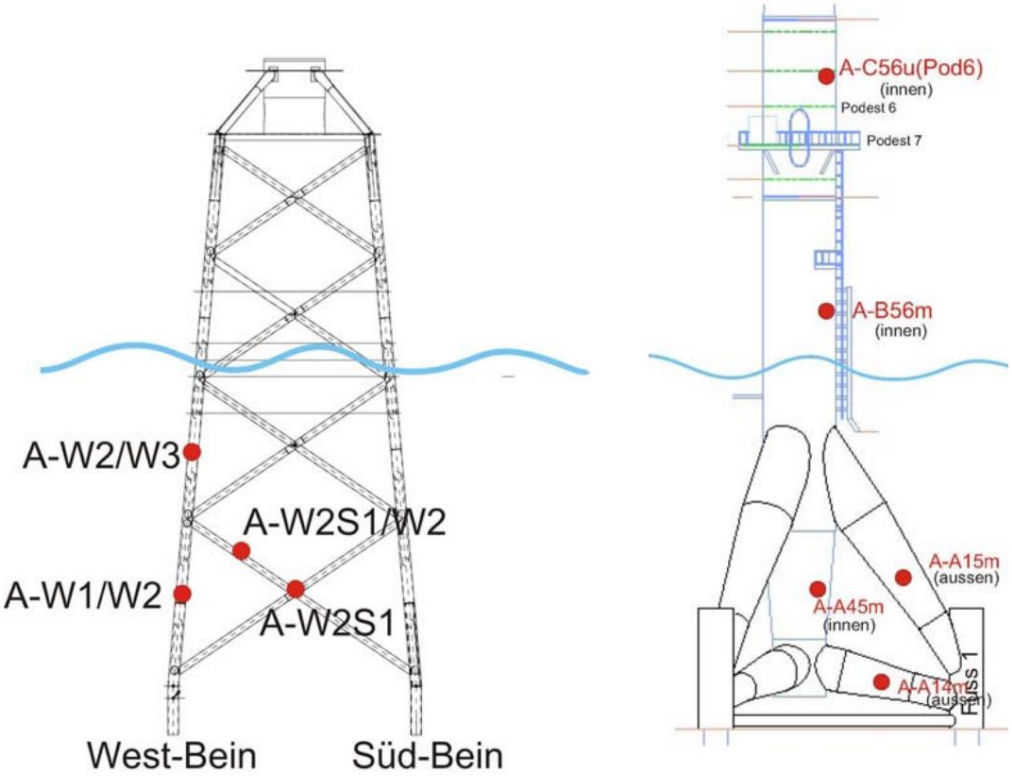

Fig. 5.1.2: Acceleration sensors on the systems, mainly under water: Left: on system AV04 Right: on system AV07 four sensors under water three sensors under water A-W2S1 at crossing A-A15m on upper crossbar on foot 1 A-W2S1 /W2 on strut A-A14m on lower cross brace on foot 1 A-W2/W3 on longitudinal beam A-AA45m in central tube A-W1/W2 on longitudinal beam two sensors above water A-C56u(Pod6)

A-B56m

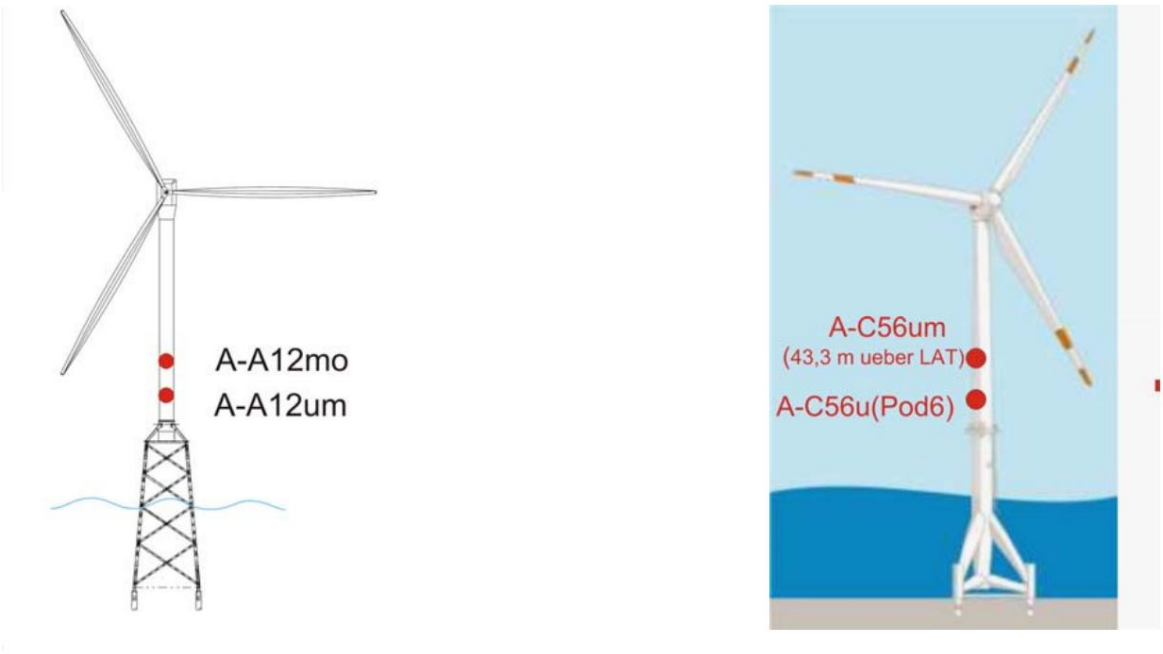

Fig. 5.1.3: Acceleration sensors on the systems AV04 left and AV07 right over water

5.2 Measurement technology

To measure the sound, 5 Brüel&Kjaer 8106 hydrophones with an integrated preamplifier were used, see Fig. 5.2.1. The nominal sensitivity was 2.24 mV/Pa corresponding to - 173 dB re 1V/ÿPa, the frequency range was 7 Hz to 80 kHz. The hydrophones each had their own power pack. The hydrophones were factory calibrated. Calibration certificates are available for each hydrophone.

The measuring chain was tested in the laboratory using the Bruel&Kjaer 4229 hydrophone calibrator including a coupler for the 8106 hydrophone. For practical reasons, the calibration of the measuring chain offshore in alpha ventus was not feasible and was not planned.

To measure the vibrations, 12 accelerometers of the type PCB/IMI Model 625B11 were used in the two plants, see Fig. 5.2.2 below. Six each were installed at each facility under and above water, see Fig. 5.1.2 and 5.1.3 above.

For data acquisition, 3 measuring systems with measuring computers (PXI measuring computer, Buffalo RAID network file server 500 GB, ANEL-LAN switchable plug connector) were used on site in the two systems and at FINO1, see Fig. 5.2.3. 24-bit A/D converters with a maximum sampling rate of 204.8 kHz were integrated.

The measuring computers were synchronized by GPS signals, see Fig. 5.2.4. The measurements of the three measuring computers began within a time window of T0 = ± 100 ns, with the sample time clocks being fixed in their phases. The synchronization enabled, among other things, correlation analyses.

The sampling of the measurement signals was 50 kHz. The measurement time was 300 s for all channels in parallel. The measurement times were chosen for 3 measurement periods per day (duration 5 minutes) in the rather non-work-intensive time at 4:00, 18:00 and 22:00 UTC. The measurement data was temporarily stored as a time series in the measurement computers on the local file servers. The data volume was 3 GB per day. The data was transported offline in blocks to the RAVE research archive via the RAVE data network. The capacity of the file server was designed for 500 GB, so that the data could be stored locally for several weeks if the network were to fail. The digitized data from all sensors were saved as uncompressed time series, so that all important variables such as sound level (Leq, Lpeak, etc.) and frequency spectra (third-octave, narrow-band spectra, etc.) could be calculated from the time series. The corresponding evaluation programs were written in LabView 8.5.

The procedure and procedures for data transmission through the network have been defined in the RAVE coordination body.

Sensoren

Hydrophone: Brüel & Kjaer 8106

Technical Data:

Sensitivity: -173dB re 1 V/µPa (±3dB)
Nominal Voltage Sensitivity: 2.24mV/Pa
Frequency Response (re 250Hz):
10 Hz to 10 kHz:+0.5/-3.0 dB
7 Hz to 30 kHz: +0.5/-6.0 dB
3 Hz to 80 kHz: +6/-10.0 dB
Dimensions: Length: 182 mm; Dia.: 32 mm
Weight: 382 g

Max. Output Signal:
12 V supply: 3.5V or 28mA
24 V supply: 7.0V or 28mA
Max. Power Output: 50mW
Output Impedance: <30Ω
High-Pass Filter 3 dB at 7Hz (±2Hz)
DC Ripple Rejection 20 Hz to 20 kHz: 70 dB
Overload Sound Pressure Level
12 V supply: 182 dB re 1 µPa
24 V supply: 188 dB re 1 µPa
Supply Voltage:12 to 24VDC
Power Consumption: 6mA without load

Fig. 5.2.1: Hydrophone von Brüel & Kjaer

Beschleunigungssensoren: PCB/IMI Model 625B11

Technical Data:

Ring-style, industrial, ceramic shear ICP® accel

Sensitivity: 100 mV/g (±5%) (10.2 mV/(m/s^2))

Frequency Range: 0.5 to 6500 Hz (±5%)

Frequency Range: 0.2 to 10500 Hz (±3dB)
Measurement Range:±50 g (±490 m/s^2)

Mounting: Through Hole

Fig. 5.2.2: Accelerometer

Messsystem:

Messrechner:
National Instruments PXI
1031 Chassis,
8105 Controller,
6682 Synchronisation,
2 x 4462 AD-Wandler
(Fino1: 1x4462)

Abtastrate: max. 204.8 kHz
AD-Wortbreite: 24 Bit
Analog-Kanäle: 8 (Fino1: 4)
Synchronisation: GPS-Signal

10 MHz Referenzoszillator:
Trimble Thunderbolt GPS disciplined clock

Fileserver:
Buffalo Terastation
2x 500 GB, Raid1

Hydrophon-Netzgerät:

3 x 18 Volt, je 110 mA
linear geregelt
(ExElec LM2 Module)
Restwelligkeit 1 mV_{pp}

Fig. 5.2.3 Measuring computer and accessories

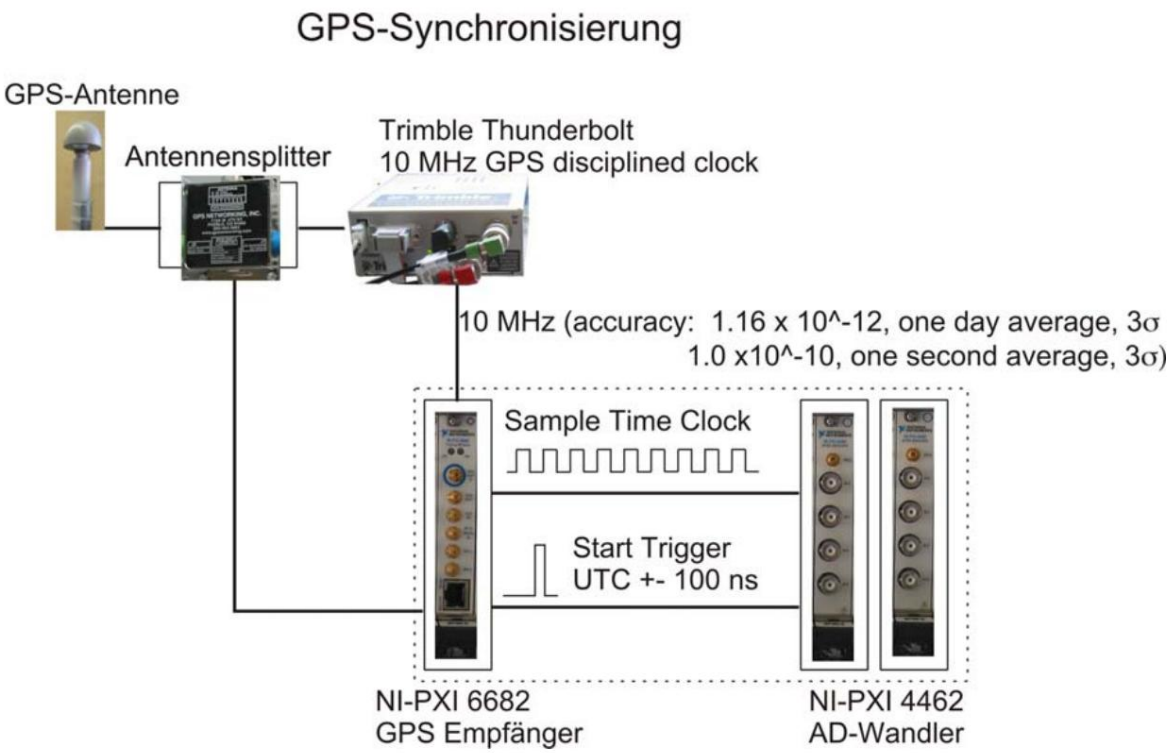

Fig. 5.2.4: GBS receiver and integration into the measuring system for synchronization

The hydrophones were permanently wired to a measuring computer with a hydrophone cable. Fig. 5.2.5 shows the type Hydrophone Cable Rawcable AC-0101 (JJ-0738, JP-0735) fully assembled and not installed.

Fig. 5.2.5: Hydrophone cable, ready-made

6. Installation, position

The installation of the measuring devices and the positions of the hydrophones are shown below.

6.1 Installation

The measuring equipment was installed on the AV04 system, the AV07 system and on FINO1.
Fig. 6.1.1 shows the deployment of a hydrophone on the AV04 by the BSH. Two hydrophones were installed at a distance of approx. 80 m and approx. 140 m west of the AV04 system. The hydrophone at FINO1 was operated in cooperation with DEWI. It was installed at a distance of about 100 m from FINO1.

The acceleration sensors on the tripod foundation of the AV07 system were already installed in Norway in August 2008 by DEWI. The BSH installed the acceleration sensors on the jacket foundation of the AV04 plant in Scotland in autumn 2009. Fig. 6.1.2 shows acceleration sensors. On the left is an accelerometer on the jacket construction of the AV04, on the right an accelerometer on the lower brace of the tripod construction of the AV07. For the installation, cylindrical intermediate bodies made of metal were previously welded onto the metal body of the foundation construction, to which the sensors were glued. The intermediate bodies were required in order to avoid notch effects caused by direct hole drilling. To protect against corrosion, the sensors and fuses could only be bonded with an electrically insulated screw.
Fig. 6.1.3 shows a measuring computer and the other measuring equipment installed at sea on the AV04 system (photo: BSH). In a similar way, measuring computers and other measuring equipment were installed on the AV07 facility and on FINO1.
Fig. 6.1.4 shows the deployment of the hydrophone frame used in 2010 at FINO1.

Fig. 6.1.1: Deposition of the hydrophone at the AV04 system (Photo: BSH)

Fig. 6.1.2: Acceleration sensors on the foundation of the AV04 (left photo, source BSH) and on the lower brace of the foundation of the AV07 (right photo, source DEWI)

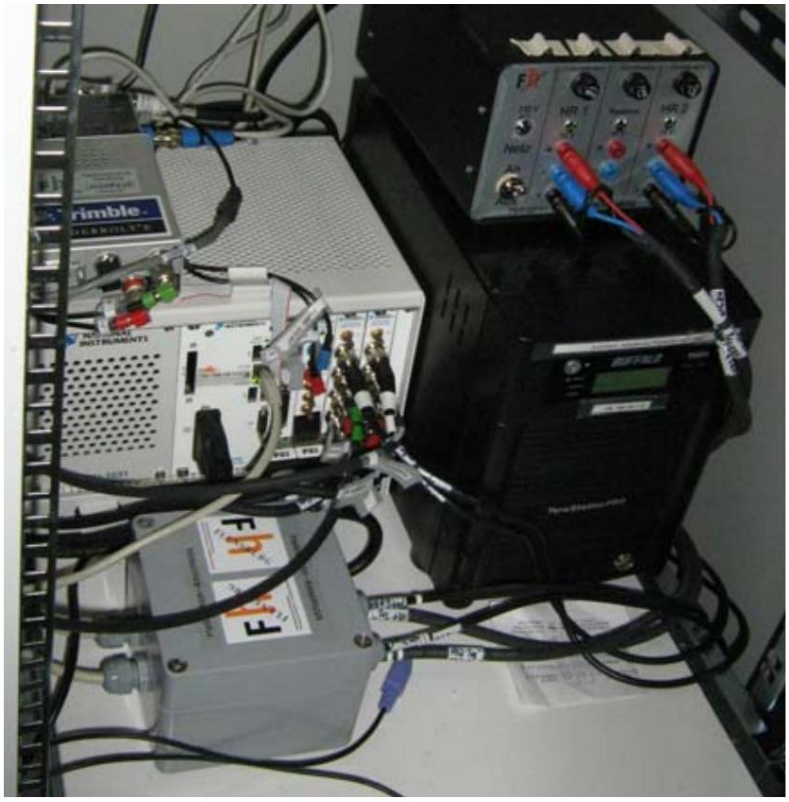

Fig. 6.1.3: Measuring computer and measuring equipment on AV04 (Photo: BSH)

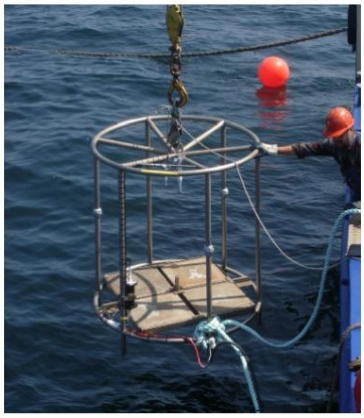

Fig. 6.1.4: Hydrophone frame, originally used on FINO1 (Photo: BSH)

6.2 Positions

In May 2010, the position of the two hydrophones (R4-HR1, R4-HR2) west of the AV04 facility was checked using a sonar measurement. In Fig. 6.2.1, the AV04 system can be seen as a white or black shadow in the sidescan. The positions of the hydrophones were measured by the BSH according to length and width in WGS84 and entered on maps, see Fig. 6.2.2, Fig. 6.2.3 and Fig. 6.2.4.
With the online tool from the geodata center (2012), the coordinates were converted into the UTM32 coordinate system, which is very similar to the Gauss-Krüger system and is increasingly used in land surveying. The coordinates of the hydrophones and the distances to the two closest systems as well as the coordinates of all other systems are shown in Tab. 6.2.1. The attenuation due to the distance (transmission loss, see below), which was calculated as a good approximation according to TL = 15.log (r), is also given. Due to the distances, every other system has at least 4 dB less sound input to the three hydrophones. For the coordinates of the facilities see also RAVE (2012).

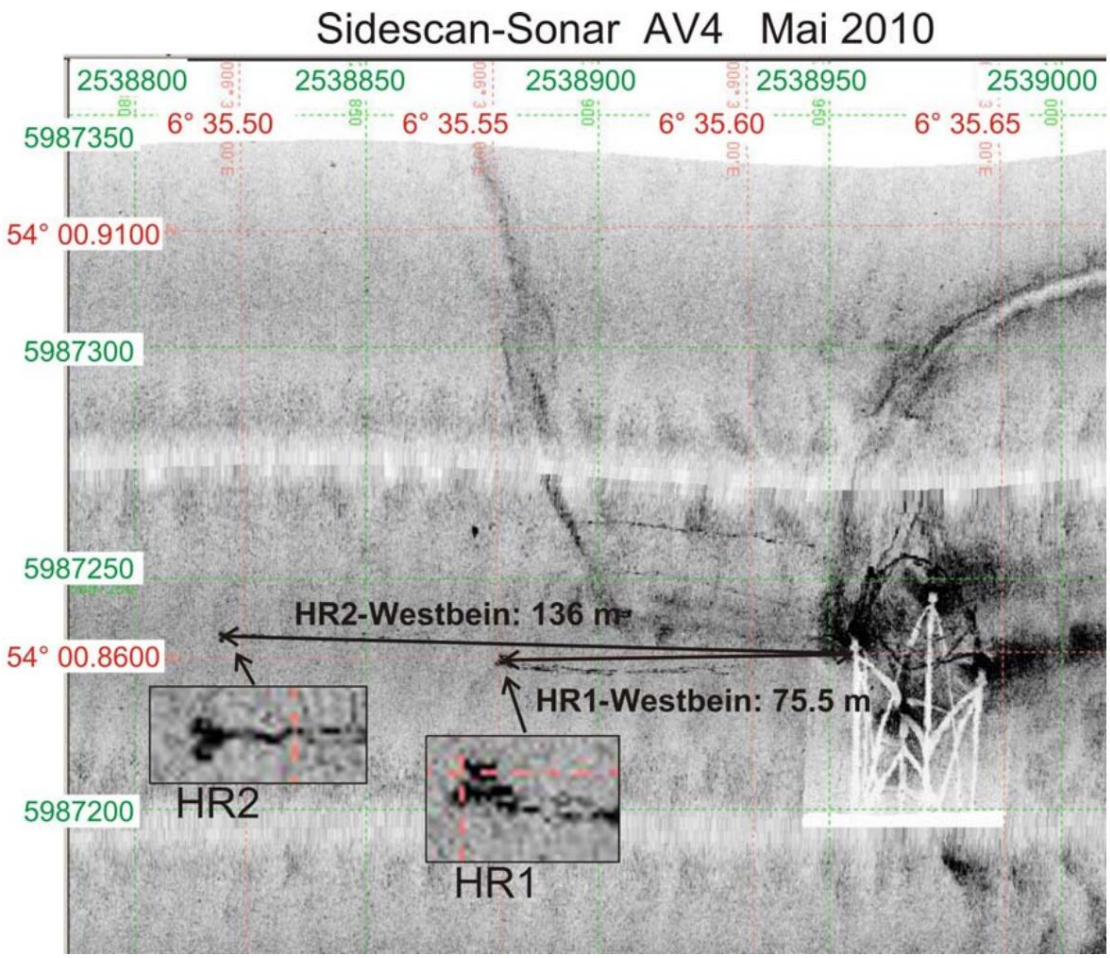

Fig. 6.2.1: Position of the 2 hydrophones (R4-HR2, R4-HR1) west of the AV04 facility (white and black shadow, designation HR2, HR1) in the first measurement period 2010, sonar sidescan in May 2010 coordinate systems WGS84 (length, width, red) and Gauss-Krüger (meter, green)

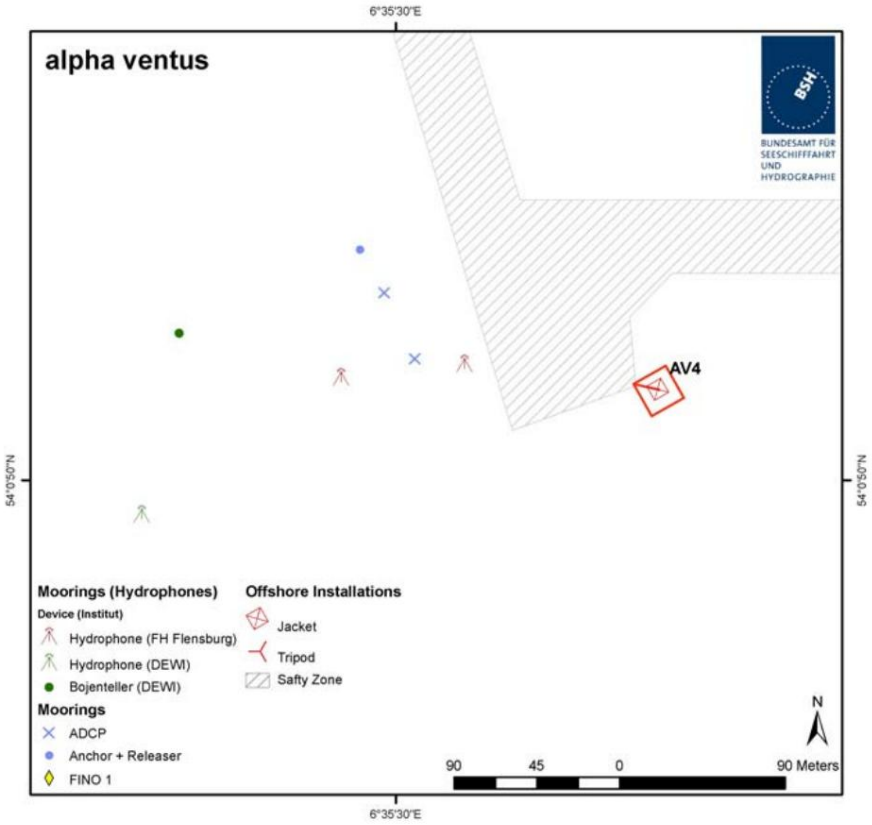

Fig. 6.2.2: Position of the two hydrophones (R4-HR1 and R4-HR2) west of the AV04 facility (AV04 = AV4)

Map BSH

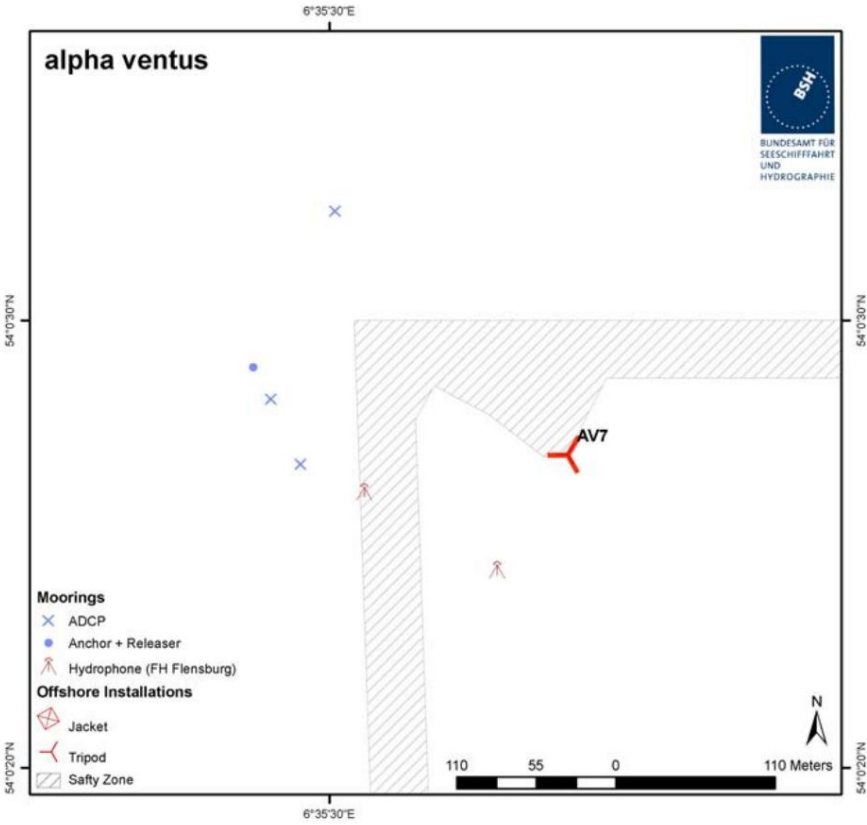

Fig. 6.2.3: Position of the 2 hydrophones (M7-HM1 and M7-HM2) west of the AV07 facility (AV07 = AV7)

Map BSH

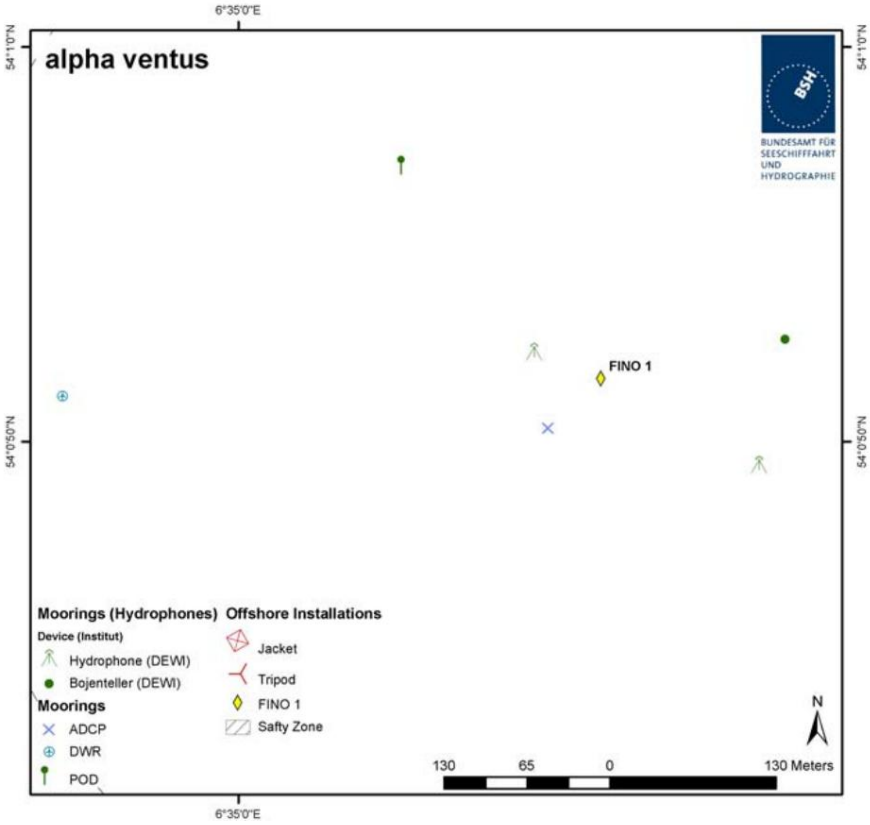

Fig. 6.2.4: Position of one hydrophone (F1-H8106-2) in 2011 and (F1-H8106) in 2010 on FINO1 map BSH

2010/2011	coordinates	UTM32	Distance TL Distance TL Distance AV04	AV04 AV07 AV07			R4-HR1 (2011)	TL
Hydro	Easting x Northing y Easting	Northing	[m]	[dB]	[m]	[dB]	[m]	[dB]
facility. R4-HR1 (2010)	342.257	5.987.796	75	28	765	43		
Hydro. R4-HR2 (2010)	342.196	5.987.796	136	32	775	43		
Hydro. F1-H8106 (FINO1, 2010)	342.063	5.987.737	275	37	755	43		
Hydro. R4-HR1 (2011)	342.241	5.987.813	92	29	785	43	0	
Hydro. R4-HR2 (2011)	342.174	5.987.808	159	33	791	43		
Hydro. F1-H8106-2 (FINO1, 2011)	341.887	5.987.828	446	40	914	44		
Hydro. M7-HM1	342.291	5.986.956	840		93			
hydro. M7-HM2 **plant**	342.201	5.987.014	793		142			
AV04 west leg	342.332	5.987.796	0		761		92	29
Appendix AV07	342.341	5.987.035	761		0		785	43
Appendix AV01	342.351	5.988.612					806	44
Appendix AV05	343.191	5.987.767					950	45
Appendix AV02	343.192	5.988.584					1223	46
Appendix AV08	343.189	5.987.006					1245	46
Appendix AV10	342.336	5.986.237					1579	48
Appendix AV06	343.984	5.987.740					1744	49
Appendix AV11	343.188	5.986.208					1863	49
Appendix AV03	343.978	5.988.557					1889	49
Appendix AV09	343.990	5.986.979					1937	49
Appendix AV12	343.996	5.986.181					2397	51
FINO1 Mast	341.941	5.987.806						

Tab. 6.2.1: Coordinates of the hydrophones and connection to wind farms with spatially closest systems AV04 and AV07 (coordinate system UTM32, similar to Gauss-Krüger), supplemented by all systems, distances in meters and sound attenuation Transmission Loss TL = 15. log(r / 1m) given in dB

7. Evaluation

The evaluation of the measurements that could be carried out in this project is presented below. The measurement times and viewing of the data, mean sound level Leq and peak level Lpeak, percentiles, third-octave analyses, narrow-band analyzes of the sound and acceleration signals, coherence and transfer functions are shown. Sound sources are assigned.

7.1 Measuring times,

viewing The measuring times and viewing of the data are presented below.

The following measurement times could be evaluated: 10
Sep. 2010 - Oct 6, 2010 27 days, Jul 20, 2011
- Dec 16, 2011 138 days.

The measurement positions of the hydrophones and their names in the diagrams are given in Table 7.1.1 below. listed, see also Tab. 6.2.1.

Coordinate System UTM32 Year Designation Easting Hydrophone 1 at	Northing
AV04 2010 R4-HR1 342.257 Hydrophone 2 at AV04 2010 R4-HR2	5.987.796
342.196 Hydrophone FINO1 2010 F1-H8106 342.065 Hydrophone 1 at	5.987.796
AV04 2011 R4-HR1 342.241 Hydrophone 2 at AV0 4 2011 R4-HR2	5.987.736
342.171 Hydrophone FINO1 2011 F1-H8106-2 341.887	5.987.813
	5.987.808
	5.987.828

Tab. 7.1.1: Position of the hydrophones

All sound data had to be viewed, ie a selection had to be made. The control of the sound data is very complex. The authors listened to and looked at all of the time series in order to identify clear background noise and sort out these measurement series from the evaluation.
Unambiguous and easily identifiable disturbing noises are pile driving, see Section 7.8, from the construction areas for the offshore wind farms Borkum West II and BARD Offshore 1, which are approx. 7 km and 50 km away removed by culling.

In the next step, the frequencies below 10 Hz and above 3.0 kHz were removed using a bandpass filter. Low-frequency pressure fluctuations were identified as disturbances, which were detected as pseudo-sound, and high-frequency signals were identified as electromagnetic radiation.
This filtering is justified by the spectra, see Section 7.4, which show that the main part of the sound energy is preserved in the frequency range examined.

7.2 Leq time series, peak time series, effect of the band filter, Leq-5s, mean values The following is an overview of all measurement data from 2011 and 2010 as time series in their development of processing by selection. In order to document the selection, the time series that have not yet been selected are shown first, then the time series after the selection, then the time series after bandpass filtering. Finally, the differences in dB generated by the bandpass filtering are shown.

Furthermore, the mean sound levels are shown averaged over the shorter time of 5 seconds in order to get a quantitative impression of the greater spread of the mean values due to the shorter averaging time.

Finally, mean values of the Leq and peak values for 2011 and 2010 are given.

In Fig. 7.2.1 the time series in 2011 of the unfiltered (no bandpass) 300s-Leq and peak values from all 3 hydrophones are shown. From the end of October to the beginning of November there is a data gap due to a complete system failure. In the following evaluation, the result will be that the continuous sound level Leq averaged over 300 seconds (5 minutes) for all 3 hydrophones (empty symbols) averaged energetically over the entire time is 118 dB re 1ÿPa, the peak level Lpeak is 17 dB higher. The unfiltered values of all measurements are shown in Fig. 7.2.1, the dB values are somewhat higher.

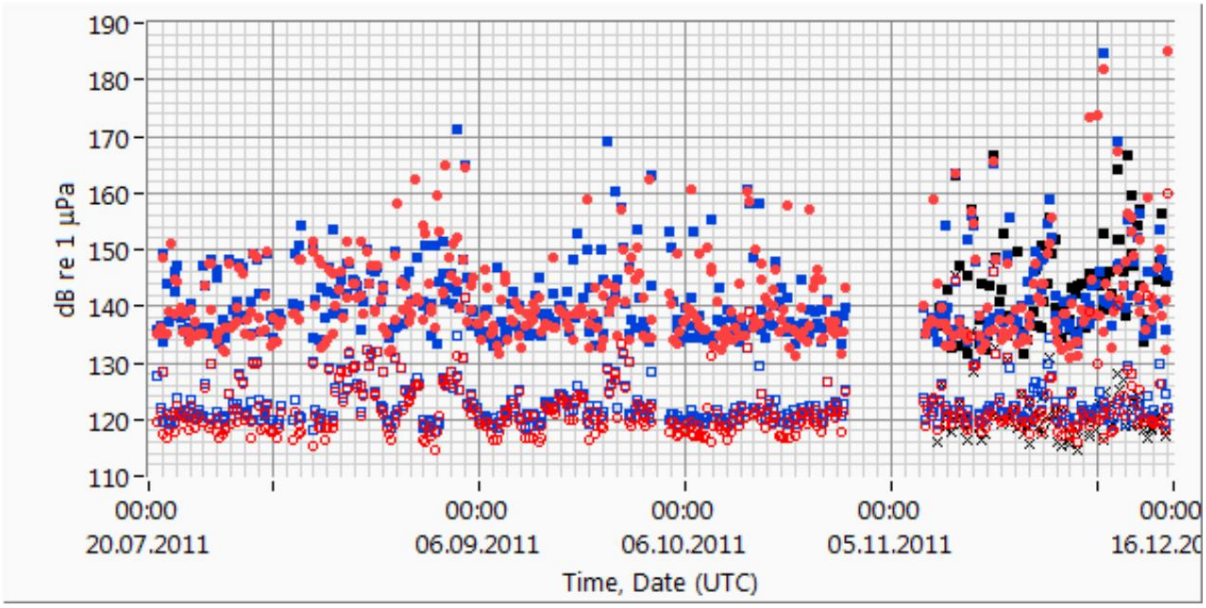

Fig. 7.2.1: Leq (empty symbols), Lpeak (solid symbols), 2011, all hydrophones, all data, unfiltered Leq: R4-HR1: red empty circles, R4-HR2: blue empty squares, F1-H8106- 2: black crosses Peak values: R4-HR1: red filled circles, R4-HR2: blue filled squares, F1-H8106-2: black filled squares

In the next step, the series of measurements (duration 300 s) that have acoustic or electrical noise are removed. Selected, non-bandpass filtered 300s-Leq and peak values 2011 of all three hydrophones are shown in Fig. 7.2.2. The scatter is less than in the figure above, the dB levels hardly drop.

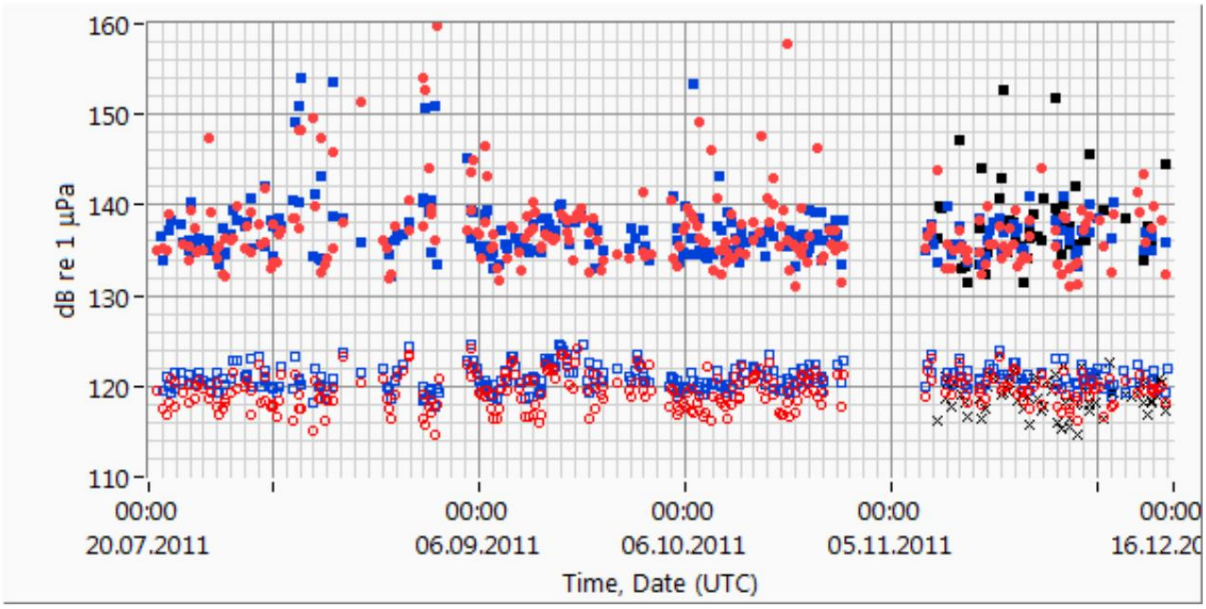

Fig. 7.2.2: Leq, Lpeak, 2011, all hydrophones, selected, not filtered Leq: R4-HR1: red open circles, R4-HR2: blue open squares, F1-H8106-2: black crosses Peak values: R4 -HR1: red filled circles, R4-HR2: blue filled squares, F1-H8106-2: black filled squares

In the next step, see Fig. 7.2.3, the selected measurement series 300s-Leq and peak values 2011 are filtered with the bandpass (10 Hz - 3 kHz). All hydrophones are shown. The scatter and the dB levels drop somewhat.

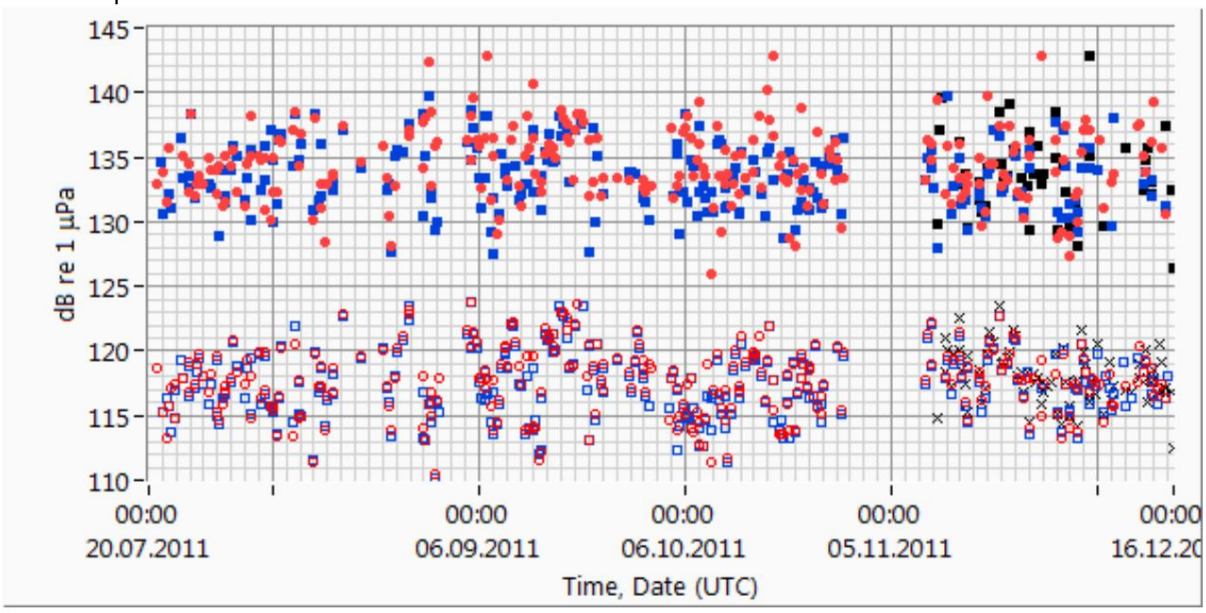

Fig. 7.2.3: Leq, Lpeak, 2011, all hydrophones, selected, filtered Leq: R4-HR1: red open circles, R4-HR2: blue open squares, F1-H8106-2: black crosses.
Peak values: R4-HR1: red filled circles, R4-HR2: blue filled squares, F1-H8106-2: black filled squares

Bandpass filtering is justified. In order to get a quantitative impression of how many dB the bandpass filtering reduces, the differences between the selected unfiltered measurement series and the selected bandpass-filtered 300s-Leqs from 2011 are shown in Fig. 7.2.4 for all hydrophones. The Leq values drop by a few dB due to bandpass filtering.

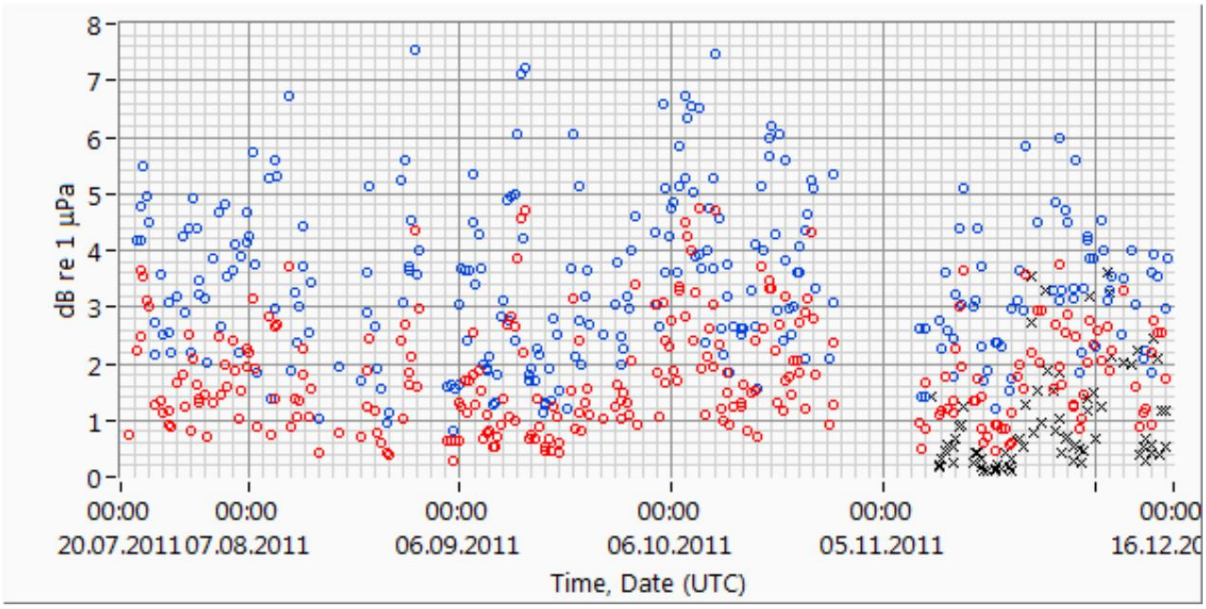

Fig. 7.2.4: Difference Leq by bandpass filtering R4-HR1: red empty circles, R4-HR2: blue empty squares, F1-H8106-2: black crosses

As expected, the difference between the peak values and the mean values Leq is greater due to the bandpass filtering, see Fig. 7.2.5. From the selected series of measurements, the differences between the unfiltered and the bandpass filtered 300s peak values 2011 for all hydrophones are shown. Individual values with a negative difference are not shown. Their magnitude is insignificant and less than 1 dB in magnitude. The cause lies in the phase shift caused by the filtering, see above, and has no relevance to the sound.

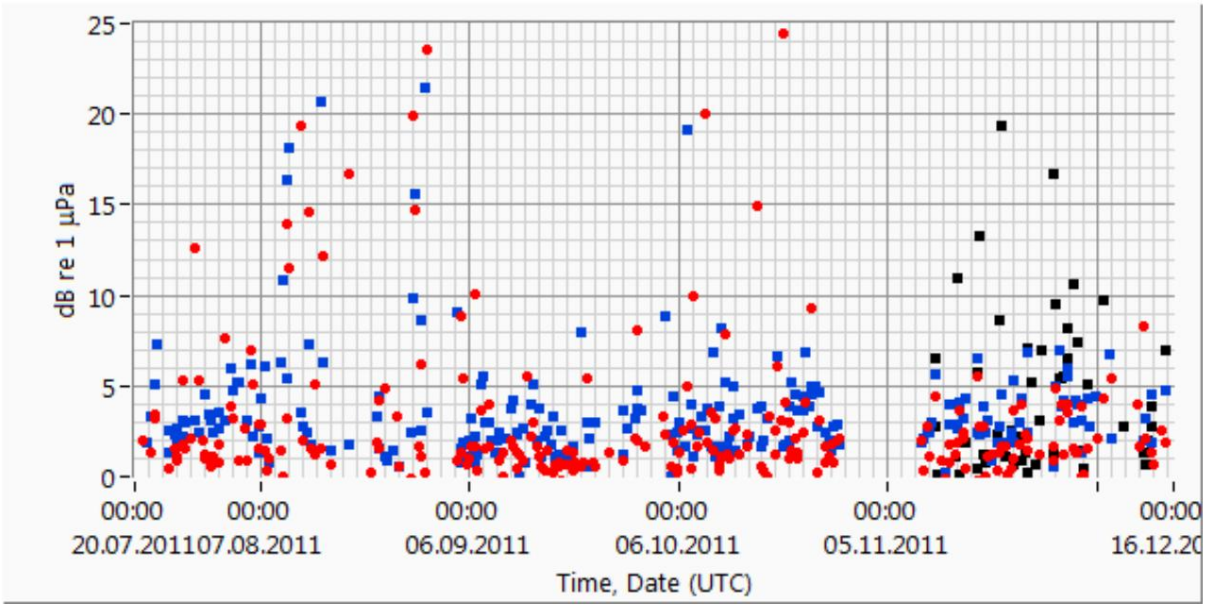

Fig. 7.2.5: L-peak difference by filtering, all hydrophones, 2011 R4-HR1: red filled circles, R4-HR2: blue filled squares, F1-H8106-2: black filled squares

The processing of the measurement data for data from 2010 shown above is shown below.
Fig. 7.2.6 shows an overview of all measurement data from 2010 as a time series. Shown are the unfiltered (no bandpass) 300s Leq and Peak values from all three hydrophones (R4-HR1, R4-HR2 and F1-H8106). The continuous sound level Leq averaged over 300 seconds is constant for all 3 hydrophones (empty symbols) just under 120 dB re 1ÿPa, the peak level is approx. 20 dB higher.

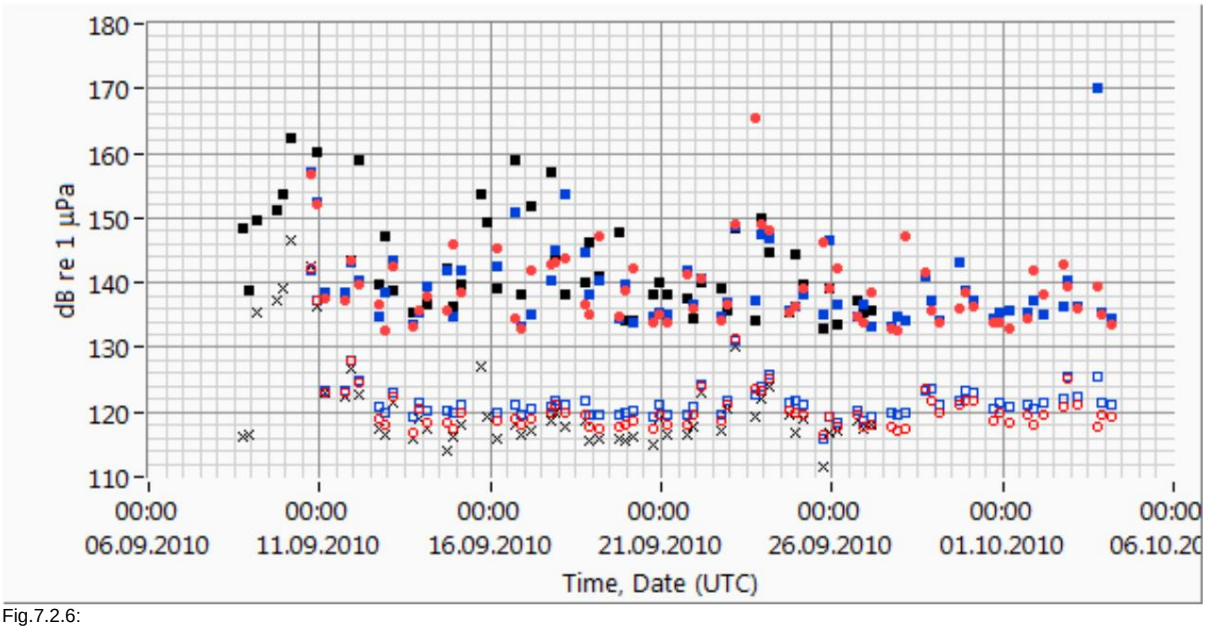

Fig.7.2.6:

Leq: R4-HR1: red empty circles, R4-HR2: blue empty squares, F1-H8106: black crosses Peak values: R4-HR1: red filled circles, R4-HR2: blue filled squares, F1-H8106: black filled squares

In the next step, the measurement series that have acoustic or electrical noise are removed. Fig. 7.2.7 shows selected, non-bandpass filtered 300s Leq and peak values from 2010 for all three hydrophones. The scattering becomes smaller and the level sinks.

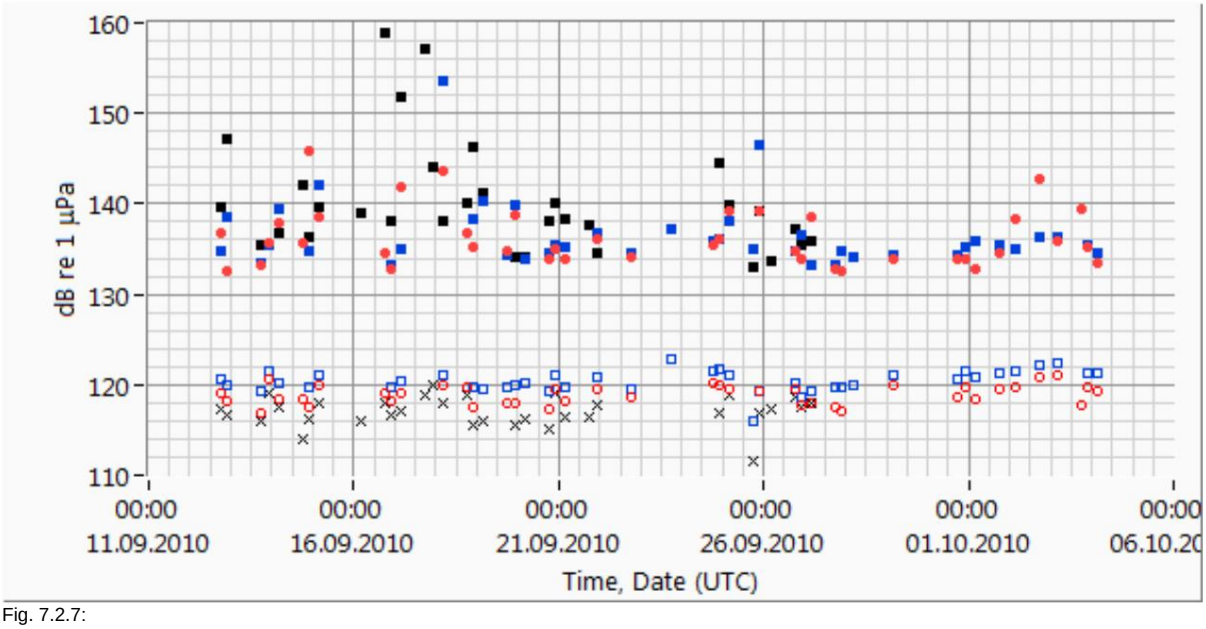

Fig. 7.2.7:

Leq: R4-HR1: red empty circles, R4-HR2: blue empty squares, F1-H8106: black crosses Peak values: R4-HR1: red filled circles, R4-HR2: blue filled squares, F1-H8106: black filled squares

In the next step, see Fig. 7.2.8, the selected measurement series 300s-Leq and peak values from 2010 are displayed filtered with the bandpass (10 Hz - 3 kHz) for all hydrophones. The scatter and the level decrease somewhat.

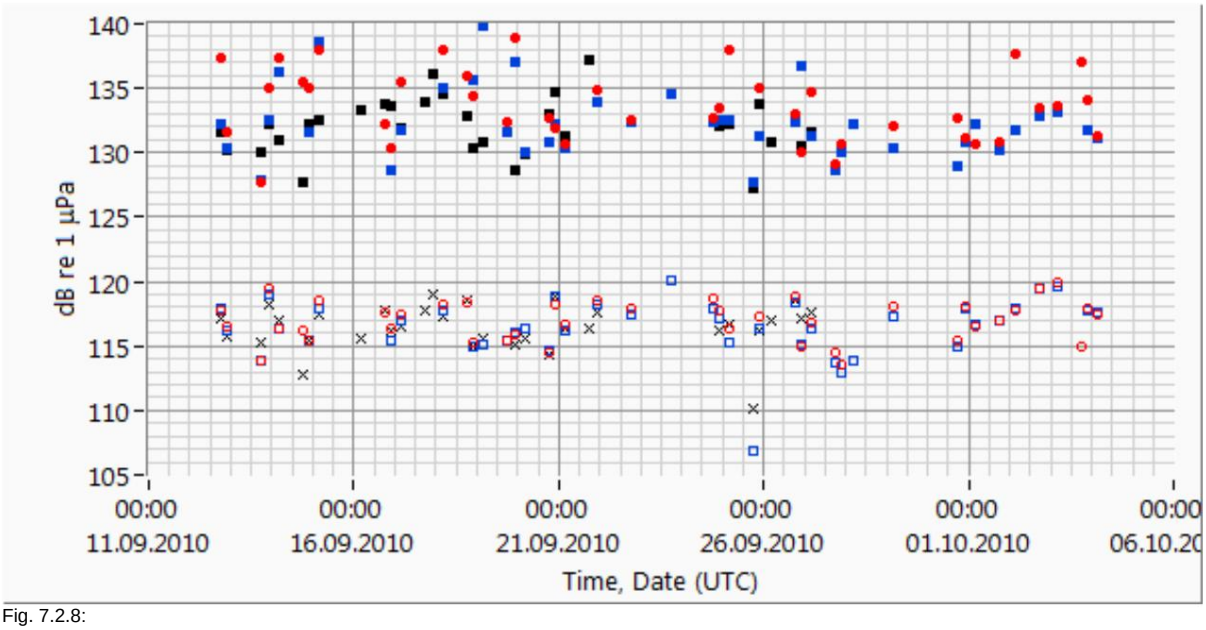

Fig. 7.2.8:
Leq: R4-HR1: red empty circles, R4-HR2: blue empty squares, F1-H8106: black crosses Peak values: R4-HR1: red filled circles, R4-HR2: blue filled squares, F1-H8106: black filled squares

Bandpass filtering is justified. In order to provide quantitative evidence of how many dB attenuation the filtering generates, the difference between the unfiltered selected measurement series and the band-pass filtered selected 300s-Leqs from 2010 is shown in Fig. 7.2.9 for all hydrophones. The Leq value drops by a few dB as a result of the bandpass filtering.

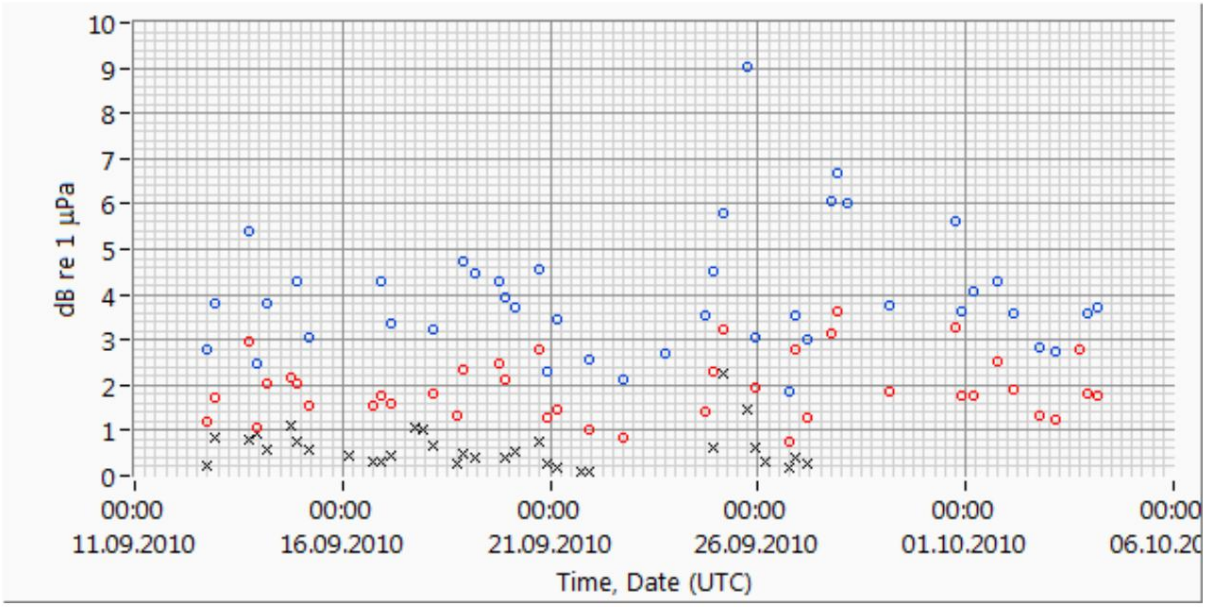

Fig. 7.2.9: Difference Leq by filtering R4-HR1: red
empty circles, R4-HR2: blue empty squares, F1-H8106: black crosses

As expected, the difference in the peak values is greater due to the bandpass filtering. Fig. 7.2.10 shows the differences between the unfiltered and the bandpass filtered 300s peak values from 2010 for all hydrophones from the selected series of measurements. A few individual values with a negative difference that are less than 1 dB are not shown. The cause lies in the phase shift caused by the filtering, see above, and has no relevance for the sound.

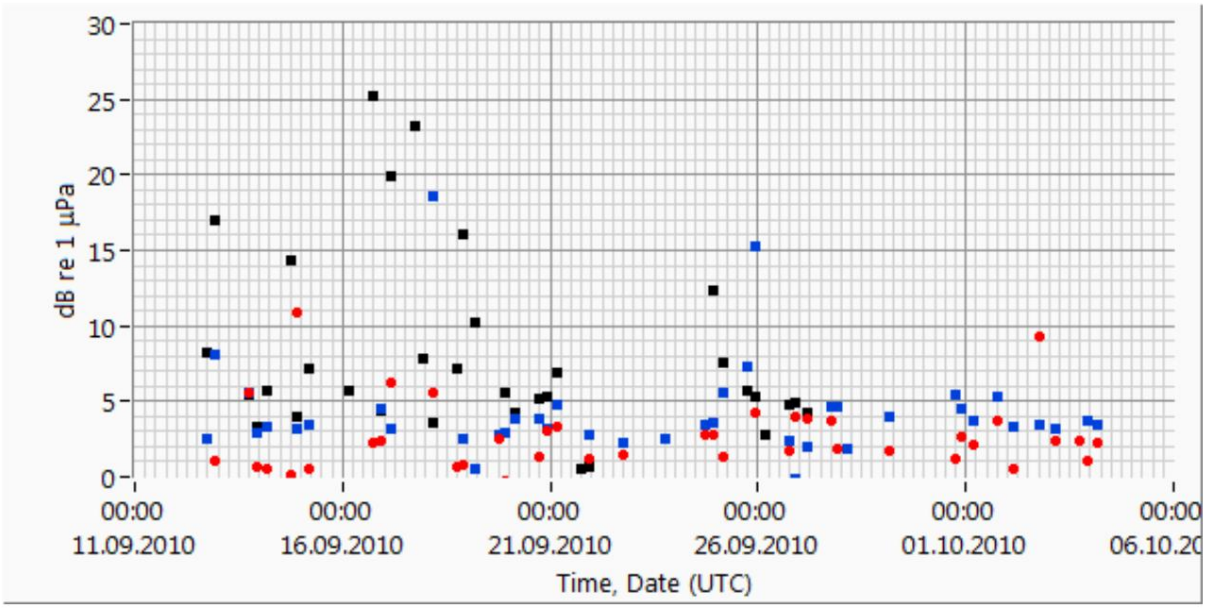

Fig. 7.2.10: L-peak difference by filtering R4-HR1: red filled circles, R4-HR2: blue filled squares, F1-H8106: black filled squares

Below, see Fig. 7.2.11, the mean sound level Leq is shown as a time series over a 5-second averaging period for all three hydrophones in 2011. For comparison, Fig. 7.2.12 shows the mean sound levels Leq averaged over 300 seconds for the same period under the same conditions (same selection of measurement series, band filter 10Hz-3kHz). As expected, the spread of the 5s-Leq is greater than the spread of the 300s-Leq, but the range, i.e. the maximum and the minimum, is only slightly more extreme. A closer look at the 5% percentile and the 95% percentile shows the same weak widening.

Fig. 7.2.13 shows the continuous sound level Leq and its percentiles L95, L50, L5 for all three hydrophones for 5 seconds of measurement series from 2010 with a bandpass of 10 Hz – 3 kHz. The scatter of the L95 and L5 values is not very pronounced, also compare 300 second series of measurements from 2010 in Fig. 7.2.8 above.

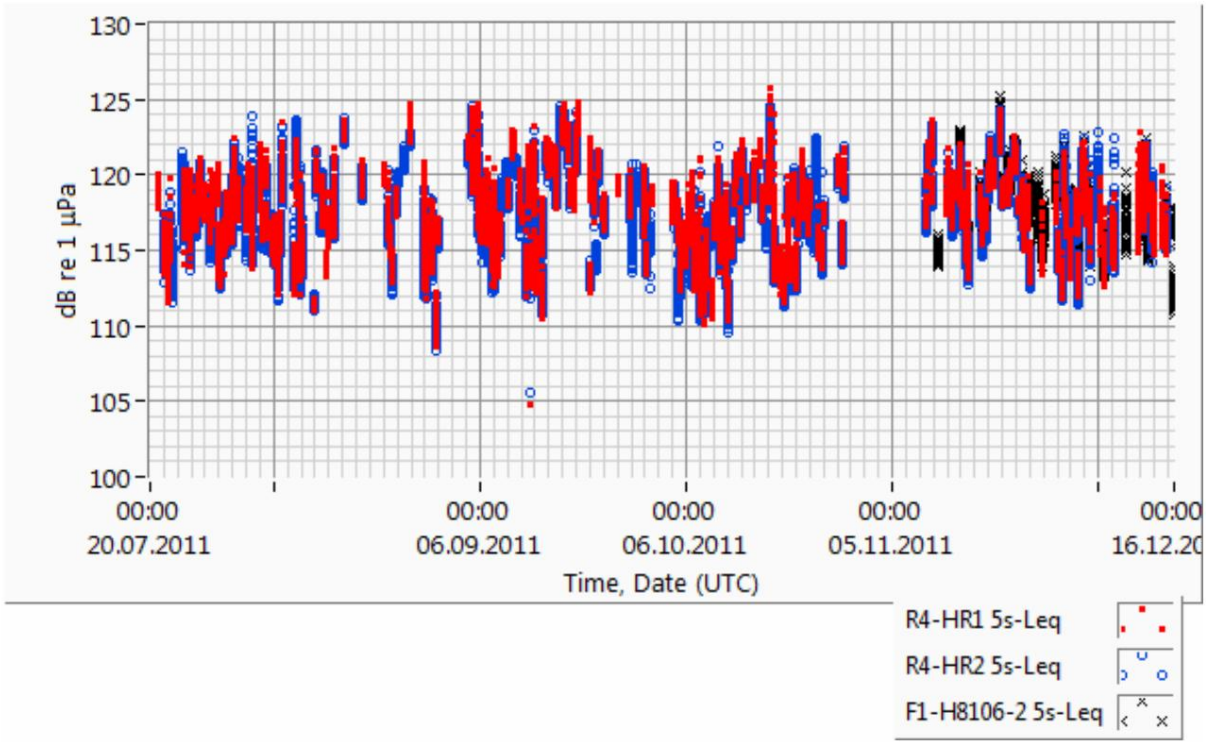

Fig. 7.2.11: 5s-Leq, 2011, Leq over 5 s, all hydrophones

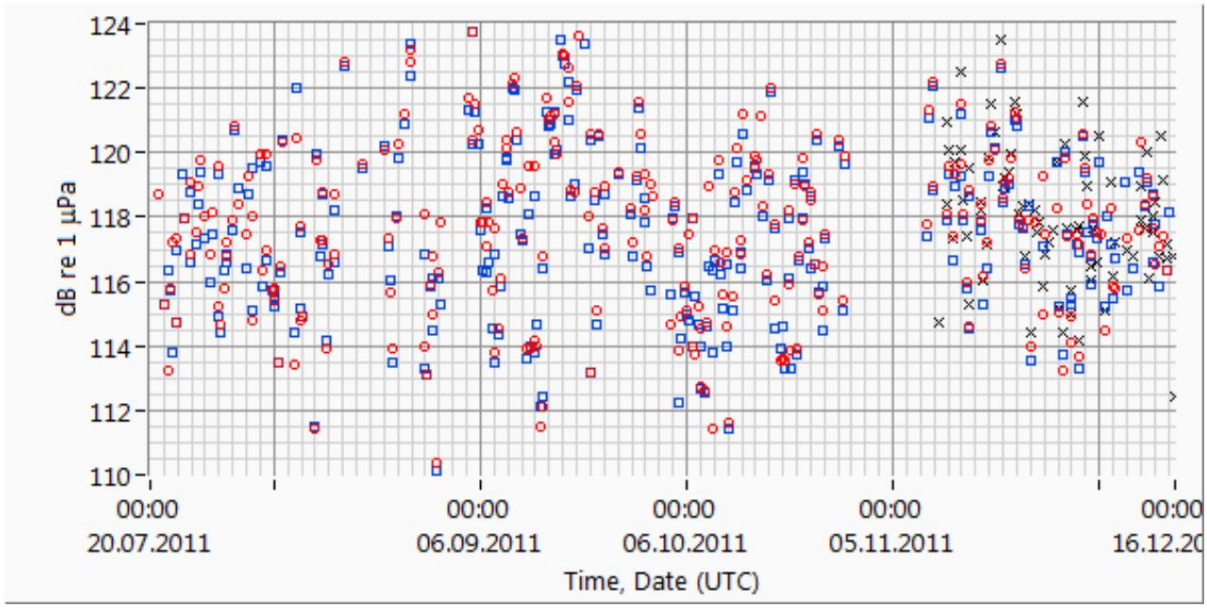

Fig. 7.2.12: 300s-Leq, 2011, Leq over 300 s, all hydrophones Red circles R4-HR1, blue squares R4-HR2, black crosses F1-H8106-2

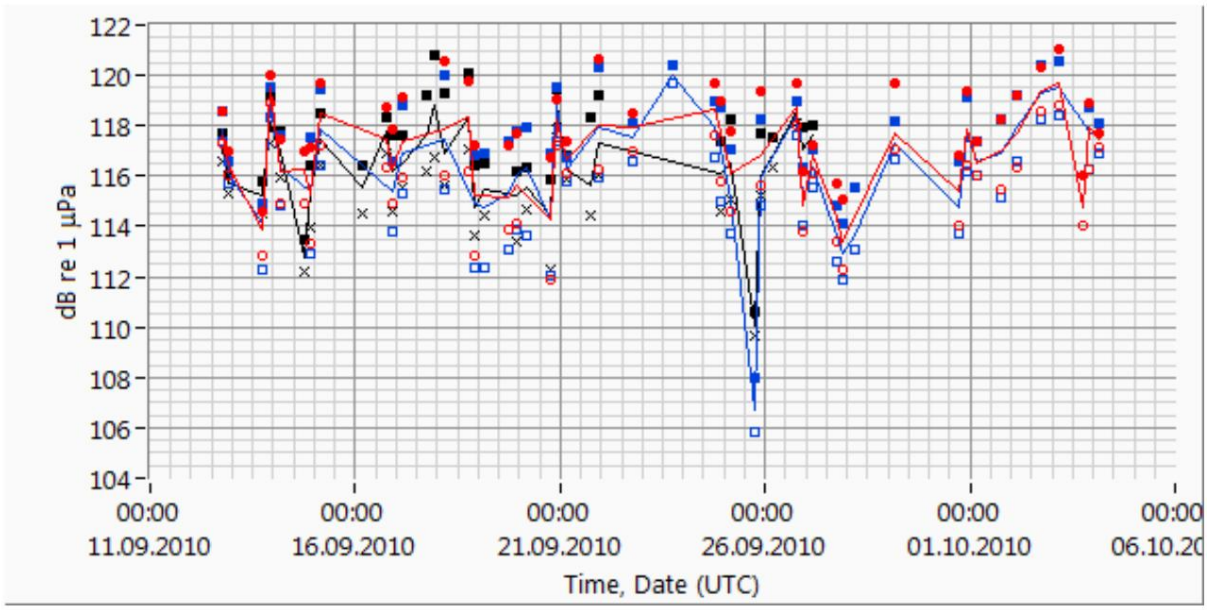

Fig. 7.2.13: Leq 5 s, percentile, all 3 hydrophones, bandpass 10Hz-3kHz, 9 measurement curves, 2010 3x L50 (median) without symbols, red R4-HR1, blue R4-HR2, black F1-H8106 (middle) 3x L5 full symbols, red circles R4-HR1, blue squares R4-HR2, black squares F1-H8106 (top) 3x L95 empty symbols, red circles R4-HR1, blue squares R4-HR2, black crosses F1-H8106 (bottom)

Finally, mean values for Leq and Lpeak values for 2011 and 2010 are given.
The time series for the measurement periods 2011 and 2010 show that the fluctuations are surprisingly small. As an overview of the measured sound levels, the mean values of the continuous sound values Leq and the peak values Lpeak averaged over all measurements are given, separated according to 2010 and 2011, separated according to the hydrophones, as physically meaningful energetic mean values, see Table 7.2.1, and additionally as arithmetic mean values, see Table 7.2.2, which are surprisingly slightly lower. The Leq values of the three hydrophones are almost the same, so that no distance effect can be demonstrated by the AV04 system. It must be proven that the wind farm became louder from 2010 to 2011, with all disturbing noises that were reliably identified being removed.

Energetic mean values		**Leq**		Lpeak	
[dB re 1ÿPa]		2010	2011	2010	2011
AV04 Hydro. 1	R4-HR1	117,23	**118,43**	134,49	135,44
AV04 Hydro. 2	R4-HR2	116,89	**118,21**	133,21	134,24
FINO1 Hydro.	F1-H8106-2	116,71	**118,52**	132,59	134,86

Tab. 7.2.1: Energetic mean values Leq and Lpeak over 2010 and 2011

Arithmetic means		Leq		Lpeak	
[dB re 1ÿPa]		2010	2011	2010	2011
AV04 Hydro. 1	R4-HR1	116,69	117,69	133,64	134,48
AV04 Hydro. 2	R4-HR2	116,43	117,45	132,24	133,51
FINO1 Hydro.	F1-H8106-2	116,41	118,02	132,07	133,60

Tab. 7.2.2: Arithmetic mean values Leq and Lpeak over 2010 and 2011

In the following sections, the sound values are presented according to various parameters.

7.3 Leq arranged over v, hs, P and n, Lpeak over P In
the following, all continuous noise levels Leq from 2011 and 2010 from all three hydrophones are presented over different sizes in order to show their dependencies. The ordering variables are wind speed v, wave height hs and power P. To keep track of who is using the 300s-Leq. Only the selected measurement series recognized as valid are used, i.e. those without background noise.

Fig. 7.3.1 shows all Leq values (300 s) from 2011 and 2010 of all hydrophones over the wind speed. The wind speed was measured in 2011 at hub height on the nacelle of the AV04 system and in 2010 on FINO1 at a height of 100 m. It was to be expected that the noise level would increase with the wind speed and thus with the power of the turbines, as can be found in airborne noise. Here under water, the sound level decreases with increasing wind speed. The reason is that the sound is essentially not determined by the equipment but by the background noise. The background noise is generated partly by natural noise and mainly by ship noise. The background noise is of the same order of magnitude as the turbine noise, or to put it another way, the turbines are as quiet or as loud as the background noise in the North Sea. This statement is substantiated by the following diagrams.

This relationship becomes even clearer when the sound level is plotted against the significant wave height hs given in m measured at the FINO1 station, see Fig. 7.3.2. The sound level drops from a wave height of 2 m. The turbines themselves are not getting any quieter, the noise level on the sea floor is increasing due to the waves (Urban 2002 p. 221 ff), but the reason for the decrease is, on the one hand, that the service boats in the wind farm are no longer used at these wave heights because they can no longer moor at the facilities, and secondly, because the sound transmission of the ships in the traffic separation schemes 14 km away is dampened by more air bubbles entering at higher waves, see third-octave and spectral analyzes Sections 7.4 and 7.5 and verification by Wille (1988) Section 7.8 .3.

Fig. 7.3.3 shows the dependency on the total output of the wind farm. It shows that the decrease in noise noted above is not due to downtimes or reduced performance of the systems. The total output is the sum of all 12 plants in percent, where 100% is defined as the nominal output of the park here with 12 times 5 MW. Rated power is also called full load. An accumulation of the measuring points can be seen under full load, which was often reached. It can be seen that the wind farm tends to be quieter at full load than at standstill, which is shown as 0% power. The latter represents the background noise with little wind (0 to approx. 4 m/s).

Fig.7.3.4 shows the sound levels over the output of the AV04 system in %. The facility is spatially the closest facility to the hydrophones, in particular to the hydrophones R4-HR1 and R4-HR2. Here, too, it can be seen that at a distance of approx. 100 m from the system, the underwater noise level is lower at full load than at standstill.

Fig. 7.3.5 shows the sound level over the output of the AV07 system in %. The system is spatially the closest system of type AV07 to the hydrophones. The hydrophones are about 800 m apart.
Here, too, it can be seen that the level is lower at full load than at standstill.

Fig. 7.3.6 shows the peak level Lpeak of all measurements (all hydrophones 2011 and 2010) over the total output of the park in %. The same picture emerges as with the continuous noise level Leq over the total output, but at a level that is approx. 16 dB higher. The peak level is also not dependent on the performance of the farm.

All other evaluations of the peak sound level not shown here using the above parameters confirm the similar behavior of the peak level relative to the continuous sound level.
Other evaluations of the average sound level Leq over the performance of the AV01 system, identical in construction to AV04, which are not shown here, confirm the statements on the analyzes presented here.

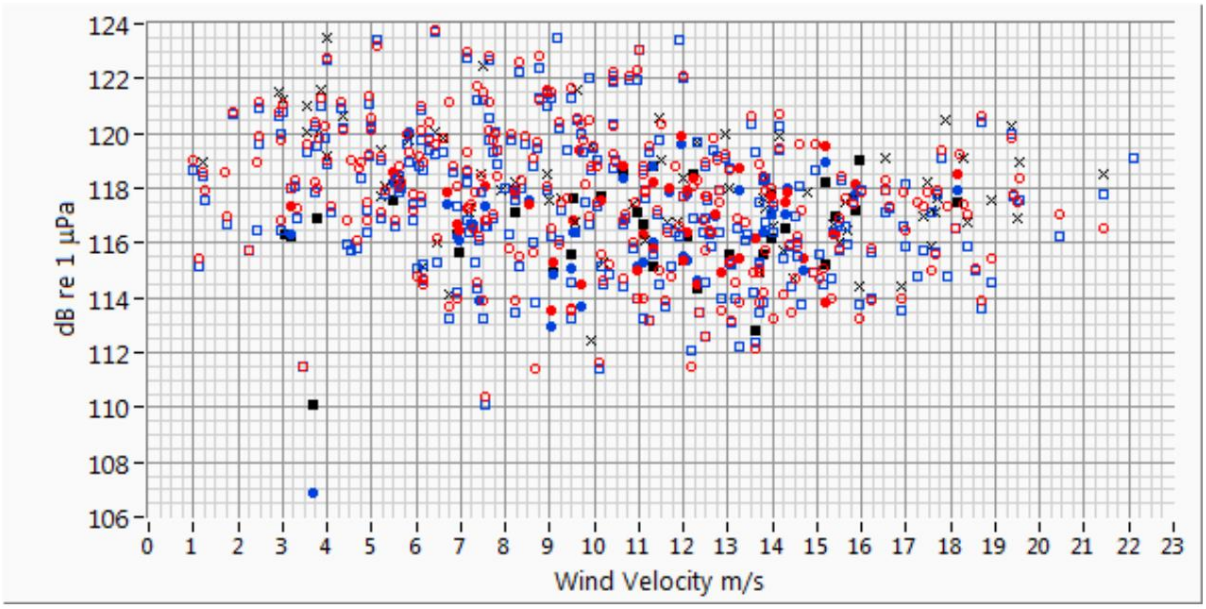

Fig. 7.3.1: Leq over wind speed v in m/s Leq 300 s, all hydrophones 2011 and 2010 Wind speed 2011: Nacelle AV04, 2010: FINO1, height 100 m Values from 2011: Empty red circles: R4-HR1, empty blue ones Squares: R4-HR2, black crosses: F1-H8106-2 Values from 2010: Solid red circles: R4-HR1, solid blue squares: R4-HR2, solid black squares: F1-H8106 Continuous noise level decreases

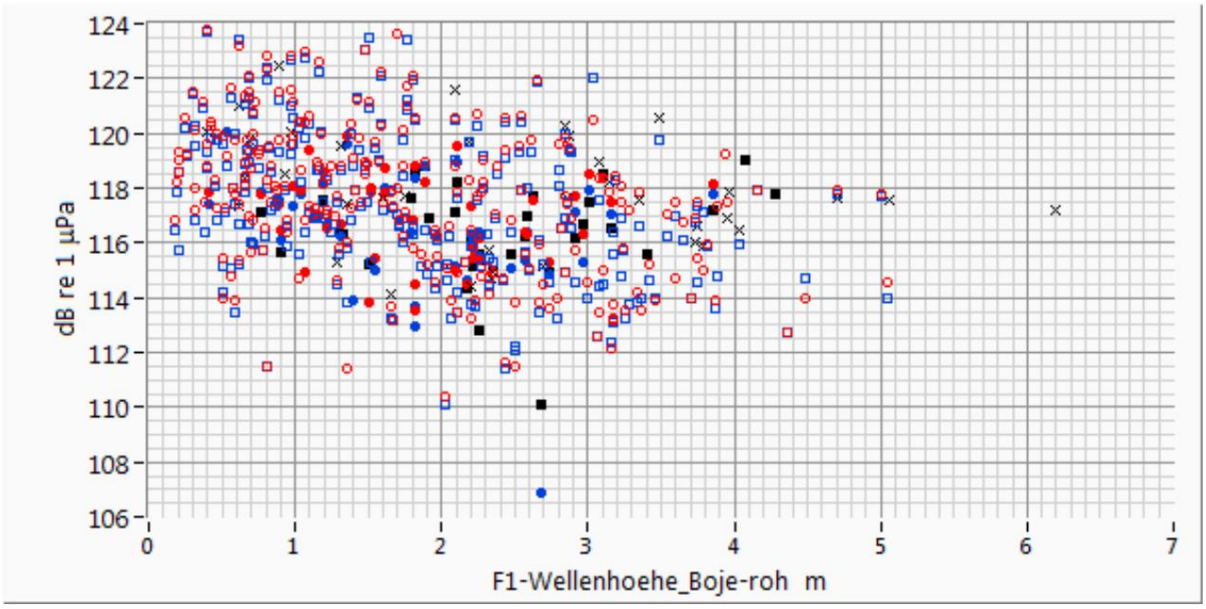

Fig. 7.3.2: Leq over wave height hs in m Leq 300 s, all hydrophones 2011 and 2010 wave height measured at measuring buoy FINO1, no post-processing of the data Values from 2011: Empty red circles: R4-HR1, empty blue squares: R4-HR2 , black crosses: F1-H8106-2 Values from 2010: Solid red circles: R4-HR1, solid blue squares: R4-HR2, solid black squares: F1-H8106 Continuous noise level decreases

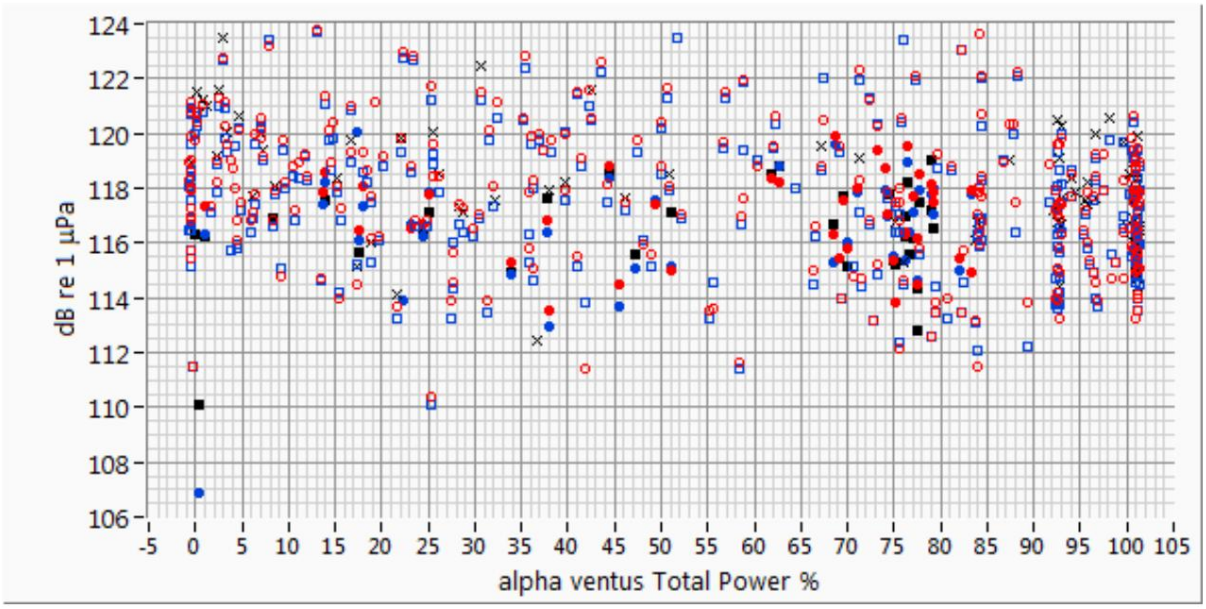

Fig. 7.3.3: Leq over total power of the wind farm in % Leq 300 s, all hydrophones 2011 and 2010 values from 2011: Empty red circles: R4-HR1, empty blue squares: R4-HR2, black crosses: F1-H8106-2 Values from 2010: solid red circles: R4-HR1, solid blue squares: R4-HR2, solid black squares: F1-H8106 continuous noise level decreases

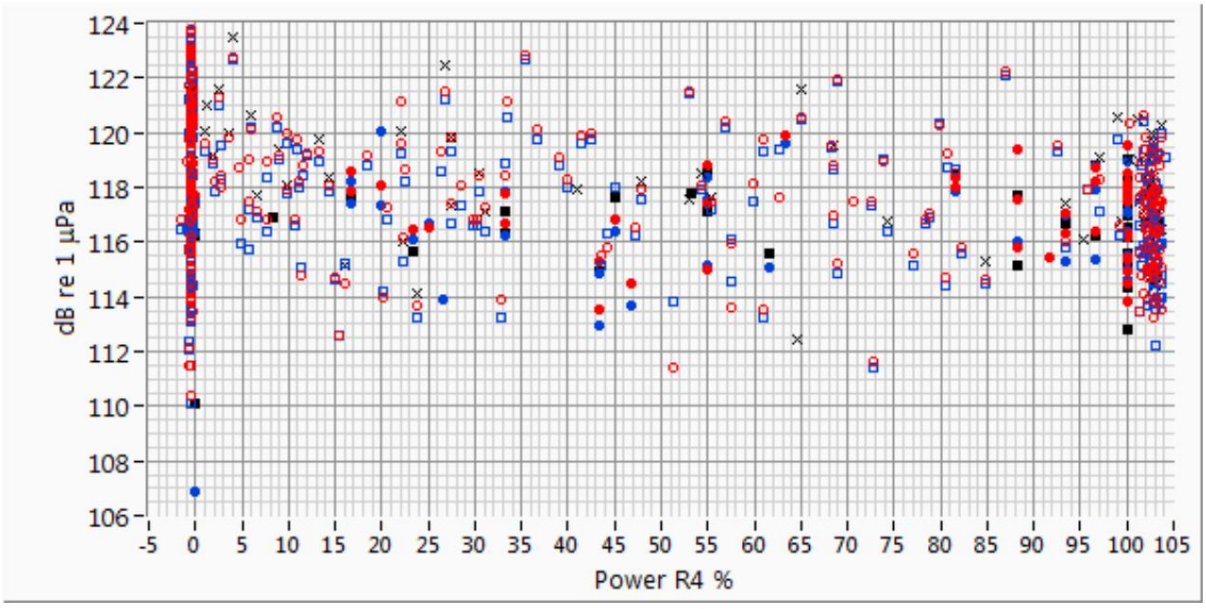

Fig. 7.3.4: Leq over the output of the AV04 system in % Leq 300 s, all hydrophones 2011 and 2010 values from 2011: empty red circles: R4-HR1, empty blue squares: R4-HR2, black crosses: F1-H8106- 2 values from 2010: solid red circles: R4-HR1, solid blue squares: R4-HR2, solid black squares: F1-H8106 continuous noise level decreases

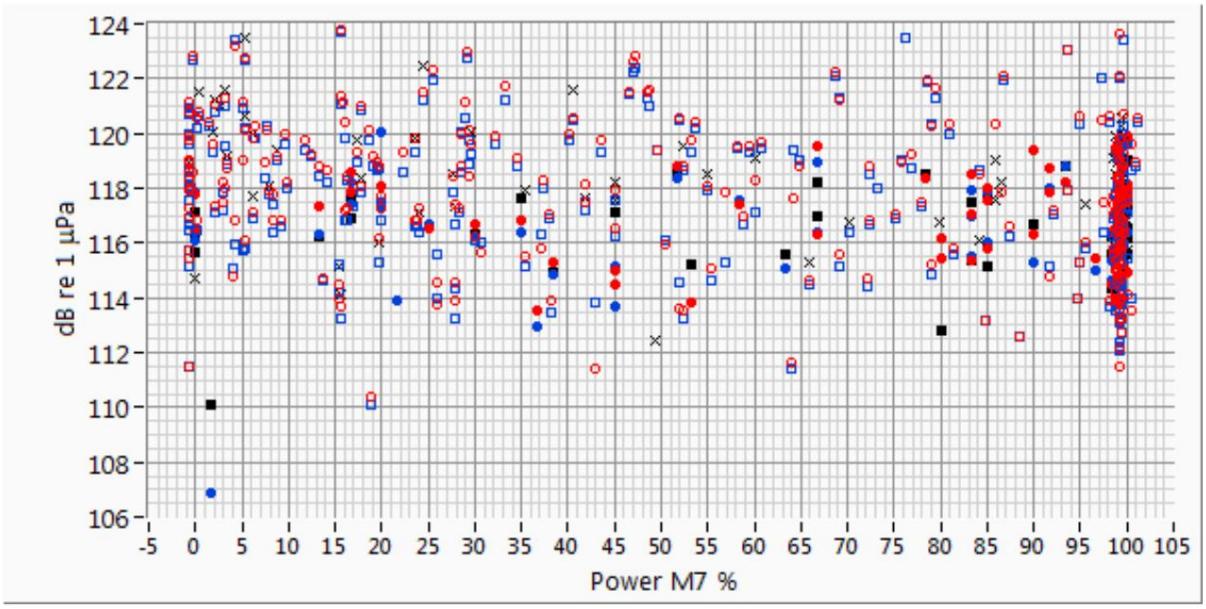

Fig. 7.3.5: Leq over the performance of the AV07 system in % Leq
300 s, all hydrophones 2011 and 2010 Values from
2011: Empty red circles: R4-HR1, empty blue squares: R4-HR2, black crosses: F1-H8106- 2.
Values from 2010: solid red circles: R4-HR1, solid blue squares: R4-HR2, solid black squares: F1-H8106 continuous noise level decreases

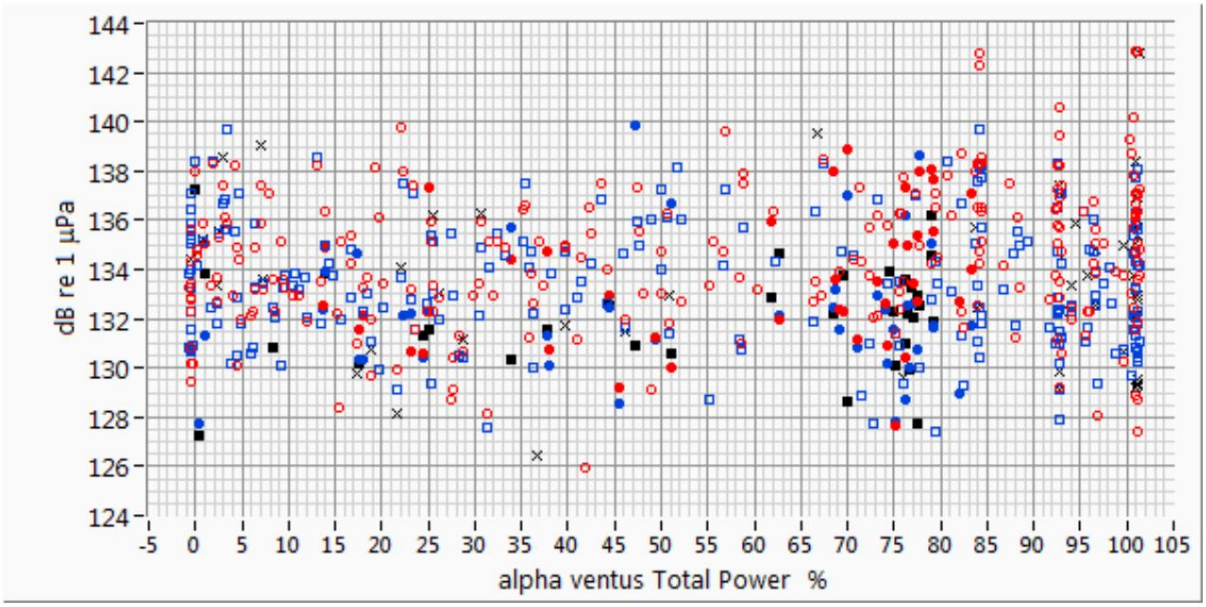

Fig. 7.3.6: Peak level Lpeak over the total power of the wind farm in % Lpeak 300 s, all
hydrophones 2011 and 2010 Values from 2011: Empty
red circles: R4-HR1, empty blue squares: R4-HR2, black crosses: F1-H8106- 2 values from 2010: Solid red circles: R4-HR1, solid blue squares: R4-HR2, solid black squares: F1-H8106 Peak level remains constant, approx. 16 dB higher than continuous sound level

7.4 Third-octave spectra

spectra The third-octave spectra with different parameters are shown below.

Fig. 7.4.1 shows all evaluable third-octave spectra from 2011, measuring time 300 s each, recorded with the hydrophone R4-HR1, which is the closest to the AV04 system, measuring time 300 seconds each. 235 spectra are shown.

Fig. 7.4.7 shows the position of the bandpass from 10 Hz to 3000 Hz in the third-octave spectra to demonstrate the bandpass, compare Fig. 7.4.1 without bandpass. The bandpass consists of a high-pass filter with a cut-off frequency of 10 Hz, which suppresses low-frequency flow-related interference, and a low-pass filter with a cut-off frequency of 3.0 kHz, which suppresses high-frequency electromagnetic radiation. The area visible in the figure is used to calculate the sound levels Leq (and Lpeak). It can be seen that the essential part of the spectrum lies in the passband of the filter and that the lowering of the Leq level through filtering, see Section 7.2, is therefore justified. This filtering is used for all Leq and Lpeak values here except for the comparison values above.

Fig. 7.4.2 shows the statistical evaluation of the third-octave spectra from 2011, measurement time 300 s, hydrophone R4-HR1, number of measurement series 235, direct comparison see Fig. 7.4.1. The maximum (red, line, square), percentile L5 (red, line), energetic mean (black, line, squares), percentile L50 (black, line), percentile L95 (blue, line), minimum (blue, line, squares). The percentiles L5 and L95 are better suited to show the spread of the measured values than the maximum and the minimum, since individual extremes, both particularly loud and particularly quiet events, occur very rarely and are therefore not statistically relevant and are not shown in the percentiles become. Betke (2012) comes to the same conclusion. The energetic mean is higher than the median L50, which is due to the logarithmic scale of the dB values. This difference is already given above with the Leq values. The spectrum shows that the difference is constant over the entire frequency range.

The spectra listed above are broken down below into wave heights below and above 2.5 m, which prevailed during the measurements. The wave height is the significant wave height and was measured at FINO1. Wave height readings are raw in the sense that extreme outliers indicative of system failures have not been removed. These do not occur in the periods considered here, which is why the raw data of the wave heights could be used.

Fig. 7.4.3 shows the third-octave spectra from 2011, measurement time 300 s, hydrophone R4-HR1, measured at wave heights 0 to 2.5 m, number of measurement series 151. In a direct comparison with the unsorted measurements, see Fig. 7.4. 1, there is no significant difference. The same applies to the statistical evaluation of these measurements, see next Fig. 7.4.4.

Fig. 7.4.5 shows the third-octave spectra from 2011, measurement time 300 s, hydrophone R4-HR1, measured at significant wave heights greater than 2.5 m, number of measurements 53, with the systems switched on. It can be clearly seen that the spectral component has fallen above 100 Hz. The authors conclude that this part of the spectrum, which is missing above 2.5 m wave height, can be traced back to ships. Spectral components above 100 Hz are typical for ship noise, see below. From this wave height, service ships are no longer present in the wind farm, the ship noises from the shipping routes 14 km away can be heard on the hydrophones, with high waves a lot of air is introduced into the water and this dampens the propagation, see Wille (1988) and above Ab section 7.3. This explains why the noise level in the wind farm decreases with increasing wind speed and thus increasing wave height, namely the ship noise above 100 Hz is increasingly attenuated, with the system noise itself having the order of magnitude of the ship-generated background noise. The statistical analysis of the third-octave spectra at wave heights greater than 2.5 m is shown in Fig. 7.4.7.

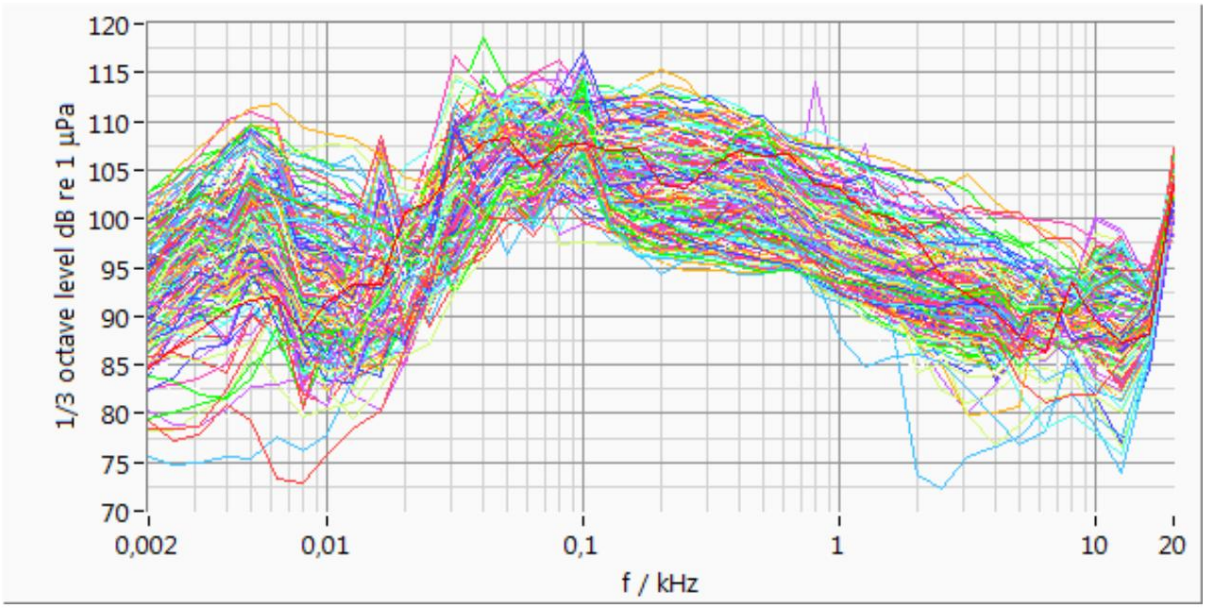

Fig. 7.4.1: Third-octave spectra, 2011, measurement time 300 s, hydrophone R4-HR1, all spectra, number 235

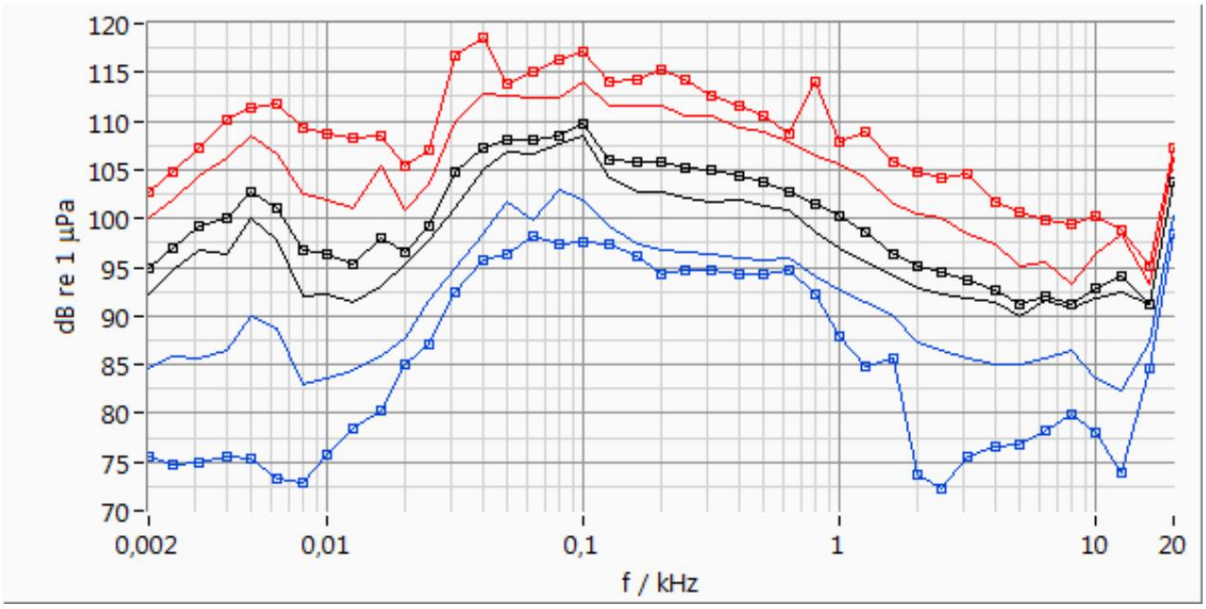

Fig. 7.4.2: Percentile, maximum, minimum, energy, all spectra 1/3-octave spectra,
2011, measurement time 300 s, hydrophone R4-HR1 direct comparison
see Fig. 7.4.1 Maximum (red), energetic
mean value (black), minimum (blue), each with squared percentiles L5 (red), L50 (black) and L95 (blue), each
with smooth lines of the third-octave band levels

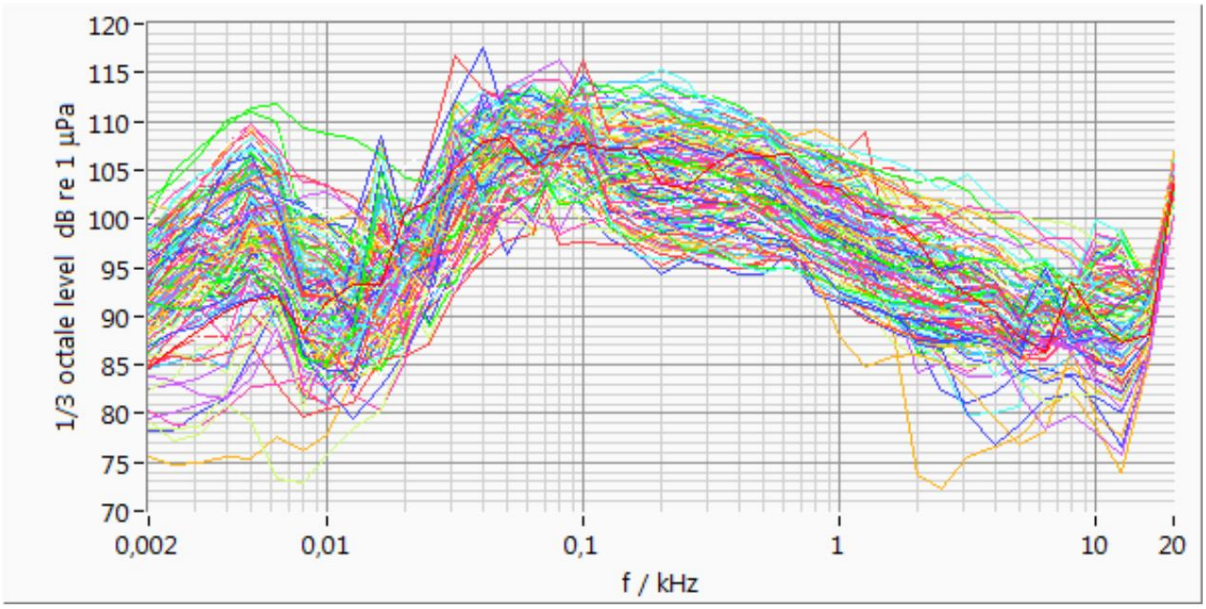

Fig. 7.4.3: Third-octave spectra, 2011, measurement time 300 s, hydrophone R4-HR1, wave height 0 to 2.5 m, number of spectra 151

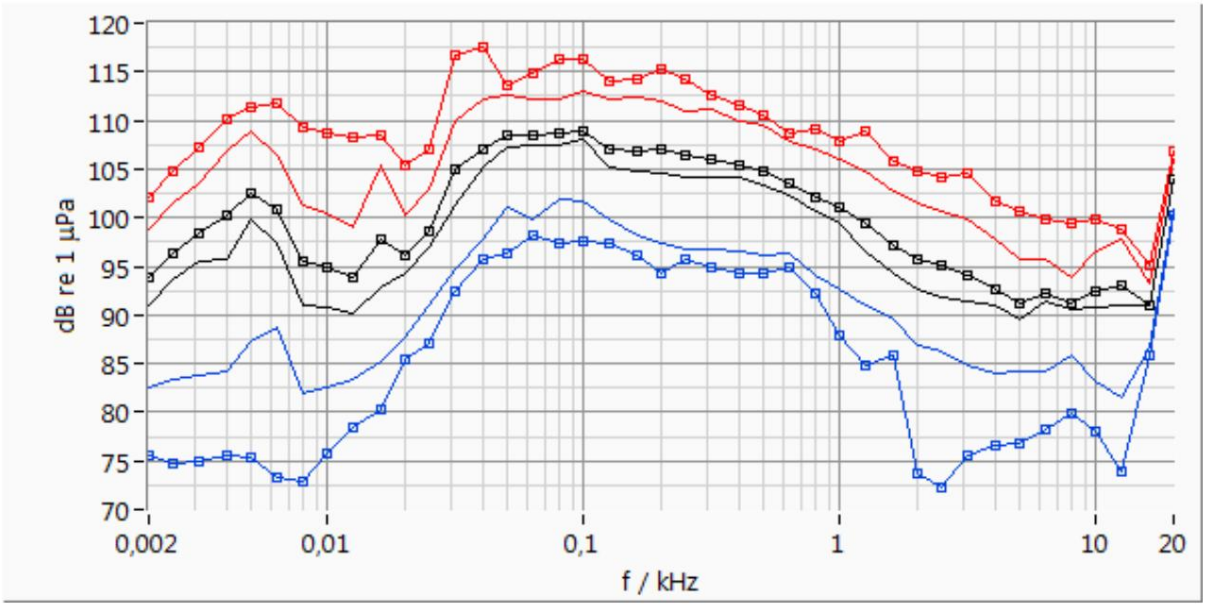

Fig. 7.4.4: Third-octave spectra, 2011, measurement time 300 s, hydrophone R4-HR1, wave height 0 to 2.5 m Number of spectra 151 maximum
(red), mean (black), minimum (blue), each with squares percentiles L5 (red), L50 (black), L95 (blue), each with smooth lines

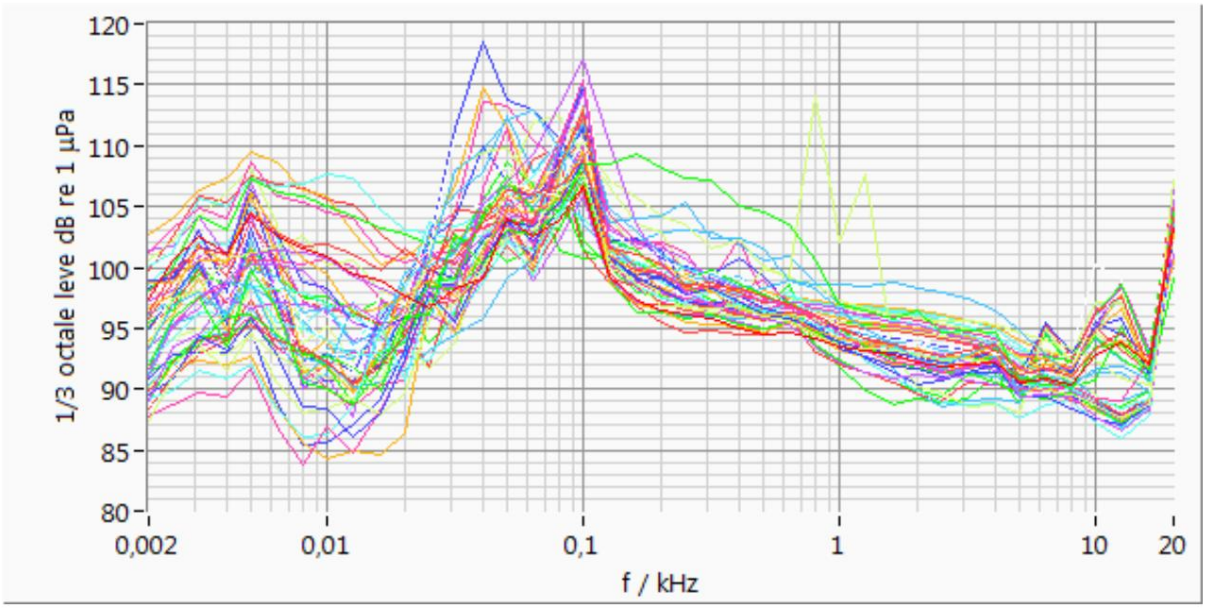

Fig. 7.4.5: Third-octave spectra, 2011, measurement time 300 s, hydrophone R4-HR1, wave height greater than 2.5 m
Number of spectra 53
Result: Frequency range above 100 Hz significantly weakened

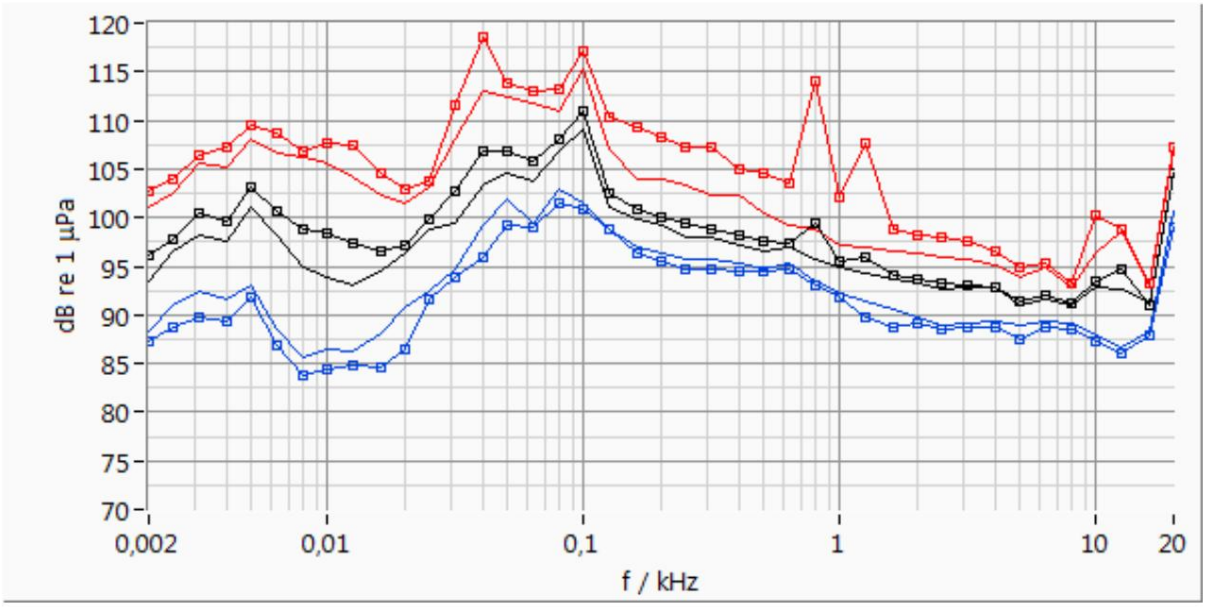

Fig. 7.4.6: Third-octave spectra, 2011, measurement time 300 s, hydrophone R4-HR1, wave height greater than 2.5 m
Number of spectra 53
Result: frequency range above 100 Hz significantly weakened maximum (red), mean value (black) and minimum (blue) , each with squares Percentiles L5 (red), L50 (black) and L95 (blue), each with smooth lines

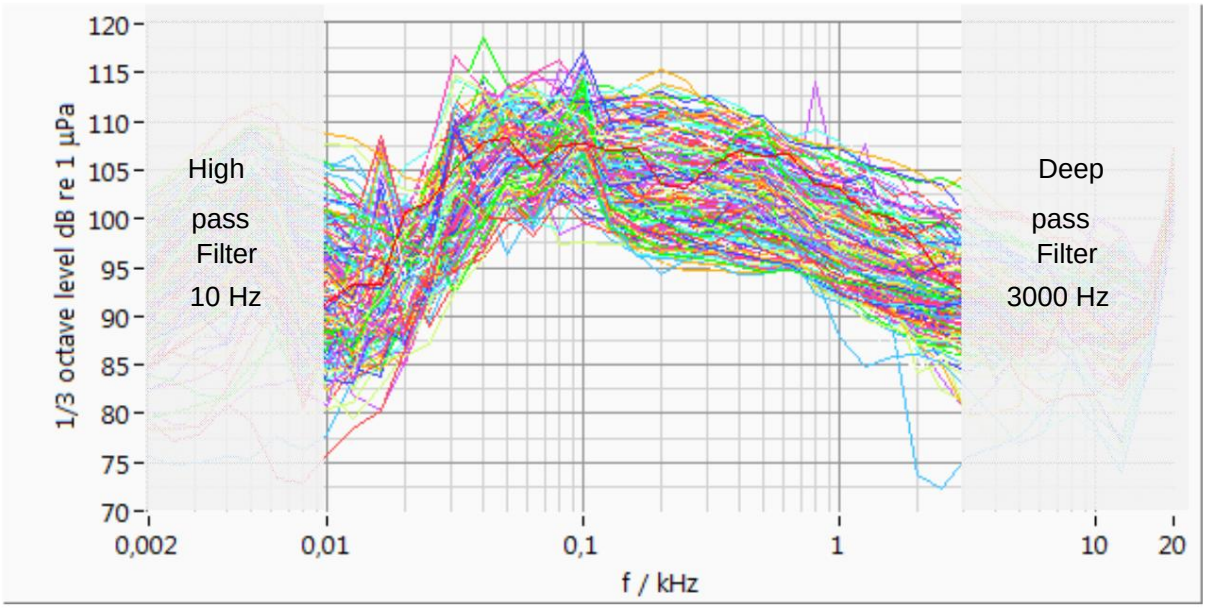

Fig. 7.4.7: Bandpass demonstration: third-octave spectra, 2011, measurement time 300 s, hydrophone R4-HR1, all spectra, number 235, shows the position of the bandpass 10 Hz to 3000 Hz, visible range used to calculate the sound level Leq, in all spectra no band filter switched on

7.5 Narrow Band Spectrum

Narrow band spectra are shown under different parameters below. There are three power classes of the total power of the wind farm and individual powers with two limits of 90% and 1% and two classes of wave height with a limit of 2.5 m. Spectra of individual measurements are shown. The frequency scale is logarithmic.

Fig. 7.5.1 above shows all narrowband spectra from 2011 that can be evaluated, measuring time 300 s each, hydrophone R4-HR1, the next to the AV04 system, with the total output of the wind farm greater than 90%, i.e. full load. 61 spectra are shown. The unit of the spectral density is dB re (1ÿPa)² / Hz. The display is true to the peak. The hydrophone is close to the AV04 facility, the influence of this facility cannot be clearly determined. The distance between the hydrophone and the next AV07 system is approx. 800 m, the 90 Hz peak can be clearly assigned to the AV07 system. The peak at 19 Hz can be attributed to plant AV04, the peaks at 24 Hz and 48 Hz can be attributed to plant AV07 as another fundamental frequency with harmonics, see Section 7.7. The spectral curves correspond to the narrowband spectra measured in alpha ventus at a comparable position by Betke (2012), Figure 4.7, there also all systems at nominal power.

Fig. 7.5.1 in the middle shows the associated narrowband spectra (2011, 300 s, R4-HR1) at the total power of the wind farm between 90% and 1%, i.e. partial load. 151 spectra are shown. Identification of peaks is not obvious. The 90 Hz peak is weakly represented.

Fig. 7.5.1 below shows the associated narrowband spectra (2011, 300 s, R4-HR1) with the total output of the wind farm being less than 1%, which represents the background noise with little wind. 16 spectra are shown. The 90 Hz peak is very weak. Other peaks emerge from the broad spectrum. As lower reference values, the spectral curves correspond to the narrow-band spectra measured in aplha ventus by Betke (2012), Figures 4.9 to 4.13, all systems there. This spectrum also basically corresponds to the third-octave spectrum measured by Betke (2008) at the alpha ventus site before the start of construction with little wind (ibid. p. 11 Figure 3.4a "low"), which represents the background noise, whereby different amplitude scales have to be taken into account due to the different frequency intervals are sighted.

Fig. 7.5.2 shows the evaluation of the spectra according to the wind speed measured on the AV04 system in the intervals above 11.5 m/s, between 11.5 m/s and 4 m/s, below 4 m/s. Evaluations based on power (above) and wind speed (here) therefore produce very similar results.

Fig. 7.5.3 shows the evaluation for the performance of the AV04 system. The plant had downtimes. Their power was cumulatively zero while other systems were in operation, so a broad band of spectra appears in the image below, and in particular the 90 Hz peak of the AV07 system that was in operation appears.

Fig. 7.5.4 shows the evaluation for the performance of the AV07 system. It can be seen that in the partial load range, middle and lower image, the 90 Hz peak is present but not dominant. It can be assumed that the 90 Hz peak is emitted by another type AV07 system (cf. Betke 2012, Figure 4.2).

Fig. 7.5.5 shows the spectra above and below 2.5 m significant wave height measured at FINO1. The upper representation corresponds to the representation of the spectra at full load in Fig. 7.5.1 to 7.5.4 above. It can be seen that with high waves, Fig. 7.5.5 upper image, the loud components are missing in the entire spectral range compared to the lower image with smaller waves, which is due on the one hand to the attenuation of the distant ship noises due to bubbles and on the other hand to the absence of service - and research ships in the area of the wind farm when there are high waves, see Section 7.4 Third-octave analysis above.

The conspicuous 90 Hz peak, which is assigned to the AV07 system, see Section 7.7 below, is not so pronounced in the partial load range, see in particular Fig. 7.5.4 middle, where the narrow-band spectra (2011, 300 s, R4-HR1) at the output of the nearest system from AV07 between 90% and 1%, i.e. partial load AV07, shown with 128 spectra. The 90 Hz peak can be seen but does not step out significantly from the spectrum. For the behavior of the significant peak at part load see section 7.7 under significant frequency variable.

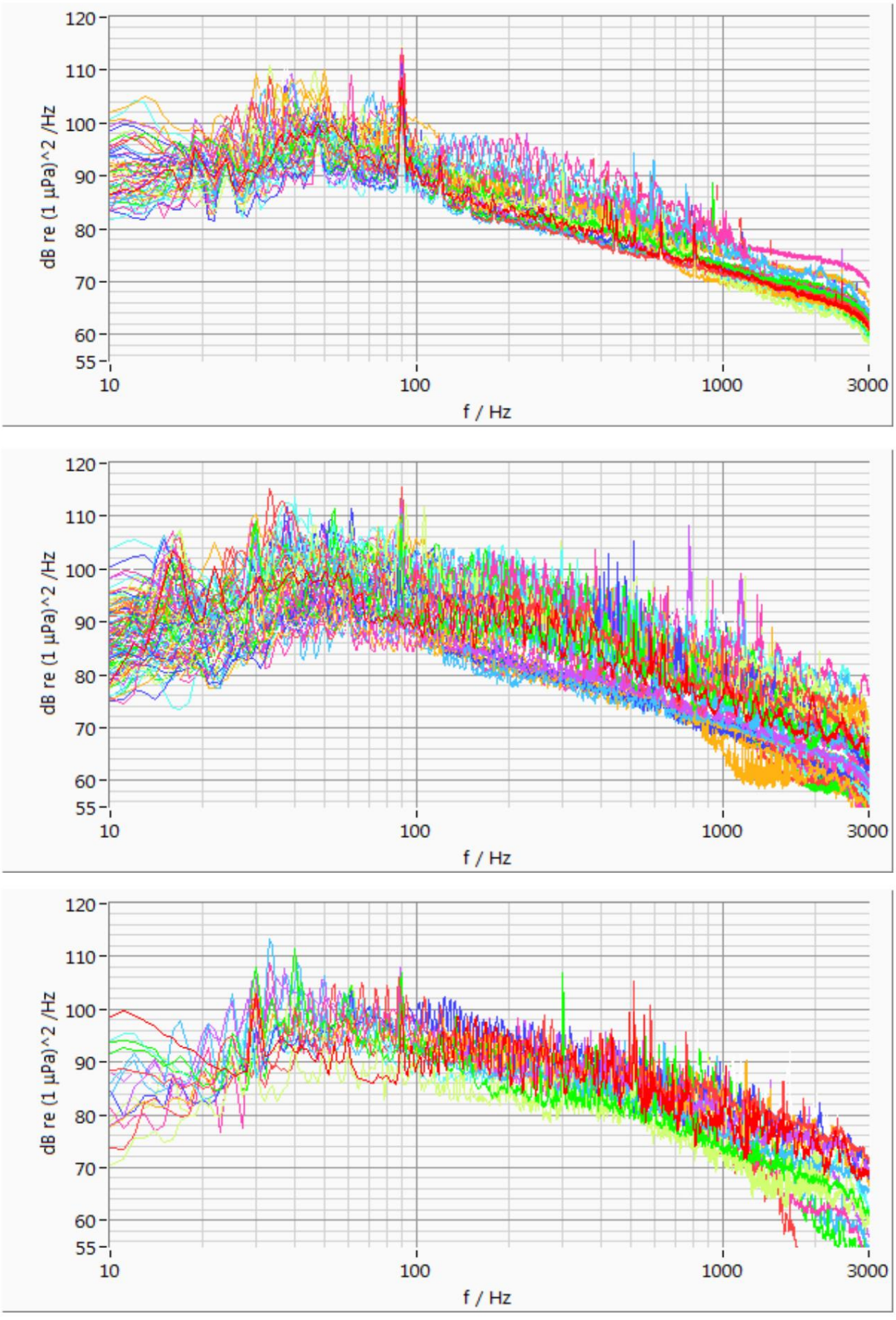

Fig. 7.5.1: Narrow-band spectra, hydrophone R4-HR1, farm power Top: Total power wind farm Pav > 90%, corresponds to full load, number of spectra 61 Middle: Total power wind farm 90% > Pav > 1%, corresponds to part load, number of spectra 151 Bottom: Total power Wind farm 1% > Pav, corresponds to background with little wind, number of spectra 16 measurement time 300 s, measurements 2011

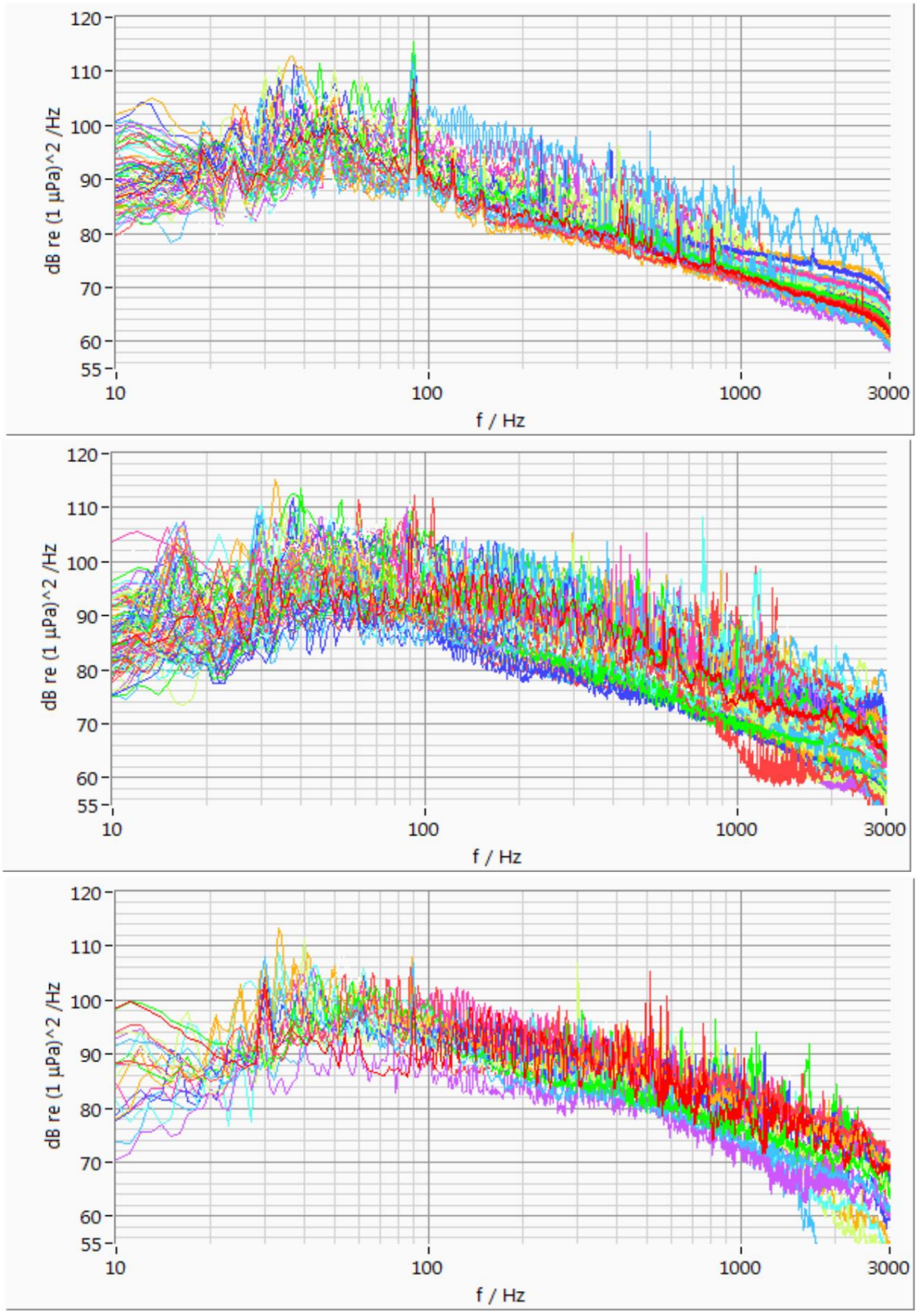

Fig. 7.5.2: Narrow-band spectra, hydrophone R4-HR1, wind Above: wind speed (on AV04) v > 11.5 m/s, corresponds to full load, number of spectra 79 middle: wind speed (on AV04) 11.5 m/s > v > 4 m/s, corresponds to partial load, number of spectra 123 Bottom: wind speed (on AV04) 4 m/s > v, corresponds to background with little wind, number of spectra 21 measurement time 300 s, measurements 2011

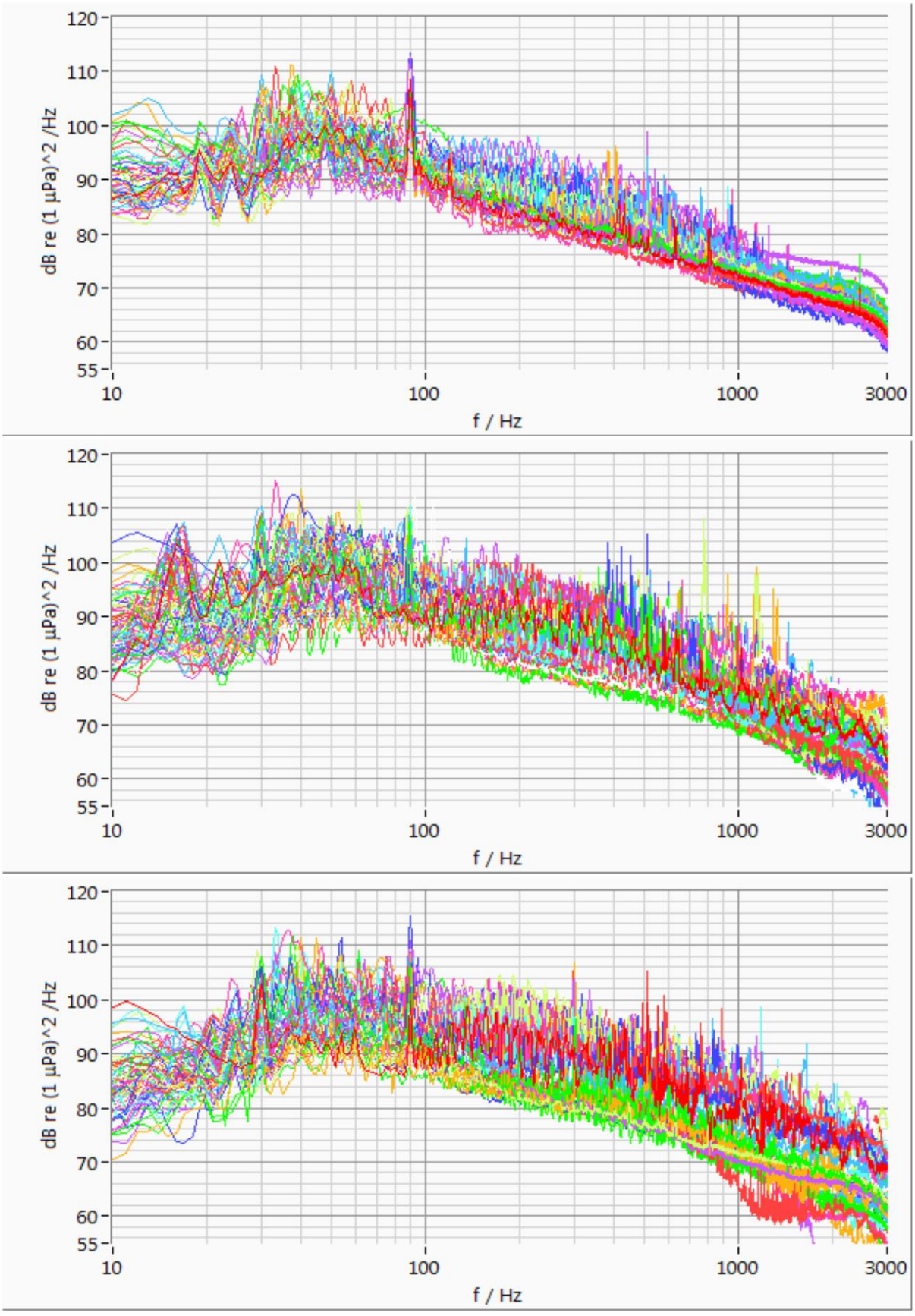

Fig. 7.5.3: Narrow band spectra, hydrophone R4-HR1, power system AV04 Above: power system AV04 PAV04 > 90%, corresponds to full load, number of spectra 58 middle: power system AV04 90% > PAV04 > 1%, corresponds to partial load, number of spectra 87 Below: Output of system AV04 1% > PAV04, corresponds to background with little wind, number of spectra 82 measurement time 300 s, measurements 2011

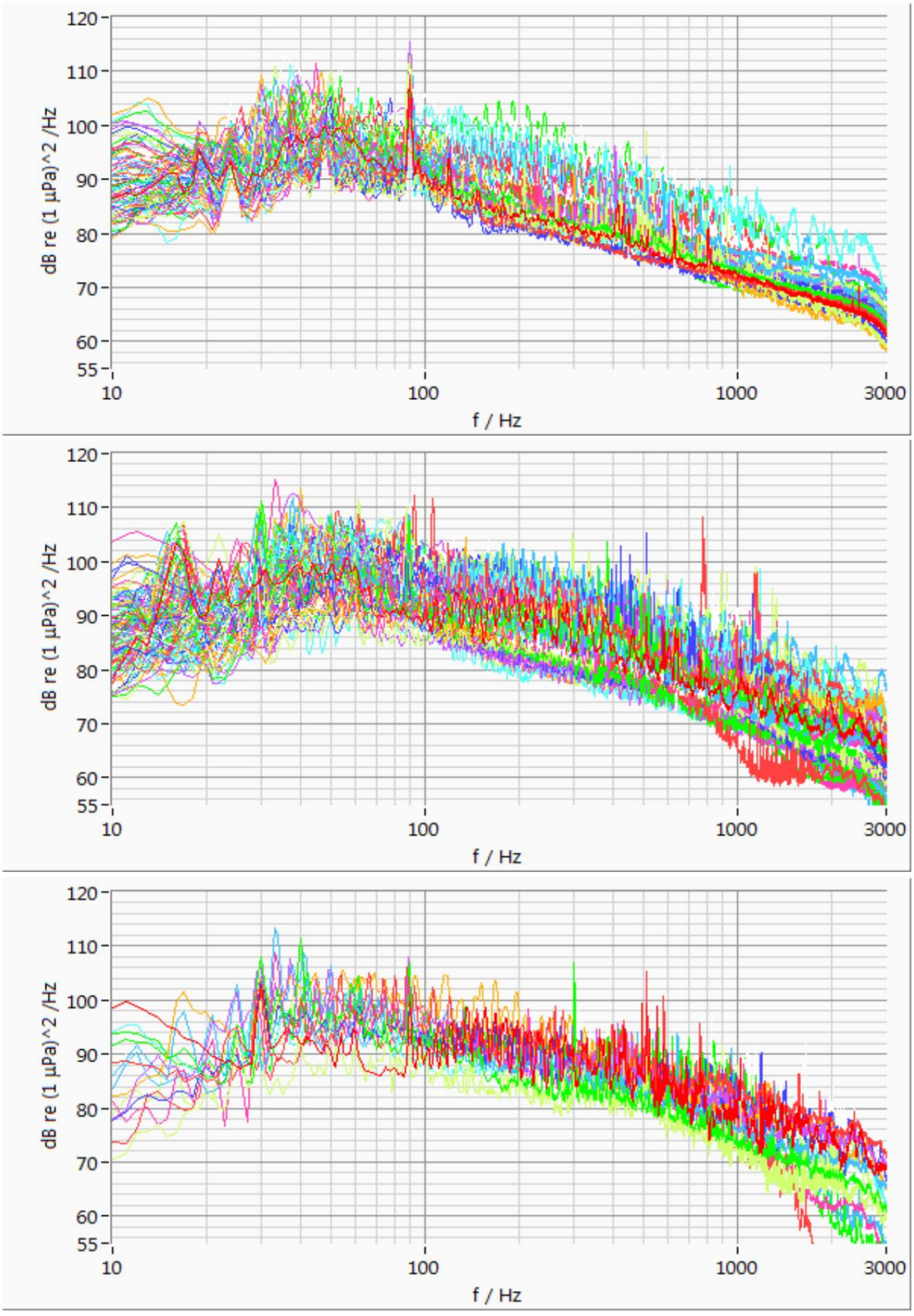

Fig. 7.5.4: Narrow band spectra, hydrophone R4-HR1, power system AV07 Above: power system AV07 PAV07 > 90%, corresponds to full load, number of spectra 91 middle: power system AV07 90% > PAV07 > 1%, corresponds to partial load, number of spectra 128 Below: Output of system AV07 1% > PAV07, corresponds to background with little wind, number of spectra 15 measurement time 300 s, measurements 2011

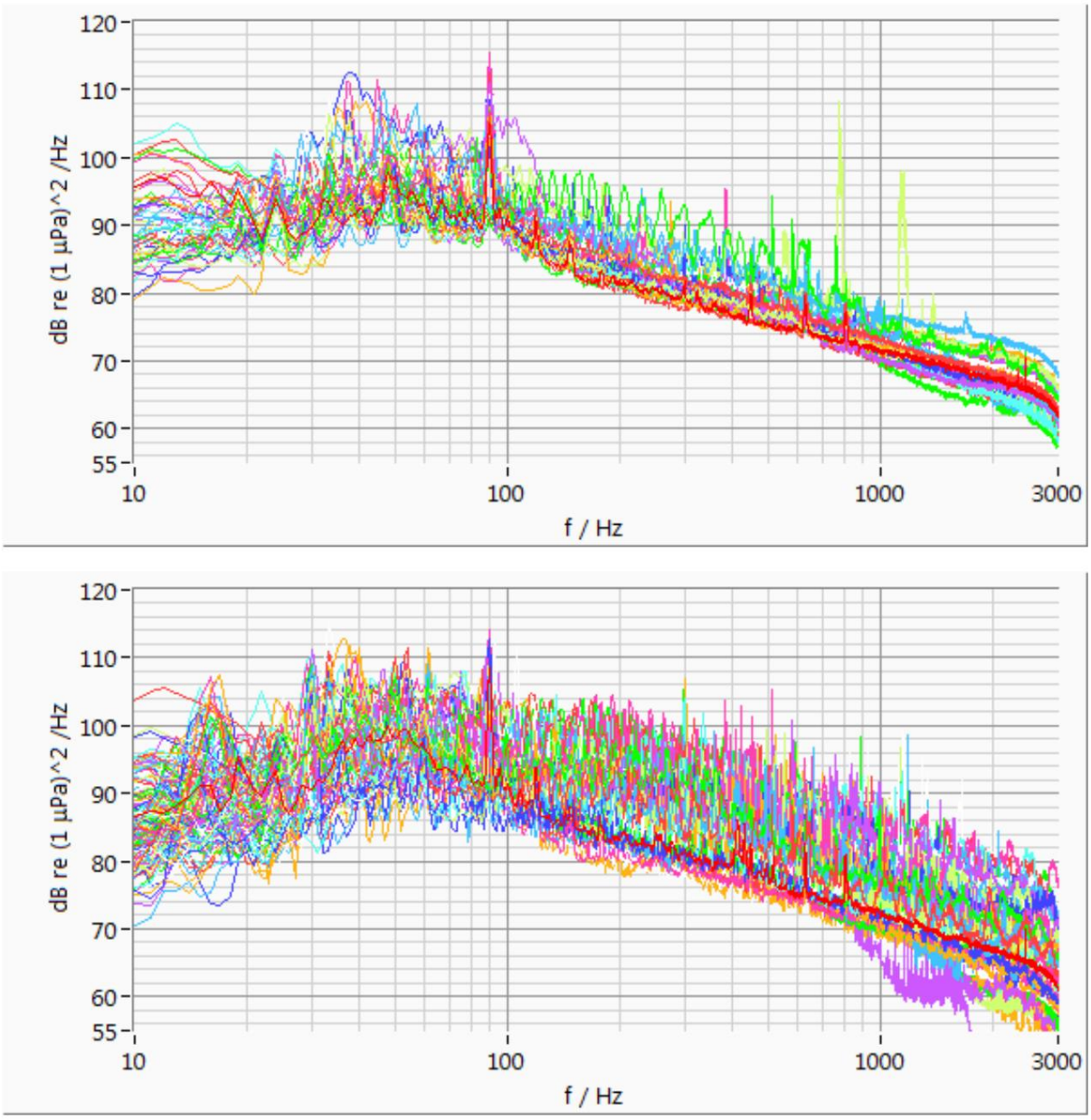

Fig. 7.5.5: Narrow-band spectra, hydrophone R4-HR1, wave height Wave height > 2.5 m, corresponds to full load, number of spectra 53 Wave height < 2.5 m, corresponds to part load, number of spectra 150 Measurement time 300 s, measurements 2011

Selected spectra are shown below.
Fig. 7.5.6 shows 7 spectra at 100% power. The sound was measured at the hydrophone close to the AV04 plant (R4-HR1). The parameters for the spectra are shown in Tab. 7.5.1.

Measurement	ink	wind speed up AV04 [m/s]	wave height [m]	overall performance of [%]	Performance AV07 [%]	Performance AV04 [%]	Performance AV01 [%]
KFS111203-180000R	Black	15.5	3,7	100,9	99,3	102,2	103,4
KFS111130-220000R	Rot	14.3	2,3	101,2	100,0	101,8	103,2
KFS111130-180000R	Green	13.7	2,4	101,0	99,4	103,0	102,7
KFS111129-180000R	Light Blue	15.9	2,2	92,8	99,5	102,8	102,9
KFS111129-040000R	Dark Grey	13.7	2,0	101,1	99,5	102,5	102,9
KFS111126-180000R	Violet	17.5	3,8	101,0	98,7	102,5	103,8
KFS111124-040000R	Orange	11.6	-	99,7	99,7	102,5	101,5

Tab. 7.5.1: Measurements at 100% power shown in Fig. 7.5.6

The peaks at 450 Hz, 630 Hz and 810 Hz are the 5th, 7th and 9th harmonics of the 90 Hz peak, the peaks at 24 Hz and 48 Hz are another fundamental frequency and its first harmonic of the AV07 system. The peak at 19 Hz is singular and can be assigned to plant AV04.
The spectrum has a level of 95 - 90 dB re (1ÿPa)²/Hz below 100 Hz, apart from the peaks, and falls above that at around 20 to 15 dB per decade.

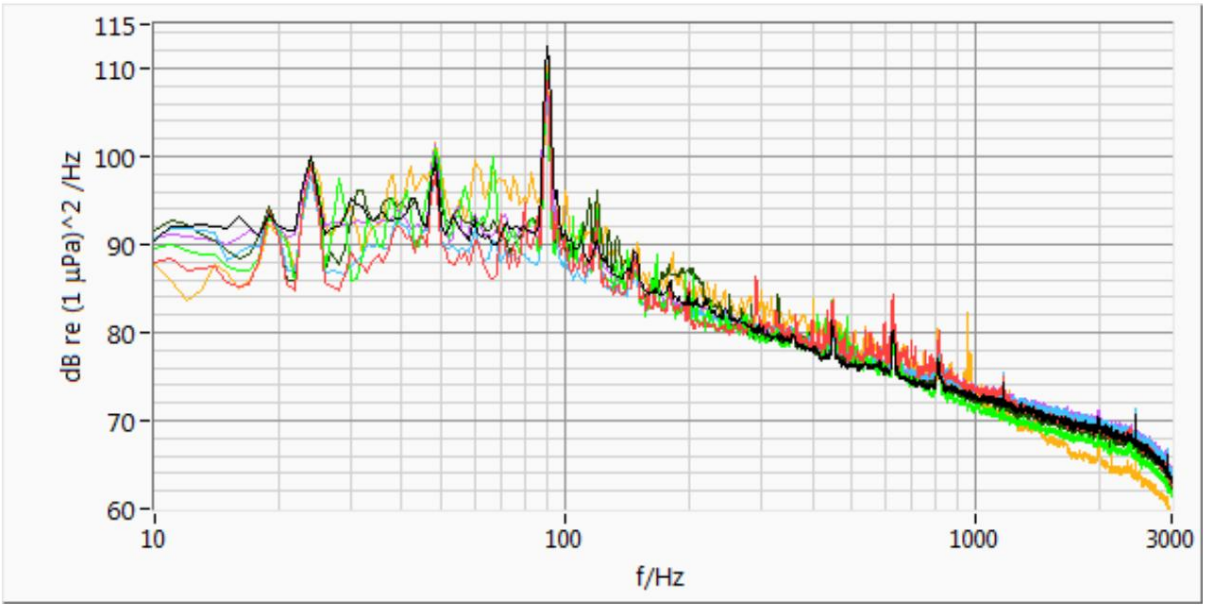

Fig. 7.5.6: Narrow band spectra, hydrophone R4-HR1, 100%
power, number of spectra 7, parameters see Tab. 7.5.1, all prominent peaks are assigned measurement time 300 s, measurements 2011

In the following, individual narrowband spectra at full power are shown as examples. The parameters of the measurements are given in Tab. 7.5.2.
Fig. 7.5.7 shows an almost identical course for all three hydrophones. The “new” DEWI hydrophone (F1-H8106-2) on FINO1, available from 11.11.2011, also shows amplitudes that are up to 3 dB higher from about 1 kHz in other measurements, the reason is unknown.
Fig. 7.5.8 shows an almost identical course for all 3 hydrophones. Here the measurements with the "old" hydrophone on FINO1 (F1-H8106) are superimposed with mains hum at 100 Hz, 200 Hz and multiples up to 600 Hz, apart from that the curve is the same.

Measurement	Abb.	wind speed up AV04 [m/s]	wave height [m]	overall performance of [%]	Performance AV07 [%]	Performance AV04 [%]	Performance AV01 [%]
KFS111129-180000R,F	7.5.7	15.9	2,2	92,8	99,5	102,8	102,9
KFS100917-040000R,F Tab.	7.5.8	14.3	3,2	79,2	100,0	100,0	14,3

7.5.2: Individual measurements at full power

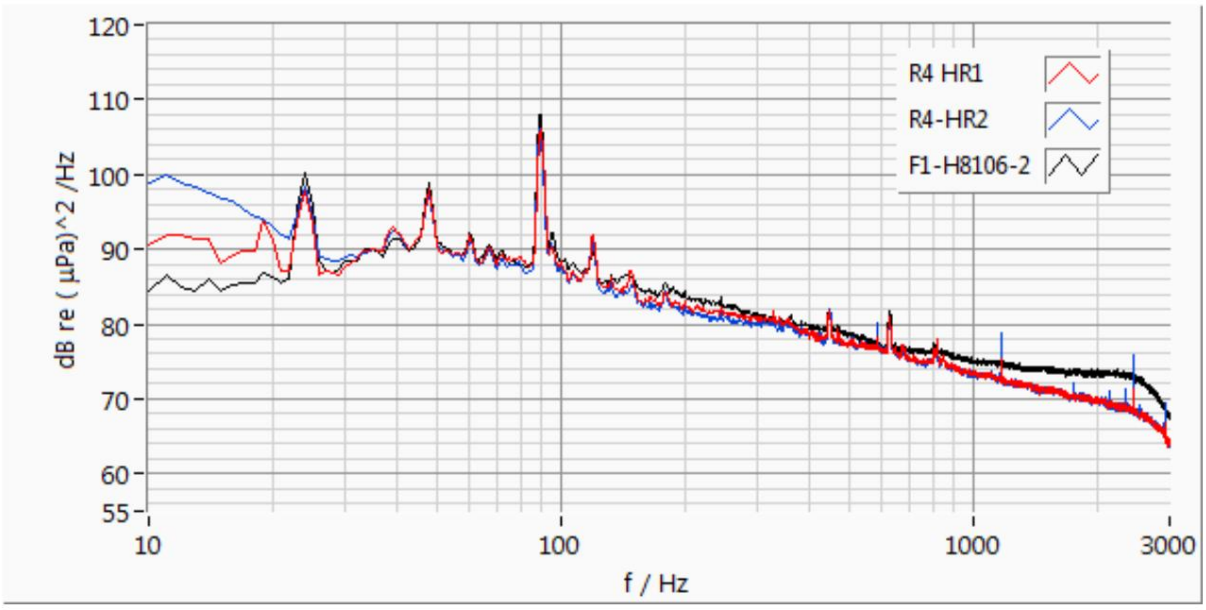

Fig. 7.5.7: Narrow band spectra, all 3 hydrophones full power, 3 hydrophones almost identical measurement time 300 s, measurement KFS111129-180000R and KFS111129-180000F

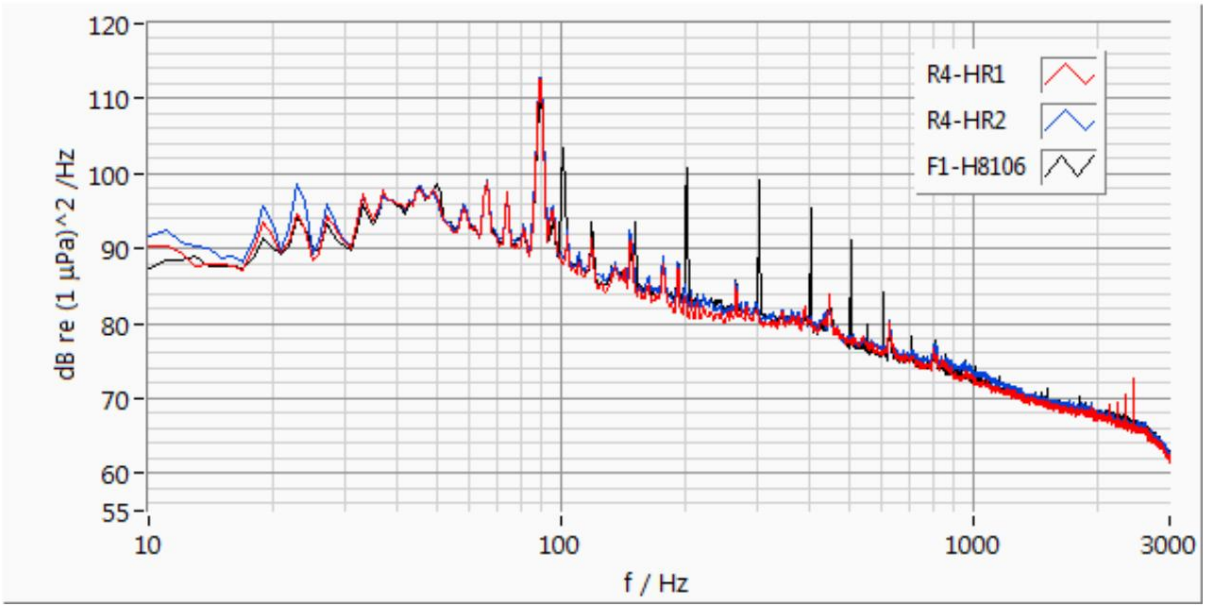

Fig. 7.5.8: Narrow band spectra, all 3 hydrophones full power, mains hum 100 Hz and harmonics on hydrophone F1-H8106 at FINO1 (black line) Otherwise 3 hydrophones almost completely identical measurement time 300 s, measurement KFS100917-040000R and KFS100917-040000F

In the following, individual narrowband spectra at medium power are shown as examples.
Fig. 7.5.9 shows an almost identical course for all three hydrophones. The "new" hydrophone F1-H8106-2 at FINO1 also shows higher amplitudes from about 1 kHz in other measurements.
Fig. 7.5.10 shows an almost identical course for all 3 hydrophones. Here the measurements with the hydrophone F1-H8106 at FINO1 are superimposed with mains hum, apart from that the course is the same.

Measurement	Abb.	wind speed up AV04 [m/s] 9.2	wave height [m]	overall performance of [%]	Performance AV07 [%]	Performance AV04 [%]	Performance AV01 [%]
KFS111201-180000R,F	7.5.9	18.2	1,6	46,2	41,9	55,5	56,5
KFS100915-040000R,F	7.5.10		3,0	77,6	83,3	83,3	18,2

Tab. 7.5.3: Individual measurements at average power

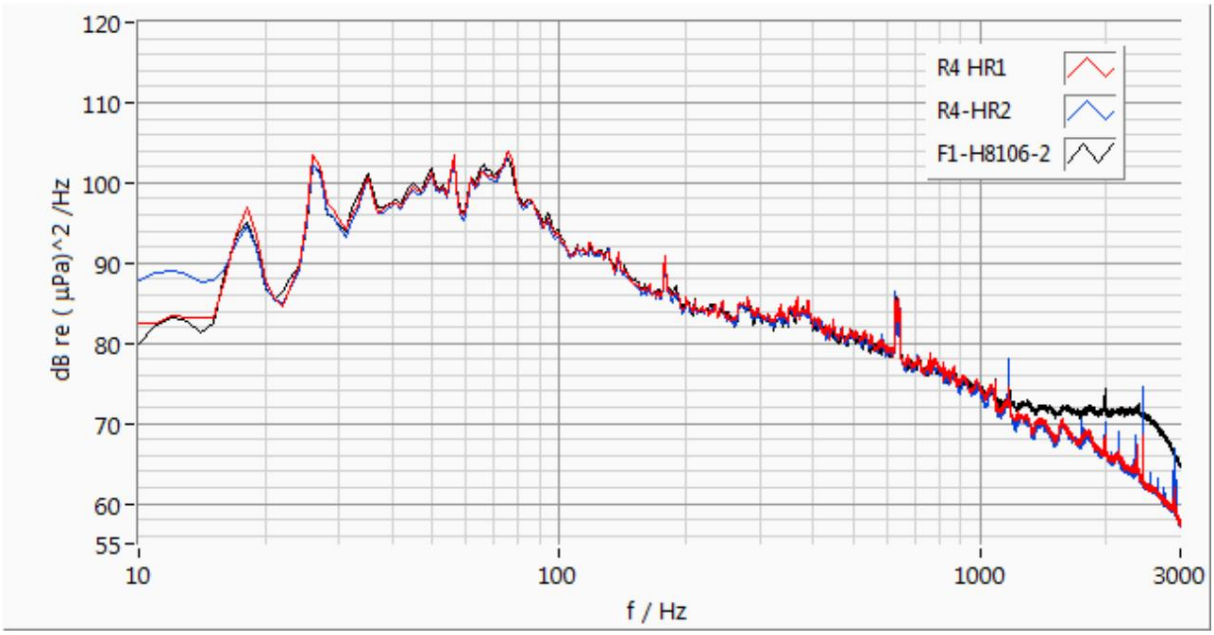

Fig. 7.5.9: Narrow band spectra, all 3 hydrophones Medium power, 3
hydrophones almost identical, from 1000 Hz possible chain clanking at FINO1 Measurement time 300 s, measurement KFS111201-180000R
and KFS111201-180000F

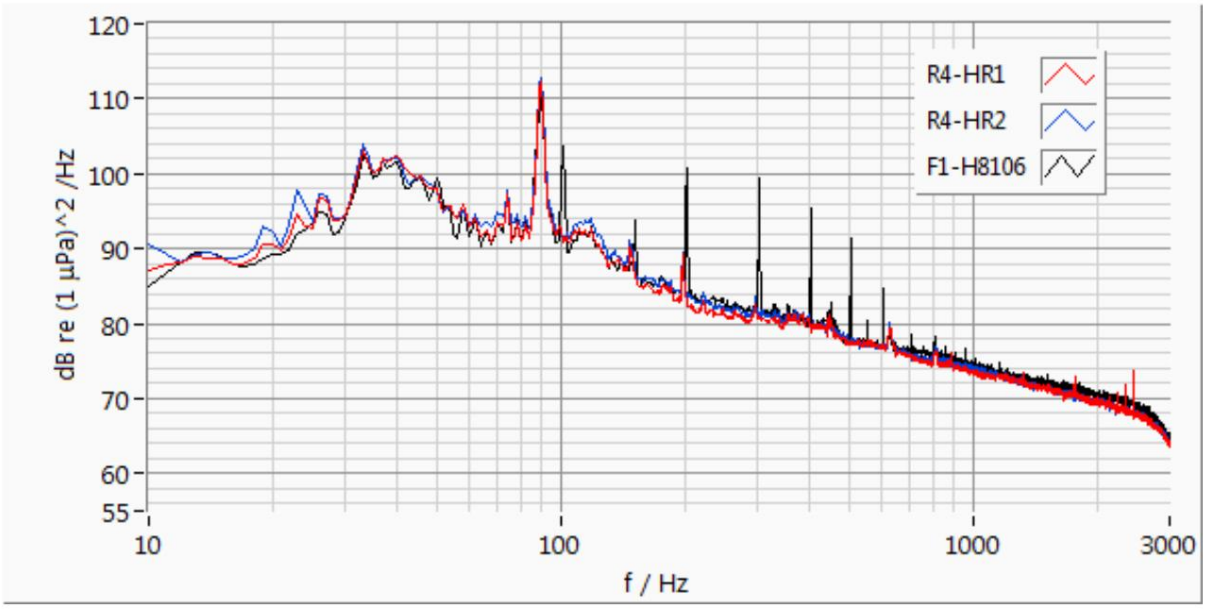

Fig. 7.5.10: Narrow band spectra, all 3 hydrophones medium power, 3
hydrophones almost identical, mains hum on hydrophone at FINO1 (black line)
Measuring time 300 s, measurement KFS100915-040000R and KFS100915-040000F

In the following, individual narrowband spectra at low power are shown as examples.
Fig. 7.5.11 shows an almost identical course for all three hydrophones. The hydrophone at FINO1 shows higher amplitudes above 1 kHz, possibly due to chain noise. Weak ship noise is present.
Fig. 7.5.12 shows an almost identical course for both hydrophones. It's quiet conditions.

Measurement	Abb.	wind speed up AV04 [m/s] 3.0	wave height [m]	overall performance of [%]	Performance AV07 [%]	Performance AV04 [%]	Performance AV01 [%]
KFS111122-220000R,F	7.5.11	1.1		0,7	2,2	-0,3	0,5
KFS111028-180000R	7.5.12	3.7	0,5	-0,5	-0,7	-0,4	-0,4
KFS100925-180000R,F Tab. 7.5.4:	7.5.13		2,7	0,3	1,7	1,7	3,7

Individual measurements at low power

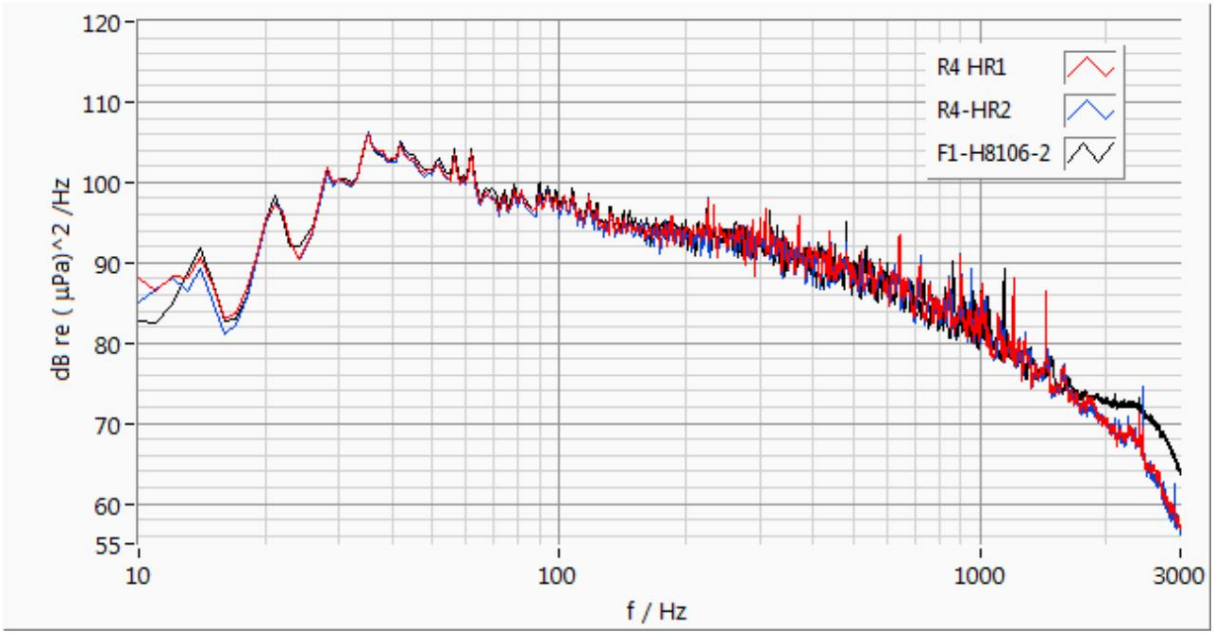

Fig. 7.5.11: Narrow band spectra, all 3 hydrophones Low power, 3 hydrophones almost identical, from 1000 Hz possible chain clanking at FINO1 Measurement time 300 s, measurement KFS111122-220000R and KFS111122-220000F

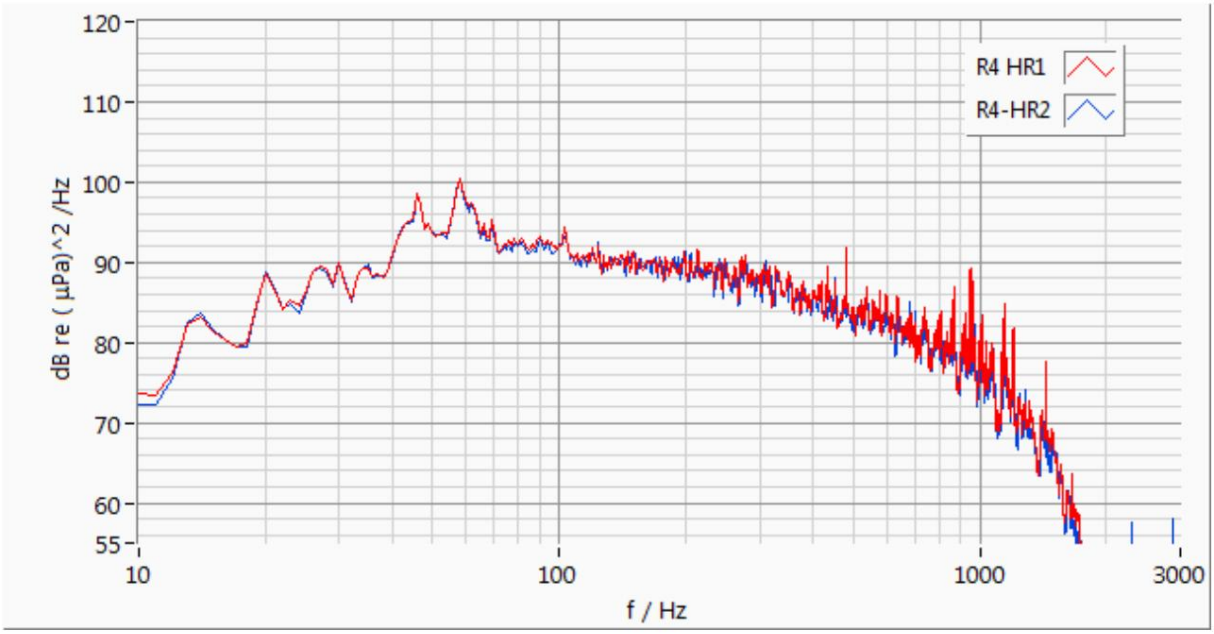

Fig. 7.5.12: Narrow band spectra, 2 hydrophones Low power, 2 hydrophones almost identical, very quiet measurement Measurement time 300 s, measurement KFS111028-180000R

An extremely quiet measurement is presented below, see Fig. 7.5.13, the measurement conditions are given in Tab. 7.5.4 above. Unfortunately, there is mains hum on the FINO1 hydrophone F1-H8106 with 100, 150, 200, 300, 400, 450, 500, 550, 600 Hz, otherwise you can see three identical hydrophone curves (measuring time 300 s, measurement KFS111028-180000R).

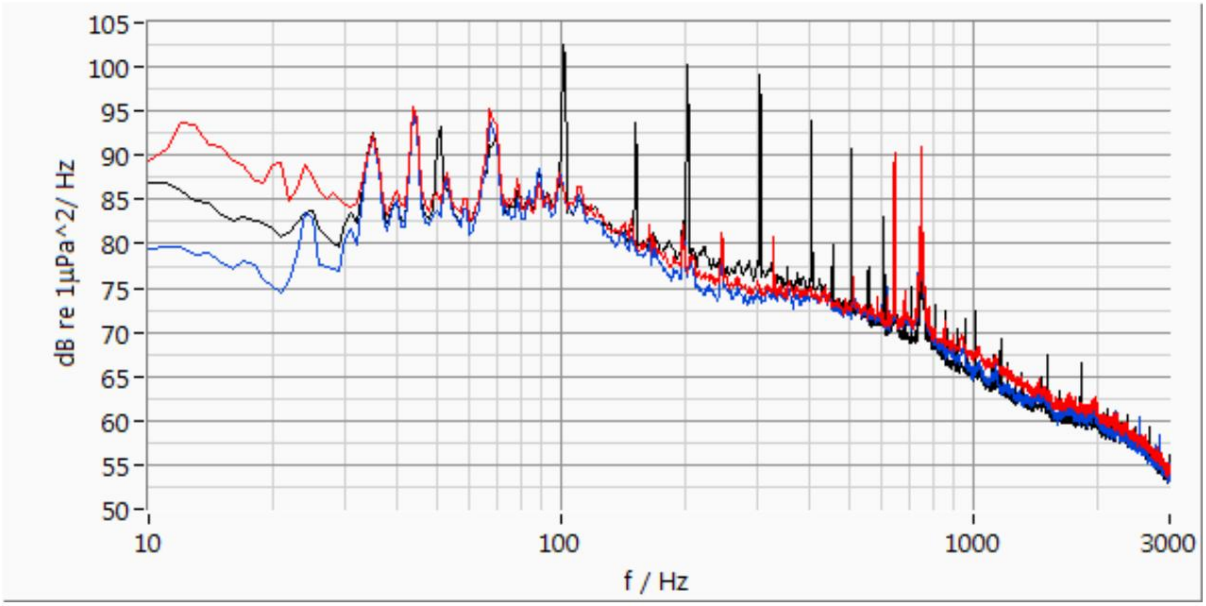

Fig. 7.5.13: Narrow band spectra, 3 hydrophones, very quiet
measurement Black lines
hydrophone F1-H8106 (FINO1) with mains hum (100, 150, 200, 300, ... Hz) otherwise 3 identical hydrophone courses,
measurement time 300 s, measurement KFS100925-
180000R and KFS100925-180000F

The influence of the AV04 system is shown below. Two measurements are shown in Fig. 7.5.14. In both, the AV07 system has 100% power, in one measurement the AV04 system has 100% power, in the other the AV04 system is switched off. The measurement conditions are given in Tab. 7.5.5. Although the two hydrophones measure in front of the AV04 system, the influence of the system is so small in relation to the overall noise that it cannot be proven to be significant. The environmental conditions in two measurements are so different that the measurements when the system is switched off sometimes have higher spectral densities (green line). Obviously, differential measurements are only possible to a very limited extent.

Measurement	Attachment AV04	Wind on AV04 [m/s]	Wave height [m]	Total	Performance AV07 [%]	Performance AV04 [%]	Performance AV01 [%]
KFS111130-220000R,F	an	14.3	2.3		100,0	101.8	103,2
KFS110828-220000R	out of	12.2	3.2	performance av [%] 99.1	91.2 84.1	-0.5	100,9

Tab. 7.5.5: System AV04 switched on, switched off

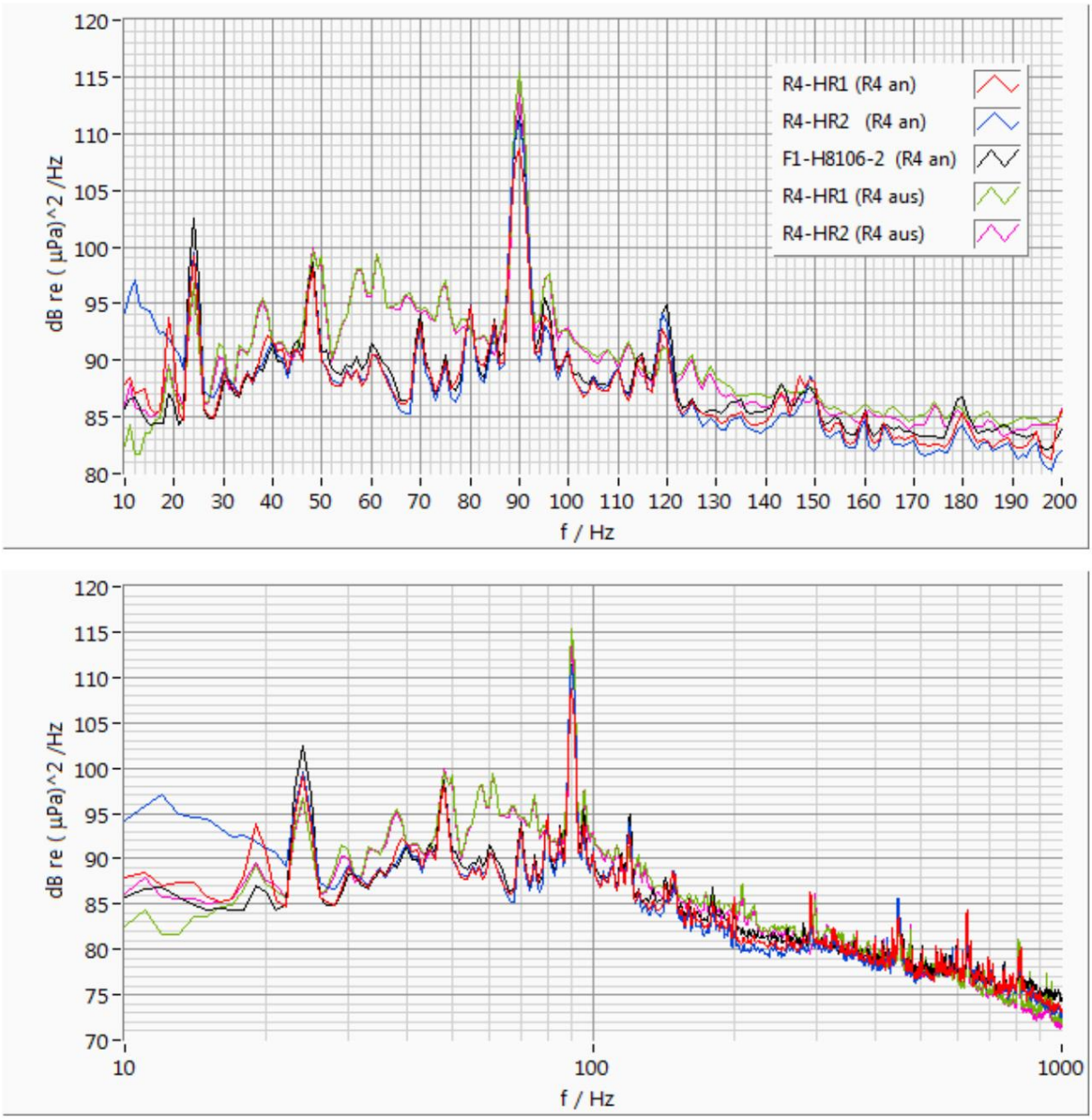

Fig. 7.5.14: Narrowband spectra, 2 hydrophones in front of the AV04 system AV04 system switched on, partly lower lines, and switched off, partly upper lines Above: 10 to 200 Hz linear, below: 10 to 1000 Hz logarithmic Result: Influence of surroundings greater than System AV04, differential measurements cannot be evaluated, measurement time 300 s, measurements KFS111130-220000R, KFS111130-220000F, KFS110828-220000R

7.6 Narrow band 90 Hz

The peak at 90 Hz in the narrow band spectrum is analyzed below with various parameters.

Fig. 7.6.1 shows a frequency section from the narrowband spectra of all valid measurements with the hydrophone R4-HR1 from 2011, in which the power of the AV07 system was greater than 90%. 56 measurements are shown, the distance between the hydrophone and the facility was 785 m. This peak can already be seen in the third-octave spectra and narrow-band spectra, see Sections 7.4 and 7.5. A tonality is evident. Section 7.7 shows that the source is plant AV07.

The frequency of the peak is constant at high power of the systems P > 90%. For the energetic estimation of the peak, the spectral lines 89, 90, 91 Hz are energetically summed and subsequently called the peak height. The lines are peak-neutral with the Hanning correction according to DIN 456681 tonality. In Fig. 7.6.2, the peak heights are plotted against the water level measured at FINO1. The water level is given in dBar (also dbar), 1 dBar equals 1 meter water column.
The water level as a time series is shown in Fig. 7.6.3. It can be seen that the level of the peak (sum of 3 frequency lines) is between 116 and 105 dB. This level determines the source level of the AV07 system, see Tab. 7.6.1. For an exact calculation, the background noise would have to be subtracted. Since the peak protrudes 10 to 15 dB from the signal, the correction is not large, so the source strength can be specified without this correction. The source strength related to 1 m with the attenuation according to Thiele at 90 Hz, see Eq. 4.3.3, between 157 and 146 dB and with the attenuation 15 log(r) two dB more 159 or 148 dB re 1ÿPa re 1m. The reason for the difference is that, according to Thiele, the attenuation is 2 dB weaker than estimated according to Eq.
4.3.1. The source strength is also given at a distance of 100 m, see Table 7.6.1. It can also be seen that the sound level increases with the water level, at 1 m by around 4 dB. The authors consider it possible that the water column is resonating in the central tube of the foundation. With different water levels, the quality of the resonance changes and the frequency is emitted differently. If all powers are taken into account, it can be seen that for powers below 90% the sound level does not increase with the water level, see the second lower branch in Fig. 7.6.4.
In Figures 7.6.5 to 7.6.10, the peak heights measured on the AV04 system with the two hydrophones R4-HR1 (red circles) and R4-HR2 (blue squares) are shown over the output of the AV07 system, the total output in the park (av Total Power), the power of the AV04 and AV01 turbines, the wind speed at hub height measured on the AV04 turbine and the wave height measured at FINO1. The number of measurements is different. Only undisturbed measurements are used. Not all parameters are available for all days. As a result, it is found that the peak height increases with power. The peak is particularly concentrated when the nearest system AV07 has 100% power, see Fig. 7.6.5. It is also noticeable that the level rises sharply from a wind speed of 11 m/s, see Fig. 7.6.9. The level also increases with the wave height, see Fig. 7.6.10. Due to the short distance, the attenuation caused by bubbles from the waves, see above, has no effect.

The peak height specified here results from the sum of the three specified frequencies. At high powers, the peak is very stable at these frequencies. At 50% power the peak is no longer at 90 Hz, a weak peak is at 80 Hz, see below.

Peakhöhe	Distance	frequency	Lwa Thiele dB	Lwa 15log(r) dB re	Lwa Thiele dB	Lwa 15log(r) dB re
dB re 1ÿPa	m	Hz	re 1ÿPa re 1m	1ÿPa re 1m	re 1ÿPa re 100m	1ÿPa re 100m
116	785	90	157	159	129	129
105	785	90	146	148	118	118

Tab. 7.6.1 Estimation of the source strength Lwa of the AV07 system calculated from peak height peak height sum of 89, 90, 91 Hz, transition loss according to Thiele Eq. 4.3.3 and after 15 log (r/r0) G. 4.3.1, Lwa related to 1 m and to 100 m

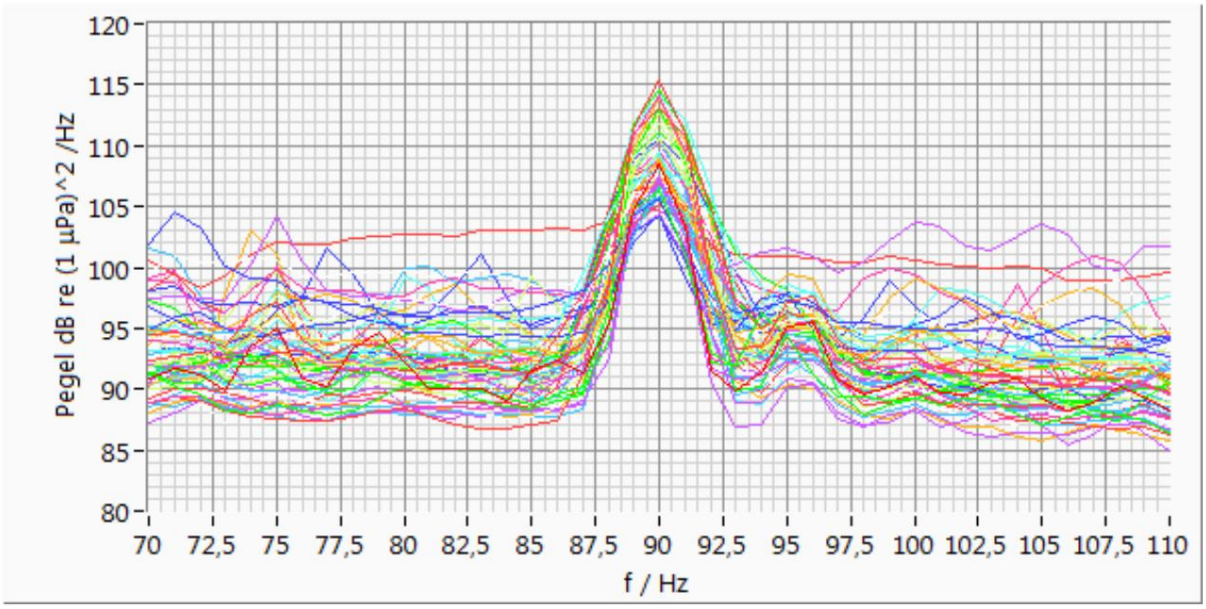

Fig. 7.6.1: Section of narrow-band spectra, 2011, measurement time 300 s, hydrophone R4-HR1, output of system AV07 > 90%, 56 measurements from 2011 are shown

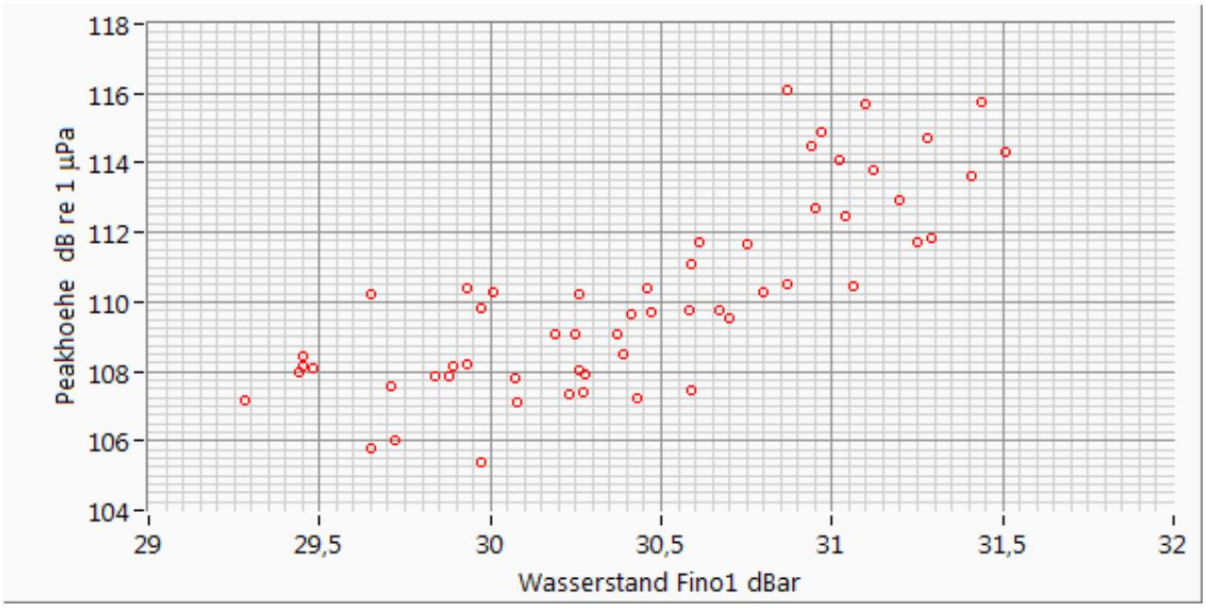

Fig. 7.6.2: Dependence of the peak height (= energetic sum of the corrected lines 89, 90, 91 Hz), only power AV07 > 90%, above the water level (1 dBar approx. 1 m), 56 measurements from 2011, hydrophone R4 -HR1 Result: At P > 90%, the sound level increases with the water level.

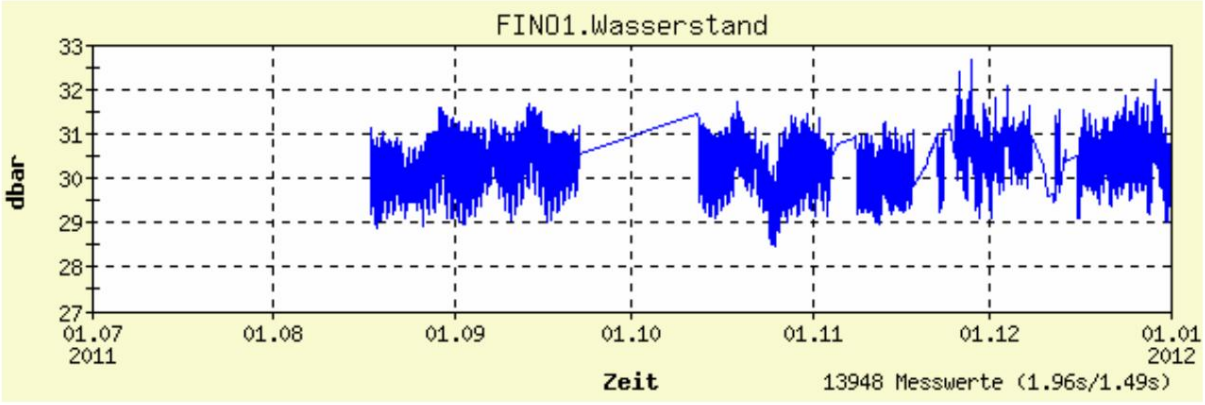

Fig. 7.6.3: Time series of water level at FINO1, unit in dbar (1 dbar identical to 1 dBar approx. 1 m water column)

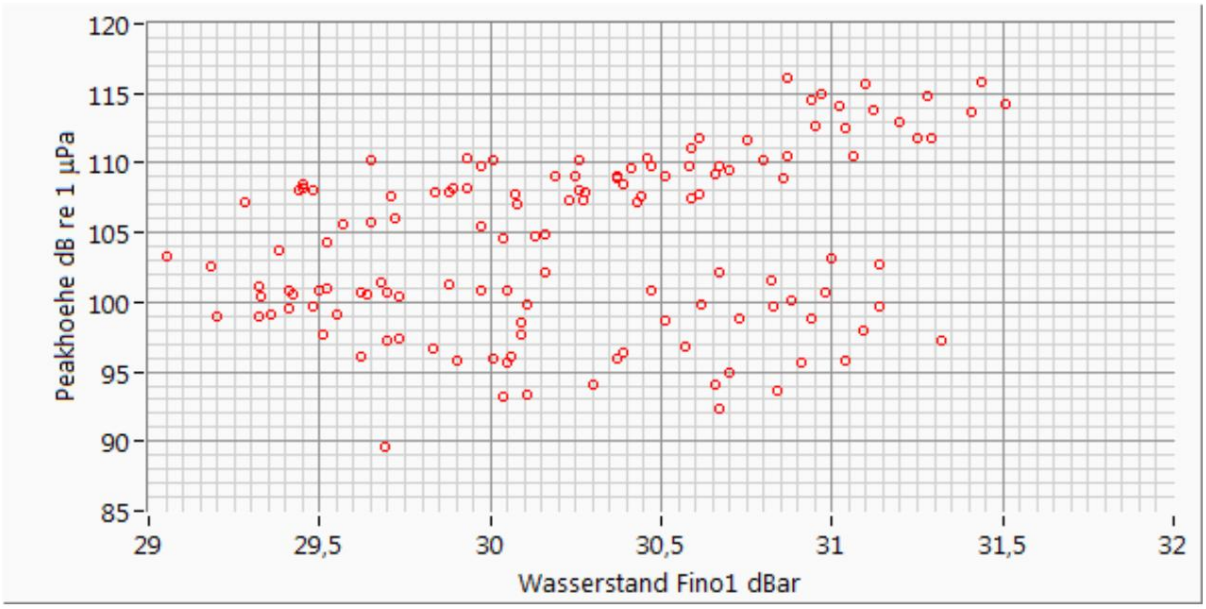

Fig. 7.6.4: Dependence of the peak height (= energetic sum of the corrected lines 89, 90, 91 Hz), all power AV07, above the water level (1 dBar around 1 m), 132 measurements from 2011, hydrophone R4-HR1 Result: A second branch, independent of the water level, arises for performances < 90%.

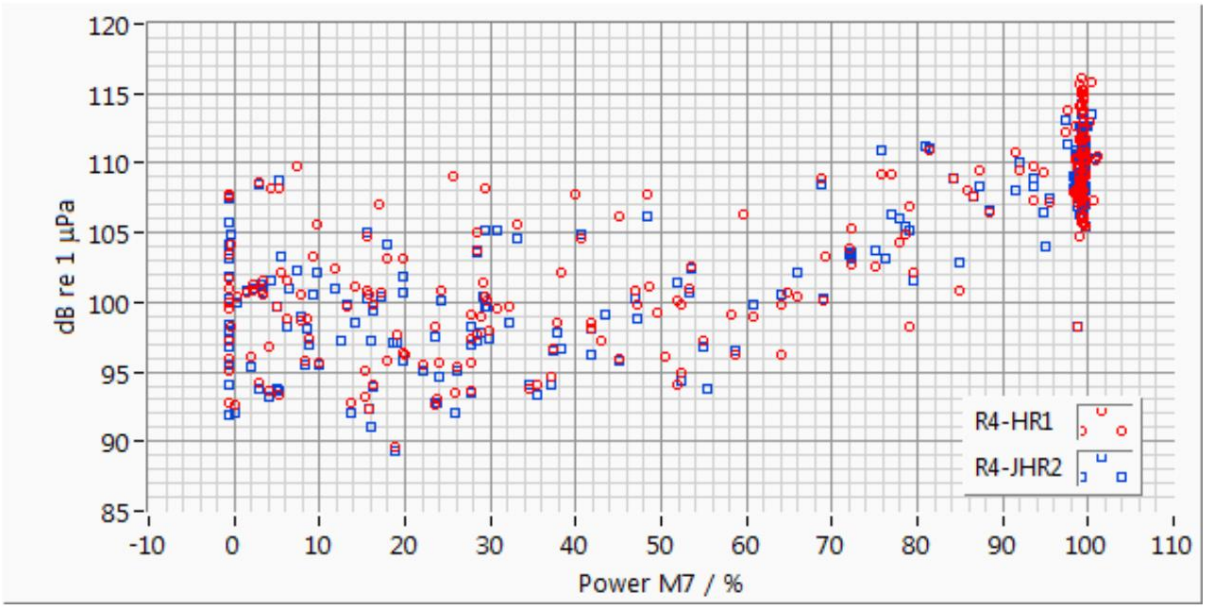

Fig. 7.6.5: Dependence of the peak height (= energetic sum of the corrected lines 89, 90, 91 Hz)
Hydrophone R4-HR1 red circles 234 measurements, hydrophone R4-HR2 blue squares 218 measurements over power system AV07 in %

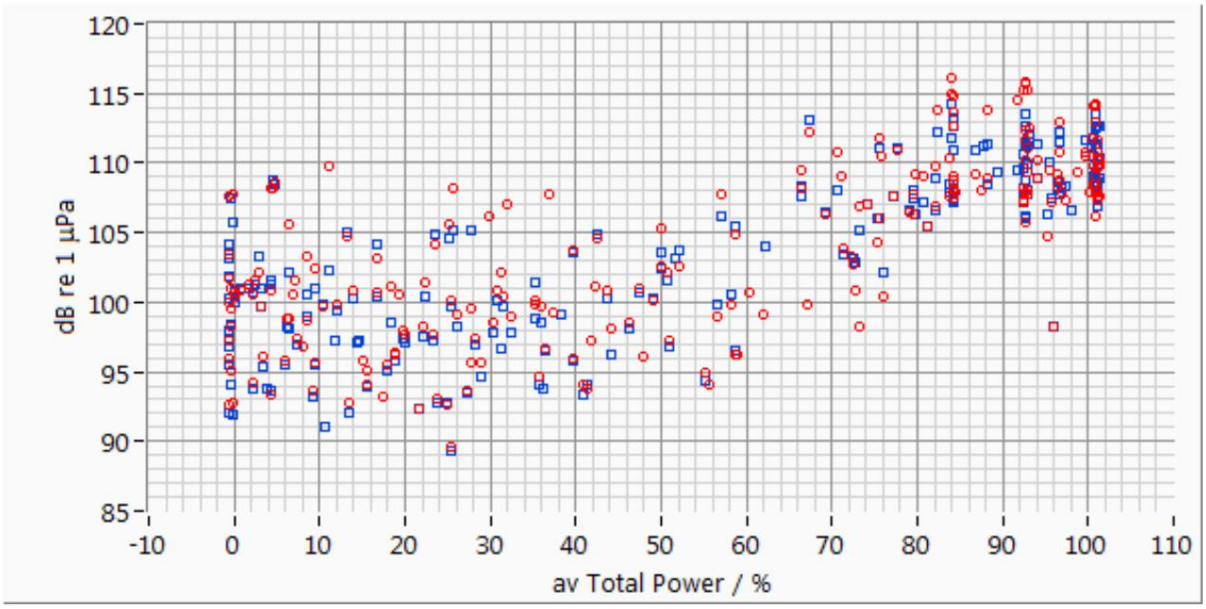

Fig. 7.6.6: Dependence of the peak height (= energetic sum of the corrected lines 89, 90, 91 Hz)
Hydrophone R4-HR1 red circles 228 measurements, hydrophone R4-HR2 blue squares 211 measurements, over total park power (av Total Power) in %

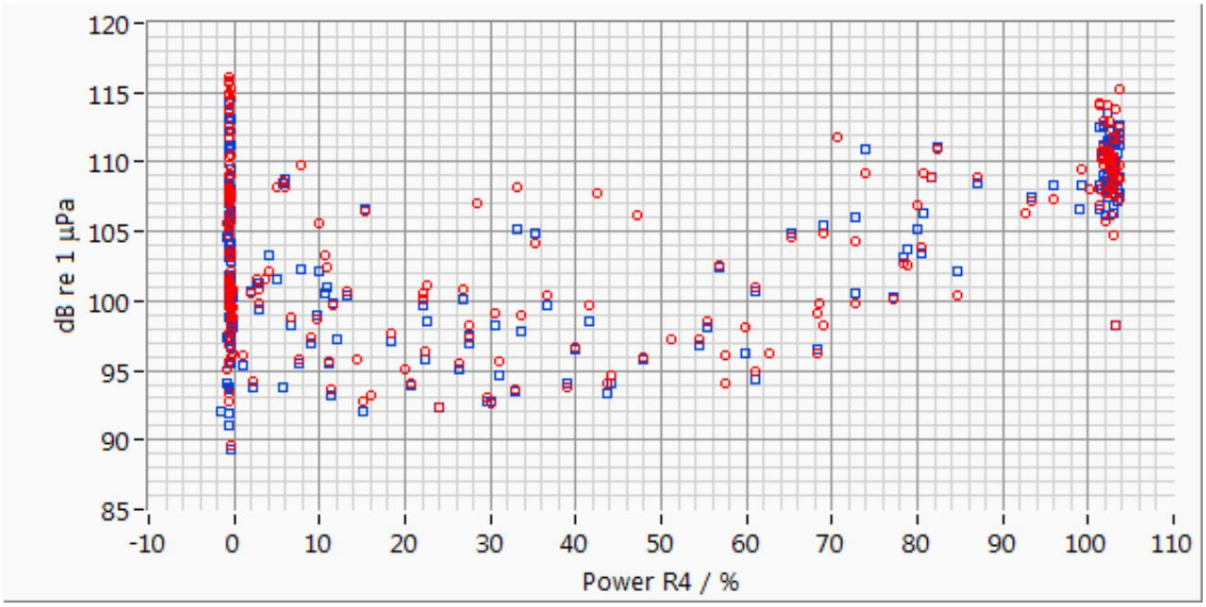

Fig. 7.6.7: Dependence of the peak height (= energetic sum of the corrected lines 89, 90, 91 Hz)
Hydrophone R4-HR1 red circles 227 measurements, hydrophone R4-HR2 blue squares 211 measurements, over power system AV04 in %

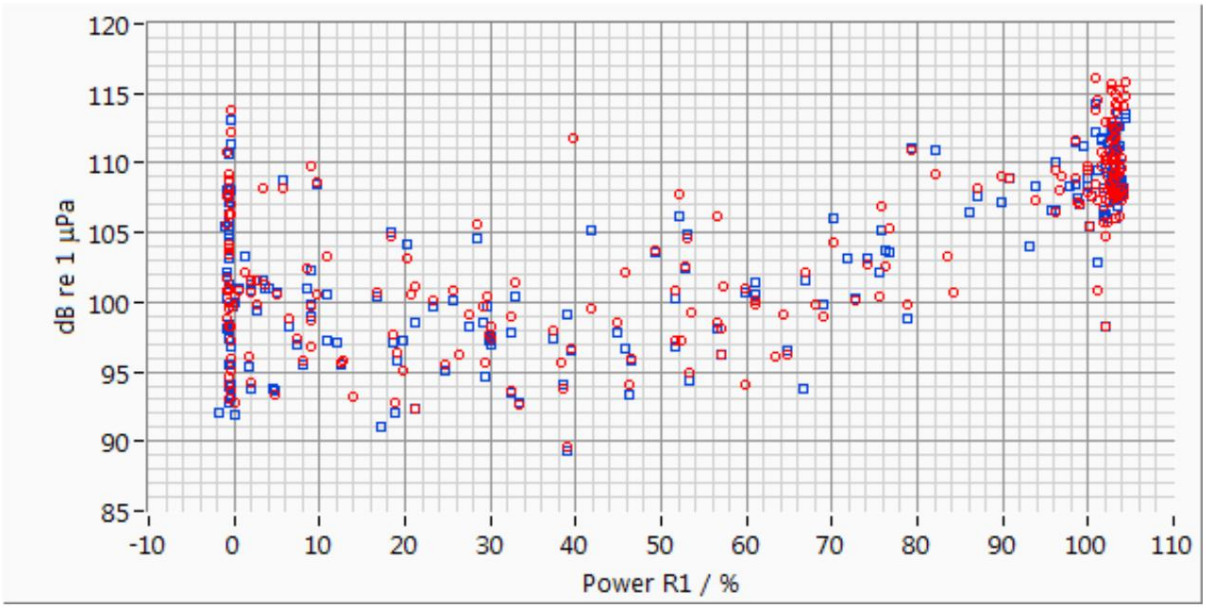

Fig. 7.6.8: Dependence of the peak height (= energetic sum of the corrected lines 89, 90, 91 Hz)
Hydrophone R4-HR1 red circles 226 measurements, hydrophone R4-HR2 blue squares 211 measurements over power system AV01 in %

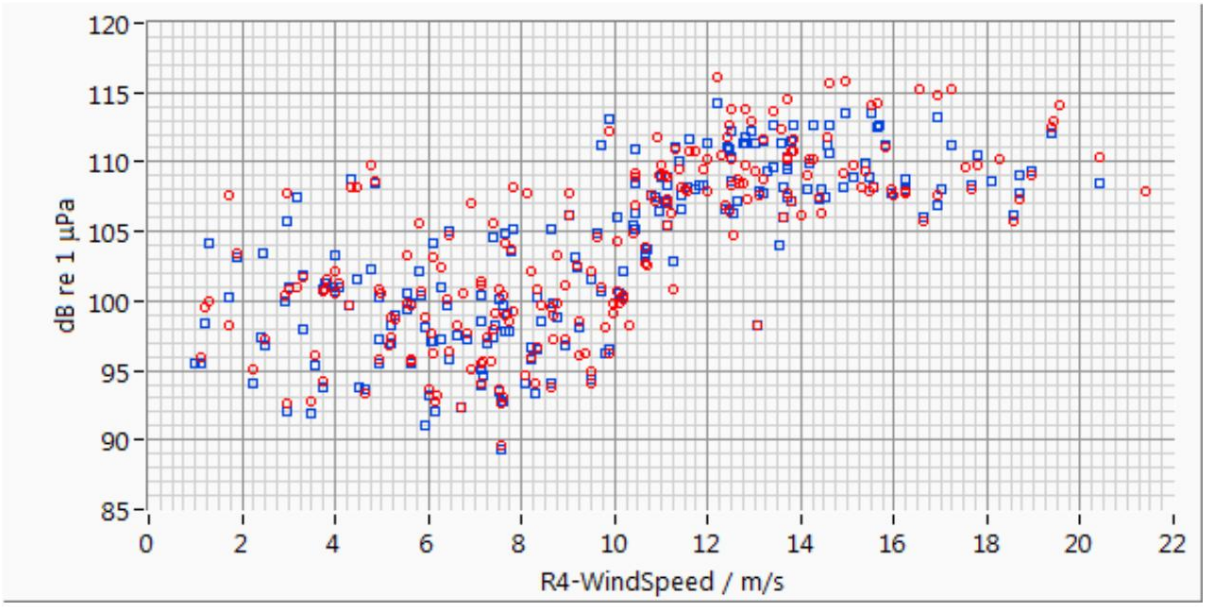

Fig. 7.6.9: Dependence of the peak height (= energetic sum of the corrected lines 89, 90, 91 Hz)
Hydrophone R4-HR1 red circles 223 measurements, hydrophone R4-HR2 blue squares 207 measurements about wind speed Hub height measured on AV04

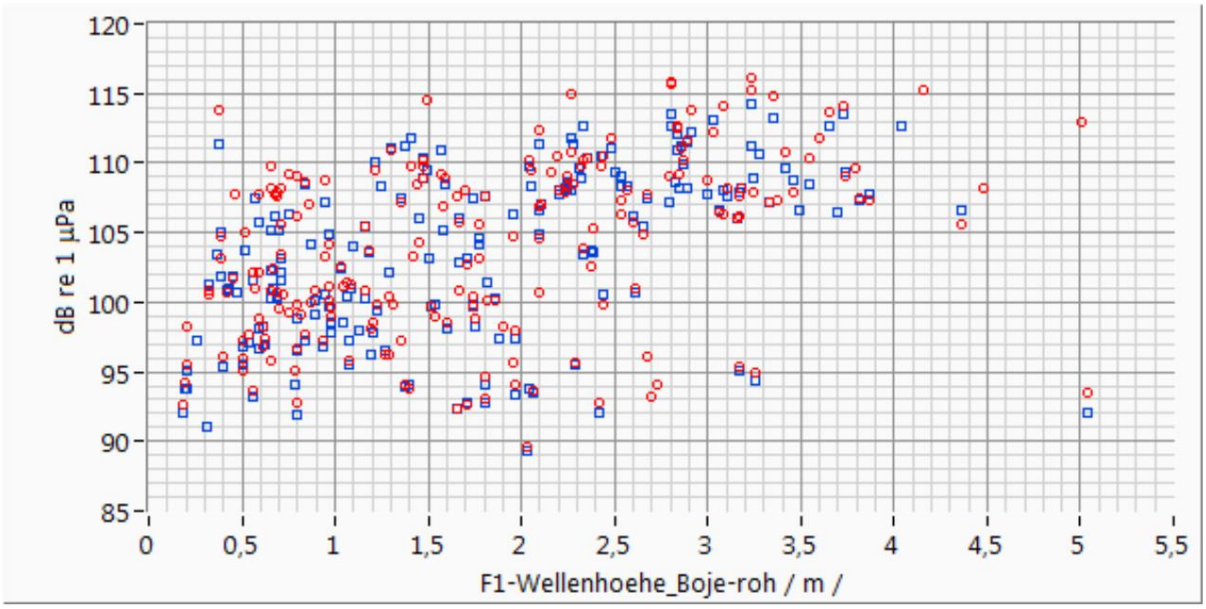

Fig. 7.6.10: Dependence of the peak height (= energetic sum of the corrected lines 89, 90, 91 Hz)
Hydrophone R4-HR1 red circles 203 measurements, hydrophone R4-HR2 blue squares 190 measurements, measured over wave height at FINO1

7.7 Acceleration spectra and sound sources The sound
and acceleration spectra are compared to identify the sound sources.

7.7.1 Sound and acceleration spectra The sound and
acceleration spectra are directly compared. Transfer and coherence functions are also considered. It turns out that coherence functions are suitable to a limited extent and transfer functions are not very suitable for making clear statements. In particular, the transfer functions create the false impression of pseudo-boosts. This is due to the many sources of noise. Overall, it makes sense to look at the spectra involved and use coherence and transfer functions to help identify sound sources.

Three different load cases are examined: 1. System AV04
and System AV07 under high load (both about 80%)
2. AV04 system off and AV07 system under high load 3. AV04 system and
AV07 system at half load (both around 50%)
Finally, the lines are determined according to their sources.

The following individual spectra are used in this section, see Table 7.7.1.1.

Measurement	Wind speed on AV04 [m/s] 11.3 12.2 8.9	wave height [m]	Total	Performance AV07 [%]	Performance AV04 [%]	Performance AV01 [%]
KFS100919-220000R		2.2		85,0	85.0	11,3
KFS110828-220000R		3.2		99,1	-0.5	100,9
KFS111115-040000R		0.9	performance av [%]	67.0	84.1 50.9	54.3 51,5

Tab. 7.7.1.1: Measurements used in this section

1. Plant AV04 and plant AV07 under high load (both about 80%)
Fig. 7.7.1.1 shows narrow-band spectra of 10 to 200 Hz of the sound measured on the hydrophone at a distance of 92 m from the AV04 system, R4-HR1 black line, two acceleration spectra measured on the AV07 system on the underwater traverses M7_A-A15 and M7_A-A14m, for the position, compare Fig. 5.1.2 (there A-A15 and A-A14m on the right), and two acceleration spectra measured on the AV04 system on the cross braces under water, R4-A-W2S1 and R4-A-W2S1_W2, compare Fig. 5.1 .2 (there on the left AW2S1 and A-W2S1/W2). The spectral densities are plotted vertically in Fig. 7.7.1.1 on a logarithmic scale but not in dB. The unit of the sound level scale is Pa^2/Hz, the unit of the acceleration scale is $(m/s^2)^2/Hz$ and multiplied by a factor of 100 for clarity. During the measurement, the wind speed on the AV04 system was 11.3 m/s, the wave height was 2.2 m, the park output was 70%, the output of the AV07 system was 85%, the output of the AV04 system was 85% and the power of the system AV01 11.3% (measurement KFS100919-220000R). Transmission from the AV07 facility to the hydrophone: the sound (black line) clearly shows the peak at 90 Hz and the peak at the same frequency in both accelerations at the AV07 facility (light red and green lines),
while in the two accelerations of the AV04 system (blue and dark
red line) there are no peaks at 90 Hz. This means that the source of the 90 Hz peak is the AV07 system.

The frequencies 22 Hz, 28 Hz, 95 Hz, 120 Hz, 180 Hz, 300 Hz are clearly weaker than other sources. The latter is not shown here.
To a far lesser extent, the 4th, 5th, 7th and 9th harmonics of 90 Hz corresponding to the frequencies 360 Hz, 450 Hz, 630 Hz and 810 Hz can be identified as sources, see Fig. 7.7.1.5. Transmission from the AV04 system to the
hydrophone: A much lower transmission than the AV07 system
can be seen from the AV04 system (Fig. 7.7.1.1) at the frequencies 19 Hz, 38 – 39 Hz and 140 – 150 Hz.

In Fig. 7.7.1.2 the transfer functions of sound to acceleration belonging to the spectra are shown. These initially give the false impression that the sound at 90 Hz is being transmitted amplified by the AV04 system (upper blue and dark red lines, R4-HR1 / R4-A-W2S1 and R4-HR1 / R4-A-W2S1_W2) and no transmission from plant AV07 (lower green and light red lines, R4-HR1 / M7_A-A15 and R4-HR1 / M7_A-A14m). In fact, the latter is transmitted well.

The former is pseudo-enhancement because spectral lines are present in the sound that are not present in the acceleration. A separation of the signals for assignment to different transmission paths using the method of multiple transmission functions (see Bendat, Piersol 1980) is not possible here at present. The transfer function is therefore only suitable for identifying sources in connection with the individual spectra.

The coherence functions are suitable here for making statements about peaks in the spectra. Figures 7.7.1.3 and 7.7.1.4 show the coherence functions between sound and acceleration of the two sensors used here on the AV04 system. In both functions, correlations can be found in the spectra that confirm the statements made about the AV04 system as the source. See the following section for the appearance of the faint coherence line at 90 Hz. The coherence of 0.3 is reached several times and considered significant in connection with the background noise.

In Fig. 7.7.1.5 to 7.7.1.7 the same spectra and transfer functions are shown over the larger frequency range of 10 Hz - 1000 Hz. The above statements on the sources of the sound, which are summarized in Table 7.7.1.2, result from the illustrations, taking into account the property of the transfer functions.

In summary, it is established that the following frequencies are transmitted	
From the AV07 system to the hydrophones	Far less transmission from the AV04 system to the
22 Hz 28 Hz 90 Hz (clearly strongest line) 95 Hz 120 Hz 180 Hz 300 Hz Weak 4th, 5th, 7th, 9th harmonic of 90 Hz corresponding to 360 Hz, 450 Hz, 630 Hz, 810 Hz	hydrophones than with AV07 19 Hz 38 – 39 Hz 140 – 150 Hz

Tab. 7.7.1.2: Sound sources (plants approx. 80% power)

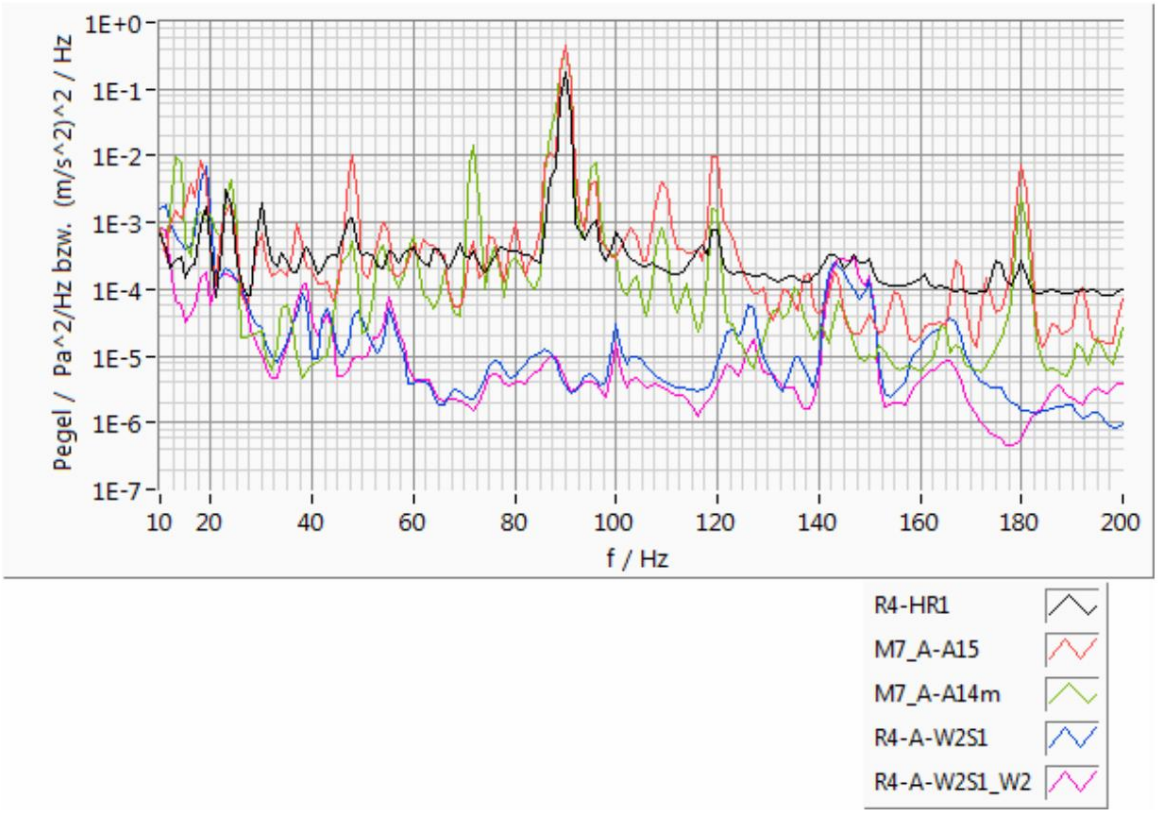

Fig. 7.7.1.1: Narrowband spectra of 1 sound (hydrophone 75 m distance, system AV04, R4-HR1, black line)
2 accelerations of facility AV07 under water (M7_A-A15 and M7_A-A14m, light red and green)
2 accelerations plant AV04 under water (R4-A-W2S1 and R4-A-W2S1_W2, blue and dark red)
Acceleration scale times 100, wind speed 11.3 m/s, power AV07 85%, power AV04 85% Result: 90 Hz peak in sound and acceleration system AV07, not in acceleration system AV04, sound source is system AV07, other sound sources see text (Measurement KFS100919-220000R).

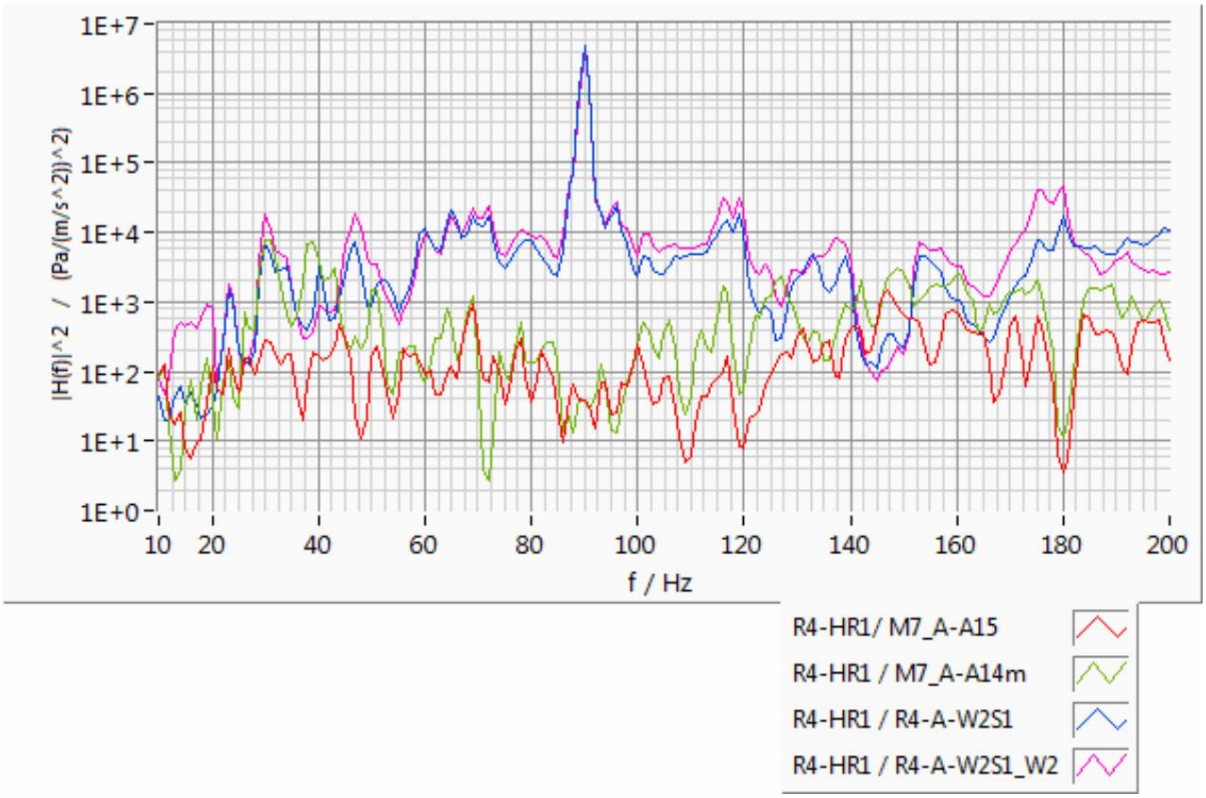

Fig. 7.7.1.2: Transfer functions sound / acceleration to system AV04 with R4-HR1 / R4-A-W2S1 and R4-HR1 / R4-A-W2S1_W2, upper blue and dark red lines to system AV07 with R4-HR1 / M7_A-A15 and R4-HR1 / M7_A-A14m, lower green and light red lines for interpretation see text (measurement KFS100919-220000R)

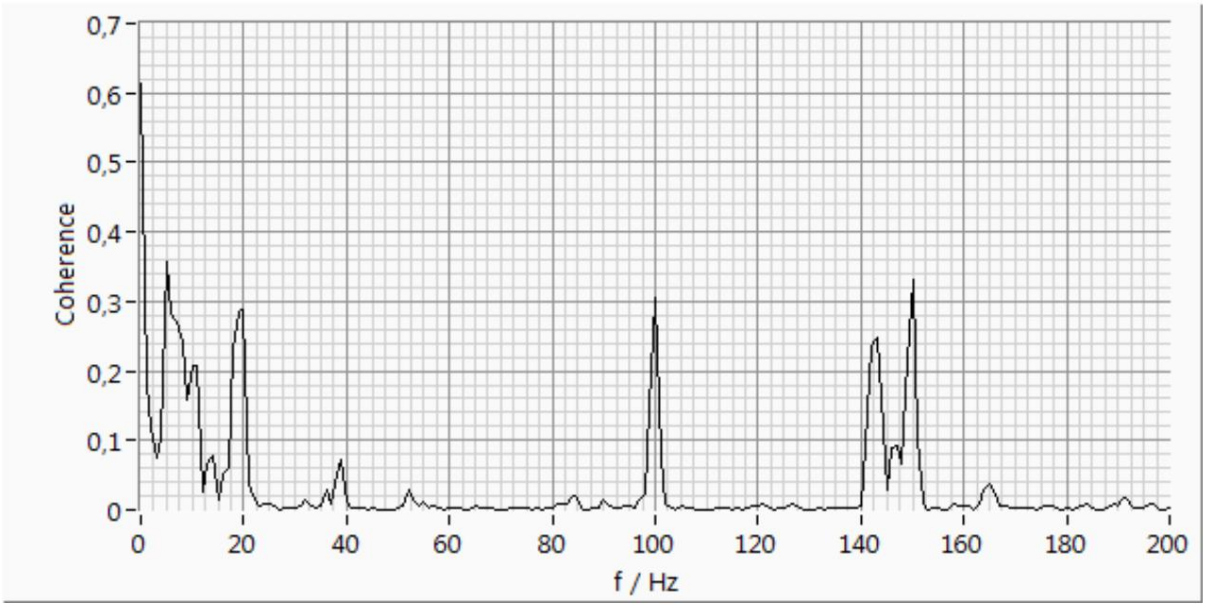

Fig. 7.7.1.3: Coherence function sound to acceleration system AV04 with (R4-HR1 to R4-A-W2S1)
Confirms statements about sources at Annex AV04, see text (measurement KFS100919-220000R)

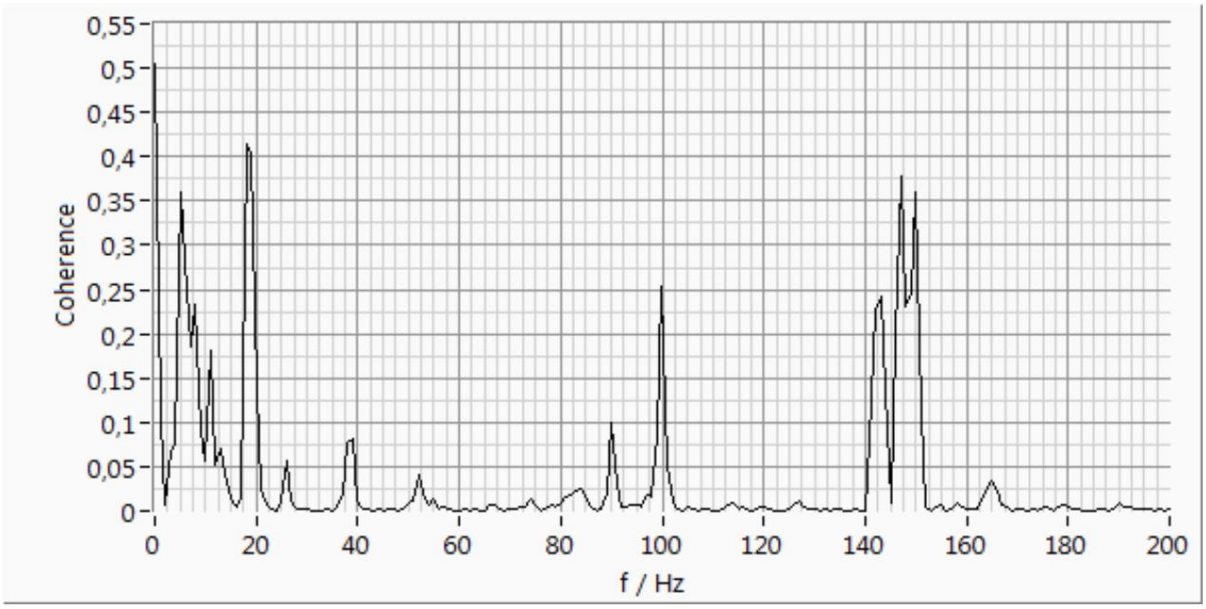

Fig. 7.7.1.4: Coherence function sound to acceleration system AV04 with (R4-HR1 to R4-A-W2S1_W2)
Confirms statements about sources at Annex AV04, see text (measurement KFS100919-220000R)

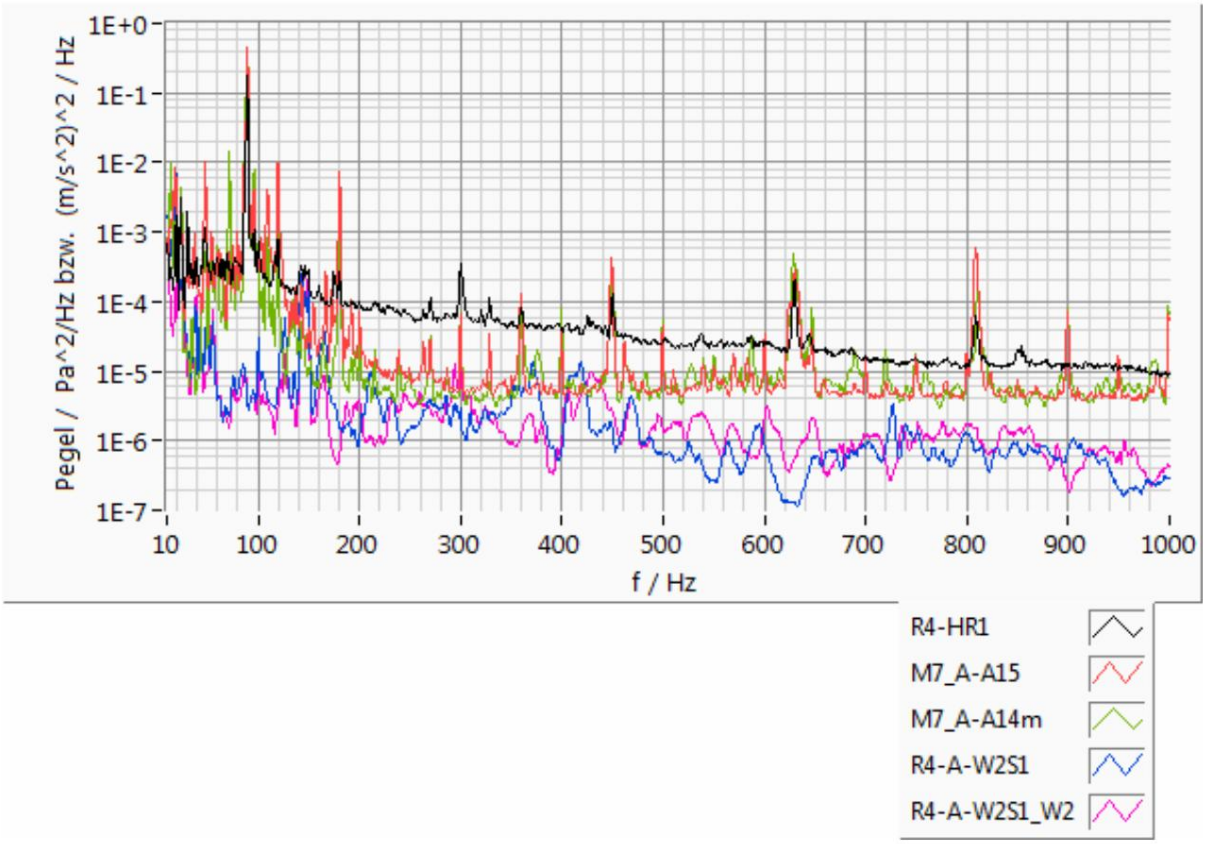

Fig. 7.7.1.5: Narrow band spectra of 1
sound (hydrophone 75 m distance, system AV04, R4-HR1, black line)
2 accelerations of facility AV07 under water (M7_A-A15 and M7_A-A14m, light red and green)
2 accelerations plant AV04 under water (R4-A-W2S1 and R4-A-W2S1_W2, blue and dark red)
As above but frequency range up to 1000 Hz (measurement KFS100919-220000R)

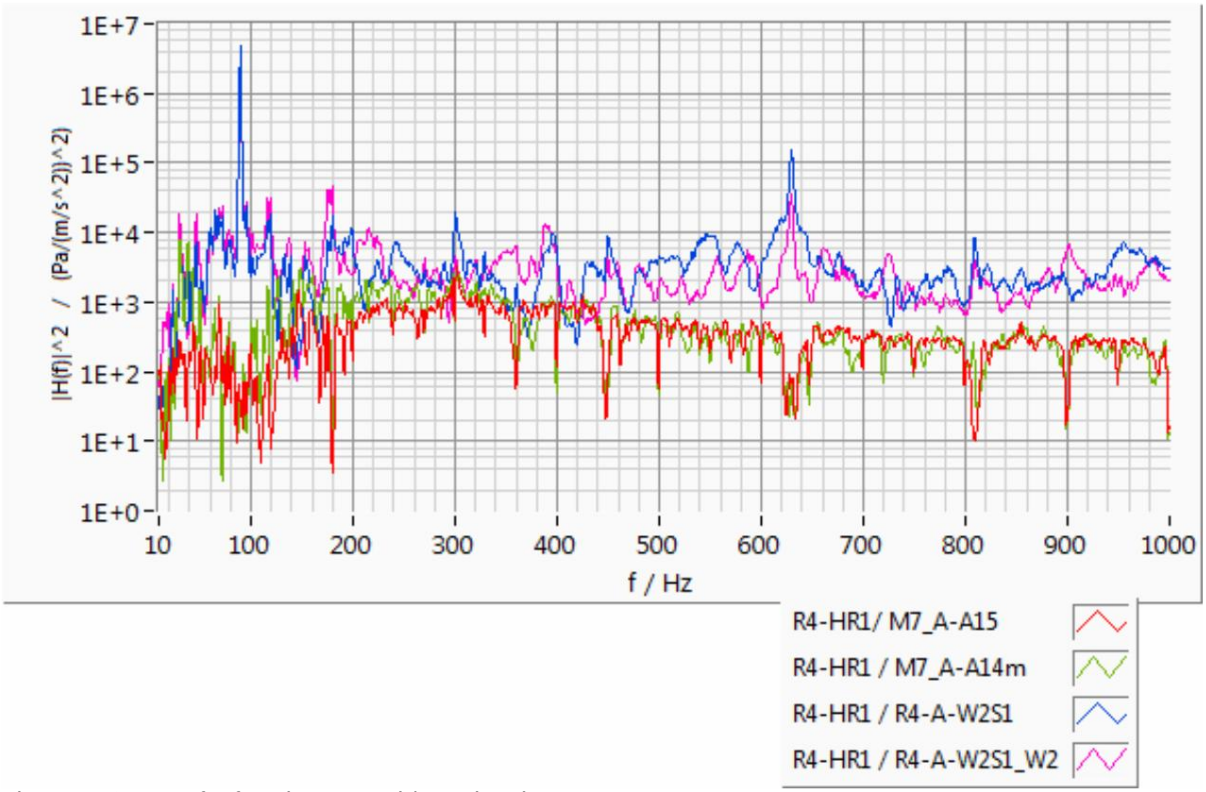

Fig. 7.7.1.6: Transfer functions sound / acceleration to system
AV04 with R4-HR1 / R4-A-W2S1 and R4-HR1 / R4-A-W2S1_W2, upper blue and dark red lines to system
AV07 with R4-HR1 / M7_A-A15 and R4-HR1 / M7_A-A14m, lower green and light red lines As above
but frequency range up to 1000 Hz (measurement KFS100919-220000R)

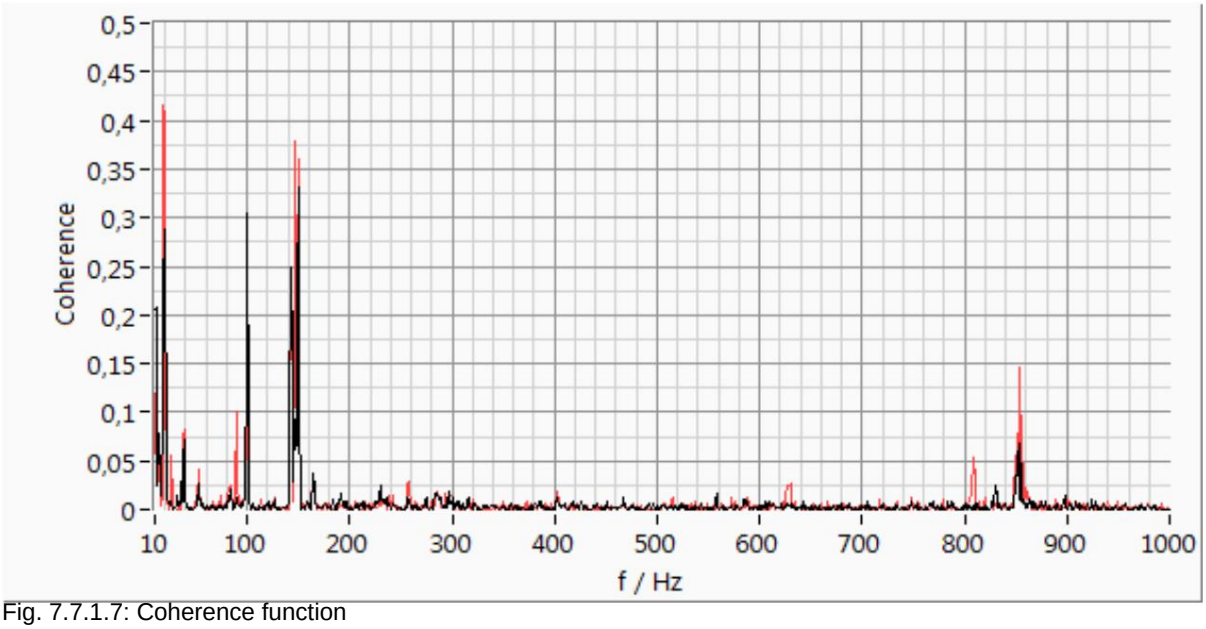

Fig. 7.7.1.7: Coherence function
sound to acceleration system AV04 (R4-HR1 to R4-A-W2S1 black line) to
acceleration system AV04 (R4-HR1 to R4-A-W2S1_W2) red line) Similar
to above but frequency range up to 1000 Hz (measurement KFS100919-220000R)

2. System AV04 switched off and system AV07 under high load In the following,
sound and acceleration spectra are compared with the 92 m distant system AV04 switched off.

During the measurement, the wind speed on the AV04 turbine was 12.2 m/s, the wave height was 3.2 m, the park capacity was 84.1%, the capacity of the AV07 turbine was 99.1%, the capacity of the AV04 turbine was -0.5 %, the performance of the AV01 system 109.9% (measurement KFS110828-220000R).

Fig. 7.7.1.8 shows narrow-band spectra of the two hydrophones at the AV04 facility (red line R4-HR1 and blue line R4-HR2). The AV07 facility is 785 m and 791 m away respectively. The AV01 facility is 806 m and 824 m away respectively. There is good agreement between the two hydrophones.
Fig. 7.7.1.9 shows narrowband spectra of sound from a hydrophone, R4-HR1 black line, two acceleration spectra measured at facility AV07, light red line and green lines M7_A A15 and M7_A-A14m, and two acceleration spectra measured at facility AV04, blue line and dark red line R4-A-W2S1 and R4-A-W2S1_W2. The accelerations, units $(m/s^2)^2/Hz$, are multiplied by 100. The peak at 90 Hz can again be clearly seen in the sound (black line) and in the accelerations on the AV07 system (light red and green lines). The 2nd harmonic can be found in the accelerations at 180 Hz (light red and green lines), but not in the sound.
Fig. 7.7.1.10 shows the associated transfer functions.
Fig. 7.7.1.11 shows the coherence function of the hydrophone for the two acceleration sensors used here on the AV04 facility, black line R4-A-W2S1 and red line R4-A-W2S1_W2. There is weak coherence e.g. B. at 90 Hz, although the AV04 system is switched off. The authors interpret that the transmission is the other way around here, ie that sound from the water is converted into acceleration at the facility. In other words, the accelerometer facility works as a hydrophone. The effect is so weak that it cannot be seen in the acceleration spectrum. The loud piling noise signals, not shown here, can be clearly "heard" with the acceleration sensors under water on the foundation.

Fig. 7.7.1.12 shows the spectra of the two hydrophones up to 1000 Hz and Fig. 7.7.1.13 up to 3000 Hz. The hydrophones measure identically. The spectral density falls continuously apart from individual peaks, some of which can be traced back to harmonic multiples of 90 Hz, see above.
Fig. 7.7.1.14 shows the sound spectrum as narrow band spectra up to 1000 Hz, R4-HR1 black line, two acceleration spectra of the AV07 system, light red line and green line M7_A-A15 and M7_A A14m, and two acceleration spectra of the AV04 system, blue line and dark red line R4-A W2S1 and R4-A-W2S1_W2. The accelerations, units $(m/s^2)^2/Hz$, are multiplied by 100. The 90 Hz peak and some harmonics can be seen in the sound and acceleration spectra of the AV07 system, which therefore have their origin in the AV07 system.
Fig. 7.7.1.15 shows the associated transfer functions.

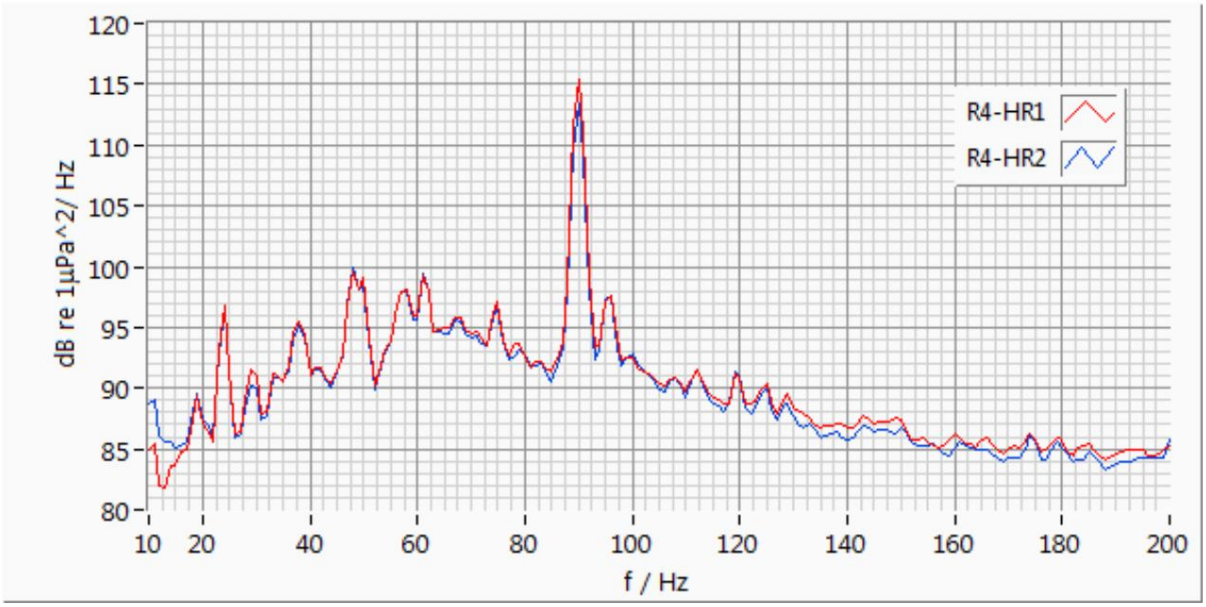

Fig. 7.7.1.8: Narrow band spectra of 2
hydrophone system AV04 (red line R4-HR1, blue line R4-HR2)
Distance to system AV07 765 m or 775 m, system AV01 822 or 831 m Result: good agreement
between the two sound spectra (measurement KFS110828-220000R)

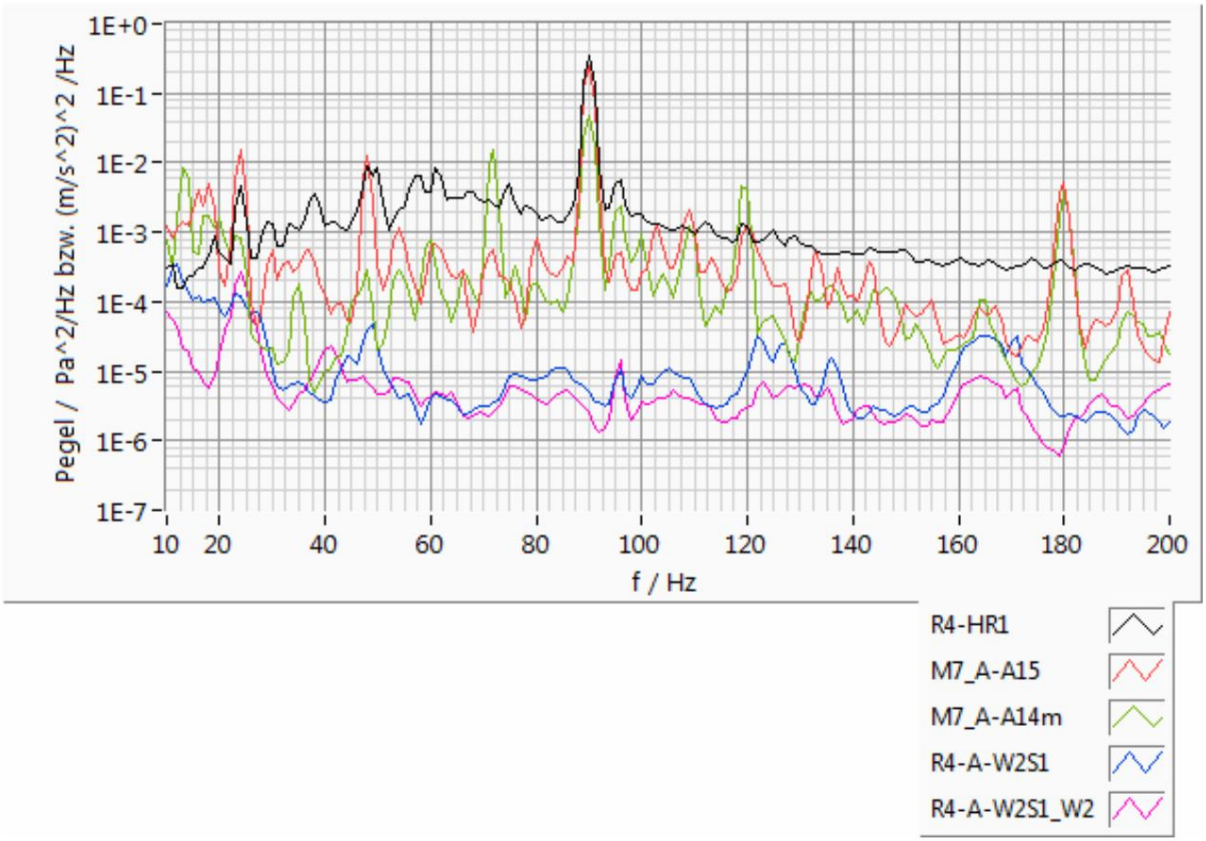

Fig. 7.7.1.9: Narrow band spectra, system AV07 power 99.1%, system AV04 from 1 hydrophone black line R4-HR1 2 acceleration spectra AV07, light red line M7_A-A15 and green line M7_A-A14m 2 acceleration spectra AV04, blue line R4-A -W2S1 and dark red line R4-A-W2S1_W2 Accelerations ((m/s²)²/Hz) multiplied by 100 Result: peak at 90 Hz source AV07 (measurement KFS110828-220000R)

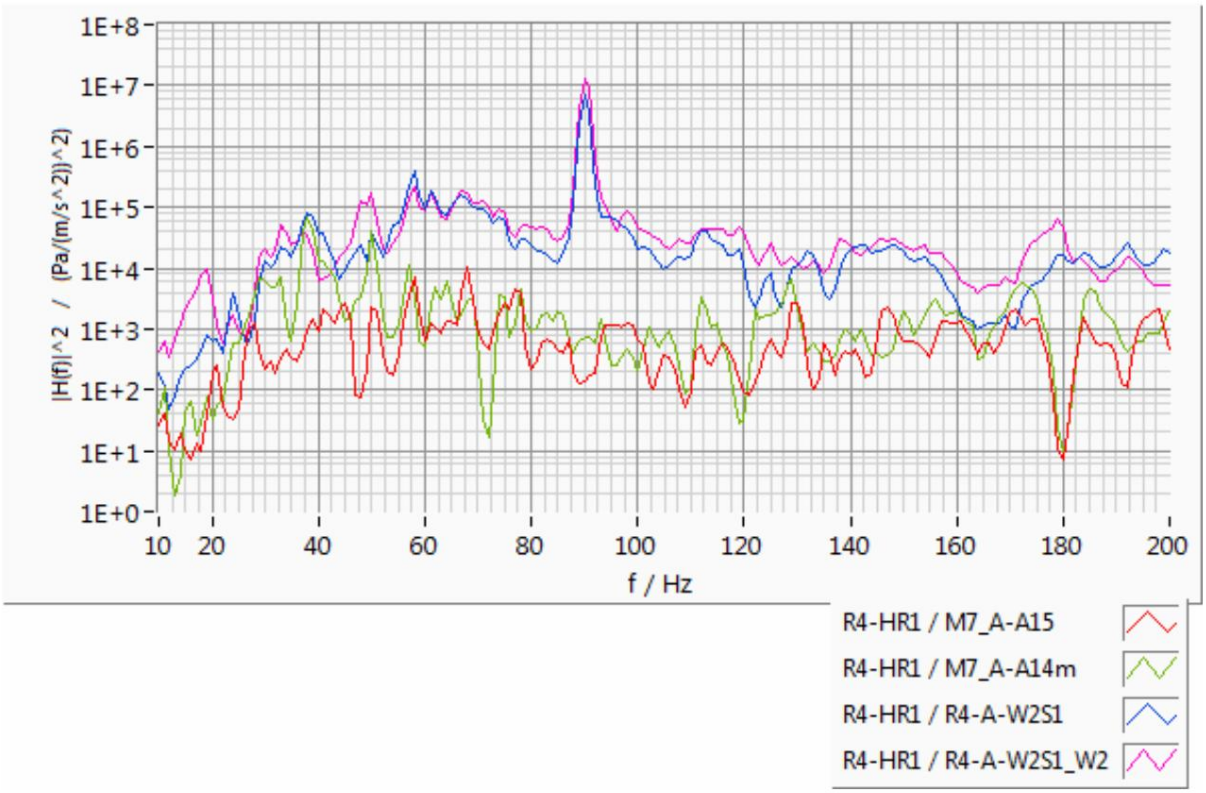

Fig. 7.7.1.10: Transfer functions sound / acceleration to system AV04 with R4-HR1 / R4-A-W2S1 and R4-HR1 / R4-A-W2S1_W2, upper blue and dark red lines to system AV07 with R4-HR1 / M7_A-A15 and R4-HR1 / M7_A-A14m, lower green and light red lines, system AV07 power 99.1%, system AV04 off (measurement KFS110828-220000R)

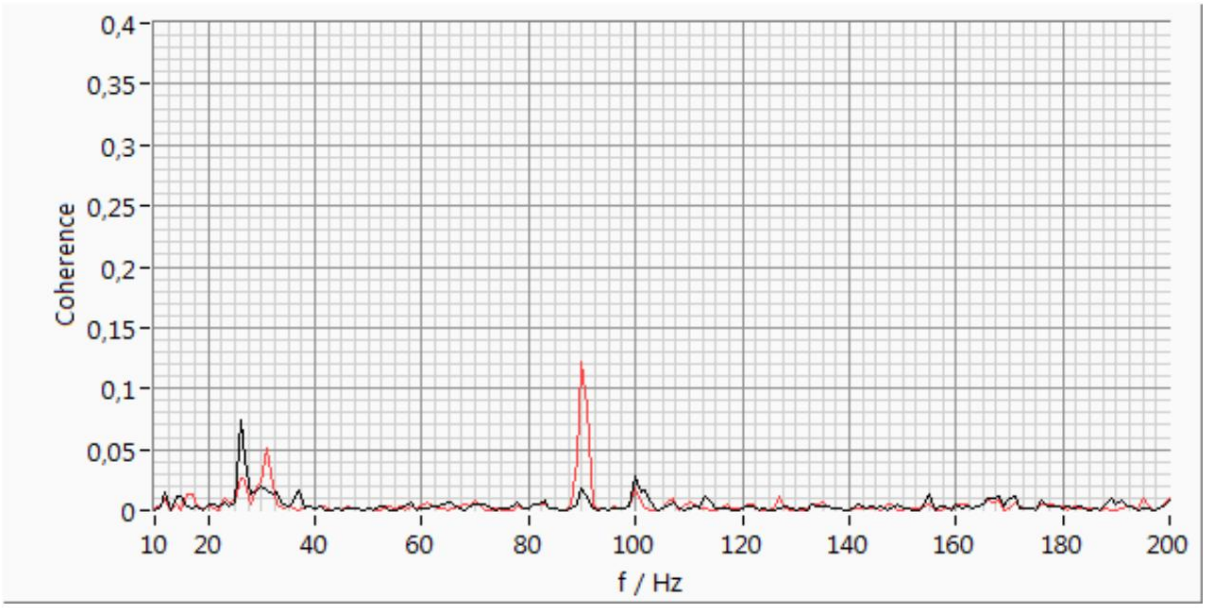

Fig. 7.7.1.11: Coherence function sound / acceleration for system AV04 with R4-HR1 / R4-A-W2S1_W2, red line for system AV04 with R4-HR1 / R4-A-W2S1, black line Result: waterborne noise generates weak acceleration in the Underwater structure of the AV04 system AV07 system output 99.1%, AV04 system off (measurement KFS110828-220000R)

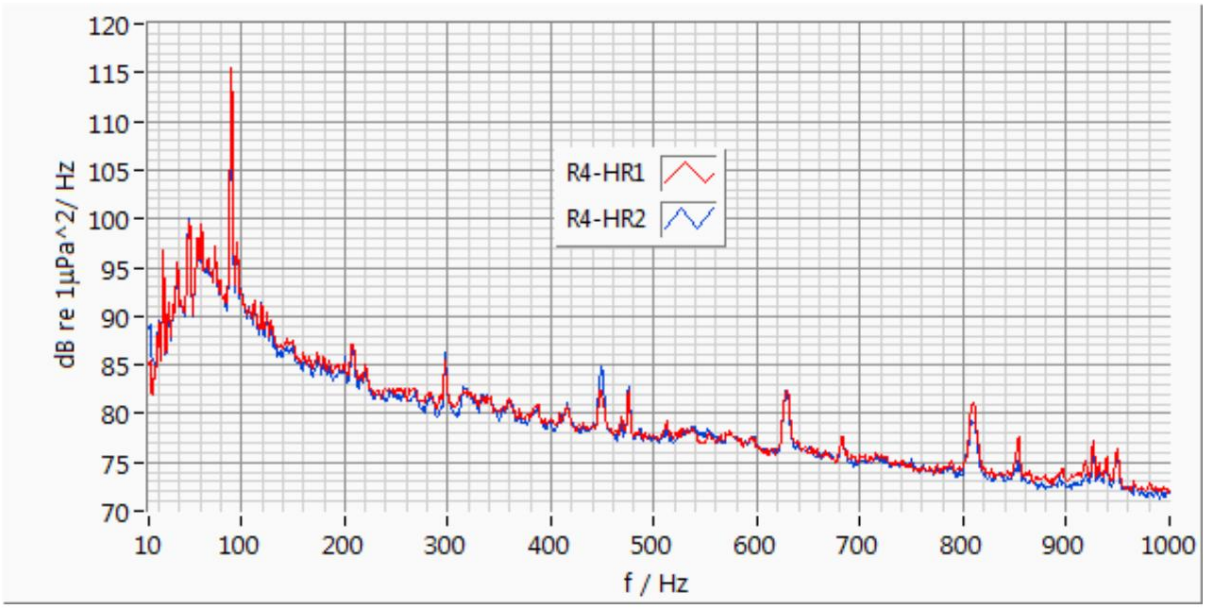

Fig. 7.7.1.12: Narrow-band spectra of 2 hydrophones at AV04 Result: good agreement, spectral density decreases, individual peaks in part harmonics of 90 Hz AV07 system power 99.1%, AV04 system off (measurement KFS110828-220000R)

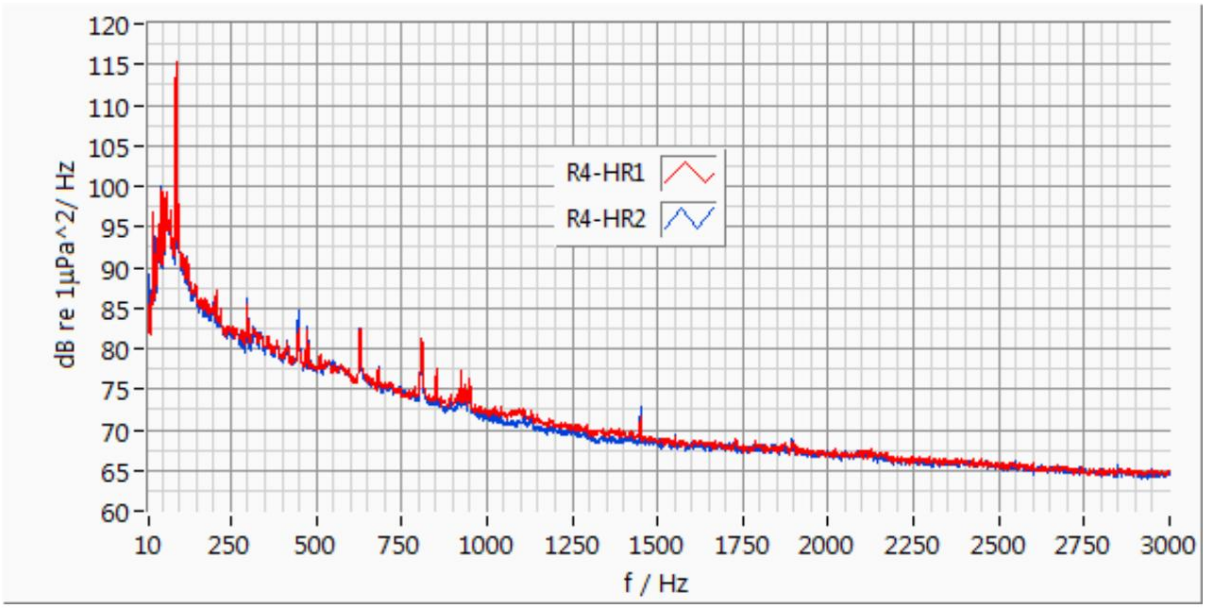

Fig. 7.7.1.13: Narrow-band spectra of 2
hydrophones at AV04 Result:
good agreement, spectral density decreases, individual peaks in part harmonics of 90 Hz system AV07 power 99.1%, system AV04 off
(measurement KFS110828-220000R)

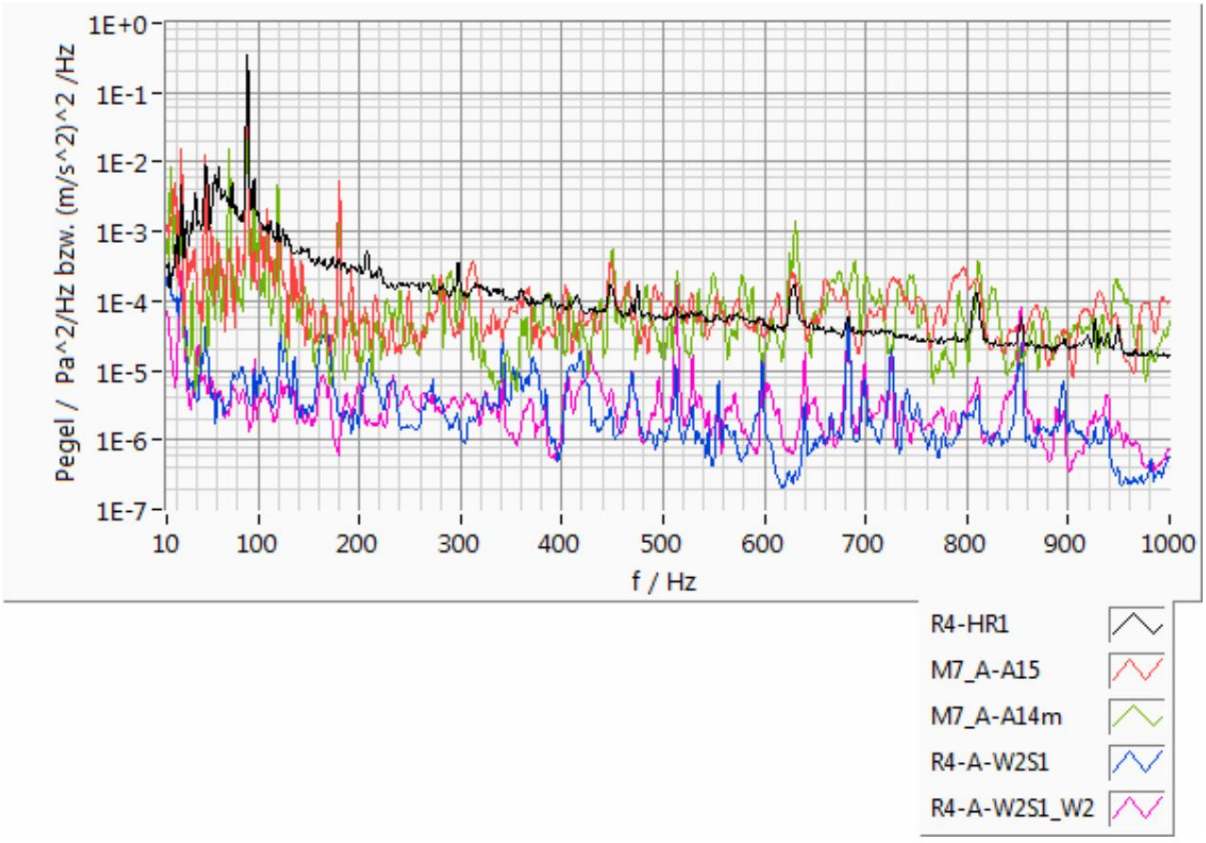

Fig. 7.7.1.14: Narrow band spectra 1
hydrophone black line R4-HR1 2 acceleration
spectra AV07, light red line M7_A-A15 and green line M7_A-A14m 2 acceleration spectra AV04, blue line R4-A-
W2S1 and dark red line R4-A-W2S1_W2 accelerations ((m/s²)²/Hz) multiplied by 100 Result: Peak at 90 Hz and harmonics
Source AV07 system AV07 power 99.1%, system AV04 off
(measurement KFS110828-220000R)

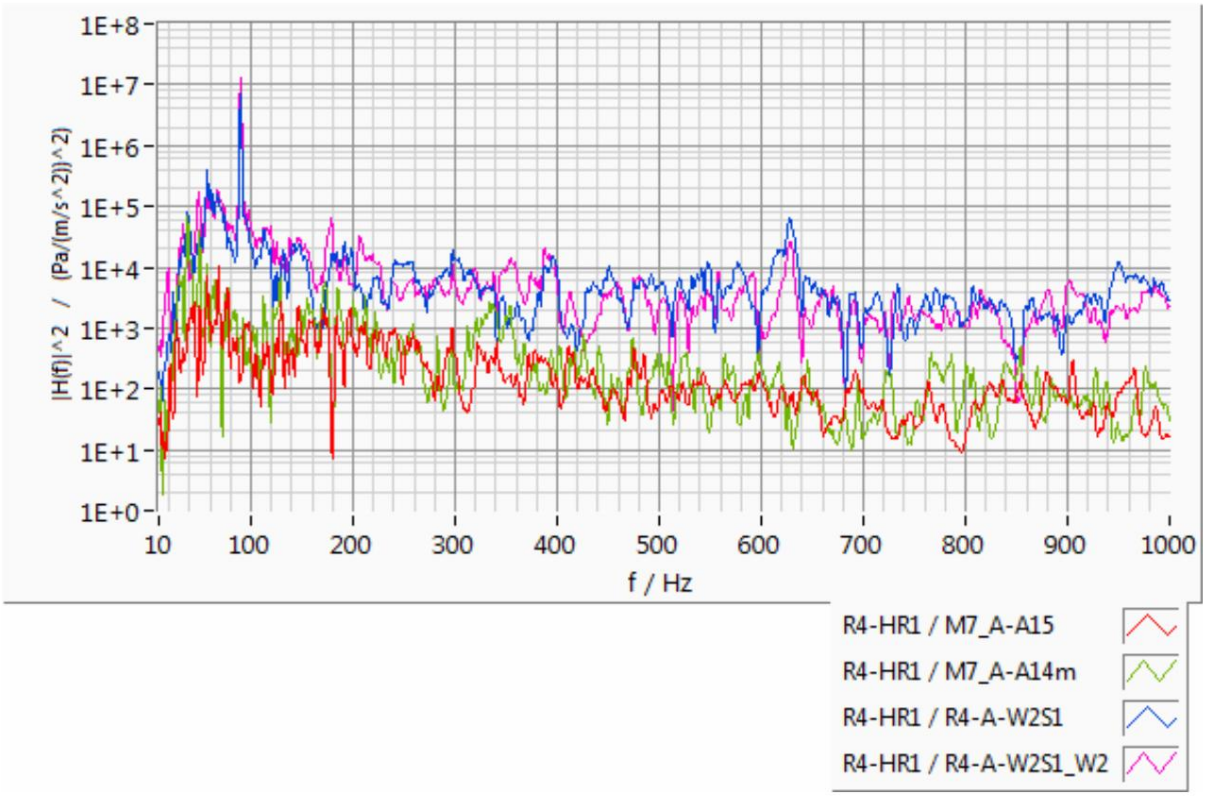

Fig. 7.7.1.15: Transfer functions sound / acceleration to system AV07 with R4-HR1 / M7_A-A15 and R4-HR1 / M7_A-A14m, lower green and light red lines to system AV04 with R4-HR1 / R4-A-W2S1 and R4-HR1 / R4-A-W2S1_W2, upper blue and dark red lines, AV07 system output 99.1%, AV04 system off (measurement KFS110828-220000R)

3. Plant AV04 and plant AV07 at half load (both about 50%)

The sound and acceleration spectra are compared below, with both systems, AV07 and AV04, each running at half power.

During the measurement, the wind speed on the AV04 turbine was 8.9 m/s, the wave height was 0.9 m, the park output was 50.9%, the outputs of the AV07 turbines were 55.0%, AV04 54.3%, AV01 51%, 5% (measurement KFS111115-040000R).

Fig. 7.7.1.16 shows the narrow-band spectra of the two hydrophones at the AV04 facility (red line R4-HR1 and blue line R4-HR2). The spectra show surprisingly good agreement. The differences for frequencies below 20 Hz are obviously due to flow separation at the hydrophone R4-HR1 due to a local wave-induced flow. If the AV04 system were the only sound source, the difference between the two hydrophones would be 3.5 dB. The small difference points to the relatively small part of the AV04 system with a relatively high proportion of noise from the wind farm and from the background.

Fig. 7.7.1.17 shows narrowband spectra of sound from a hydrophone, R4-HR1 black line, two acceleration spectra measured at facility AV07, light red line and green lines M7_A A15 and M7_A-A14m, and two acceleration spectra measured at facility AV04, blue line and dark red line R4-A-W2S1 and R4-A-W2S1_W2. The sound level scale is entered on the left in Pa^2/Hz, the acceleration scale is entered on the right in $(m/s^2)^2/Hz$. The AV07 system does not emit at 90 Hz but at 80 Hz. All three spectra (black, light red, green line) form a peak. The AV04 system emits weakly at 138 Hz. All three spectra (black, blue, dark red line) form a peak. The plant AV04 continues to emit at 18 Hz.

The transfer function does not contain any further information and is not shown.

Fig. 7.7.1.18 shows the coherence function of the hydrophone closer to facility AV04 to the two accelerometers on facility AV04, red line R4-A-W2S1_W2 and black line

R4-A-W2S1. Here the relationships between the frequencies at 136 Hz and especially at 18 Hz are clear.

Fig. 7.7.1.19 shows the spectra of the two hydrophones up to 1000 Hz. The hydrophones measure identically. The spectral density falls almost continuously.

Fig. 7.7.1.20 shows the sound spectrum as narrow band spectra up to 1000 Hz, R4-HR1 black line, two acceleration spectra of the AV07 system, light red line and green line M7_A-A15 and M7_A-A14m, and two acceleration spectra of the AV04 system, blue line and dark red line R4-A-W2S1 and R4-A-W2S1_W2. The accelerations $(m/s^2)^2/Hz$ are multiplied by 100. The peak group from 630 to 650 Hz can be found in the sound and acceleration spectra of the AV07 system.

The transfer function is not shown.
The coherence function is not shown.
Determining the peaks is relatively difficult. In summary, the following results: The AV04 system emits at 17.9 Hz, 136.5 Hz, 730 Hz.
The AV07 system emits at 80 Hz, 630 – 650 Hz.
The 45-65 Hz peak group could be divided into AV04 with 45-55 Hz and AV07 with 55-65 Hz and the peak at 37.5 Hz (with weak peak at A-A15) could be generated by AV04 and AV07 or issued by one or more other investments.

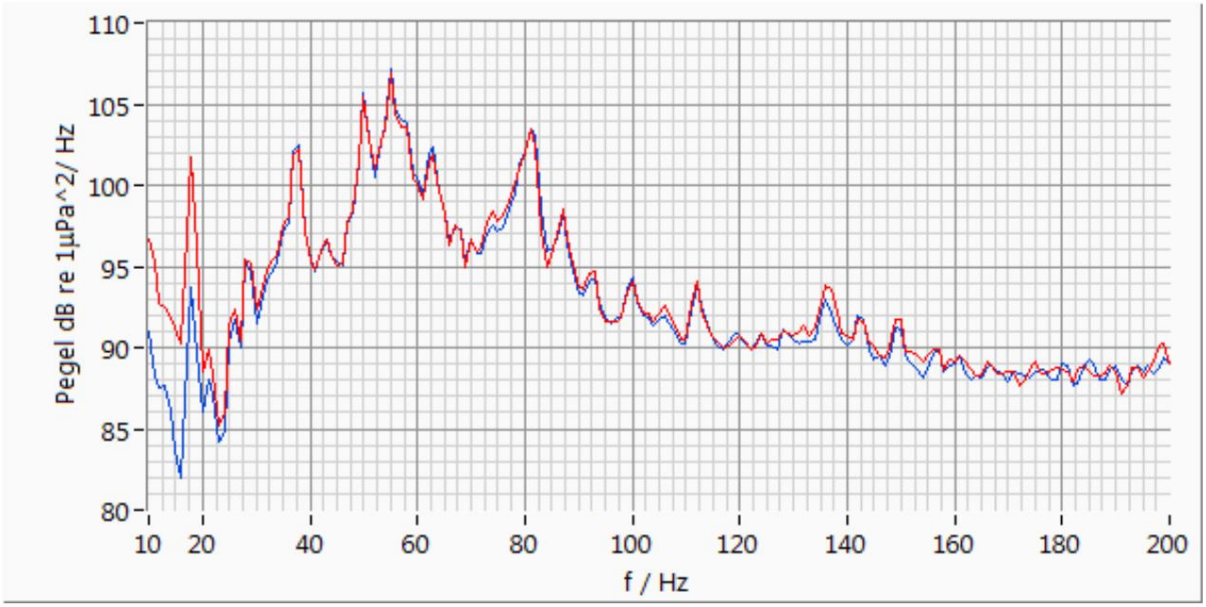

Fig. 7.7.1.16: Narrow band spectra of 2 hydrophone system AV04 (red line R4-HR1, blue line R4-HR2) Distance to system AV04 75 m or 136 m, system AV07 765 m or 775 m Result: agreement, red line 61 m closer to the next system AV04 than blue line Power system AV07 and system AV04 approx. 50% (measurement KFS111115-040000R)

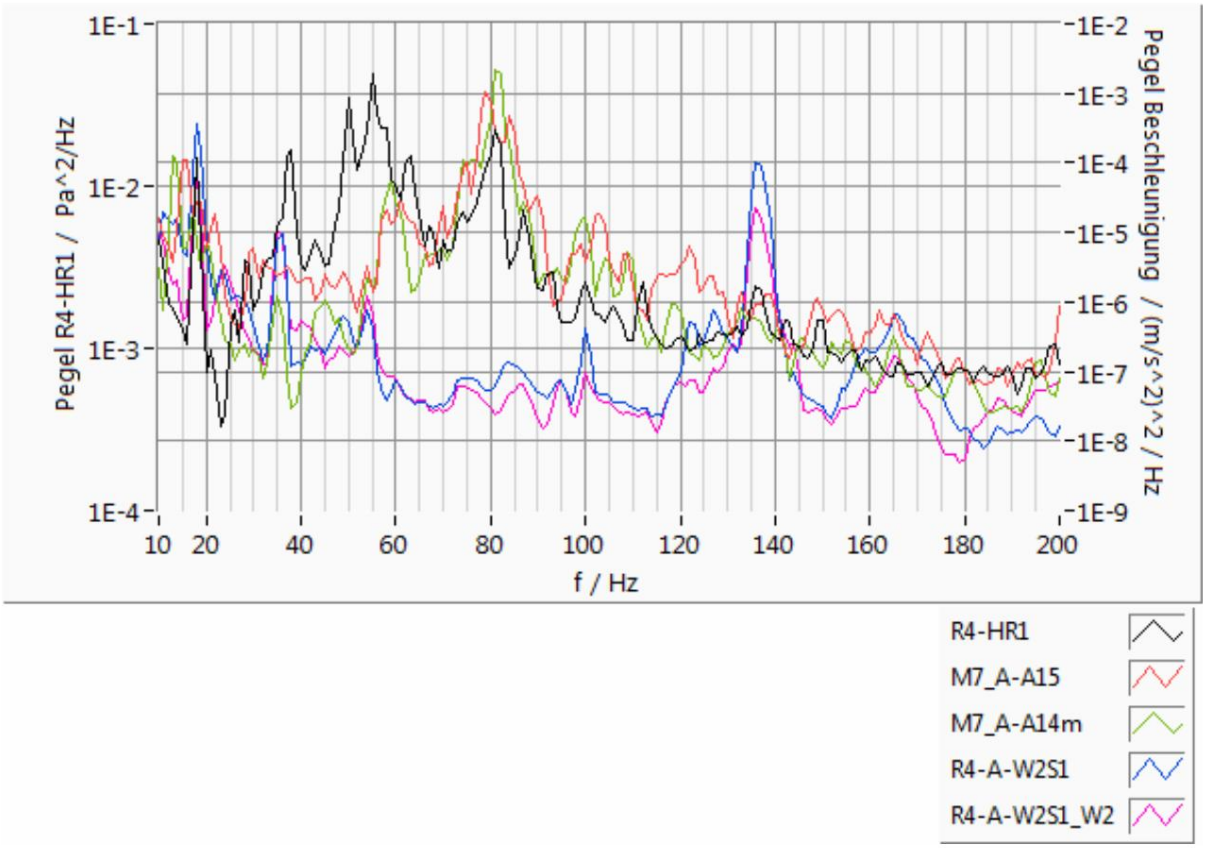

Fig. 7.7.1.17: Narrow band spectra 1
hydrophone black line R4-HR1 2 acceleration
spectra AV07, light red line M7_A-A15 and green line M7_A-A14m 2 acceleration spectra AV04, blue line R4-A-
W2S1 and dark red line R4-A-W2S1_W2 hydrophone scale left , acceleration scale on the right Result: AV07 does not
emit strongly at 90 Hz but weakly at 80 Hz, system AV04 emits
weakly at 18 Hz, 2x 18 Hz and 138 Hz, power of system AV07 and system AV04 approx. 50% (measurement KFS111115-040000R)

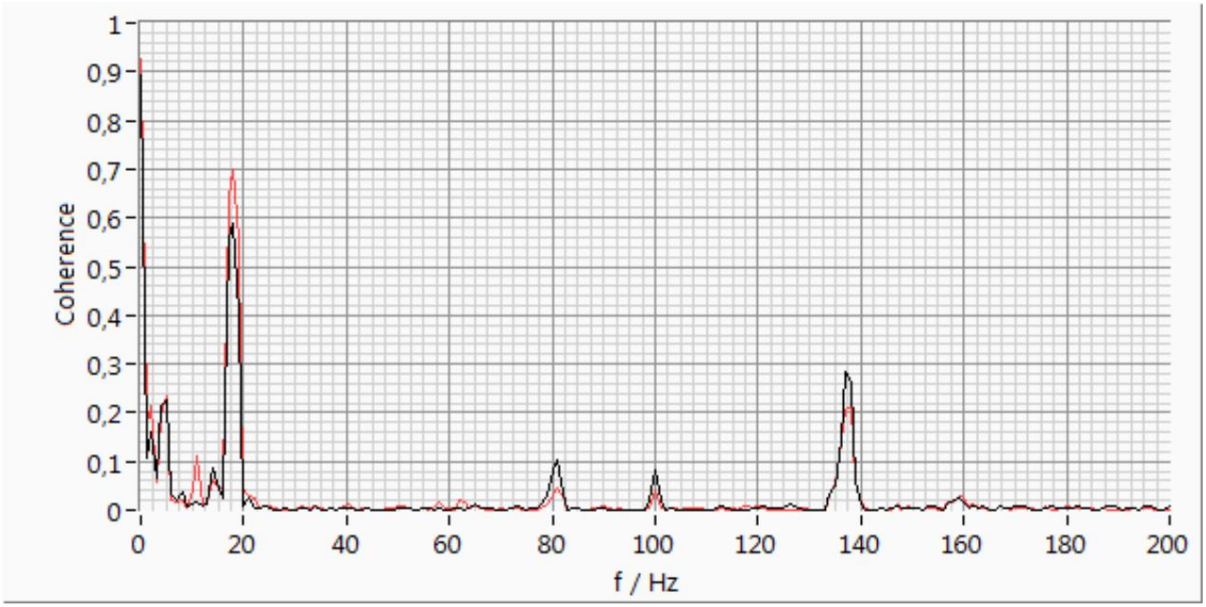

Fig. 7.7.1.18: Coherence function sound / acceleration for system AV04
with R4-HR1 / R4-A-W2S1_W2, red line for system AV04 with R4-HR1 /
R4-A-W2S1, black line Result: System AV04 emits at 138 Hz and 18 Hz
system AV07 power 55.0%, system AV04 54.3% (measurement
KFS111115-040000R)

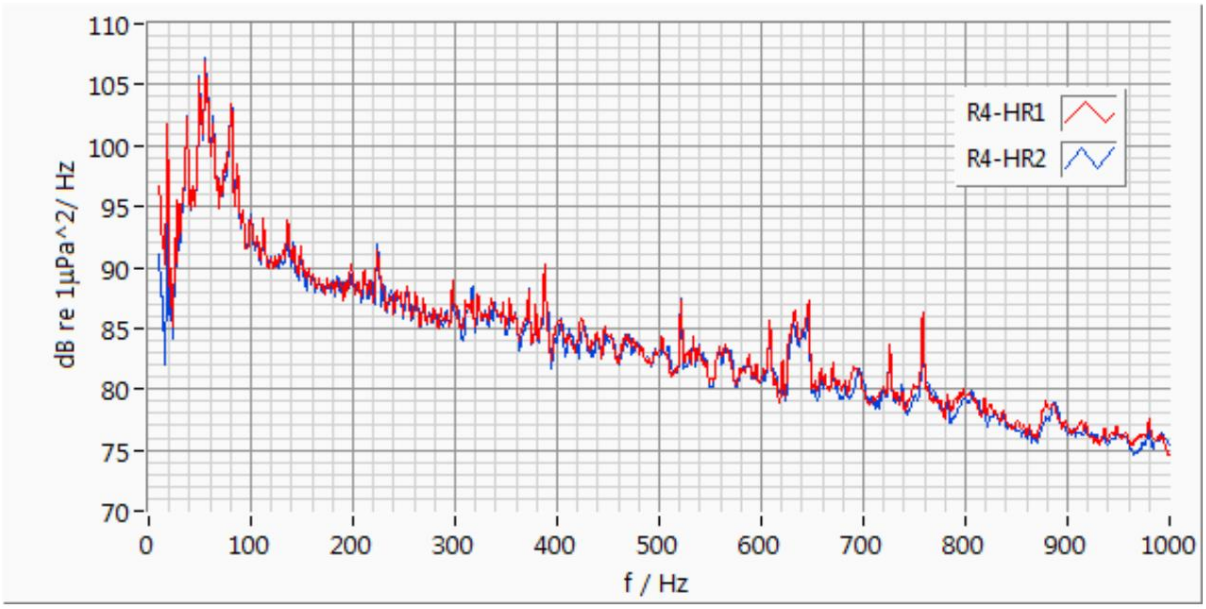

Fig. 7.7.1.19: Narrow band spectra of 2
hydrophones at AV04 Result:
agreement, spectral density decreases, individual peaks plant AV07 power 55.0%, plant
AV04 54.3% (measurement KFS111115-040000R)

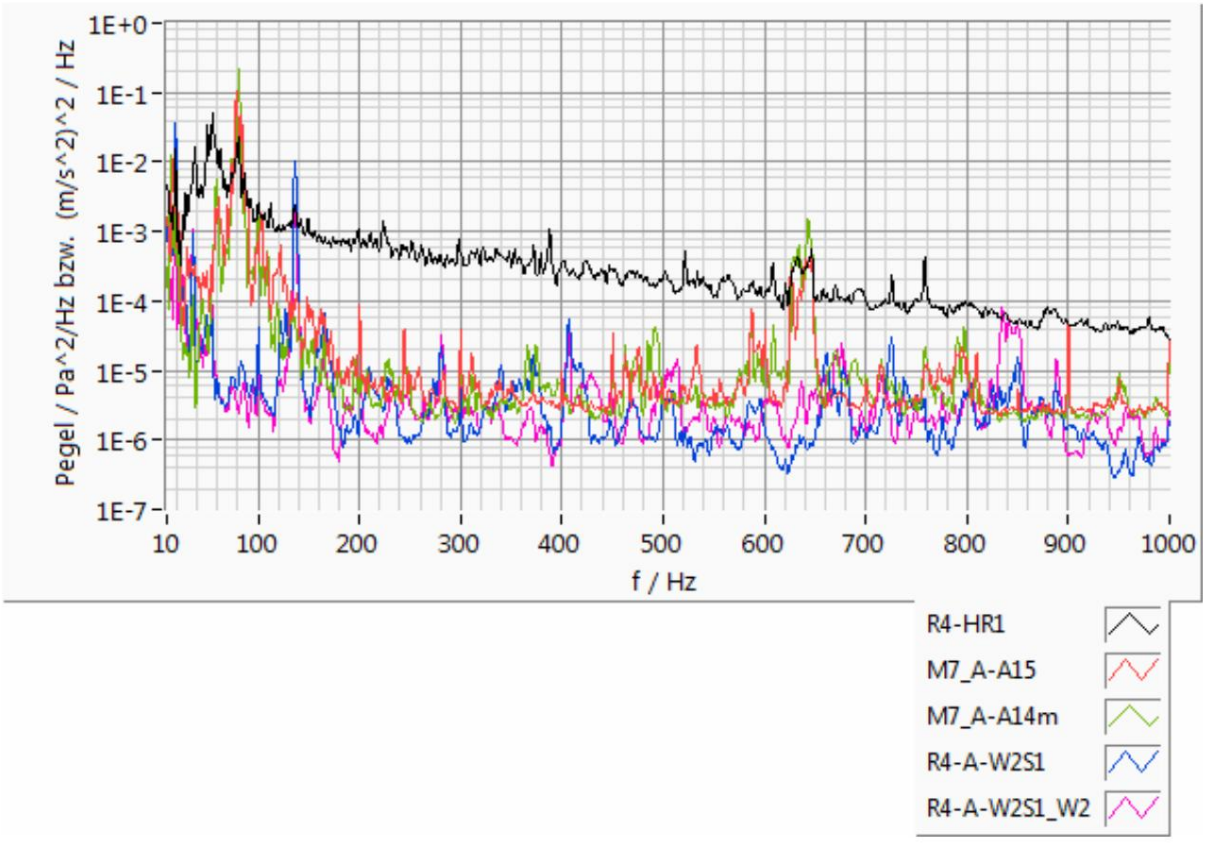

Fig. 7.7.1.20: Narrow band spectra 1
hydrophone black line R4-HR1 2 acceleration
spectra AV07, light red line M7_A-A15 and green line M7_A-A14m 2 acceleration spectra AV04, blue line R4-A-
W2S1 and dark red line R4-A-W2S1_W2 accelerations ((m/s²)²/Hz) multiplied by 100 Result: Peak group 630 - 650 Hz
source AV07 system AV07 power 55.0%, system AV04 54.3%
(measurement KFS111115-040000R)

7.7.2 Determine peaks

In the following, various peaks in the sound spectra of the hydrophones and acceleration spectra of the systems AV07 and AV04 are determined primarily as harmonics of the fundamental fre
quench

The pronounced 90 Hz peak is possibly the 3rd harmonic of a 30 Hz oscillation. To check this, the frequency in the narrowband spectrum is shown as a multiple of the frequency f0 as f/f0.

Fig. 7.7.2.1 and Fig. 7.7.2.2 show narrowband spectra of the sound measured with the hydrophone at the AV04 facility, R4-HR1 black line, and two acceleration spectra of the AV07 facility of the sensors M7_A-A15 and M7_A-A14m, red and green line , via f/f0 with f0 = 30 Hz of the orders 0 to 20 or 10 to 30. A considerable number of orders of the harmonics are met, see Table 7.7.2.1 below. In some cases, the agreement in the acceleration spectra is even stronger. The AV07 system supplied 85% load (measurement KFS100919-220000R).

The fundamental frequency f0 = 24 Hz also forms several harmonics in the sound spectrum. The spectra normalized with this frequency are shown in Fig. 7.7.2.3.

The harmonics of the fundamental frequencies that are visible in the sound spectra are listed in Table 7.7.2.1 below. The harmonics can sometimes be seen more clearly in the acceleration spectra.

order 1		2	3	4	5	6	9	10	11	12 13 14 15 21					27
f /Hz 30 60			**90** 120 150 180 270 300 330 360 390 420 450 630 810												
Strength		weak **strong**			hardly hardly hardly weakly hardly hardly								stark stark stark		

order 1		2	3	4	5	6	11	15
f /Hz 24 48			72 96 120 144 264 360					
Strength					=4x30 hardly hardly =12x30			

Tab. 7.7.2.1: Harmonics (order n) of 2 fundamental frequencies f0 (order =1) in the sound spectrum and the acceleration spectra of the AV07 system

The frequencies at 18.5 Hz, 38 Hz, the broad peak of 140 to 150 Hz and 850 Hz can be assigned to the AV04 system. Fig. 7.7.2.4 shows narrow band spectra of hydrophone sound at facility AV04, R4-HR1 black line, and two acceleration spectra of facility AV04, blue line R4-A-W2S1 and red line R4-A-W2S1_W2, over f/f0 with f0 = 17.937 Hz. (The acceleration spectra in the unit $(m/s^2)^2/Hz$ are multiplied by 100.) In the sound spectrum, the fundamental frequency is 17.937 Hz, the 2nd harmonic is 35.874 Hz and the 3rd harmonic is 53.811 Hz visible.

These three lines are particularly clearly visible in the acceleration spectra. In this measurement, both systems have a partial load of 50%, measurement KFS111115-040000R. This assignment confirms the assignment of the lines to plant AV04, shown in Figs. 7.7.2.5 and 7.7.2.6, for which the performance of the plant was different.

This means that most of the peaks in the hydrophone spectrum can be assigned as harmonics of 30.0 Hz (green circles) and harmonics of 24.0 Hz (blue circles), these have the AV07 system as their source.

There are individual lines that have the AV04 system (black circles) as their source. In Fig. 7.7.2.5 and 7.7.2.6 the sound spectra are shown over the frequency range 0 to 200 Hz and 0 to 1000 Hz with the assignments mentioned.

Fig. 7.7.2.7 shows the narrowband spectrum of the sound spectra of the two hydrophones of the measurement KFS110728-180000R over f/f0 with f0 = 14.841 Hz (upper scale). The performance of the AV07 plant is indeed weak with only 4.2%, which is 210.4 kW, but the 90 Hz peak occurs and a lot of harmonics of 14.841 Hz can be seen at the low level. Only the circled lines belong to a different series. This measurement should be viewed as an isolated case and does not reflect the sound emissions of a representative operating condition of the system. However, it indicates that the actual excitation frequency is 15 Hz and thus the frequency of 90 Hz as the 6th harmonic of the excitation due to a resonance effect of the water column in the

Central tube or the central tube itself is preferably radiated. Irrespective of the quality of the radiation, an excitation of the frequency from the machine itself is usually to be expected due to rollover frequencies in bearings or tooth meshing frequencies.

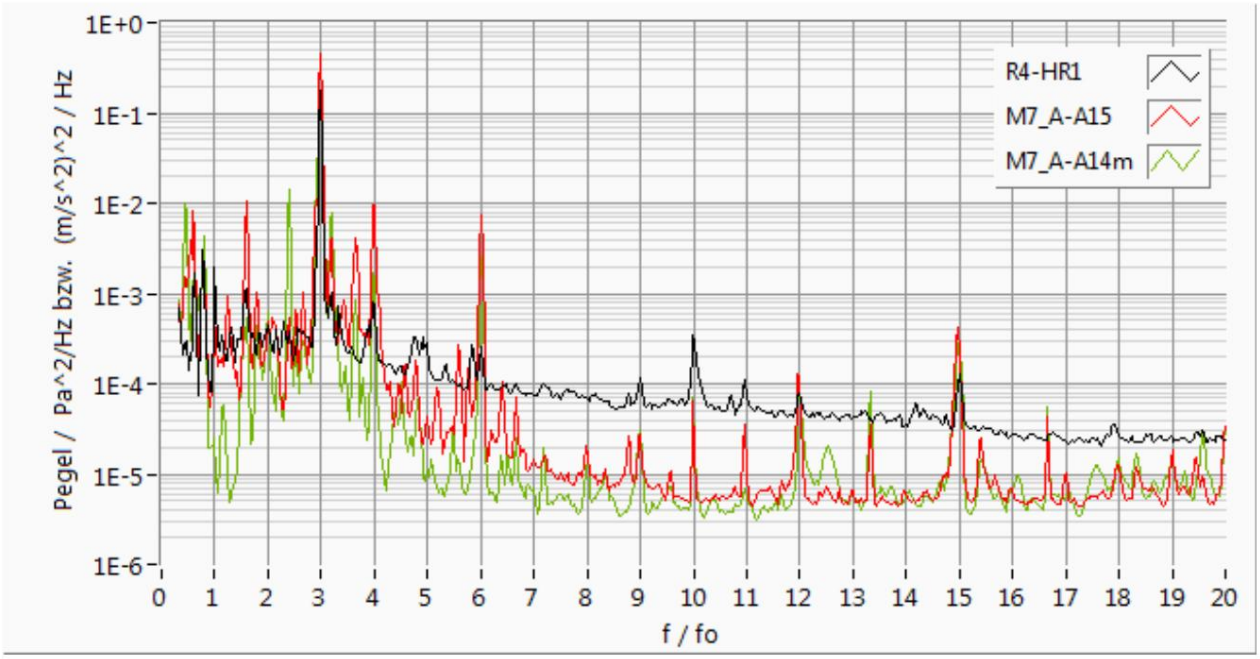

f0 = 30.0 Hz
Fig. 7.7.2.1: Narrow band spectra over f/
f0 system AV07, harmonic order 0 to 20 1
hydrophone black line R4-HR1 2
acceleration spectra AV07, light red line M7_A-A15 and green line M7_A-A14m
accelerations ((m/s²)²/Hz) multiplied by 100
Result: many multiples of 30 Hz (measurement KFS100919-220000R)

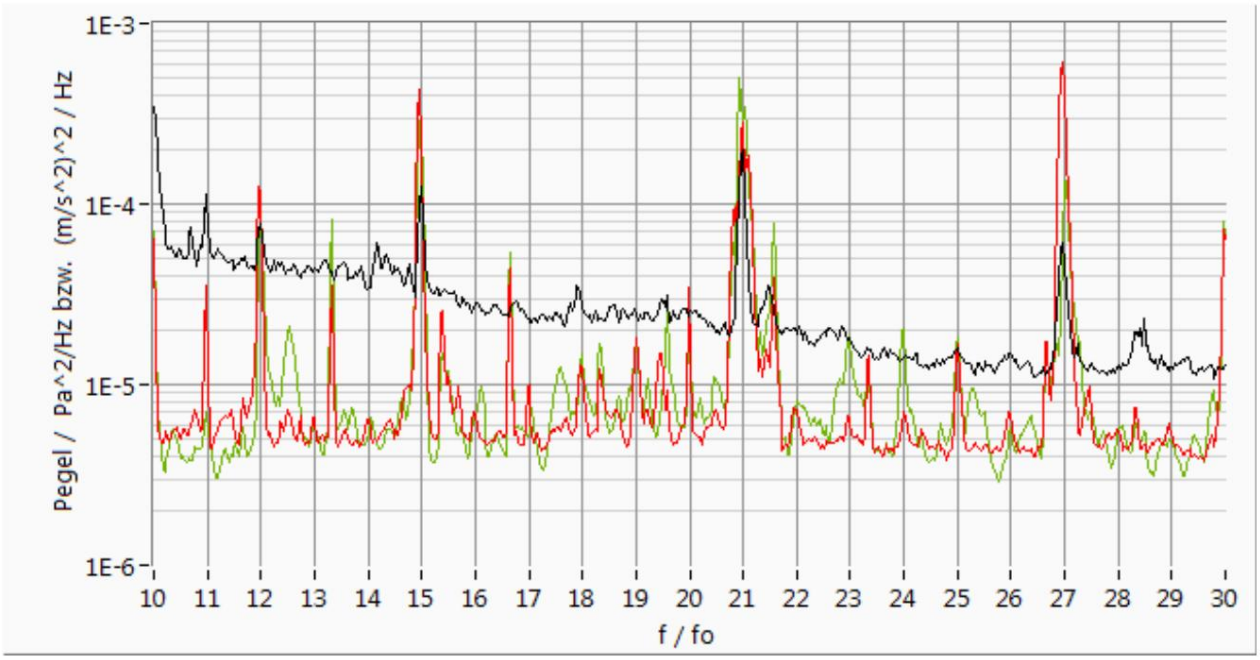

f0 = 30.0 Hz
Fig. 7.7.2.2: Narrow band spectra over f/
f0 system AV07, harmonic order 10 to 30 1
hydrophone black line R4-HR1 2
acceleration spectra AV07, light red line M7_A-A15 and green line M7_A-A14m
accelerations ((m/s²)²/Hz) multiplied by 100
Result: many multiples of 30 Hz (measurement KFS100919-220000R)

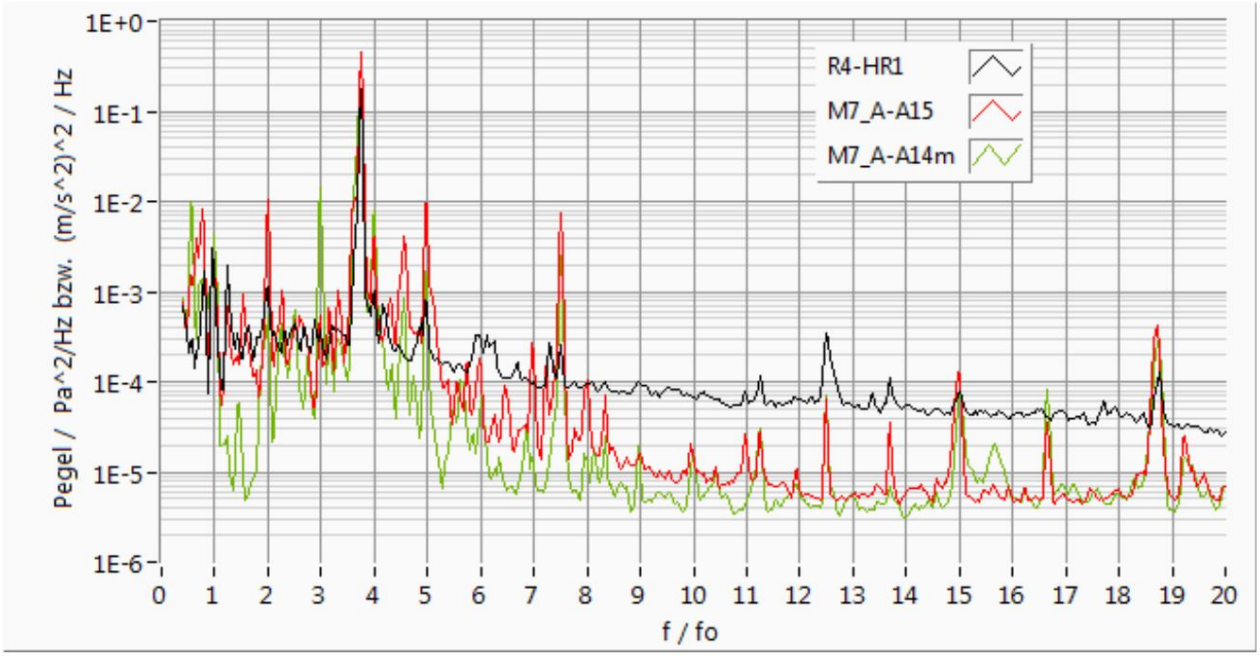

f0 = 24.0 Hz
Fig. 7.7.2.3: Narrow band spectra over f/
f0 system AV07, harmonic order 0 to 20 1
hydrophone black line R4-HR1 2
acceleration spectra AV07, light red line M7_A-A15 and green line M7_A-A14m
accelerations ((m/s²)²/Hz) multiplied by 100
Result: Several multiples of 24 Hz (measurement KFS100919-220000R)

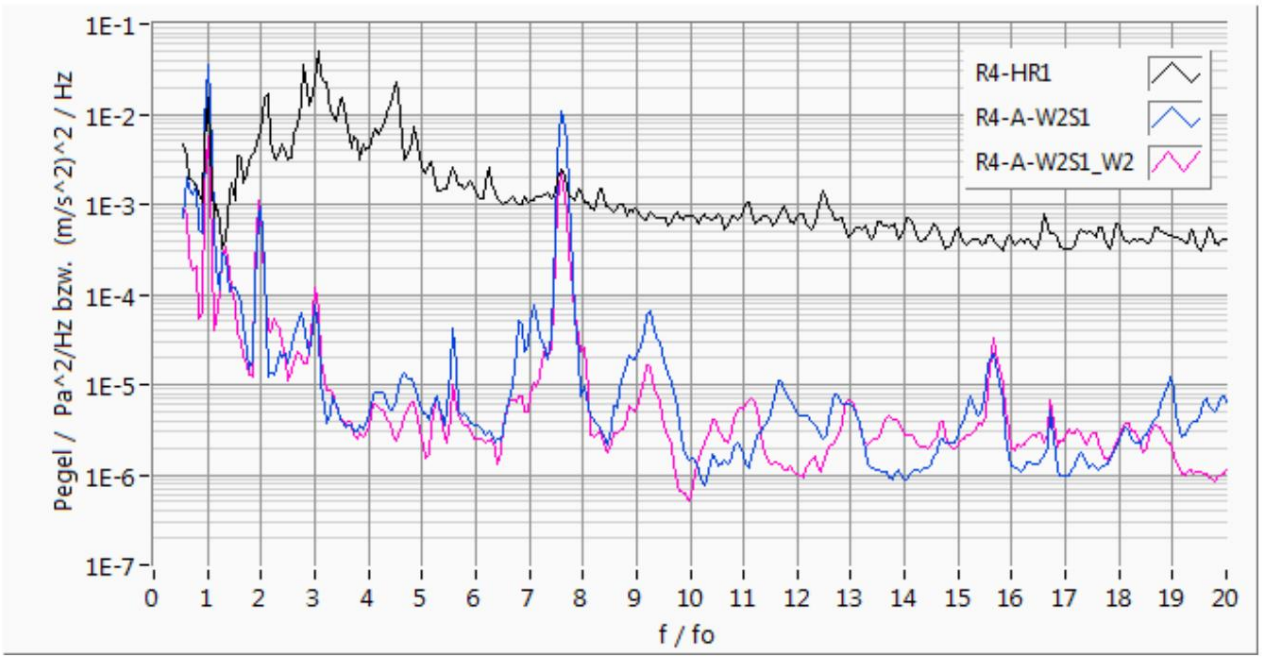

f0 = 17.9370 Hz
Fig. 7.7.2.4: Narrow band spectra over f/
f0 system AV04, harmonic order 0 to 20 1
hydrophone black line R4-HR1 2
acceleration spectra AV04, blue line R4-A-W2S1 and red line R4-A- W2S1_W2
accelerations ((m/s²)²/Hz) multiplied by 100
Result: 17.937 Hz visible in the sound spectrum, orders 2 and 3 (35.874 Hz and 53.811 Hz)
contribute (measurement KFS111115-040000R)

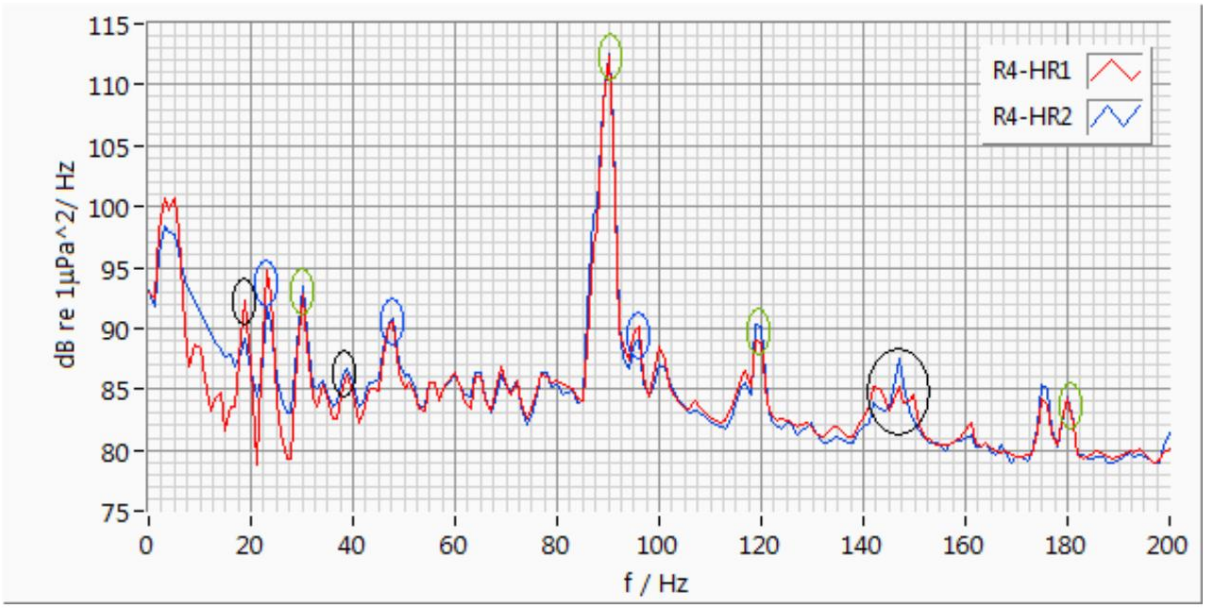

Fig. 7.7.2.5: Narrow band spectra of 2 hydrophones at AV04 (R4-HR1 and R4-HR2), frequency 0 to 200 Hz Green circles: source AV07, harmonics of 30.0 Hz Blue circles: source AV07, harmonics of 24.0 Hz Black circles Source AV04, single lines Result: hydrophone spectrum with associated lines (measurement KFS100919-220000R)

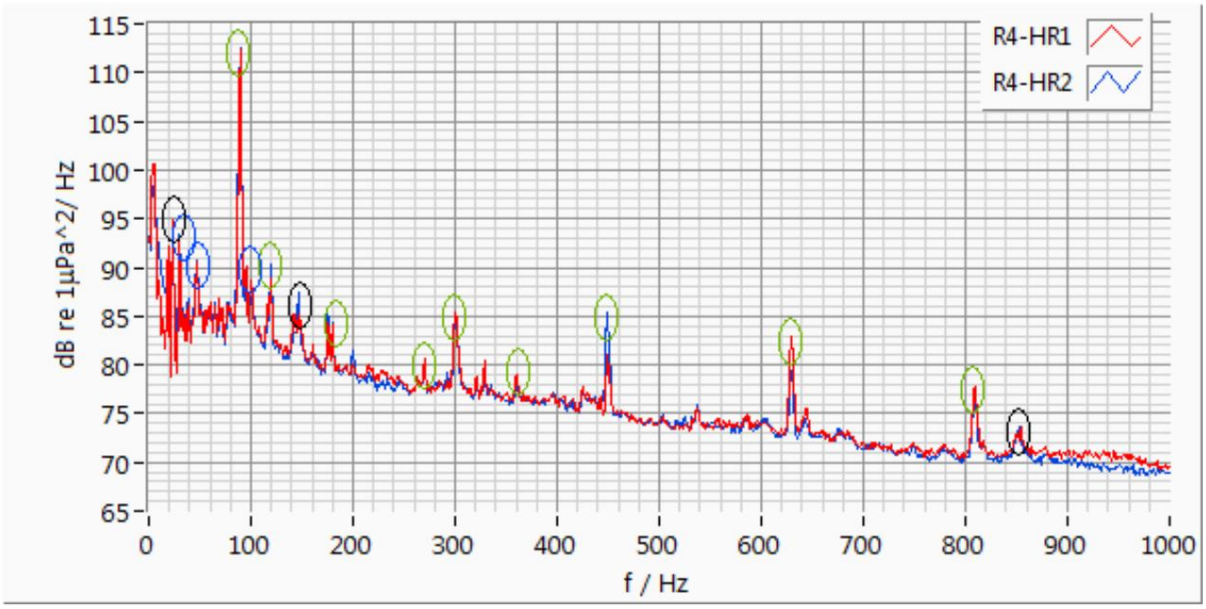

Fig. 7.7.2.6: Narrowband spectra of 2 hydrophones at AV04 (R4-HR1 and R4-HR2), frequency 0 to 1000 Hz Green circles: source AV07, harmonics of 30.0 Hz Blue circles: source AV07, harmonics of 24.0 Hz Black circles Source AV04, single lines Result: hydrophone spectrum with associated lines (measurement KFS100919-220000R)

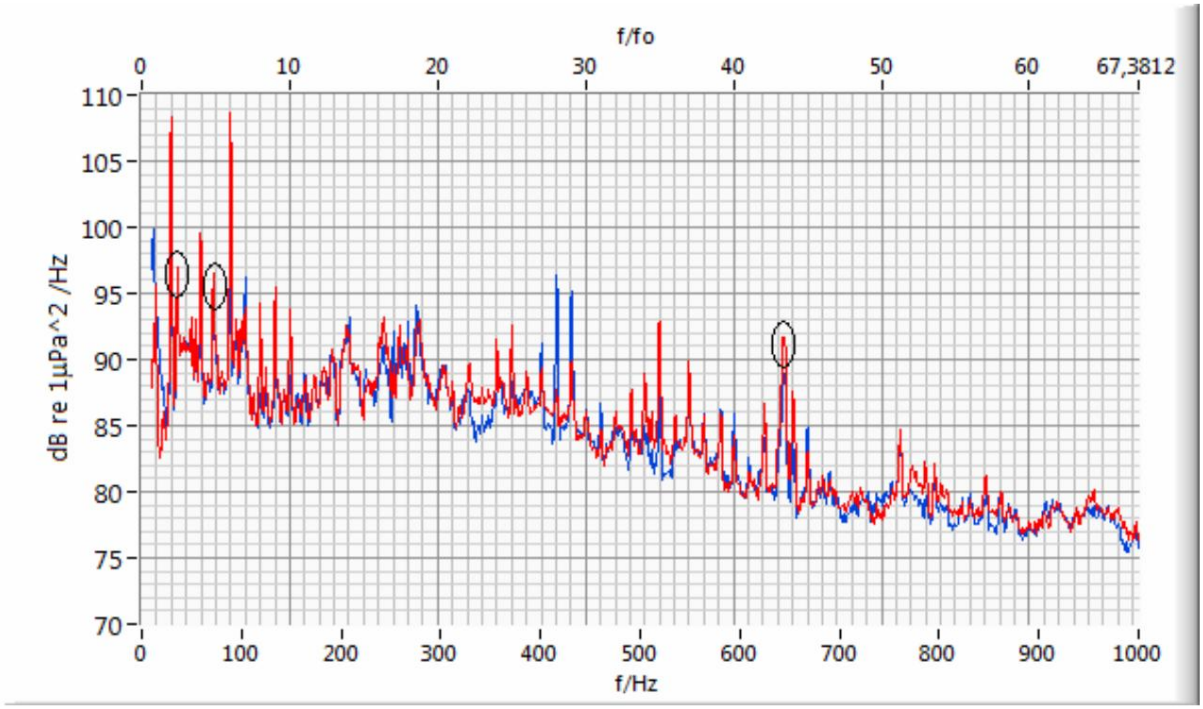

f0 = 14.841 Hz Fig.
7.7.2.7: Narrow band spectra over f/f0 2 hydrophones
at AV04 (R4-HR1 red, R4-HR2 blue), harmonic order 0 to 67.3812 upper scale measurement KFS110728-180000R at low power from AV07 this Multiples visible in the sound Result: harmonics of 14.8 Hz around 15 Hz multiples, 90 Hz (exactly 89 Hz) is 6th harmonic, 15 Hz could be exciting frequency in machine The marked peaks are fundamental, 2nd and 18th harmonics of 35.795 Hz and are a separate excitation.

The measurement data are shown in the table below.

Measurement	Abb.	Wind speed AV04 4.5 m/s	wave height	In total perfomance of	Performance AV07	Performance AV04	Performance AV01
KFS110728-180000R	7.7.2.7		0,7 m 4,4 %		4,2 % 210,4 kW	4,9 % 3,4 %	

Tab. 7.7.2.2: Measurement parameters

7.7.3 Marked variable frequency

The authors interpret that the marked peak at 90 Hz of the AV07 system in the partial load range is excited with a basic frequency in the drive train of the system, tooth engagement frequency or rollover frequency, and follows the variable speed. In the noise measurement, the sound is distributed in different spectral lines when the wind changes as a narrowband spectrum, so that it is hidden and, unlike at full load, is no longer visible as a peak.

In the following, a measurement is evaluated in several spectrograms that show that a frequency increases from 77 Hz to 86 Hz and decreases back again in the period of 30 seconds. This frequency can be detected in the accelerometers of the AV07 installation and in the sound at the hydrophones, while the accelerometers of the AV04 installation do not contain this frequency. This means that the source of the excitation is the vibration in the AV07 installation and as sound in the water is radiated.

The measurement is from September 26, 2010, time axis of the display 20:00:00 + t with t in seconds, time in UTC. The spectrogram has a vertical scale from 50 Hz to 125 Hz in the six representations. Fig. 7.7.3.1, 7.7.3.2 and 7.7.3.3 show three spectrograms measured with three acceleration sensors on the AV07 system. The positions of the sensors are shown in Fig.5.1.2. All three accelerations show a clear increase in frequency along a line in the spectrogram from 77 Hz at t = 30 s to 86 Hz at t = 45 s and a subsequent decrease back to 77 Hz at t = 60 s a red to red-yellow arc can be seen, red means high amplitude.

Fig. 7.7.3.4 and 7.7.3.5 show two spectrograms measured with the two hydrophones in front of the AV04 system. This frequency variation from 77 Hz to 86 Hz and back to 77 Hz can be clearly recognized in these spectrograms of the hydrophones. This means that the AV07 system emits sound of this frequency, which is detected at a distance of 800 m. In addition, weaker lines of constant frequency at about 90 Hz can be observed than horizontal lines. These tones are presumably emitted by other systems of the AV07 type.
Fig. 7.7.3.6 shows the spectrogram measured with an acceleration sensor on the AV04 system (sensor R4-A-W2S1 on the cross of the strut). All frequencies do not change over time and no lines can be seen at 86 to 77 Hz. All spectrograms of the four acceleration sensors on the AV04 system (sensors R4-A-W1_W2, R4-A-W2_W3, R4-A-W2S1, R4-A-W2S1_W2) show the same behavior for this measurement; only one diagram is shown here . This means that the AV04 system is not the source of the sound shown here.

Measurement	Abb.	Wind on AV04	wave height	overall performance	Performance AV07	Performance AV04	Performance AV01
KFS100926-220000	7.7.3.1 - 7.7.3.6	11,0 m/s	2,1 m 51 %		45 %	55%	72 %

Tab. 7.7.3.1: Measurement parameters

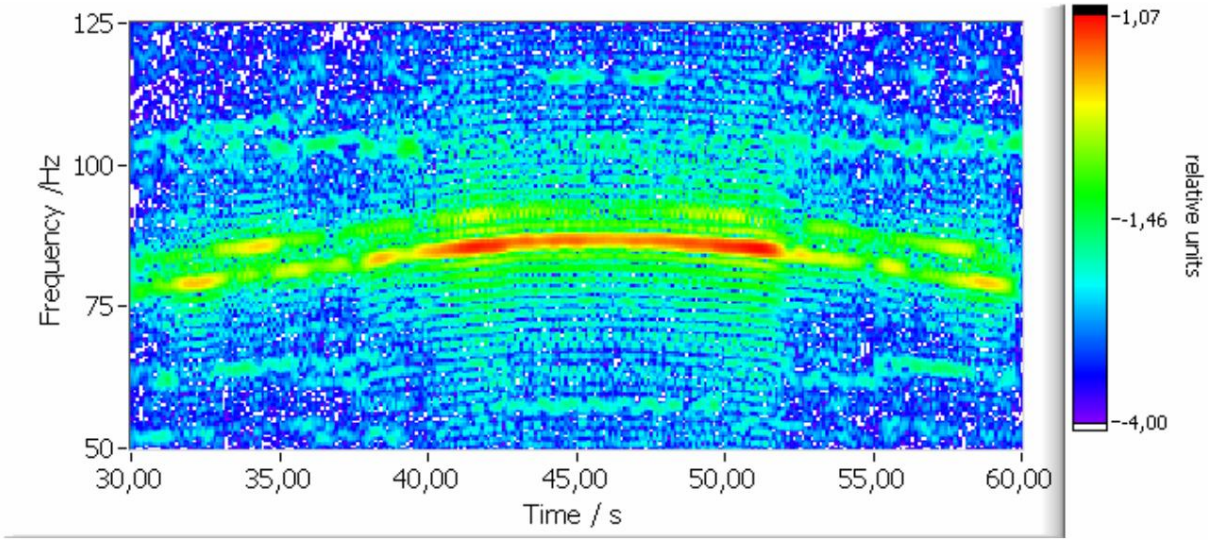

Fig. 7.7.3.1: Acceleration spectrogram on system AV07 sensor M7_A-A15 color scale red high acceleration, decreasing via yellow, green to blue low, measurement KFS100926-220000 Result: Red arc = frequency increases from 77 Hz to 86 Hz and decreases to 77 Hz in approx. 30 s

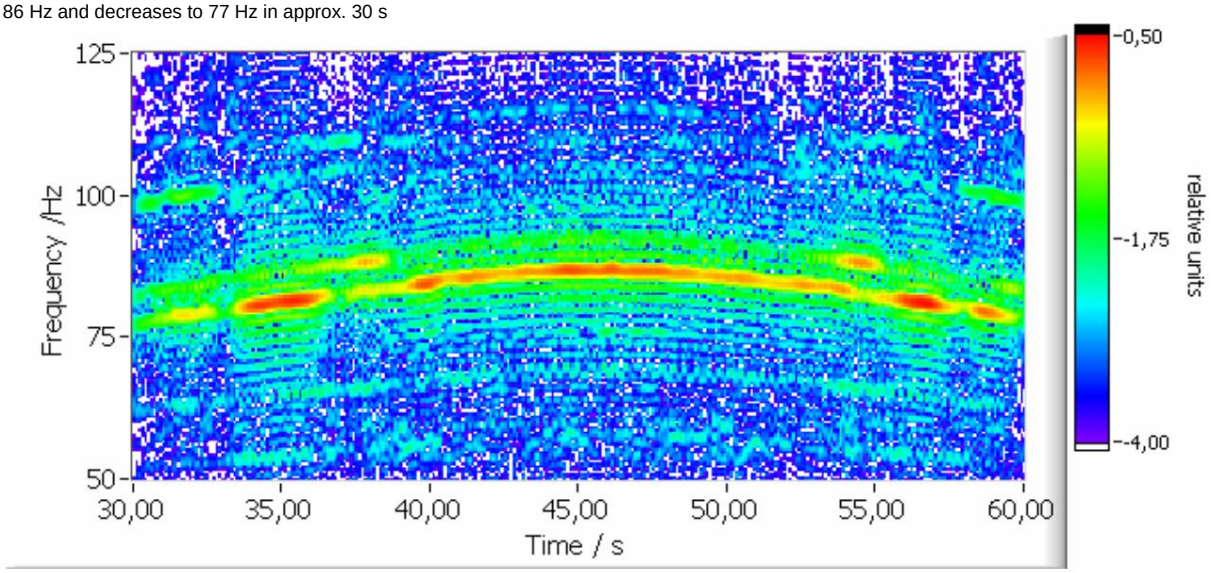

Fig. 7.7.3.2: Acceleration spectrogram on system AV07 sensor M7_A-A14 color scale red high acceleration, decreasing via yellow, green to blue low, measurement KFS100926-220000 Result: Red arc = frequency increases from 77 Hz to 86 Hz and decreases to 77 Hz in approx. 30 s

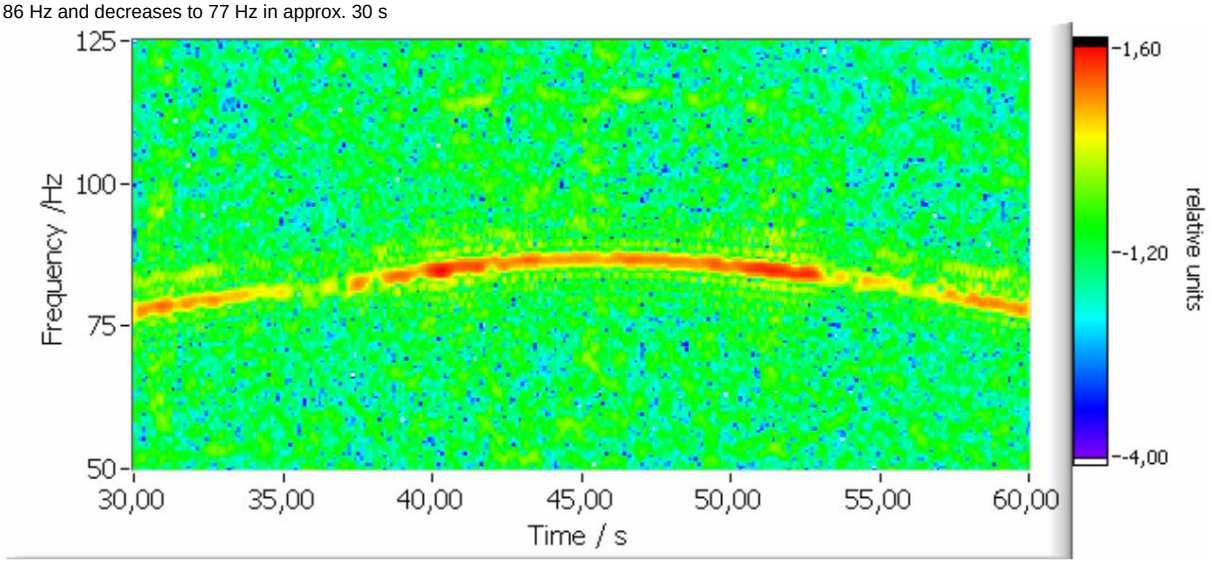

Fig. 7.7.3.3: Acceleration spectrogram on system AV07 sensor M7_A-A56um color scale red high acceleration, decreasing via yellow, green to blue low, measurement KFS100926-220000 Result: Red arc = frequency increases from 77 Hz to 86 Hz and decreases to 77 Hz in approx. 30 s

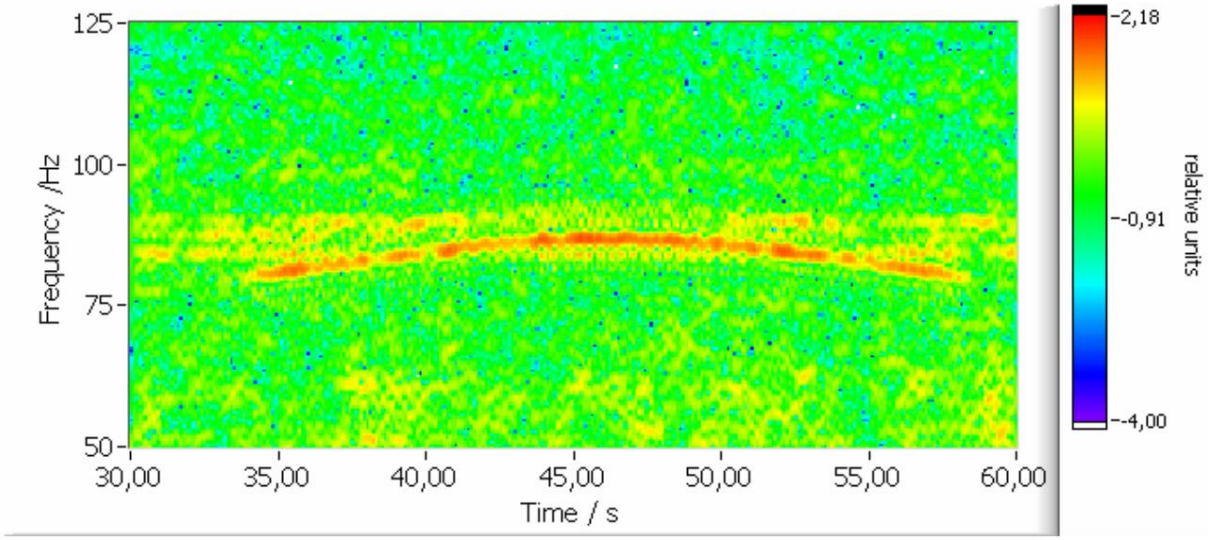

Fig. 7.7.3.4: Spectrogram sound hydrophone 1 near system AV04 (R4-HR1)
Color scale red high sound amplitude, decreasing via yellow, green to blue low, measurement KFS100926-220000 Result: red arc = frequency increases from 77 Hz to 86 Hz and decreases to 77 Hz in approx. 30 s

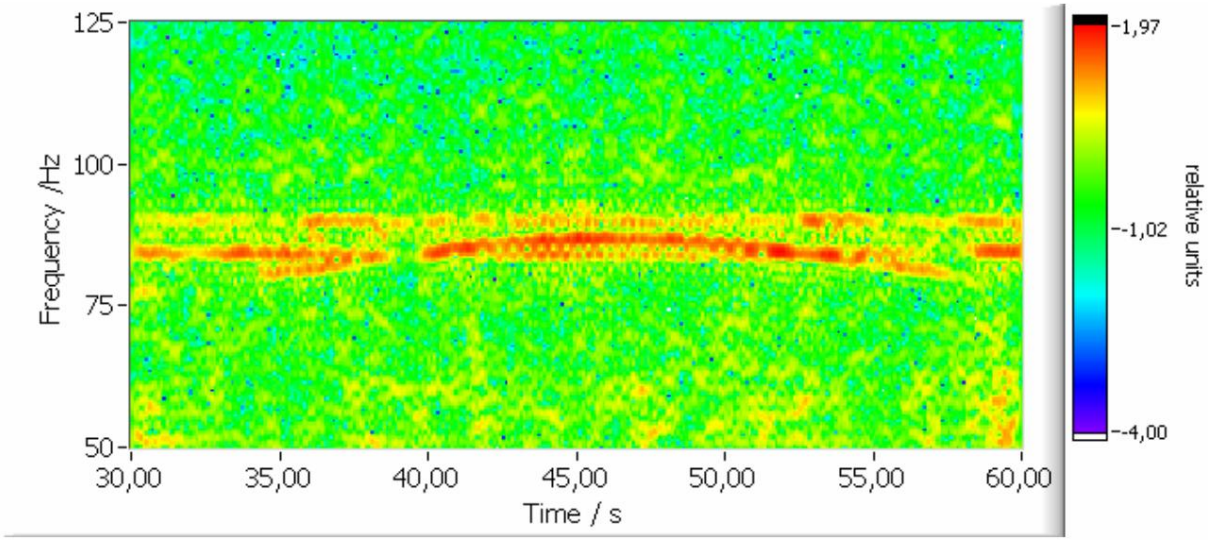

Fig. 7.7.3.5: Spectrogram sound hydrophone 2 near system AV04 (R4-HR2)
Color scale red high sound amplitude, decreasing via yellow, green to blue low, measurement KFS100926-220000 Result: red arc = frequency increases from 77 Hz to 86 Hz and decreases to 77 Hz in approx. 30 s

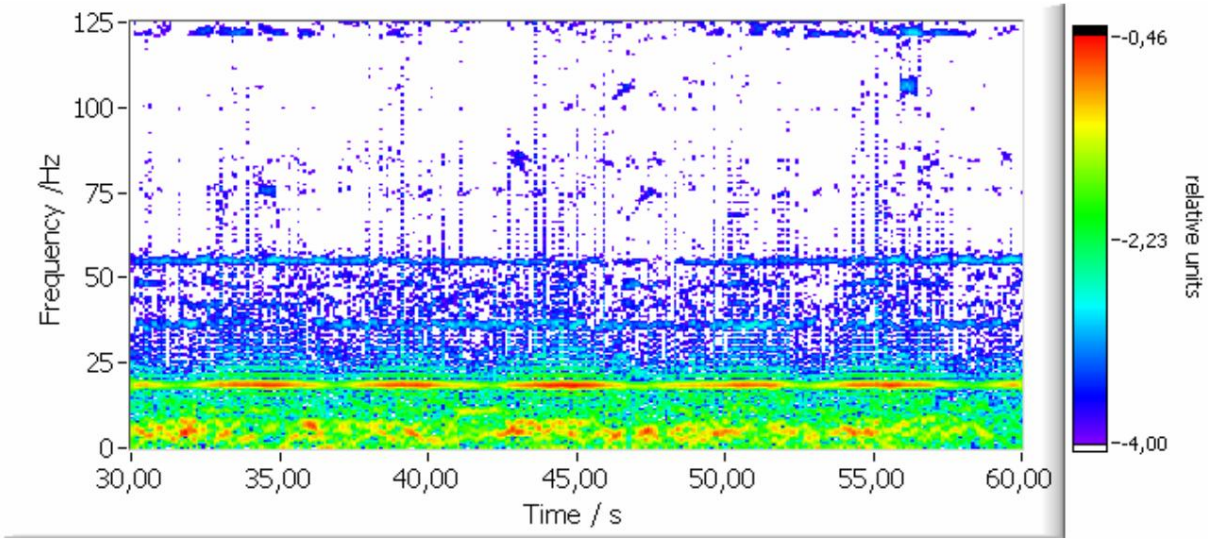

Fig. 7.7.3.6: Acceleration spectrogram on the AV04 system sensor R4-A-W2S1 color scale red high acceleration, decreasing via yellow, green to blue low, measurement KFS100926-220000 result: no arc = all frequencies constant, no source of the sound 77- 86-77Hz

7.8 Ramming and other disturbances

In Table 7.8.1 below, disturbing noises and irradiation are shown that the authors have identified in the measurements and the measures that were taken are named.

Disturbance	measure		
	Sort out measurement	Hochpass – Filtering 10Hz	Tiefpass – Filtering 3.0kHz
piling noise	x		
ship sounds	x		
chain jingle			x
Sonar			x
Interference from the converter			x
Pseudoschall an Hydrophonen	(X)	x	
animal sounds	x		
Mains interference FINO1	see text section 7.8.2		

Table 7.8.1: Overview of various interferences and measures to minimize them Measurements were only discarded if the interference could be clearly identified High- and low-pass filtering were combined as band-pass filtering in measurements to calculate the Leq and Peak values regardless of the presence of the corresponding ones disruption used

Section 7.8.1 deals with ramming noises and Section 7.8.2 with tidal currents, chain clanking, scour sonar and electrical radiation from inverters, among other things. How the interference was removed is described. Section 7.8.3 deals with ship noise, calculates its potential contribution to background noise based on literature and proves that it becomes quieter under water when it gets windier. Animal sounds are discussed in Section 7.8.4.

7.8.1 Ramming noises

In the measurement periods 2010 and 2011, ramming was carried out in the BARD Offshore 1 wind farm, 50 km away, and in 2011 also in the Borkum West II offshore wind farm, also called Trianel, 7 km away. The ramming impacts recorded by the two hydrophones at the AV04 facility and partly by the hydrophone at FINO1 were so loud that they were easy to identify. Upon identification, the complete measurement over 300 s was sorted out and not used to evaluate the operating noise. The time series, third-octave spectra and spectrograms of the piling blows are shown here.

Wind farm Borkum West
II Fig. 7.8.1.1 and 7.8.1.2 show excerpts from the time signals of the two hydrophones at the AV04 facility (R4-HR1 red, R4-HR2 blue) with different time resolutions. Date is 2011-11-14 04:00 UTC, the source is Trianel BW61 Pile 1.2, the driving energy is 800 to 1000 kJ, the data for the sound level as Leq over 300 s and peak value as Lpeak for the two hydrophones are in Tab. 7.8.1.1 specified. The single event level SEL, definition corresponding to the Leq deviating with integration over one second including the ramming impact in time, see as an example Fig. 7.8.1.2, lies between the specified values for Leq and Lpeak. According to Müller (2011) p. 15, the single-event sound pressure level can be determined with the equivalent continuous sound level Leq and the number of impacts n per time T according to SEL = LE ÿ Leq -10. log(n.T0 /T). With T0 = 1 s, T = 20 s, n = 15, SEL ÿ 145 dB re 1 ÿPa follows. With L750 = LE + 15.log(r/750m) the estimate is L750 = 160 dB re 1 ÿPa.
The UBA precautionary value, which is the maximum reference value for piling noise SEL = 160 dB re 1 ÿPa at a distance of 750 m, see et al. Betke (2010) p.3, has this size. However, the comparison is not suitable as a check because of the large distance (Müller 2011 p. 17).
Fig. 7.8.1.2 shows the same time series (piling noise Borkum West II) resolved over one second. The above-mentioned individual event level SEL is always calculated over this time interval. The time lag of the impact can be seen on the two hydrophones (R4-HR1 red, R4-HR2 blue, start of display at 4:00 a.m.). The ramming is close, the scale indicates the sound pressure in Pa, you can read the peak level directly with 161 dB = 20 log (112 Pa / 1 ÿPa), in fact there were louder ones

Blows, see Fig. 7.8.1.1. The peak decays relatively continuously with only weak subsequent secondary maxima.

Fig. 7.8.1.3 shows the associated third-octave spectra (piling noise Borkum West II) measured on the hydrophone at AV04 (R4-HR1), averaging time of the spectra 5 s each.
Fig. 7.8.1.4 shows the statistical quantities within a third of the third-octave spectra (piling noise Borkum West II): maximum (red), energetic mean value (black), minimum (blue), each with squares, percentile L5 (red), L50 (black) and L95 (blue), both smooth lines. The hydrophone is closer to AV04 (R4-HR1), the averaging time of the spectra is 5 s each. The center frequency is about 100 Hz, strong signals can be seen from about 30 Hz to 300 Hz. (Note on logarithmic averaging: In contrast to arithmetic averaging with the addition and division functions, logarithmic averaging is carried out with the multiplication and root extraction functions, here 100 ÿ root (30*300), compare also section 4.4.) Driving noise spectra of similar spectral distribution of different construction noise Wind farms are presented in Betke (2008) and (2012).

Fig. 7.8.1.5 shows the spectrogram of the Borkum West II sound. The color scale means red with high amplitude, decreasing via yellow, green to blue to low amplitude. The frequency associated with the amplitude is read on the left and the time at which this amplitude occurred at this frequency is read below. The spectral density is red and the amplitude is therefore high in the frequencies from 30 Hz to 300 Hz according to the third-octave spectra, see the above evaluation and Fig. 7.8.1.3 and 7.8.1.4. Very low frequencies in Fig. 7.8.1.5 have a much smaller time shift on the scale to the right, which means that these sound waves arrive later and the phase velocity c of these waves with low frequency f and thus large wavelength ÿ is lower. The connection c = ÿ . f is always valid (Gerthsen 1993, p. 150). Urban (2002) p. 42 points out that the phase velocity c = c(ÿ) of waterborne sound decreases with decreasing wavelength, so that dc/dÿ > 0 applies, which is called normal dispersion (Gerthsen 1993, p.185). Here, however, the unusual relationship dc/dÿ < 0 is proven, which is generally called anomalous dispersion (ibid.). The effect of the delay can be seen several times in the figure and indicates multipath propagation (Urban 2002, p. 123). The hydrophone was that at AV04 (R4-HR1).

Fig. 7.8.1.6 shows the same spectrogram with a frequency of up to 25 kHz; no other frequencies occur. The horizontal lines are electrical noise and are irrelevant here.

Those	Distance approx. [km]	Hydrophone	Leq over 300 s [dB re 1 ÿPa] 144.53	L peak [dB re 1 ÿPa]	Measurement
Borkum West II	7	R4-HR1		163,10	KFS111114-040000R
Borkum West II	7	R4-HR2	144,20	162,88	KFS111114-040000R
Bard I	50	R4-HR1	131,39	149,58	KFS100923-040000R
Bard I	50	R4-HR2	130,97	148,30	KFS100923-040000R
Bard I	50	F1-H8106	130,00	148,03	KFS100923-040000R

Tab. 7.8.1.1: Driving noise from distant wind farms measured at the hydrophones in alpha ventus

BARD 1 wind farm

Fig. 7.8.1.7 shows the narrow-band spectra of the two hydrophones on the AV04 system (R4-HR1 red, R4-HR2 blue). The date is 09/23/2010 04:00 UTC, the source is the BARD 1 wind farm about 50 km away.
The Leq and peak levels measured at the three hydrophones at the AV04 and FINO1 system (R4-HR1, R4-HR2, F1-H8106) are given in Tab. 7.8.1.1, see above. The levels are approx. 13 dB lower than in Borkum West II, which roughly corresponds to the attenuation due to the greater distance with 13 = 15 log(50km/7km). With this level, with the equation given above, with T0 = 1 s, T = 20 s and n = 7, the single-event sound pressure level SEL ÿ 136 dB re 1 ÿPa follows, which is almost identical to the measurement results from Betke (2012), the on p. 43 for comparable hydrophone positions indicates SEL = 132 to 134 dB re 1 ÿPa as measured values. With the conversion given above

Distance follows L750 = 163 dB re 1 ÿPa, which would mean slightly exceeding the guideline value. But the distances are too large to represent reviews, see above.
The measurement has the number KFS100923-040000R.
Fig. 7.8.1.8 shows the same time series resolved over one second. The time lag of the impact can be clearly seen on the two hydrophones (R4-HR1 red, R4-HR2 blue, start of display at 4:00 a.m.). The ramming is distant, the scale gives the sound pressure in Pa and is smaller than above, the peak decays more slowly than above and is not continuous.
Fig. 7.8.1.9 shows the associated 5s third-octave spectra (BARD 1) measured on the hydrophone at AV04 (R4-HR1).
Fig. 7.8.1.10 shows the statistical quantities within a third of the 5s third-octave spectra (BARD 1): maximum (red), energetic mean value (black), minimum (blue), each with squares, percentile L5 (red), L50 (black) and L95 (blue), both smooth lines. The hydrophone is at AV04 (R4-HR1), the averaging time of the spectra is 5 s.

Fig. 7.8.11. shows the spectrogram (BARD 1). The color scale means high intensity with red, decreasing through yellow, green to blue to low intensity of a frequency read on the left at a time read on the bottom. The spectral density is red and therefore high from 50 Hz to 200 Hz, corresponding to the third-octave spectrum in the previous Fig. 7.8.1.10. Low frequencies below 100 Hz have a clear time lag of more than half a second. The dispersion effect is strong here because of the long distance of 50 km. It is confirmed that the phase velocity decreases with decreasing frequency and thus increasing wavelength. Two propagation paths can be clearly seen. The hydrophone was that at AV04 (R4-HR1).

Fig. 7.8.1.12 shows the same spectrogram with the frequency up to 25 kHz, no other frequencies appear. The horizontal lines are electrical noise and are irrelevant here.

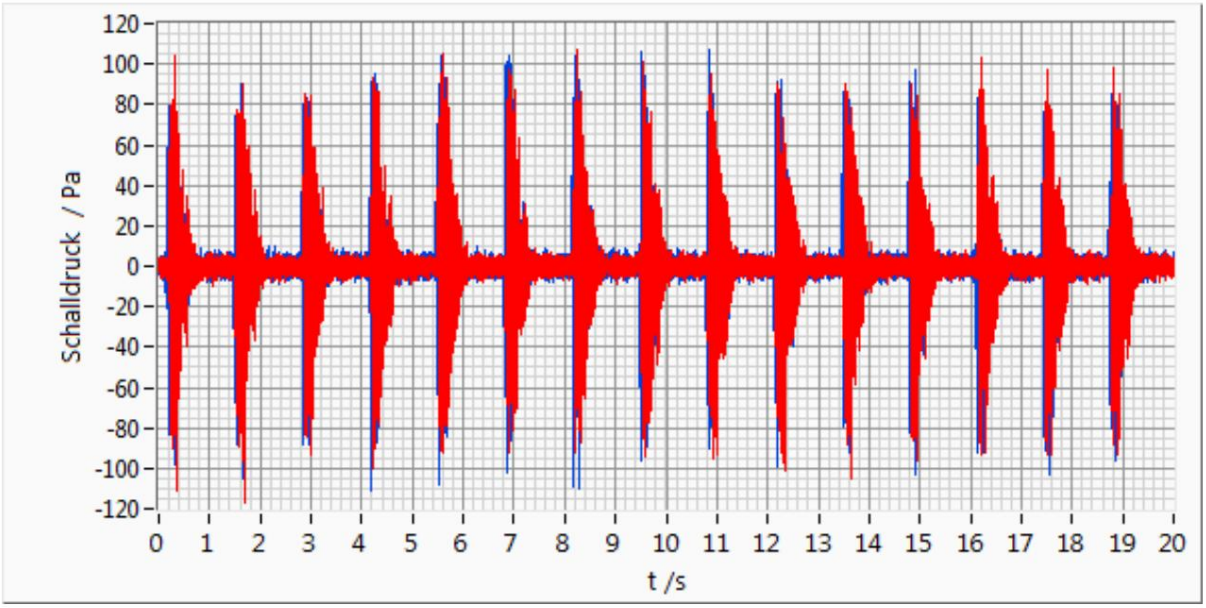

Fig. 7.8.1.1: Time series of ramming sound Borkum West II 2
hydrophones at AV04 (R4-HR1 red, R4-HR2 blue), start of display at 4:00 a.m., excerpt 20 seconds

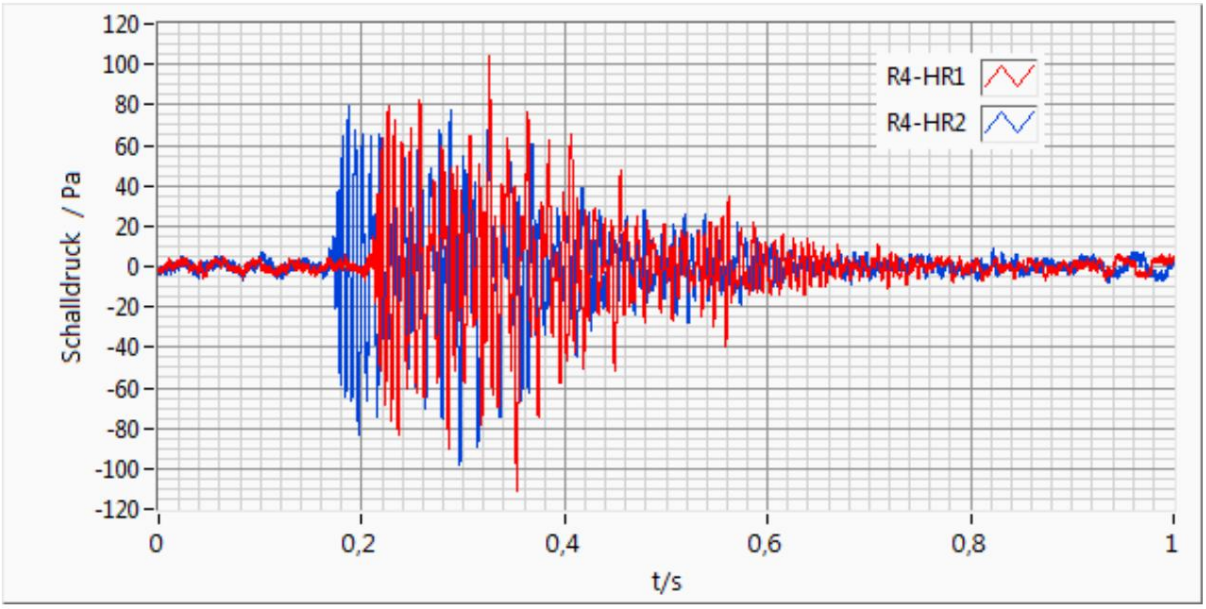

Fig. 7.8.1.2: Time series of ramming sound Borkum West II 2
hydrophones at AV04 (R4-HR1 red, R4-HR2 blue), start of display at 4:00 a.m., excerpt 1 second

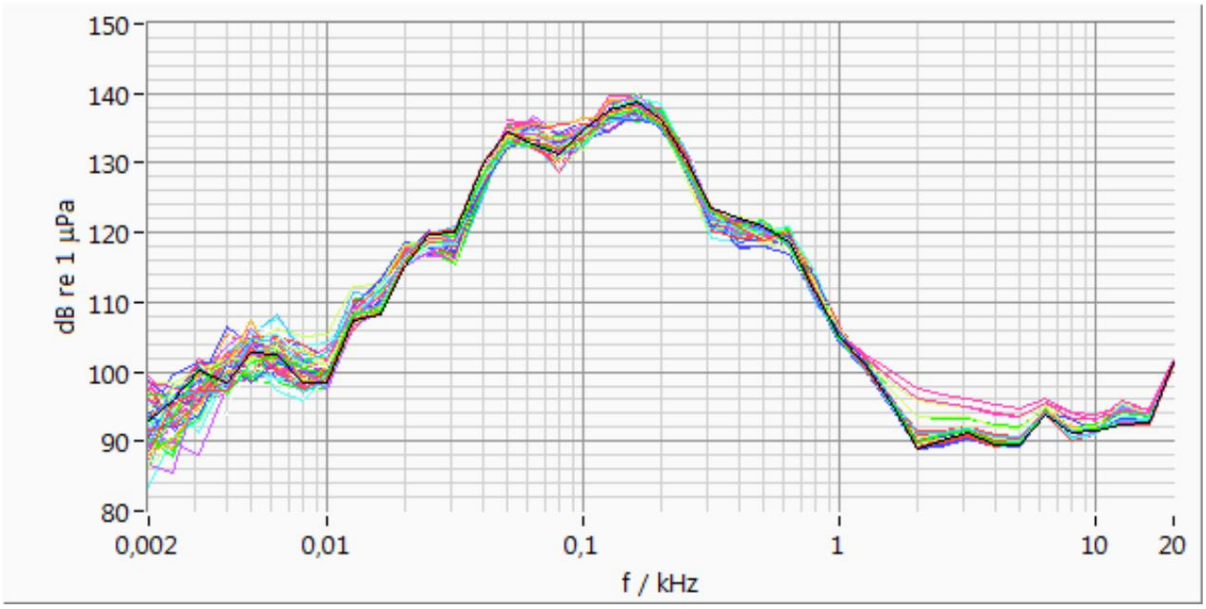

Fig. 7.8.1.3: 5s third-octave spectrum of the Borkum West II hydrophone
on the AV04 (R4-HR1), averaging time of the spectrum in each case 5s

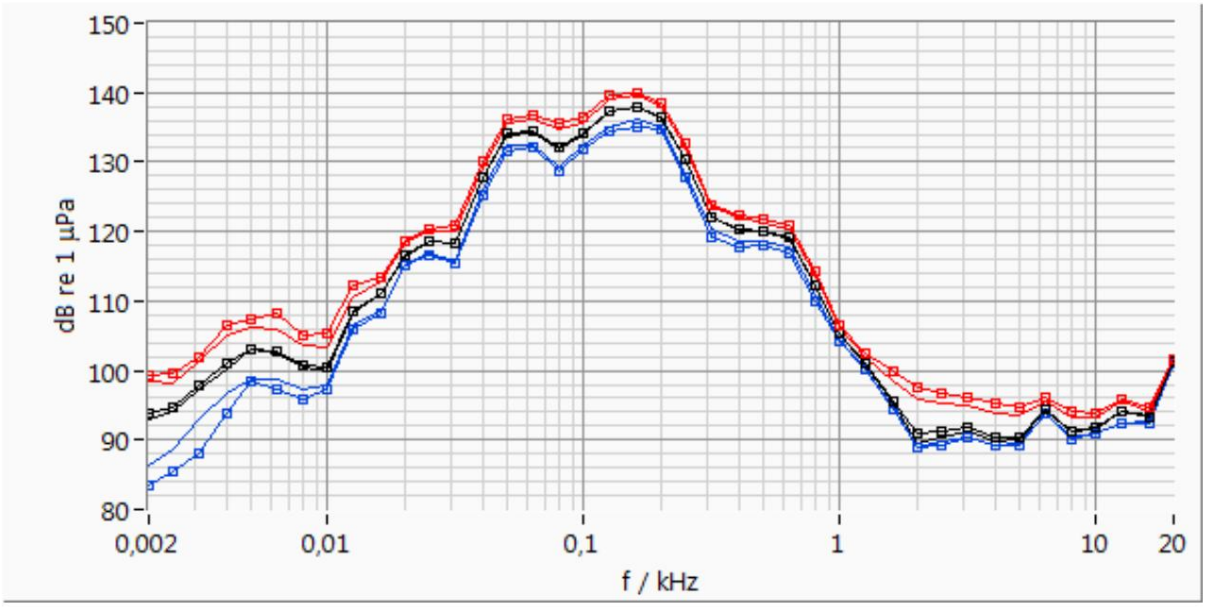

Fig. 7.8.1.4: 5s third-octave spectrum Pile driving sound Borkum West II
percentiles, maximum, minimum, energy maximum
(red), energy mean value (black), minimum (blue), each with squares percentiles L5 (red), L50 (black) and L95
(blue), each smooth lines hydrophone at AV04 (R4-HR1), spectrum averaging time 5 s
each

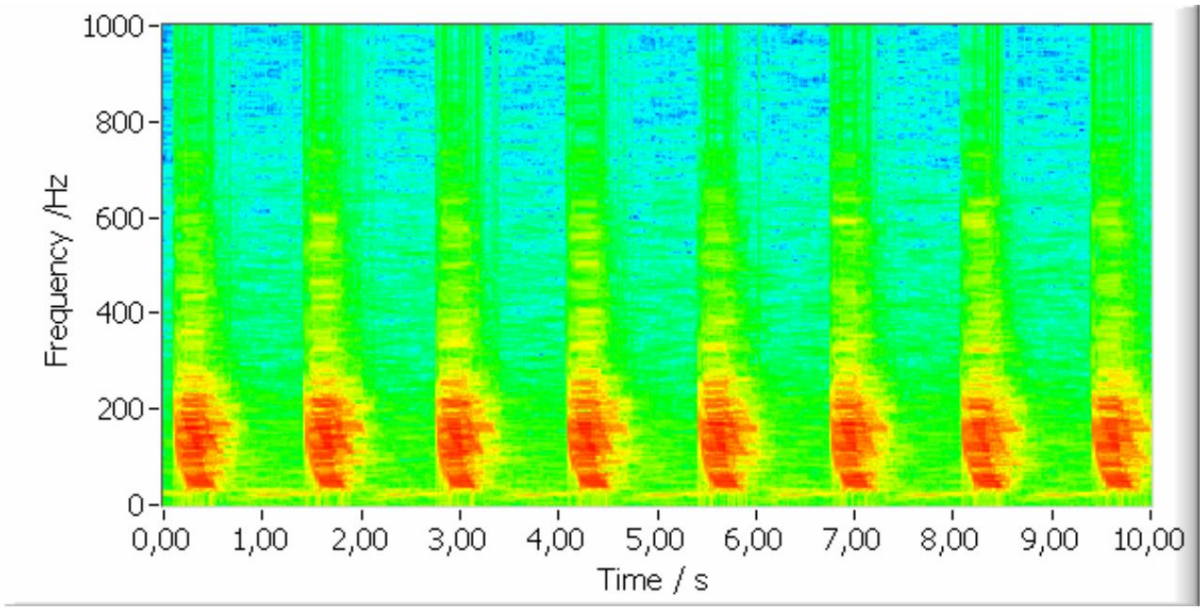

Fig. 7.8.1.5: Spectrogram pile driving noise Borkum West II Color scale
red high intensity, decreasing via yellow, green to blue low Result: spectral density high from
30 to 300 Hz according to third-octave spectrum, low frequencies have lower speed, multipath propagation hydrophone at AV04 (R4- HR1)

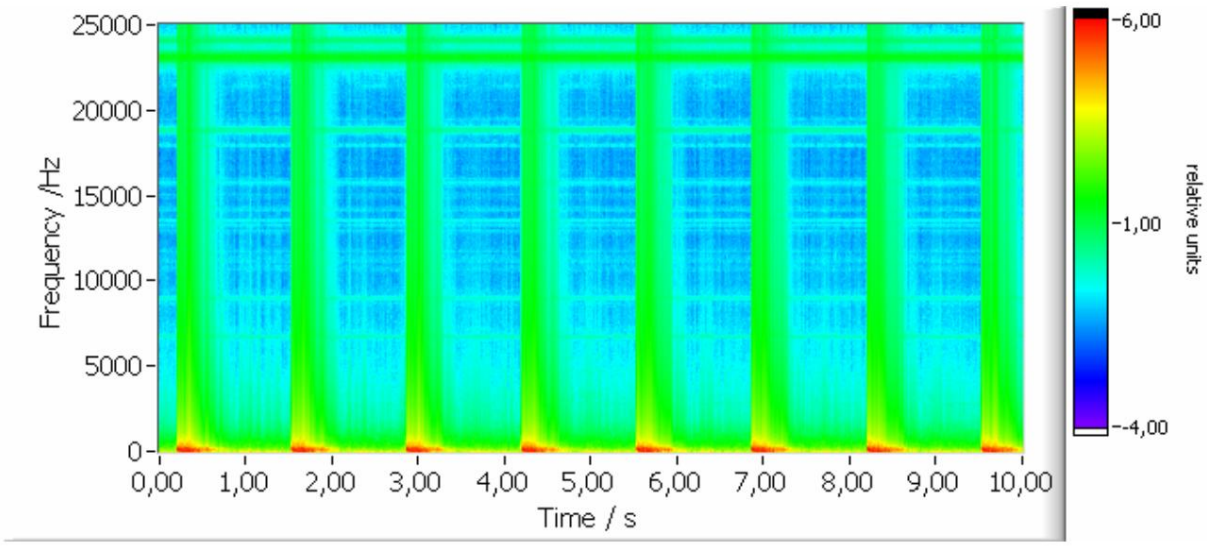

Fig. 7.8.1.6: Spectrogram pile driving noise Borkum West II As above
figure, frequency scale up to 25000 Hz, result: no high frequencies involved

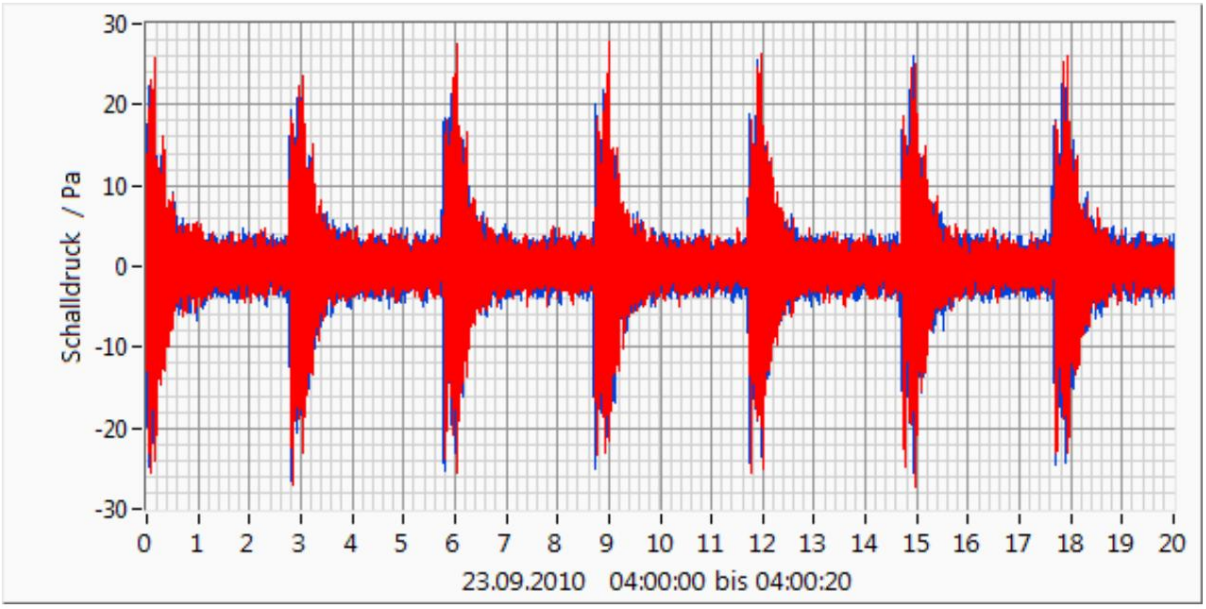

Fig. 7.8.1.7: Time series of piling noise BARD 1 2
hydrophones at AV04 (R4-HR1 red, R4-HR2 blue), start of display at 4:00 a.m., excerpt 20 seconds

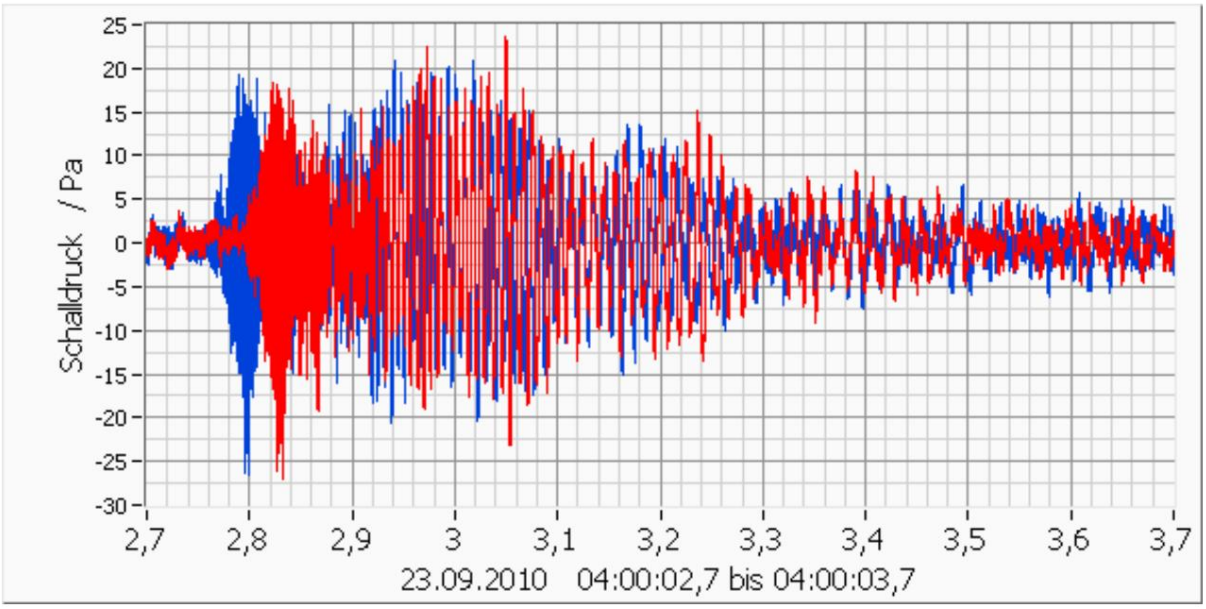

Fig. 7.8.1.8: Time series of piling noise BARD 1 2
hydrophones at AV04 (R4-HR1 red, R4-HR2 blue), start of display at 4:00 a.m., excerpt 1 second

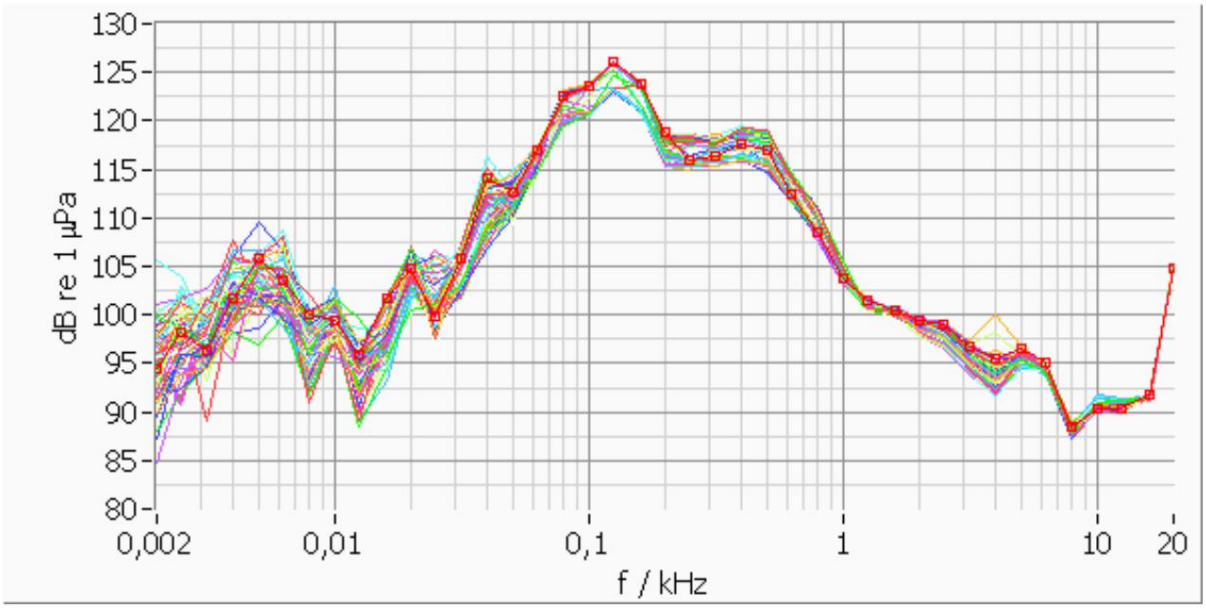

Fig. 7.8.1.9: 5 s third-octave spectrum of pile driving sound BARD
1 hydrophone at AV04 (R4-HR1), number 60, spectrum averaging time 5 s each

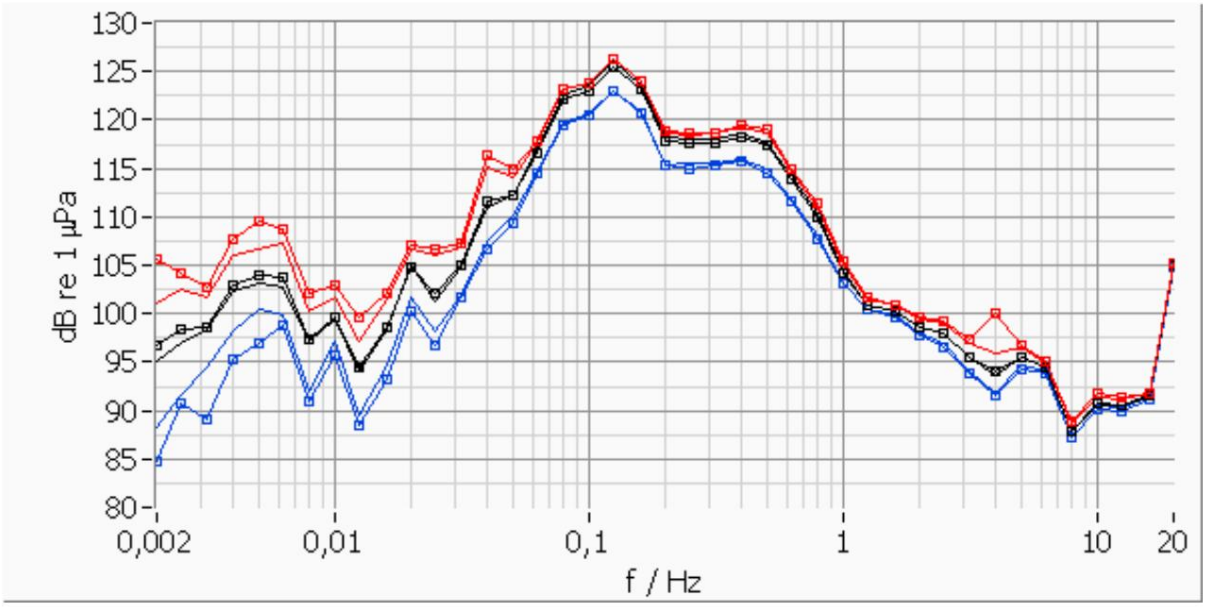

Fig. 7.8.1.10: 5s third-octave spectrum of piling noise BARD 1
percentile, maximum, minimum, energy maximum
(red), energy mean value (black), minimum (blue), each with squared percentiles L5 (red), L50 (black) and L95
(blue), in each case smooth lines hydrophone at AV04 (R4-HR1), averaging time
spectrum in each case 5 s

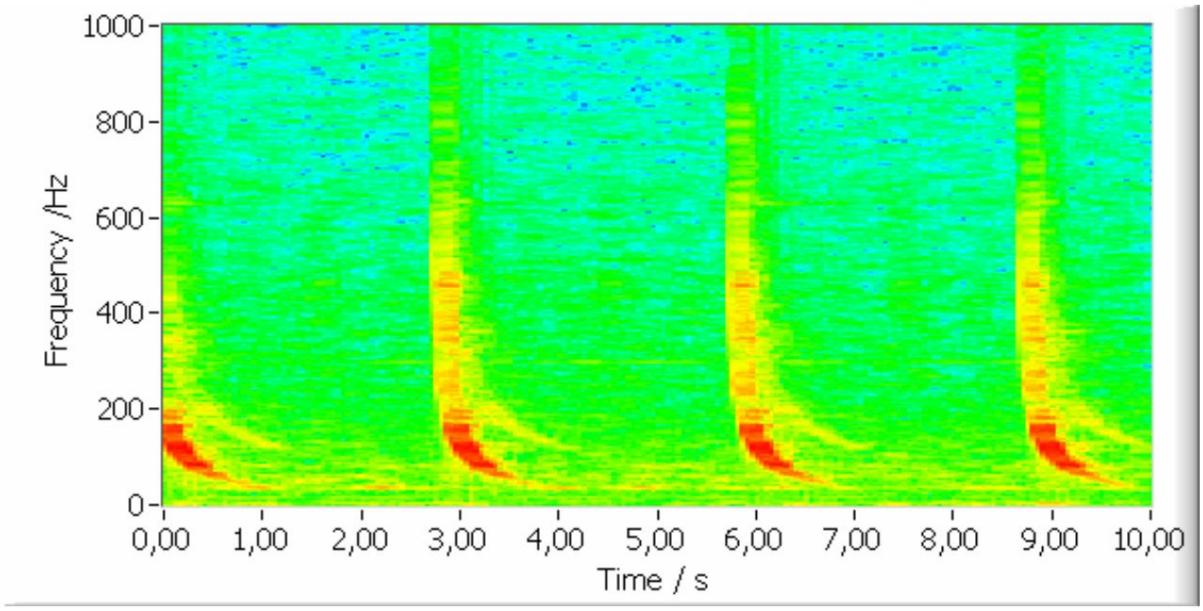

Fig. 7.8.1.11: Spectrogram of piling noise BARD 1 color scale
red high intensity, decreasing via yellow, green to blue low Result: spectral density high from
50 to 200 Hz according to third-octave spectrum, low frequencies have significantly lower speed, visible two propagation paths hydrophone at AV04 (R4-HR1)

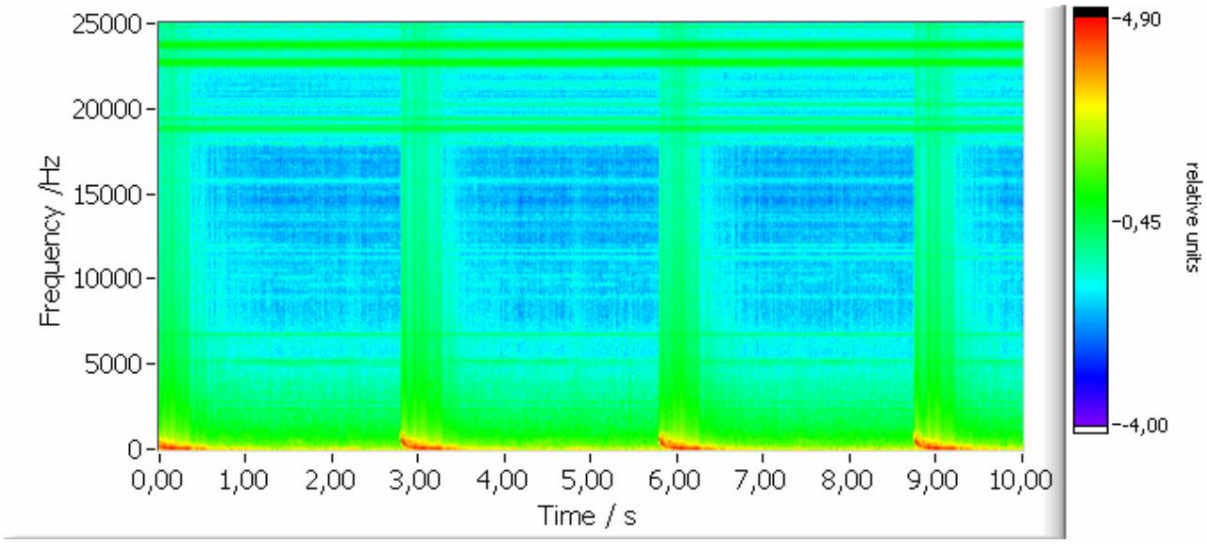

Fig. 7.8.1.12: BARD 1 piling noise spectrogram As shown above,
frequency scale up to 25,000 Hz, result: no high frequencies involved

7.8.2 Acoustic and electrical interference

Acoustic and electrical interference are described below. This interference prompted the authors to use a bandpass filter from 10 Hz to 3 kHz, with which all of this interference could be removed when calculating Leq and Peak values.

The disturbances are in detail:

Acoustic:

Below 10 Hz - low-frequency flow separations at the hydrophone due to tidal currents and wave-induced speeds, 3.5 kHz to 4.2 kHz -
periodic chain clanking, particularly strong at FINO1, 15.6 kHz - radiation
from scour sonar at the plant AV04.

Electrical:

Over 4 kHz - interference from the frequency converter in the AV04 system, the hydrophone cables are routed into the system, the measuring computer is in the system, 50.5 Hz,
101 Hz, 202 Hz and other harmonics - mains interference from the generator to FINO1.

In this case, to calculate the Leq values, the narrowband spectra were calculated variance-neutral and the spectral densities of the affected frequency lines were replaced by the mean values of the spectral densities of the surrounding lines plus 1.5 dB. Finally, the variances corrected in this way were determined by summing the spectral densities over the entire spectra, and the corrected Leq values were calculated from them. This procedure was made more difficult by the fact that the generator speed and thus the grid frequency on FINO1 fluctuated slightly from measurement to measurement. In addition, individual discrete lines can be found at the frequencies 4.8 kHz, 9.6 kHz, 14.4 kHz, 19.2 Hz, which were probably interspersed by a measuring computer or modem installed on FINO1.

Fig. 7.8.2.1 shows an unfiltered narrowband spectrum, i.e. without a bandpass, of the sound recorded with the hydrophone on AV04 (R4-HR1). Below 0.01 kHz pseudonoise is generated by flow separation, see below for explanation of pseudonoise. Electrical radiation above 3 kHz mainly generates interference from the inverters in the AV04 system.

Fig. 7.8.2.2 shows an unfiltered narrowband spectrum, i.e. without a bandpass, of the sound recorded with the hydrophone on FINO1 (F1-H8106). Below 0.01 kHz, pseudo-sound is generated by flow detachment. In the middle range from 0.1 kHz to 0.6 kHz and weaker up to 1 kHz there is mains hum, the band filter to be used does not help here. At 3.5 to 4.5 kHz the clanking of anchor chains can be heard. At 15.6 kHz is the interfering signal from Kolk sonar.

Fig. 7.8.2.3 shows the filtered narrowband spectrum. The filter is a bandpass, Butterworth filter 8. Order with the corner frequencies 10 Hz and 3.0 kHz. It was measured on the hydrophone at AV04 (Re-HR1). The result is that the interference is removed and the essential part of the acoustic spectrum is preserved. This filtering is used when forming the Leq and Peak values. In most representations, the frequency range is limited to 10 Hz to 3 kHz.

The faults are described in detail below.

Fig. 7.8.2.4 shows the vortex shedding frequency at the hydrophone as a function of the flow velocity according to Strouhal (Prandtl 2008). A stable von Karman vortex street forms at the Strouhal number Sr = 0.2. The hydrophone has a diameter of D = 32 mm. With f = v . Sr / D results in the shedding frequency f in Hz. The flow velocity v in m/s is generated by tidal currents and waves. Tidal currents affect the sound level of all three hydrophones in almost the same way, wave-induced velocities affect the three hydrophones very differently. Both were observed in the spectra. Tidal currents alone are 0.7 m/s, mainly in an east-west direction (ADCP measurements according to RAVE 2012). According to Strouhal, flow velocities between 0 and 2 m/s result in frequencies of 0 to 12 Hz, see figure.

These frequencies can be found in Fig. 7.8.2.1 and 7.8.2.2. They do not represent sound but vortex shedding. This phenomenon is called pseudo sound. For information on pseudo-sound, see also Betke

(1998). For some measurements in high seas, the wave-induced pseudo-sound was so strong that these measurements were discarded.
Fig. 7.8.2.5 shows the chain clanking spectrum between 3.5 and 4.2 kHz, also identified as such by Betke (2012) in Fig. 4.1. In addition, one of the discrete lines listed above can be seen at 4.8 kHz.

Fig. 7.6.2.6 shows the spectrum of Kolk sonar. It consists of individual lines symmetrically around 15.6 kHz at a distance of 50 Hz. A total of up to 24 devices were used in the wind farm (RAVE 2012). In addition, one of the discrete lines is present at 14.4 kHz.

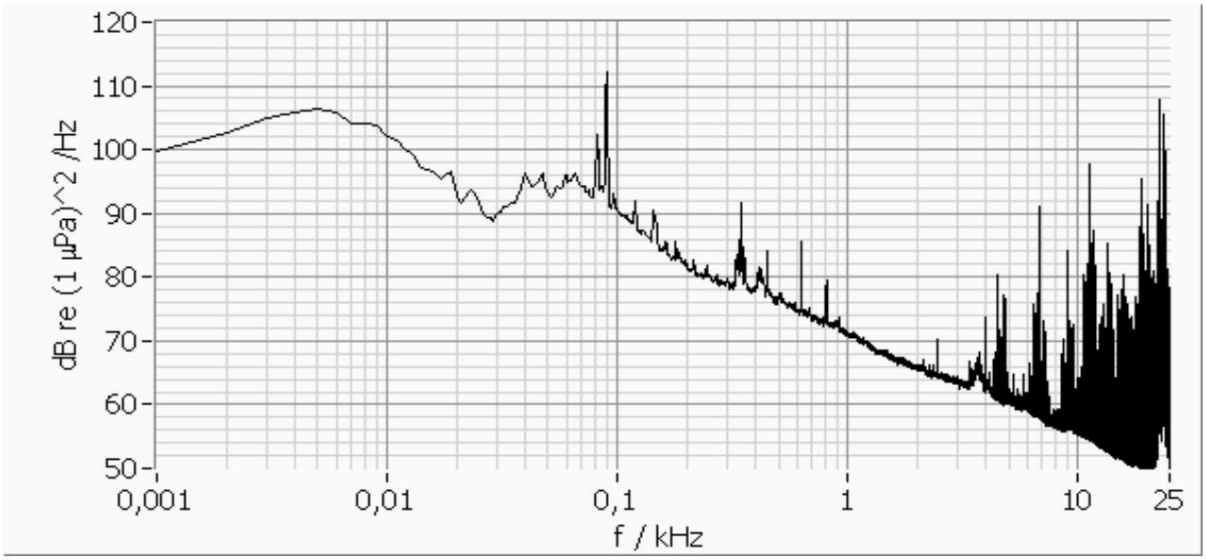

Fig. 7.8.2.1: Narrow-band spectrum, unfiltered, hydrophone at AV04 (R4-HR1), without bandpass Result: Below 10 Hz pseudo-sound due to flow separation, above 3 kHz electrical interference

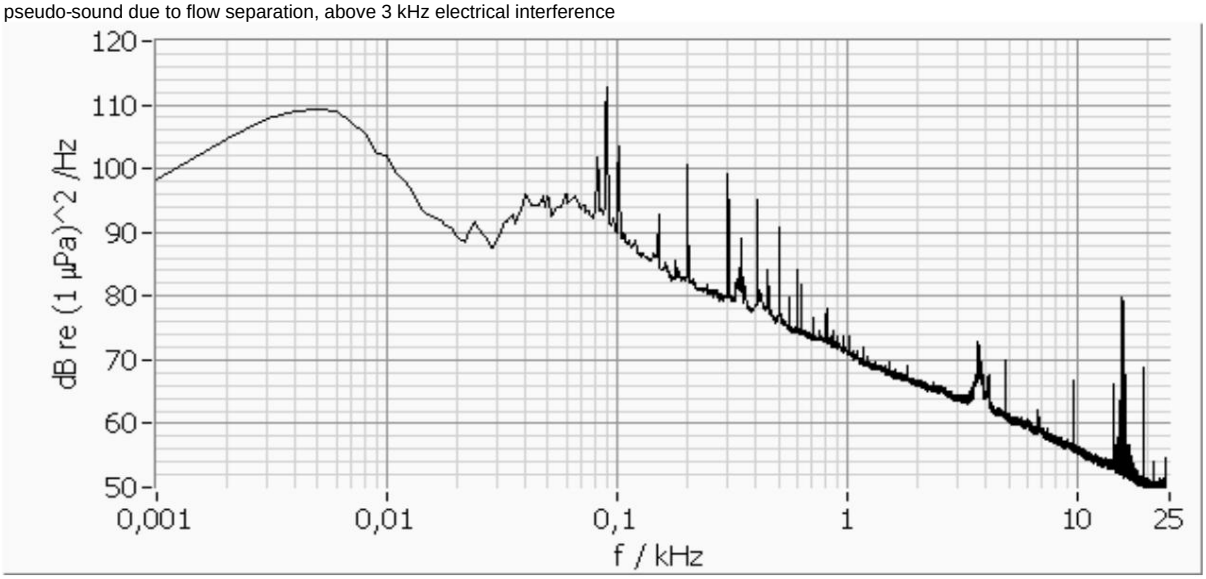

Fig. 7.8.2.2: Narrowband spectrum, unfiltered, hydrophone at FINO1 (F1-H8106), without bandpass Result: Below 10 Hz pseudo sound due to flow separation, 101, 202, 303, 404, 505, 606 Hz individual harmonics of the local mains frequency, at 15.6kHz sonar

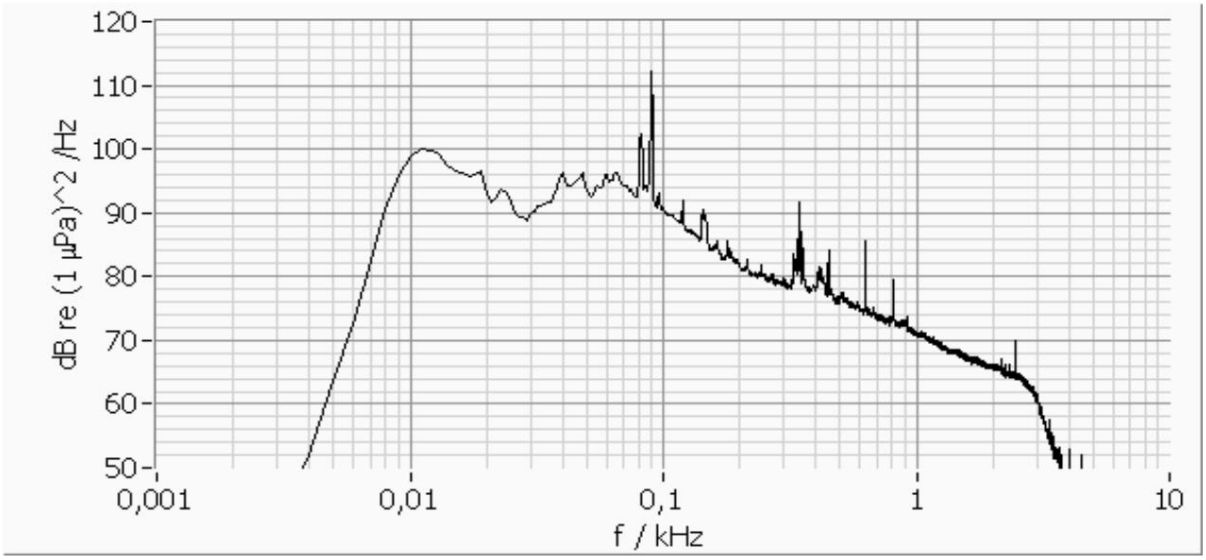

Fig. 7.8.2.3: Narrowband spectrum, according to Fig. 7.8.2.1 but filtered with bandpass, hydrophone on AV04 (R4-HR1), bandpass filtering 10 Hz to 3.0 kHz Butterworth filter 8th order Result: interference removed, the essential part of the acoustic spectrum is preserved

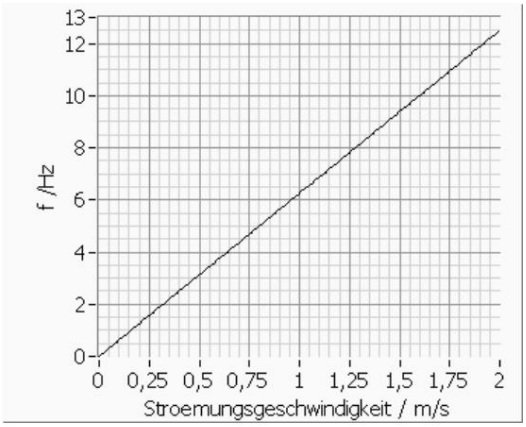

Fig. 7.8.2.4:
Vortex shedding frequency at the hydrophone f = f(v) as a function of flow velocity according to Strouhal

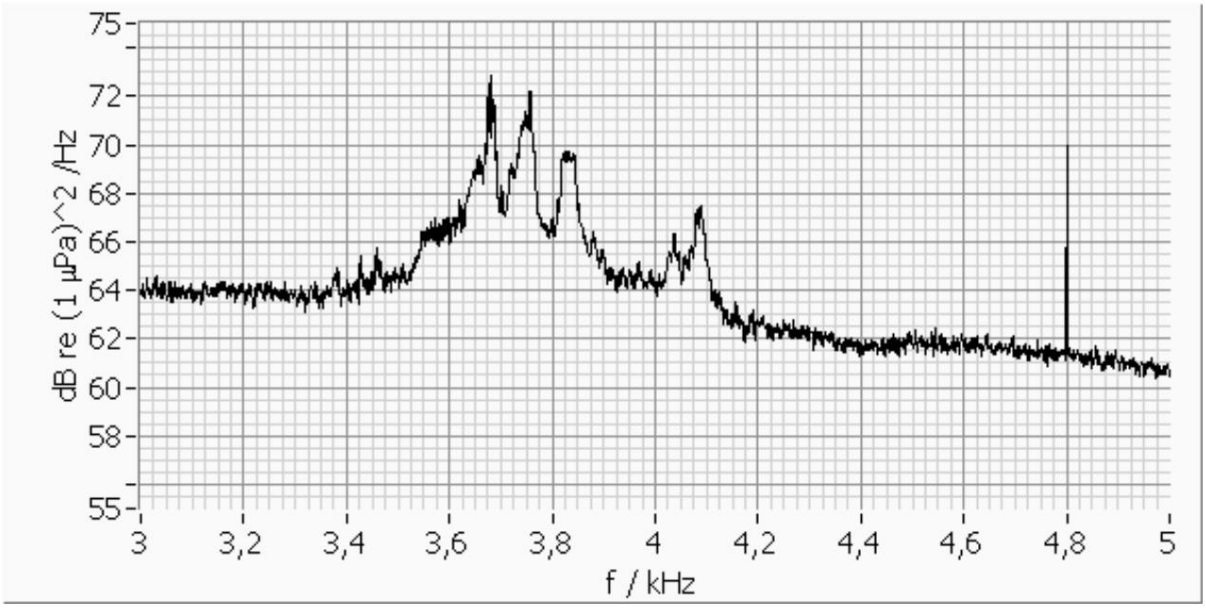

Fig. 7.8.2.5: Narrow band spectrum, hydrophone on FINO1 F1-H8106 chain clutter 3.5 kHz to 4.2 kHz, discrete line 4.8 kHz

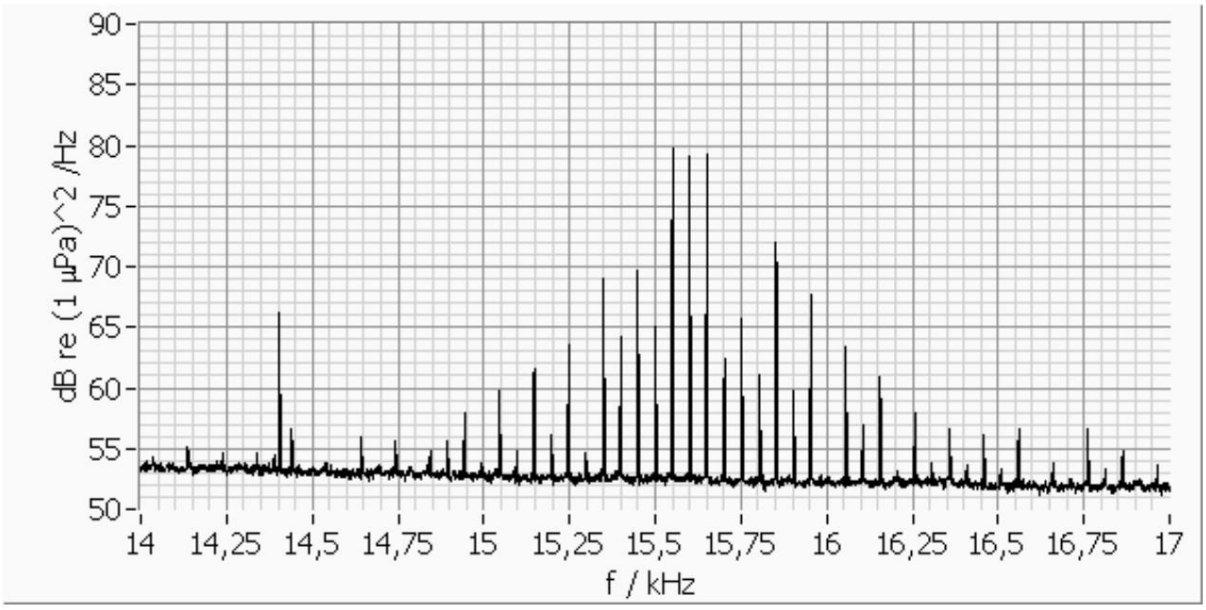

Fig. 7.8.2.6: Narrow-band spectrum, hydrophone on FINO1 F1-H8106 Kolk sonar, individual lines symmetrically around 15.6 kHz at a distance of 50 Hz, discrete line at 14.4 kHz

7.8.3 Ship noise When
listening to the time series of the sound, ship noise could be partially identified.
If clearly identified, the time series were sorted out. This mainly affected the intense sounds of ships in the immediate vicinity. If the identification was not clear, the corresponding measurements were not sorted out and left in the evaluation. This means that a not inconsiderable proportion of the measurements include quiet ship noise, as explained in Section 7.5, among other things.

In the following, it is shown mathematically that the ship noise of the traffic separation areas 14 km away to the north and south of the wind farm, see Section 3, generate background noise in the wind farm of the same order of magnitude as was measured there. It is shown with a literature value that the third-octave spectrum of a ship corresponds to the frequency ranges of the spectra measured here and that the propagation of the sound is dampened by waves, i.e. it becomes quieter with more wind. A frequency-dependent propagation calculation, which changes the spectrum at large distances, is not carried out here. The calculation basically points out that the background noise in alpha ventus is so high that it is difficult to calculate the source strength of the systems using noise measurements.

Sources of noise from ships are engine noise and noise from auxiliary units, propeller noise and hydrodynamic noise (Urban 2002 p. 226). According to Kipple (2004), ships have a source strength of up to 180 dB re 1ÿPa re 1 yd, see Fig. 7.8.3.1. The specified ships are not very noisy. A yard (yd) is 0.9144 m, so the source strength related to 1 m is insignificantly 0.6 dB lower because of -0.6 dB = 15 . log(1yd/ 1m). With the attenuation TL = 15 . log(14000m/1m) = 62 dB results from Eq. 4.3.2 as a sound level in the wind farm 118 dB re 1ÿPa, which was measured as mean values in 2011 and almost identical values in 2010 on the three hydrophones, compare Leq values in Tab. 7.2.1. If there are several ships, the level increases to TSKonvois = 10 . log(n)+TSsingle ship, where n is the number and TSsingle ship is the source strength of a ship (Urban 2002 p. 230).
Fig. 7.8.3.2 shows a third-octave spectrum (Arveson 2000) of a cargo ship, length 173 m, speed 15.6 knots at propeller speed 145 per minute (RPM), width 23 m, draft 10 m, power 8.232 MW, propeller diameter 4.9 m , built in 1977. The maximum exceeds 180 dB and is between 50 Hz and 63 Hz. Other sources (Coral Princess 2004) show similar behavior. Overall, it is confirmed that ship noise is in the frequency range that was examined here and that the volume is large enough to be measured in the background noise. The authors suspect that ship noises between approx. 100 Hz and 1.5 kHz shown in Figs. 7.5.11 and 7.5.12 are the cause of the discontinuous progression of the narrowband spectra shown there. A further analysis specifically of the frequency-dependent attenuation according to Thiele is not carried out here because the ships with their spectra and routes that have passed the paths during the measurement period are difficult to analyze.
Wille and Geyer (Wille 1988) carried out measurements of the sound attenuation in the North Sea, water depth 30 m, distance transmitter to receiver 10.5 km, depending on the wave height. The measurement setup is shown in Fig. 7.8.3.3a. The conditions (North Sea, water depth 30 m, distance 10 km) correspond very precisely to the conditions of the present study. They have proven that with increasing wave height, shown in the figure with increasing wind speed, the transmission loss, e.g. B. increase with tones of 1 kHz, see Fig. 7.8.3.3b.
This increase in damping could also be shown when a bad weather front passed through with a correspondingly large amount of wind and waves, see Fig. 7.8.3.3c. The increasing damping is explained by the increasing entry of air into the water due to higher waves. The effect is the one used in Bubble Veil. Due to waves, this effect makes itself felt at large distances, with Wille et al. from 10 km, noticeable at alpha ventus from 14 km. This relationship proves that it becomes quieter under water with increasing wind and thus waves, as is the case with the continuous sound levels Leq, Fig. 7.3.2, in the third-octave spectra Fig. 7.4.1 and 7.4.5 and in the narrow-band spectra Fig. 7.5.5 is shown.

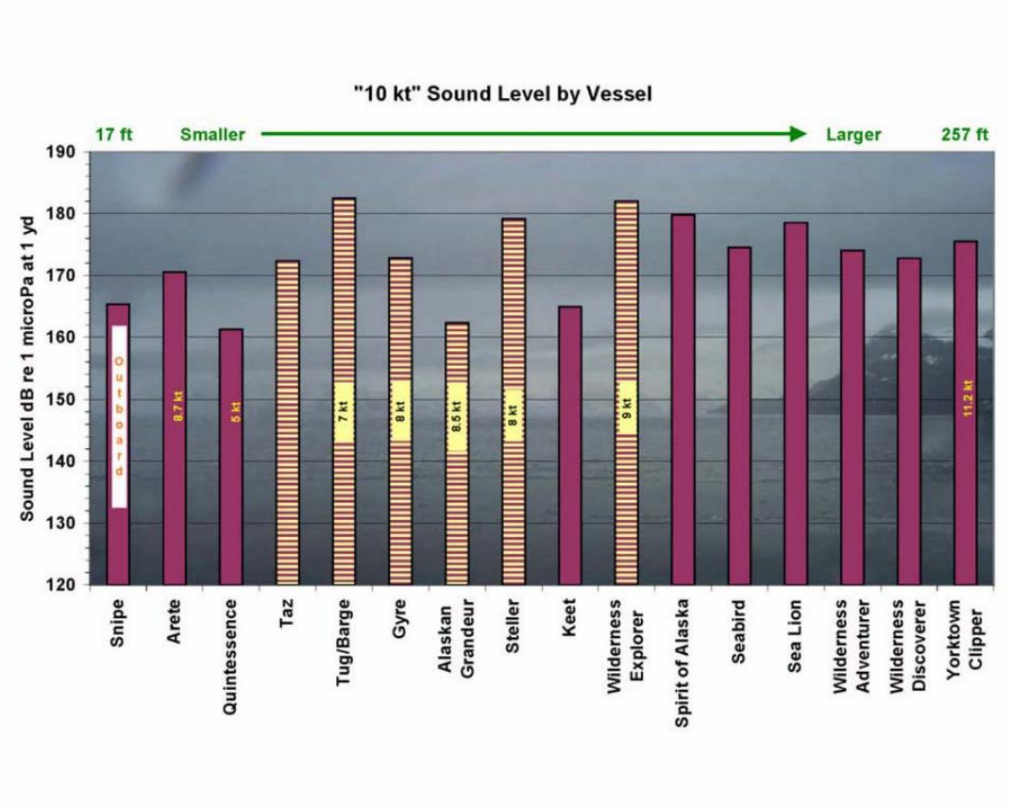

Fig. 7.8.3.1: Source strengths of ships according to Kipple (2004), result: source strength Lwa approx. 180 dB re 1ÿPa re 1m

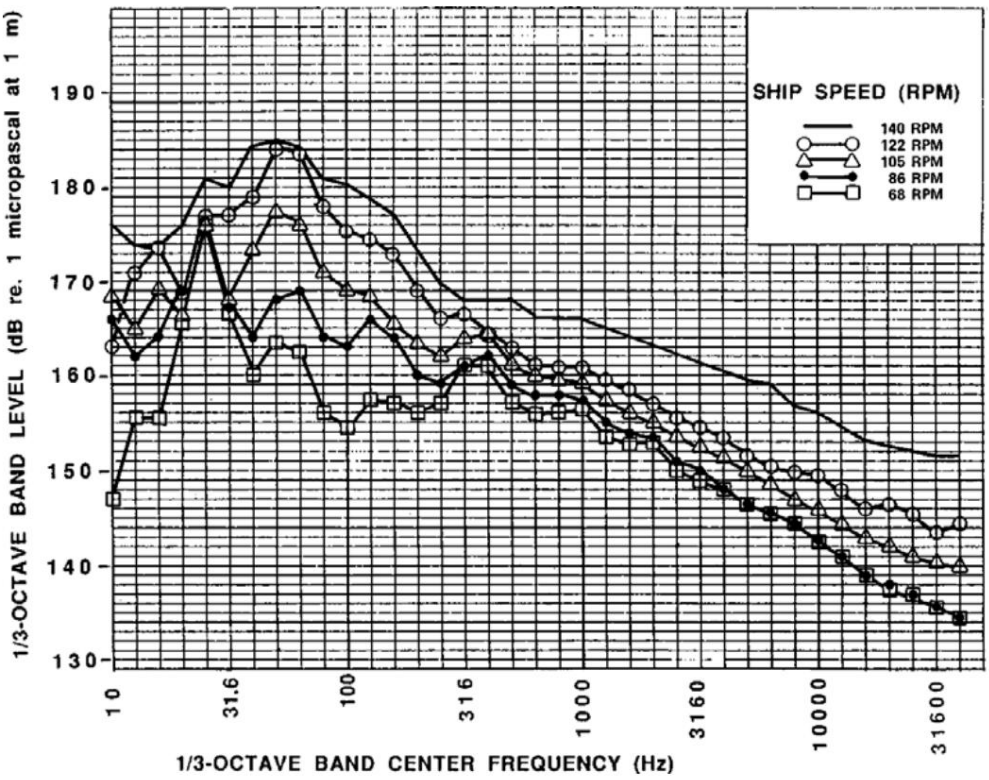

Fig. 7.8.3.2: Source strength as a third-octave spectrum, freighter, length 173 m, 140 RPM full speed (Arveson 2000)
Result: Ships emit in the frequency range of the wind turbines examined here

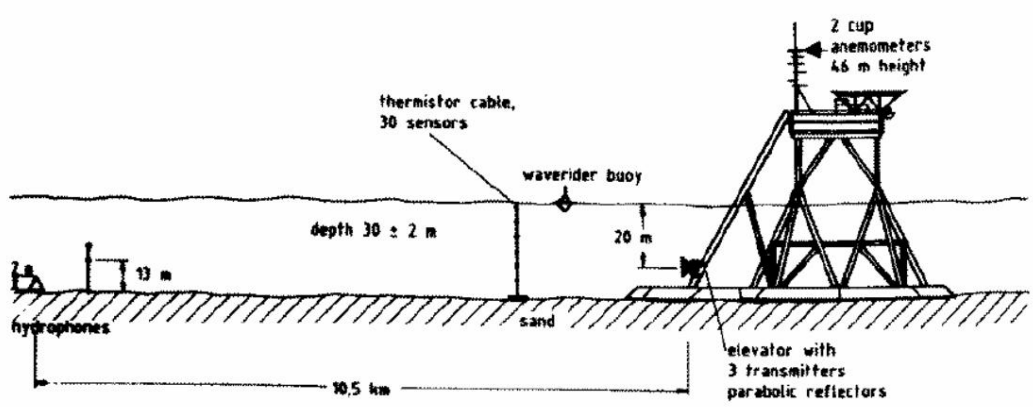

Fig. 7.8.3.3a Measurement of sound propagation in the North Sea
Measurement setup: Loudspeaker and hydrophone at a distance of 10.5 km, water depth 30 m (Wille 1988)

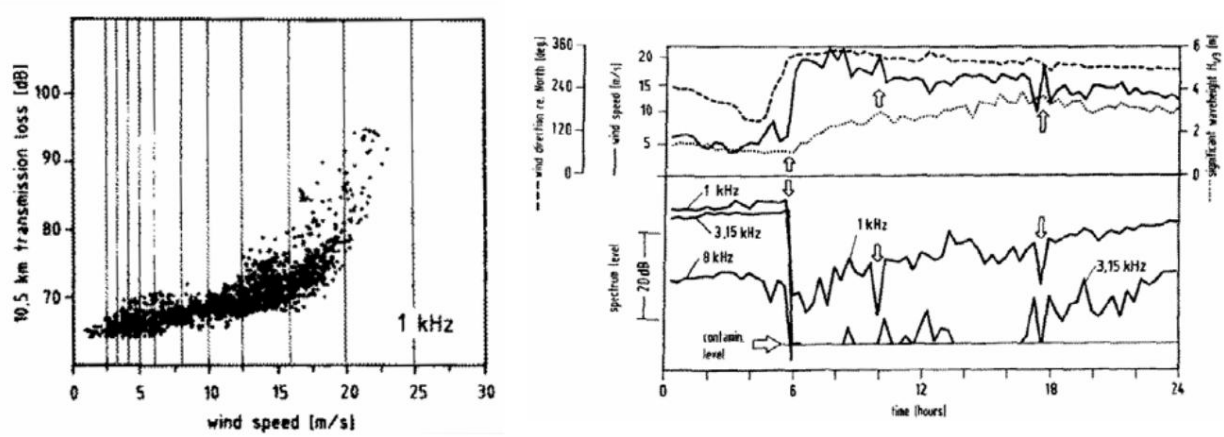

Fig. 7.8.3.3b,c Measurement of sound propagation in the North Sea
Left b: Transmission losses at 1 kHz sound over wind speed, each point a measurement over 10 minutes Result: Transmission losses increase with increasing wind speed Right c: Bad weather front passing through with strong wind increase as a time series 0 to 24 hours Upper figure: Wind speed over time, strong wind increase in hour 5 Lower figure: Third-octave spectra for 1 kHz and 3.15 kHz over time, strong drop in the signal (high transmission losses) in hour 5, 1 kHz drops sharply by approx 20 dB, 3.15 kHz barely visible Overall result: Transmission losses increase with increasing wind (Wille 1988)

Cause: Air bubbles introduced by waves
Remarkable: Conditions (water depth 30 m, distance between transmitter and receiver 10 km) almost identical to alpha ventus and shipping routes

7.8.4 Animal noises

When viewing and listening to the time series, see Section 7.1, some very unusual and some very loud noises were heard, e.g. B. scraping noises. These sounded the way you know it when someone touches a microphone or moves their hand. The authors interpret these noises as movement of animals that are directly on the hydrophone or touch the hydrophone to e.g. B. to eat the vegetation or to search for food.

Time series in which such noises were identified were removed from the analysis unless comparable noises also occurred on at least one other hydrophone in the same time window.

8. Discussion of the measurement

results The measurement results have already been largely interpreted in their presentation in Section 7. The measurement results are summarized below.

The mean sound level Leq at all 3 hydrophones is 118 dB re 1 ÿPa in 2011, see Table 7.2.1, which is identical to measurements by Betke at a comparable position (Betke, 2012, p. 43). In 2010, around 1 dB less was measured on all hydrophones.

The peak value Lpeak was determined to be about 15 dB higher than Leq.

Mean sound levels averaged over 5 seconds (5s-Leq) generate only a slightly larger spread than sound levels averaged over 300 seconds (300s-Leq), see Fig. 7.2.11-7.2.13.

The broadband sound level Leq decreases with the wind and especially with the waves, see Section 7.3. The background noise level could be measured at 0% power, especially for the next systems AV04 and AV07, and was higher than at 100% full load, see Fig. 7.3.3 – 7.3.5. The reason is that the background noise is about the same size as the system noise (see also Betke 2012 p. 34 ff). The background noise is essentially determined by ships, whereby service ships no longer operate when there is a lot of wind in the park (see also Betke ibid.) and the sound of distant ships is more strongly damped when there is a lot of wind, see below.

The third-octave spectra, Fig. 7.4.1 – 7.4.6 show that the spectral component drops above 100 Hz when there is a lot of wind and there with waves. This spectral component, which is represented in the spectrum when there is little wind, does not have its source in the turbines, but is background noise. The authors interpret that the ships on the two shipping lanes 14 km apart sail independently of the wind, but the damping increases with wind and especially with waves. The spectra of the ships are in the frequency range that has an influence here. The authors interpret that Fig. 7.5.11 and Fig. 7.5.12 show the influence of ship noise above 100 Hz. The source strength of the ships is so great that they can generate a significant part of the sound in alpha ventus despite the transmission losses. For details on ship noises, see Section 7.8.3.

The background noise is relatively high compared to the noise of the AV04 system, which means that the noise in front of the AV04 system is occasionally larger when the AV04 system is switched off than when the AV04 system is switched on, see Fig. 7.5.14. Betke (Betke 2004, p. 34) comes to the same conclusion when comparing the spectra of systems that are switched on and off, that in some cases the spectra of systems that are switched off are higher than those of systems that are switched on, apart from the distinctive peak at 90 Hz assume that the targeted and only very limited potential for shutting down plants, which the research group was told, might have led to less precise statements.

The third-octave spectra also show that sound energy is present in the frequencies 10 to 100 Hz.
These essentially have their source in the systems, in particular the distinctive peak in the third to 100 Hz, the tonal part is 90 Hz, see narrowband spectra. Here it is indicated that although the sound in the 10 to 100 Hz range from the systems increases with increasing wind, the damping in the 100 Hz to 10 kHz range dampens the background noise so much that the overall level decreases.

Frequencies below 10 Hz can also be detected in the third-octave spectra. As shown in Section 7.8.2, these are to be assigned to currents, so they are not operational noise and can be removed with the band filter.

The narrow-band spectra in the frequency range from 10 Hz to 3 kHz in the 3 power classes and the 2 wave classes, see Fig. 7.5.1 - 7.5.5, confirm the statements made about the third-octave spectra.

The spectrum at full load is represented by Fig. 7.5.6. At 10 to 100 Hz there is a level between 90 to 100 dB/Hz (spectral density unit is exactly dB re (1ÿPa)²/Hz) with individual lines belonging to plants and the very prominent line 90 Hz, which clearly belongs to plant AV07 assigned, see section Accelerometers below. The spectrum falls between 100 Hz and 3 kHz at around 18 dB per decade. Overlaid are individual lines that are multiples of the 90 Hz line.

The sound of the AV04 system can hardly be detected, although the hydrophones are only 100 m in front of it, see Fig. 7.5.14.

With the narrow-band analysis, the 3 lines around 90 Hz, i.e. 89, 90 and 91 Hz, are initially examined at full load. Impressive evidence of the peak is shown in Fig. 7.6.1. The energetic addition of the 3 lines results in an upper value of 116 dB re 1 ÿPa and a lower value of 105 dB re 1 ÿPa.
At a distance of around 800 m between the hydrophone and the AV07 system, converted using the distance- and frequency-dependent transmission loss according to Thiele, the source strength Lwa of the AV07 system is 157 dB re 1 ÿPa, for details see Table 7.6.1. This level is calculated at a distance of 1 m from the system. At 15 dB, the peak emerges so prominently from the spectrum that the other frequencies in the system hardly make any further contribution to the source strength. The audibility of this sound for harbor porpoises and seals is described in Section 9.
It has been proven that the level of this 90 Hz tone increases with the output of the AV07 system, see Fig. 7.6.5, i.e. there is a clear direct dependency here, in contrast to the overall noise. When the rated output is reached, this tonal component is noticeable. This tonal component is also noticeable when the nominal wind speed is reached from 11 m/s, see Fig. 7.6.9.
It is also striking that the level of the tonal component depends on the water level, see Fig. 7.6.2.
The authors assume that a period in the drive train, rollover frequency in the bearing or tooth meshing frequency excites the water column in the central body of the foundation structure into resonance.
In the partial load range, this tone changes its frequency and has been proven to be strictly coupled to vibrations in the foundation structure, see spectrograms in Section 7.7.3. The latter is presumably linked to the speed of the drive train. The sound level is relatively weak in part-load operation for two reasons: Firstly, the frequency of the sound is demonstrably not constant due to the speed variability and is distributed over many lines. Secondly, the excitation is probably weaker.
With the acceleration spectra, see Section 7.7, the sources of all important sound lines could be identified. The AV07 system is assigned the very strong 90 Hz peak, see Fig. 7.7.1.1 for clear evidence, and harmonics between 300 and 800 Hz as well as harmonics of 30 Hz, so that the 90 Hz can be seen as the 3rd harmonic of 30 Hz. see fig. 7.7.2.1 and 7.7.2.2. 22 Hz, 28 Hz and 24 Hz and harmonics can also be assigned to the system AV07, see Fig. 7.7.2.3.

The AV04 system is assigned the weak frequencies of 140 to 150 Hz, see Fig. 7.7.1.1 and 17.937 Hz and harmonics, see Fig. 7.7.2.4.
Thus, all significant lines in the sound spectra from below 20 Hz to 1000 Hz can be assigned to their sources, see Fig. 7.7.2.5 and 7.7.2.6.
The ramming impacts from the offshore wind farm Borkum West II and BARD Offshore 1, 50 km and 7 km away, could be identified: The peak values were determined as 149 and 162 dB re 1 ÿPa, the Leq values were 130 and 144 dB re 1 ÿPa determined at beat intervals of 1.3 s and 3.0 s.
Betke (Betke 2012 p. 32) measured a Leq value of 130 dB re 1 ÿPa at 0.38 s between the impacts at a similar position in alpha ventus for driving impacts of Borkum West II.
The third-octave spectrum of the pile driving could be shown. The maximum for Borkum West II is 140 dB re 1 ÿPa, center frequency around 100 Hz and drops to 120 dB at 30 Hz and 300 Hz. The maximum for BARD 1 is 124 dB, center frequency slightly higher than 100 Hz and is noticeable 115 dB down at 70 Hz and 200 Hz. A second peak is visible here at around 400 Hz. Betke (2012), p. 40, finds almost identical spectra for this wind farm.
Sound with frequencies below 10 Hz is identified as pseudo-sound generated by currents and removed by high-pass filtering.
Signals above 3 kHz are essentially identified as electrical interference and removed by a low-pass filter.

A high-frequency signal between 3.5 and 4.2 kHz is a sound event, but not from installations but from chain anchorages, Betke (2012) p. 19 identifies the same.
Marine mammal audibility is described in the next section.

9. Marine Mammals Audibility The
audibility of underwater noise is shown below. In addition, hearing curves of the marine mammals harbor porpoise and seal are shown, as well as sound spectra at full load.

Porpoises hear very well in the high frequency range of 1 kHz to 100 kHz. Various investigations are by Lucke et. al (2009), see Fig. 9.1.1. Harbor porpoises use high-frequency echolocation for orientation and hunting because of the good spatial resolution of the short wavelength.

Fig. 9.1.2 shows the narrow-band hearing curves (hearing thresholds) of the porpoise, upper curve, and the seal, lower curve, which hears much better in this frequency range. 7 sound spectra are entered at full load, the position of the hydrophone (R4-HR1) is around 100 m in front of the AV04 system and 800 m in front of the AV07 system, with both systems running at full load, see also Fig. 7.5.6. There are no hearing thresholds for the prominent frequency of 90 Hz. By comparison with the measured spectra, see also Fig. 7.5.1 to 7.5.5, the following becomes clear. For the porpoise u.
U., apart from a few exceptions, especially in the case of the harmonics of 90 Hz between 700 and 1000 Hz, the sound levels at these distances are below the hearing threshold. The authors suspect that the harbor porpoise can hear the facility if it is close enough to the facility. The system is clearly audible to the seal. In the entire frequency range above 125 Hz, the level is 10 dB to 15 dB higher than the hearing threshold at the measured distance and 20 dB higher at the peaks. Since the peaks originate from a facility 800 m away, they fall to the hearing threshold at 15 dB per decade at 8 km away.

At present, one can assume with a certain degree of certainty that the biological effects on marine animals are rather small. The energies generated by the operating noise are relatively small but could lead to masking of the communication. These are assumptions, since there are no studies on this.
There is also a lack of data on the hearing threshold for the distinctive tonal noise of 90 Hz. As also explained by Betke (2012), the biological relevance of the physical results demonstrated here is not certain. Statements from marine biologists and bioacousticians and the resulting legal requirements for avoiding noise are required.

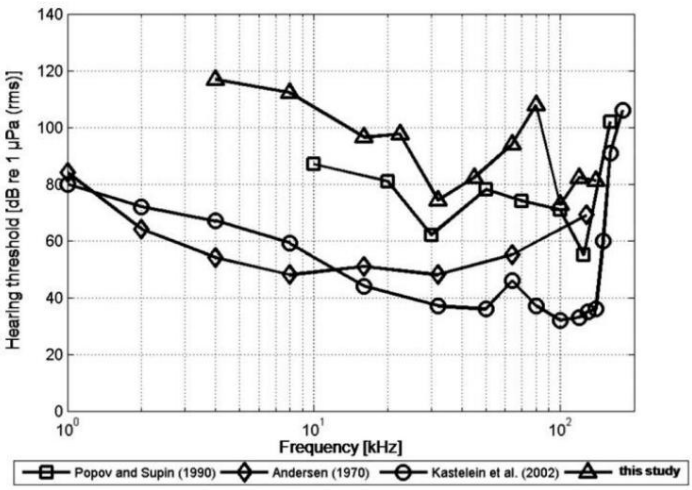

Fig. 9.1.1: Hearing curves (hearing thresholds) in the high frequency range from 1 kHz to 100 kHz for harbor porpoises (Lucke 2009, see also Betke 2012)

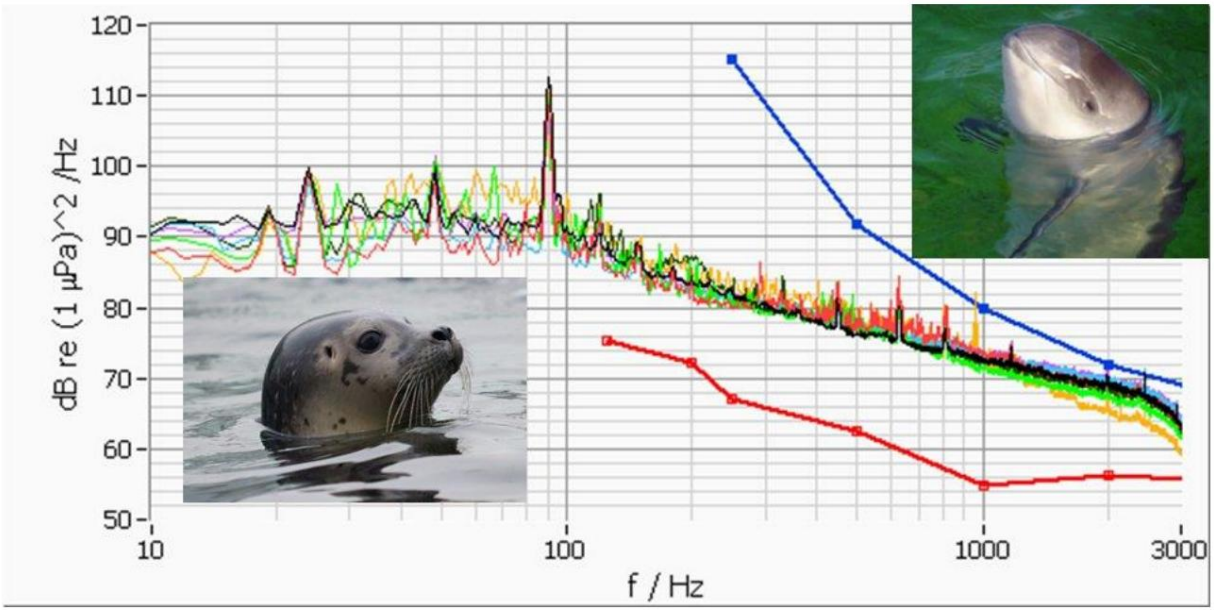

Fig. 9.1.2: Hearing thresholds for harbor porpoise (blue line), seal (red line), own measurement (in between)
(Data from porpoise and seal Kastelein 2002 and 2011, see also Betke 2012) and 7 spectra hydrophone R4-
HR1 (all colors and black)
Position around 100 m in front of system AV04 and 800 m in front of system AV07,
both systems at full capacity, see also Fig. 7.5.6 Source of
picture seal: Aquarium GEOMAR http://aquarium-geomar.de/tiere/luna.html, access 5/ 2013 Source image porpoise: Wikimedia
AVampireTear License: CC-BY-SA-3.0 http://creativecommons.org/licenses/by sa/3.0/, accessed 5/2013

10. Simulation of sound field

The sound field is simulated below. Because of the strong background, not all source strengths can be determined with certainty. So it can only be an estimate. The values used here are the same as or higher than those in the sources given below.

The following assumptions were made: source

strength AV07-AV12 source	129 dB re 1 ÿPa re 100 m, see Tab. 7.6.1 100 dB re
strength AV01-AV06	1 ÿPa re 100 m, see Fig. 7.5.6, there only the peak below 20 Hz with 94 dB clearly from AV04, all others not from AV04 , so the estimate is conservative, measurement distance is approx. 100 m 100 dB re 1 ÿPa, see also Betke
background level	2012 third-octave spectra pp. 38, 39, lower values in the spectrum there, so the estimate is conservative 15 log (r/100m), see Eq. 4.3.1.

Sound propagation

The result is that at the position of the hydrophones R4-HR1, R4-HR2, F1-H8016-2, according to the propagation calculation, taking into account the 12 systems with the stated source levels and the background level, the sound levels are 119.8, 119.6, 118.8 dB re 1 ÿPa prevail, which is approx. 1 dB higher than the measured mean values of all measurements, compare Tab. 7.2.1.

Lines of equal volume Leq, unit dB re 1 ÿPa, are shown in Fig. 8.1. The UTM coordinates start as northings with 34 1000 and end with 34 5000, which corresponds to 4 km, the northings start with 598 5000 and end with 598 9000, which corresponds to 4 km. In the lower part of the picture, the 6 systems AV07 to AV012 are within the 125 dB lines (higher values are not shown here for the sake of clarity). The 6 systems AV01 to AV06 are shown in the upper middle 4 fields, FINO1 is marked to the west. Because the source strength of these systems is only as high as the background, these systems can hardly be seen in the isoline field.

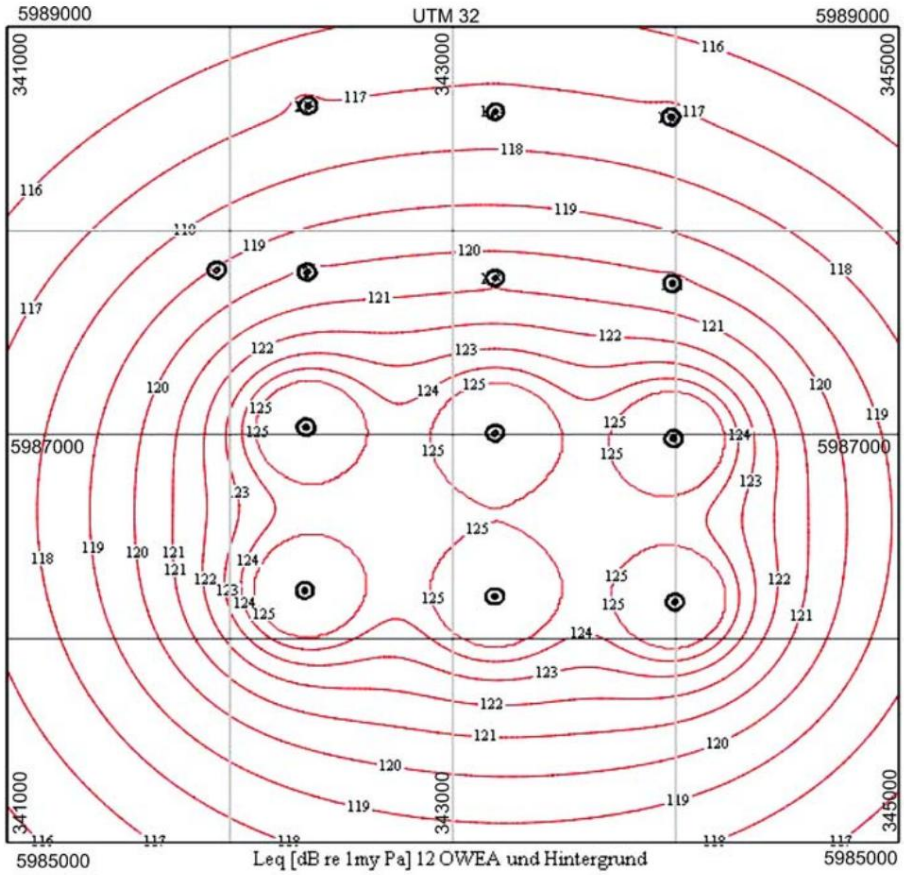

Row
AV01, AV02, AV03

FINO1 and
Row
AV04, AV05, AV06

Row
AV07, AV08, AV09

Row
AV10, AV11, AV12

Fig. 10.1: alpha ventus, lines of equal loudness, conservative estimate, values above, Leq in dB re 1 ÿPa map 4 km x 4 km, UTM coordinates northing and northing (higher values than 125 dB are not shown here)

11. Thanks

This project was funded by the Federal Ministry for the Environment, Nature Conservation and Nuclear Safety based on a resolution of the German Bundestag, funding number 0327687.

The authors would like to thank their colleagues from the German Wind Energy Institute DEWI in Wilhelmshaven, the Federal Maritime and Hydrographic Agency BSH in Hamburg and GL-Garrad Hassan formerly Windtest im Kaiser Wilhelm Koog for installing and maintaining the sensors and measuring computers in the wind farm.

The authors would like to thank the employees of the Fraunhofer Institute IWES in Kassel for their support in the coordination.

Thanks to Max Schuster from DW-ShipConsult for help with ship acoustics.

Special thanks go to the President of the Flensburg University of Applied Sciences, Herbert Zickfeld, for his support.

12. Literature

Abromeit, C. (2007): Approval notice BARD of April 11, 2007, issued by BSH, http://www.bsh.de/de/Meeresutilisation/Wirtschaft/Windparks/Genahmesbescheide/Nordsee/BARD _Offshore_1/Genahmesbescheid_BARD_Offshore_1.pdf, access 15.6 .2012

Andersson, M. H. (2011): Offshore wind farms – ecological effects of noise and habitat alteration on fish. Doctoral dissertation ISBN 978-91-7447-172-4, Department of Zoology, Stockholm University

Arveson, P.T., Vendittis, D.J. (2000): Modern cargo ship noise. J. Acoust. Soc. Am., Vol. 107, No. 1, Jan. 2000

Bendat, I.S., Piersol, A.G. (1980): Engineering Applications of Correlation and Spectral Analysis. Jon Wiley an Sons, New York

Bergström, L., Lagenfelt, I., Sundqvist, F., Andersson, M. (2009): "Fish surveys at Lillgrund - Control program for Lillgrund's wind farm". The Norwegian Fisheries Agency's annual report 2008

Betke, K., Remmers, H. (1998): Measurement and evaluation of low-frequency sound. In Daga 98, conference of the German Society for Acoustics eV Oldenburg at the ETH Zurich, http://www.daga akustik.de/publikationen/daga/DAGA_98_Inhalt.pdf, access 17.5.2012

Betke, K., Schultz-von Glahn, M. (2008): Prognosis of the underwater noise during the construction and operation of the offshore wind farm Borkum-West ("alpha ventus") and measurement of the background noise in the planning area. ITAP, Oldenburg on October 15, 2008, report no. 1169-08-d KB (commissioned work)

Betke, K., Matuschek, R. (2010): Measurements of underwater noise during the construction of wind turbines in the offshore test field "alpha ventus. Final report on monitoring according to StUK 3 in the construction phase. ITAP, Oldenburg

Betke, K., Matuschek, R. (2012): Measurements of underwater noise when operating the wind turbines in the offshore wind farm alpha ventus, final report on monitoring according to StUK 3 in the operating phase. ITAP, Oldenburg on February 3, 2012, http://www.bsh.de/de/Meeresutilisation/Wirtschaft/Windparks/StUK3/Betriebsphase/alpha_ventus_betriebsschall_20120507.pdf, accessed May 18, 2013

BSH (2007): Standard investigation of the effects of offshore wind turbines on the marine environment (StUK 3). Federal Maritime and Hydrographic Agency, BSH No. 7003, Hamburg

Cappelen, J., Jørgensen, B. (1999): Technical Report 99-13: Observed Wind Speed and Direction in Denmark – with Climatological Standard Normals, 1961-90. Danisch Meteorological Institute, Ministry of Transport, Copenhagen

Coral Princess UnderwaterAcoustic (2004): LevelsNaval Surface Warfare Center – Detachment Bremerton Technical Report October 2004

CRI, DEWI, ITAP (2004): Standard methods for determining and assessing the pollution of the marine environment through noise emissions from offshore wind turbines. Final report on research project 0327528 A

Degn, Uffe (2002): Measurements of noise induced from offshore wind turbines and ambient noise in the sea water. GIGAWIND, 2. Symposium, 9. November 2002, Hannover

DIN 45651, octave filter for electroacoustic measurements, http://www.beuth.de/de/norm, 25.6.2012

DIN EN 61672-1, (2003-10), see also DIN IEC 651

Fristedt, T., Morén, P., Söderberg, P. (2001): Acoustic and Electromagnetic noise induced by wind mills – implications for underwater surveillance systems – Pilot study. FOI-R-0233-SE, FOI, Swedish Defence Research Agency, SE-17290 Stockholm, Sweden, 2001

Geodata Center (2012), https://upd.geodatenzentrum.de/geodaten/gdz_rahmen.gdz_div?gdz_spr=deu&gdz_akt_zeile=3&gdz_anz_zeile=6&gdz_user_id=0, access 1.2.2012

Gerthsen, C., Vogel, H. (1993): Physics. Springer Verlag, Heidelberg

Heinemann, E., Feldhaus, R. (2003): Hydraulics for civil engineers, Vieweg and Teubner, Wiesbaden

Henn, H., Sinambari, GR, Fallen, M. (1999): Engineer Acoustics. Vieweg Verlag, Brunswick

IEC 1260:1995 and ANSI S1.11-2004, see (2008): User Manual, National Instruments Corporation

ISD, DEWI, ITAP (2007): Standard methods for determining and evaluating the pollution of the marine environment through noise emissions from offshore wind turbines. Final report on research project 0329947, Federal Ministry for the Environment, Nature Conservation and Nuclear Safety, Berlin

Kastelein RA, Wensveen PJ, Terhune JM, de Jong CAF (2011): Near-threshold equal-loudness contours for harbor seals (Phoca vitulina) derived from reaction times during underwater audiometry: A preliminary study. J. Acoust. Soc. Am. 129(1), 488-495

Kastelein RA, Bunskoek P, Hagedoorn M, Au WWL, de Haan, D (2002): Audiogram of a harbor porpoise (Phocoena phocoena) measured with narrow-band frequency-modulated signals. J. Acoust. Soc. Am. 112(1), 334-344

Kipple, B (2002): Southeast Alaska Cruise Ship Underwater Acoustic Noise. Naval Surface Warfare Center – Detachment Bremerton Technical Report NSWCCD-71-TR-2002/574 Okt. 2002, Zugriff 3/2012

Kipple, B., Chris Gabriele, B. (2004): Glacier Bay Watercraft Noise – Noise Characterization for Tour, Charter, Private and Government Vessels. Naval Surface Warfare Center – Detachment Bremerton Technical Report NSWCCD-71-TR-2004/545 June 2004, Zugriff 3/2012

Köller, J., Köppel, J., Peters, W. (2006): Offshore Wind Energy, Research on Environmental Impacts. Springer Verlag, Berlin

Lindell, H. (2003): Utgrunden off-shore wind farm – Measurement of underwater noise. Ingemansson Technology, Report: 11-00329-03012700, Göteborg, Sweden, 2003

Lesny, K. (2008): Foundation of offshore wind turbines - tools for planning and dimensioning. VGE Verlag, Essen

Lucke, K. (2006): Literature Review of Offshore Wind Farms with Regard to Marine Mammals, in: Ecological Research on Offshore Wind Farms: International Exchange of Experiences. BfN-Skripten 186, 2006, Part B, Federal Agency for Nature Conservation, Bonn, 2006, p 206

Lucke K, Lepper PA, Blanchet MA (2009): Temporary shift in masked hearing thresholds in a harbor porpoise (Phocoena phocoena) after exposure to seismic airgun stimuli. J. Acoust. Soc. Am. 125(6), 4060–4070

Müller, A., Zerbs, C. (2011): Offshore wind farms, measurement regulations for underwater noise measurements, current procedure with comments. Müller-BBM, Hamburg, Oct. 2011, report no. M88 607/5 (commissioned work, unpublished)

Nedwell, J. R., Parvin, S. J., Edwards. B., Workman, R., Brooker, A. G., Kynoch, J. E. (2007): Measurement and interpretation of underwater noise during construction and operation of offshore windfarms in UK waters. Subacoustech Report No. 544R0738 to COWRIE Ltd. ISBN: 978-0-9554279- 5-4. http://www.offshorewindfarms.co.uk/Pages/Publications/Archive/Soundscape/ Zugriff 1.9.2011

Prandtl, Oertel, H. (2008): Guide through fluid mechanics. Vieweg Teubner Verlag, Wiesbaden

RAVE (2012), http://www.rave-offshore.de, accessed May 17, 2012

TA Lärm (1998) - Sixth general administrative regulation for the Federal Immission Control Act (Technical instructions for protection against noise, TA Lärm), 1998

Thiele, R. (2002): Communication at the technical discussion on the UBA project "Avoidance and reduction of pollution of the marine environment by offshore wind turbines in the remote areas of the North and Baltic Seas" on January 15, 2002

Thomsen, F., Lüdemann, K., Kafemann, R., Piper, W.(2006): Effects of offshore wind farm noise on marine mammals and fish, biola, Hamburg, Germany on behalf of COWRIE Ltd. http://www.offshorewindfarms.co.uk/Pages/Publications/Archive/Soundscape/ Zugriff 1.9.2011

Tougaard, J., Henriksen, O.D., Miller, L.A. (2009): Underwater noise from three types of offshore wind turbines: Estimation of impact zones for harbor porpoises and harbor seals. The Journal of the Acoustical Society of America, 2009 June, 125(6):3766

Urban, H. (2002): Manual of waterborne sound technology. Self-published by STN ATLAS Elektronik GmbH, Bremen

Urick, R. (1983): Principles of underwater sound. McGraw-Hill Inc. Peninsula Publishing, Los Altos California

Verfuss, U., Honnef, C., Benke, H. (2004): Studies on space use by harbor porpoises in the North Sea and Baltic Sea using acoustic methods (PODs) sub-project 3. In: Final report Marine warm-blooded animals in the North Sea and Baltic Sea - Basics for the evaluation of wind turbines in the offshore area. Federal Ministry for the Environment, Nature Conservation and Nuclear Safety (FKZ: 0327520), pp.115-151

Welch, P. D. (1967): "The Use of Fast Fourier Transform for the Estimation of Power Spectra: A Method Based on Time Averaging Over Short Modified Periodograms", IEEE Transactions on Audio and Electroacoustics, Vol. AU-15, N0. 2, June 1967, pp. 70–73.

Westenberg, Hakan (2000): Impact studies of sea-based windpower in Sweden, in: Merck, T., von Nordheim, H.: Technical interventions in marine habitats. Workshop of the Federal Agency for Nature Conservation, International Nature Conservation Academy Insel Vilm, October 27 - 29, 1999, BFN - SKRIPTEN 29, Federal Agency for Nature Conservation, Bonn, 2000, pp 163 - 168

Wille, P.C., Geyer, D. (1988): Simultaneous Measurements of Surface Generated Noise and Attenuation at the fixed Acoustic Shallow Water Range “Nordsee”. in Kerman, B. R.: Sea Surface Sound. Kluwer Academic Publishers, Dordrecht